Investigating the Synergistic Signalling Mechanisms Underlying the Development of Obliterative Bronchiolitis

Aaron Gardner

PhD Thesis

Institute of Cellular Medicine

Newcastle University

June 2012

Declaration

I declare that this thesis is my own work and that I have correctly acknowledged the work of others. This submission is in accordance with University and School guidance on good academic conduct.

I certify that no part of the material offered has been previously submitted by me for a degree or other qualification in this or any other University.

I confirm that the word length is within the prescribed range as advised by my school and faculty.

Aaron Gardner

02/06/2012

Acknowledgements

I would like to thank my supervisors Professor Andrew Fisher, Professor Derek Mann and Dr Lee Borthwick for their invaluable advice and guidance throughout my studies and during my write-up.

Laura Mackay, Malcolm Brodlie, Danai Karamanou, Yonggang He, Scott Staniforth, Elizabeth Moisey, Monika Suwara, Nicola Green, Jodie Birch, Andrew Walker, Chris Ward and Gail Johnson for their friendship and support throughout my studies.

The MRC Doctoral Training Grant and the Institute of Cellular Medicine at Newcastle University for funding my studies.

Rachel Wood, Laura Ions, Andrew Henderson and Zubair Saleem for their friendship, endless cups of tea and PS3.

My parents for their love, support and encouragement in initiating and undertaking my studies.

Abstract

Therapies to limit or reverse fibrosis have thus far proved unsuccessful, highlighting the need for a greater understanding of the basic mechanisms driving fibrosis and in particular the link between fibrosis and inflammation. Obliterative Bronchiolitis (OB) is the pathological correlate of Bronchiolitis Obliterans Syndrome (BOS) a progressive disease that results in the fibrotic obliteration and blockage of the airways. Development of OB is strongly associated with elevated fibrotic, transforming growth factor beta 1 (TGF-β1), and inflammatory, tumour necrosis factor alpha (TNFα) and interleukin 1 beta, mediators; and the process of epithelial to mesenchymal transition (EMT) has been proposed as a mechanism of OB initiation and progression.

Previous work in our group has demonstrated that a physiologically relevant dose of TGF-β1 is capable of driving EMT in primary human bronchial epithelial cells (PBEC) isolated from lung-transplant recipients, an effect that was accentuated by TNFα. It was hypothesized that an unknown synergistic signalling cascade may mediate this accentuation, and identifying candidates for this role is the main aim of this thesis.

TGF-β1 and TNFα were used to induce EMT in PBEC cultures; the relative roles of several signalling proteins (SMAD3, IKKβ, TAK1, p38, ERK-1/2 and JNK-1/2) in the development of EMT were assessed by chemical inhibition and siRNA knockdown along with phosphorylation response, to describe a signalling cascade.

The results describe a mechanism whereby TGF-β1 drives EMT through SMAD3 with a requirement for TAK1 and JNK-2. TNFα signals through TAK1, IKKβ and JNK-2 but is not capable of driving EMT alone. Upon co-stimulation, TAK1 and JNK-2 display an enhanced activation that leads to an accentuation of EMT, possibly through c-Jun activation. JNK-2 sits downstream of TAK1 therefore the results indicate that TAK1 activity plays a key role both modulating TGF-β1 SMAD3 driven EMT, and its accentuation by TNFα. TAK1 was also shown to be more strongly activated in fibrotic human airway sections compared to control, suggesting that the findings have direct disease relevance.

Much further work into how TAK1 modulates SMAD3 activity after TGF-β1 stimulation and how its enhanced activation leads to accentuated EMT is required. Greater understanding of these mechanisms may lead to the discovery of novel therapeutic targets for fibrotic and inflammatory disorders.

Indexes

Main Index

Figure Index

Table Index

Appendix Figures Index

Acronyms

Acronym	Definition
BOS	Bronchiolitis obliterans syndrome
OB	Obliterative bronchiolitis
IPF	Idiopathic pulmonary fibrosis
COPD	Chronic obstructive pulmonary disease
BAL	Bronchoalveolar lavage
PBEC	Primary bronchial epithelial cell
EMT	Epithelial to mesenchymal transition
ALI	Air liquid interface
ECM	Extracellular matrix
ATP	Adenosine triphosphate
TGF-β	Transforming growth factor beta
BMP	Bone morphogenic protein
TGF-R*	TGF receptor *
LAP	Latency associated protein
SMAD*	Mothers against decapentaplegic *
SARA	SMAD anchor for receptor activation
SBE	SMAD binding element
MH2	MAD homology domain
TNFα	Tumour necrosis factor alpha
TNFR*	TNFreceptor *
TACE	TNFα converting enzyme
TRAF*	TNF-receptor-associated factor *
FADD	Fas-Associated protein with Death Domain
RIP*	Receptor interacting protein kinase *
TAK1	TGF-β activated kinase 1
TAB*	TAK1 associated binding protein *
NF-κB	Nuclear factor kappa-light-chain-enhancer of activated B cells
Iκ-Bα	NF-κB inhibitor, alpha
IKK*	IκB kinase *

Acronym	Definition
IL-*	Interleukin- *
IL-R1	IL-Receptor 1
ICE	IL-1β converting enzyme
IL-1R1A	IL-1R1 antagonist
MyD88	Myeloid differentiation primary response gene 88
IRAK*	Interleukin-1 receptor-associated kinase *
MAPK	Mitogen activated protein kinase
MAP2K	Mitogen activated protein kinase kinase
MAP3K	Mitogen activated protein kinase kinase kinase
MAPKAPK	Mitogen activated protein kinase activated protein kinase
P38	P38 mitogen-activated protein kinases
ERK*	Extracellular signal-regulated kinase *
JNK*	c-Jun N-terminal kinase *
ATF	Activating transcription factor
AP-1	Activator protein 1
EDTA	Ethylenediaminetetraacetic acid
IHC	Immuno-histochemistry
ICC	Immuno-cytochemistry
ELISA	Enzyme linked immuno-sorbent assay
SAGM	Small airway growth medium
DAPI	4',6-diamidino-2-phenylindole
FITC	Fluorescein isothiocyanate
TRITC	Tetramethyl rhodamine isothiocyanate
**i*	Chemical inhibitor of *
**si*	Small Interfering RNA targeting *
Ser	Serine amino acid residue
Thr	Threonine amino acid residue
Tyr	Tyrosine amino acid residue
Gly	Glycine amino acid residue
Glu	Glutamate amino acid residue
Pro	Proline amino acid residue
Lys	Lysine amino acid residue

1 Introduction

1.1 The Lung

The primary function of the lung is to facilitate gaseous exchange between the circulatory network and the outside environment. This is achieved by a branching network of airways; lined with a continuous epithelial sheet of varying function, which at the lower levels are intimately associated with the circulatory system to facilitate a rapid and efficient uptake of O_2 into the blood and expulsion of CO_2. This network exists within a mechanically, metabolically and immunologically supportive matrix that acts to facilitate healthy lung function.

The airways branch approximately 23 times in a normal healthy lung, transitioning from conducting airways into those where gaseous exchange can occur. The conducting zone begins with the trachea that divides into the left and right bronchi, which in turn divide into lobar, segmental and sub-segmental bronchi before concluding at the terminal bronchioles. This point onwards is known as the respiratory zone, with respiratory bronchioles with a few alveoli budding from their walls, passing into the alveolar ducts and finally terminating at the alveolar sacs. The distance between the respiratory bronchioles and alveolar sacs is small but due to the high number of branching events occurring within this zone, they make up the majority of the airway volume.

1.1.1 Large Airways

The term large airways is usually used to describe divisions of the bronchial tree from 2^0 through 2^5. The epithelium of the large airways is pseudo-stratified in nature and consists of three main types of cells, basal, goblet and ciliated, which are attached to a basal lamina composed of epithelial derived collagen IV and laminin, by hemi-desmosomes. This basal lamina in turn sits on a mature supportive ECM, produced by resident mesenchymal cells, composed predominately of collagen 1 fibres, surrounded by a protective network of smooth muscle and cartilage.

Basal cells are usually not exposed to the airway itself due to their more squat morphology, although due to the pseudo-stratified nature of the epithelium they are technically on the same plane as the other cells. Basal cells are thought to act as the progenitor cell in the upper airway (Rock et al., 2009), a fact which is demonstrated upon denudation of the airway, at which point they traverse the wound site, and expand

and divide *in situ* to reconstitute an intact epithelium (Maouche et al., 2009). Goblet cells secrete mucin, which mixes with water in the airway to form mucus, the main role of which is to trap particulate matter and pathogens preventing them from damaging the epithelium. The mucus also plays a vital role in conditioning inhaled air for efficient gas exchange by moisturising and warming it prior to reaching the alveoli. The mucus containing debris is cleared by the activity of the ciliated cells, which beat in concert to move the mucus out of the airway where it is either swallowed and degraded or cleared by coughing.

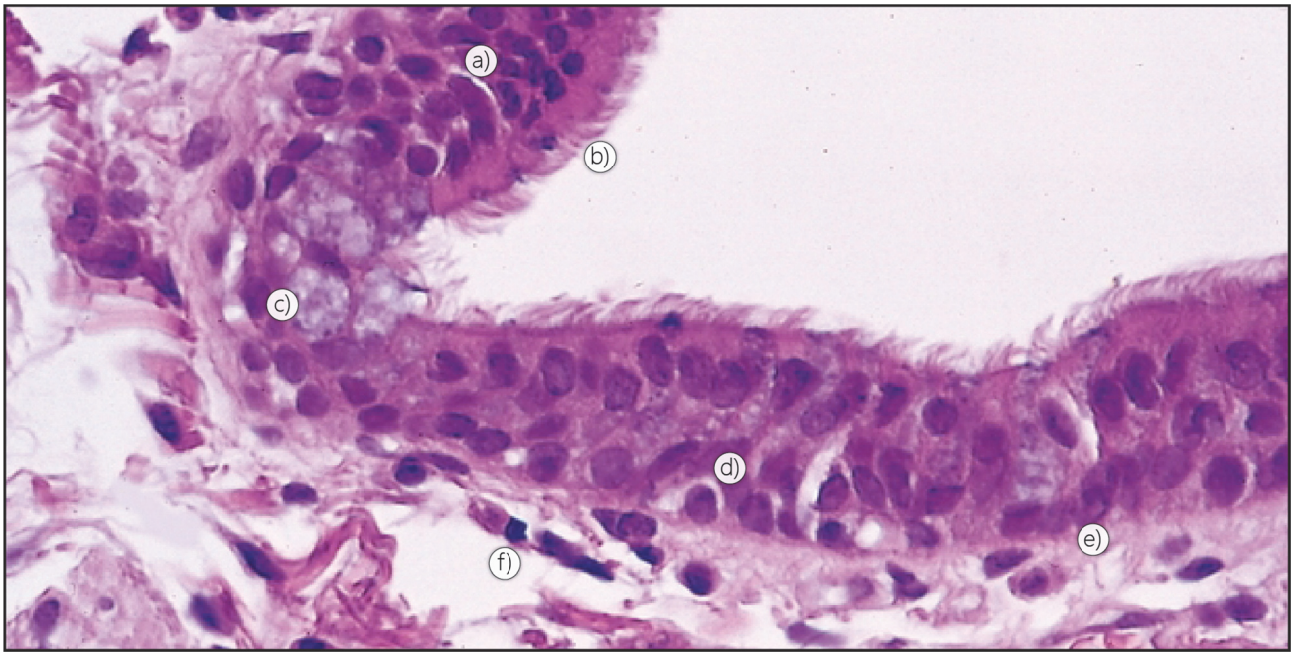

Figure 1 - Structure of the large airways

The pseudo-stratified epithelium of the large airway **a)** consists of ciliated cells **b)** along with goblet cells **c)** that are responsible for the production and clearance of mucus that traps foreign objects and prevents them reaching and damaging lower regions of the lung. Basal cells **d)** in the same plane as the other epithelial cells although more squat so they often do not have contact with the airway act as the progenitor cells of the large airways, capable of re-constituting a denuded epithelium after injury. Epithelial cells secrete a basal lamina **e)**, although in this instance basement membrane is more correct as the purely epithelial derived basal lamina cannot be differentiated by light microscopy, to which they are anchored by hemi-desmosome proteins. Beneath this lies an organized and mature ECM that is maintained by resident mesenchymal cells such as fibroblasts **f)** which are free to move around and amongst the ECM, but normally cannot pass through the basal lamina.

Images adapted from "Histology for Pathologists, Third Edition by Stacey E. Mills, 2007"

1.1.2 Small Airways

Small airways are defined as those between divisions 2^6 and 2^{22}, and as such mark the transition from the conductive to the respiratory zone of the lungs. Proximally there is little to distinguish them from the larger airways apart from the decreasing calibre of the airway. Progressing distally down the airway the cartilage support present in the airway wall decreases until it is no longer present in the smaller airways and is replaced instead by more elastic smooth muscle fibres. The respective thickness of the underlying ECM also decreases, until at the most distal regions the cells sit directly on the basal lamina closely associated with the vascular system with no cartilaginous and very little smooth muscle support. The occurrence of goblet cells decreases more distal regions of the lung, and they are replaced by the multi-functional Clara cell, there is also a transition from the cuboidal pseudo-stratified morphology to a more squat regular morphology.

Due to the small calibre of the airways at this point the surface tension of the fluid coating would be sufficient to collapse the airway under exhalation. As such Clara cells secrete a surfactant protein known as Clara cell secretory protein (CCSP) which, due to its amphiphilic nature, migrates to the surface of the fluid layer, and dramatically reduces the surface tension present (Hawgood and Clements, 1990). These Clara cells are although thought to act as the resident progenitor cell in the small airways (Stripp and Reynolds, 2008), able to divide into replacement ciliated and non-ciliated cells as required. Towards the most distal ends of the airways a squamous epithelium is found with few if any ciliated cells, it is at this point that respiratory, as opposed to conductive, features such as the alveolar ducts and sacs appear.

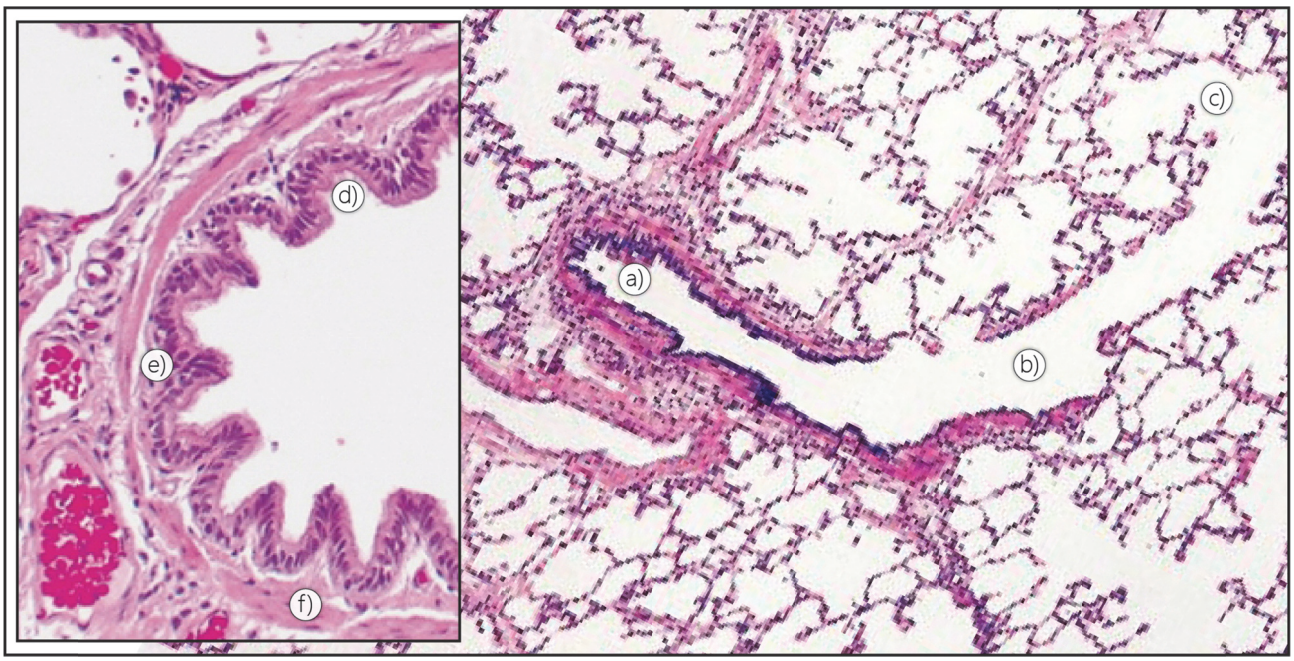

Figure 2 - Structure of the small airways

A bronchiole passes from left to right, at the more proximal end ciliated cells and a thicker ECM are apparent **a)**, passing to the right, and more distally, there is a decrease in the occurrence of ciliated cells and the epithelium becomes more squat in character **b)**, before finally terminating in the alveolar ducts and sacs **c)**. The more squat regular epithelium **d)** is attached to the basement membrane **e)** which is in turn surrounded by a ring of protective smooth muscle **f)**.

Images adapted from "Histology for Pathologists, Third Edition by Stacey E. Mills, 2007"

1.1.3 Alveoli

The alveoli are the distal termination point of the branching pulmonary network and are where the majority of gaseous exchange occurs. Alveoli initially appear budding off the respiratory bronchioles but the majority are found lining the alveolar ducts between divisions 2^{20} through 2^{22} and in the terminal alveolar sacs at division 2^{23}, there are thought to be around 500 million alveoli in a normal healthy human lung (Ochs et al., 2004). Both ducts and sacs are made up of alveoli and are responsible for the majority of gas exchange. The alveolar space is surrounded by the alveolar septa composed of Type I and Type II alveolar epithelial pneumocytes, existing upon the fibrous basal lamina described above. Interleaved throughout the alveolar walls is a dense network of pulmonary capillaries that facilitates the extremely efficient gas exchange process.

Again, due to the small size of the alveoli the surface tension of the fluid covering would be sufficient to collapse the alveoli upon themselves. To prevent this Type II pneumocytes secrete a variety of surfactant

proteins which, while distinct in structure, perform the same action as described for CCSP (Hawgood and Clements, 1990). In diseases affecting Type II pneumocytes the loss of this surfactant production can cause alveolar collapse, with the subsequent reduction in gas exchange. Alveoli also lack any mechanistic clearance mechanisms and so are dependent on the activity of alveolar macrophages in association with other immune cells to maintain their function.

Alveolar Type I pneumocytes make up the majority of the surface of the septa, approximately 95%, although due to their large flattened shape they only make up approximately 40% of total cell number. Type I cells are joined into a continuous sheet by tight junction proteins such as E-cadherin, preventing both the transmission of proteins into the alveolar space, and invasion of pathogens into the lung interstitium, although macrophages can still pass freely between through these junctions. The flattened shape of the Type I pneumocytes is designed to facilitate efficient gas exchange across the basement lamina into the associated pulmonary capillaries.

Type II epithelial cells, are typically found in the junctions between septa and are smaller and rounder than the Type I cell, although found in higher numbers. As well as producing surfactant proteins Type II cells are thought to act as the progenitor cell population within the alveoli replenishing the frequently damaged Type I cells (Evans et al., 1973, 1975), similar to the role of Clara cells found in the small airways. Type II cells have also been shown to release inflammatory cytokines in response to injury, thus contributing to the immune response (Koyama et al., 1998). Type I pneumocytes were traditionally thought to be terminally differentiated and incapable of expansion in culture, however recent advances in isolation and culture protocols have demonstrated expansion and de-differentiation capabilities (Wang and Hubmayr, 2011)

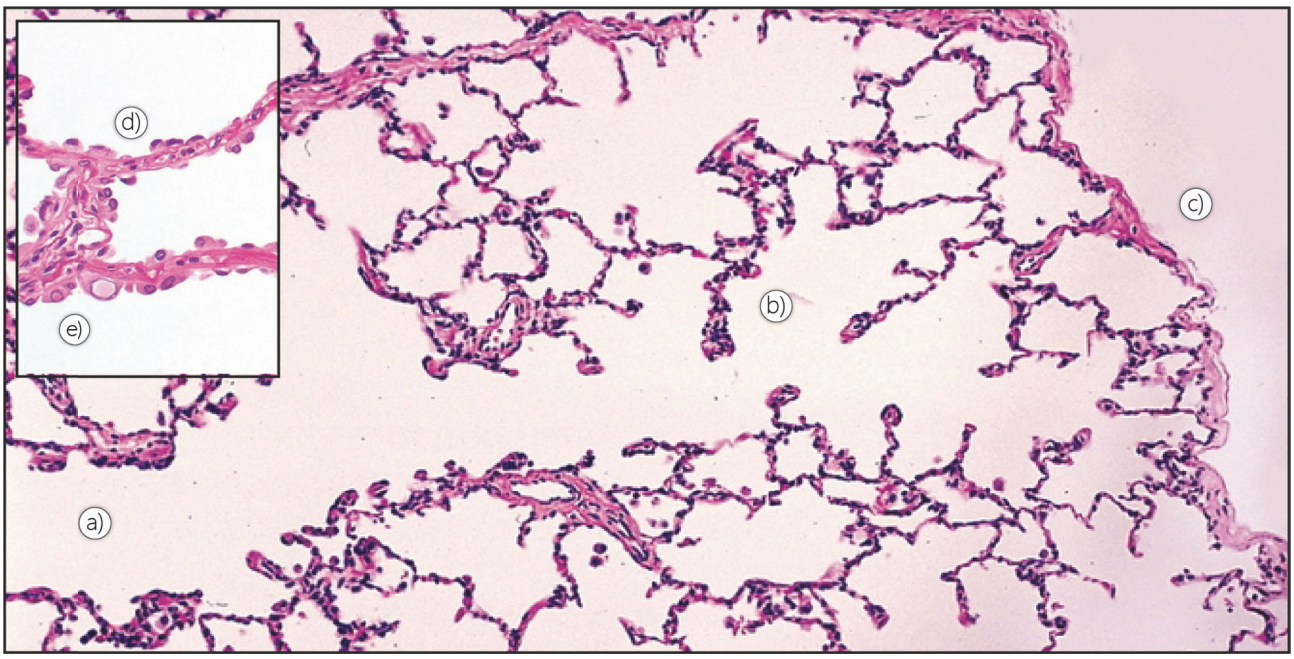

Figure 3 - Structure of the alveoli

An alveolar duct passes from left to right **a)** and is linked directly to numerous alveolar sacs **b)**. In this instance the alveolar duct terminates at the edge of the lung as evidenced by the presence of the pleura **c)**. Flattened Type I pneumocytes **d)** which line the majority of the alveolar surface and facilitate efficient gas exchange are present on either side of the pulmonary capillary containing basement membrane. A more rounded Type II pneumocyte is seen **e)** at the join between two separate alveoli, these cells are responsible for the production of surfactant protein, which allows for their separation based on innate buoyancy, and are thought to act as resident progenitor cells for Type I pneumocytes.

Images adapted from "Histology for Pathologists, Third Edition by Stacey E. Mills, 2007"

1.1.4 Supporting Matrix and Matrix Producing Cells

Beneath the epithelial cell derived basal lamina lies the supportive matrix of ECM proteins derived from non-epithelial cells. At homeostasis this ECM is composed predominantly of collagen I fibres that are cross-linked together in an organized fashion protecting the tissue it supports against damage. These fibres demonstrate a remarkable longevity *in vivo*, however, the composition of this ECM can and does vary in response to stimulation, with perhaps the most common cause being denudation of the overlying epithelium. It was initially thought that the ECM performed a supportive but generally inert role. However much recent research has described an ECM that is much more dynamic and biologically active, capable of initiating responses in resident and adjacent cells.

The ECM is predominantly maintained by fibroblasts resident within this matrix that secrete collagenous filaments and proteases, including the MMP family, maintaining the organized structure of the ECM.

Fibroblasts are generally spindle shaped, and unlike the epithelial cells they underlie are not associated into ordered sheets, display no apical-basal polarity and are free to migrate throughout the ECM. Damage to the ECM results in the recruitment of surrounding resident fibroblasts in response to stimuli such as TGF-β1 (Degryse et al., 2011) which can also induce fibroblasts to proliferate more rapidly (Hetzel et al., 2005). These resident fibroblasts may also be supplemented by fibrocytes derived from the bone-marrow and recruited from the vasculature by a chemotactic gradient, originating at the damage foci (Bucala et al., 1994). Once resident these fibrocytes are hypothesized to transition into an active fibroblast state and contribute to ECM repair and renewal (Abe et al., 2001; Lapar et al., 2011).

Myofibroblasts are typically not seen within the stable ECM, but rather are associated with the wound healing process with aggregate myofibroblast foci often associated with fibrotic disorders (Kis et al., 2011). The primary role of the myofibroblast is to contract an exposed wound site reducing the chances of infection. This is achieved by secretion of several ECM proteins including α smooth muscle actin (αSMA) in a network with other myofibroblasts around the wound site (Hinz and Gabbiani, 2003). Myofibroblasts are thought to differentiate from fibroblasts under conditions of mechanical stress within the ECM, and also in response to factors such as TGF-β1 (Ramirez et al., 2006).

Increased numbers of fibroblasts and myofibroblasts are often implicated in the development of fibrotic disorders. Whilst required in normal wound resolution their persistence can lead to excessive deposition of disorganized ECM components, often in association with an up-regulation of proteinase inhibitors such as the TIMP family. This leads to the gradual loss of structure and function within the organ affecting regions that had often suffered no direct injury themselves. Understanding the mechanisms that initiate this dysregulated production and persistence of fibroblasts and myofibroblasts is a key area of on-going research in many fibrotic disorders.

1.1.5 Pulmonary Capillaries

Pulmonary capillaries interweave throughout the majority of the alveolar walls, taking up approximately 90% of the alveolar wall volume. This high density exists to maximise the occurrence of gas exchange by maximising the surface area to volume ratio of the blood present in the lungs. The capillaries themselves have a diameter only slightly greater than that of a red blood cell, and the majority of their surface is tightly associated with the flattened portions of Type I pneumocytes, forming a fused basement membrane over which gas exchange occurs. Exchange of O_2 and CO_2 is a passive process based on the

differences in partial pressures of the two gasses, however diffusion efficiency is also affected by the thickness of the fused basement membrane. A thickening of the alveolar wall and hence reduced efficacy of gas exchange is often associated with the development of pulmonary fibrosis.

1.1.6 Resident Immune Cells

Large numbers of dendritic cells are interspersed throughout the lung, whilst often located underneath the basal lamina they are able to sample the airway space by deploying sensory protrusions between epithelial cells. Dendritic cells, in association with neighbouring epithelial cells (Upham and Stick, 2006), continually probe the airway space and are able to recognize inhaled antigens and present them to relevant immune cells, they are also capable of responding to danger signals generated by damage to resident cells (Upham and Stick, 2006).

As previously discussed, the upper airways utilise mechanistic clearance to dispose of particulate matter and inactivate prospective pathogens. However, the alveoli have no such measures and instead rely on the activity of resident alveolar macrophages as a first line of defence to ingest and clear the continuously deposited foreign materials. In homeostasis alveolar macrophages are held close to the alveolar wall in a quiescent state, with little phagocytic activity (Holt et al., 1993), consequently supressing the response of other immune cells such as the aforementioned dendritic cells (Upham and Stick, 2006). The macrophages are held in this state to prevent collateral damage to the delicate Type I pneumocytes and associated capillary networks, which may occur in response to continuous low-grade immune response. However, upon detection of potentially dangerous antigens or damage, either by themselves or through associated epithelial or dendritic cells the macrophages are released from quiescence and phagocytic and pro-inflammatory responses are initiated. Macrophages also contribute towards the initiation of correct wound resolution (Porcheray et al., 2005), however their presence is deleterious to end-stage resolution and so a decrease in macrophage number and activity is required (Martin et al., 2003).

Both macrophages and dendritic cells play key roles in the innate and adaptive immune responses of the lung. A dysregulation of their response is associated with several diseases such as asthma, where a hyper-activated response is associated with over-recruitment of other mediators of the immune system and tissue remodelling. Understanding the modulation of recruitment, activity and subsequent dispersal therefore receive much attention in the development of fibrotic disorders.

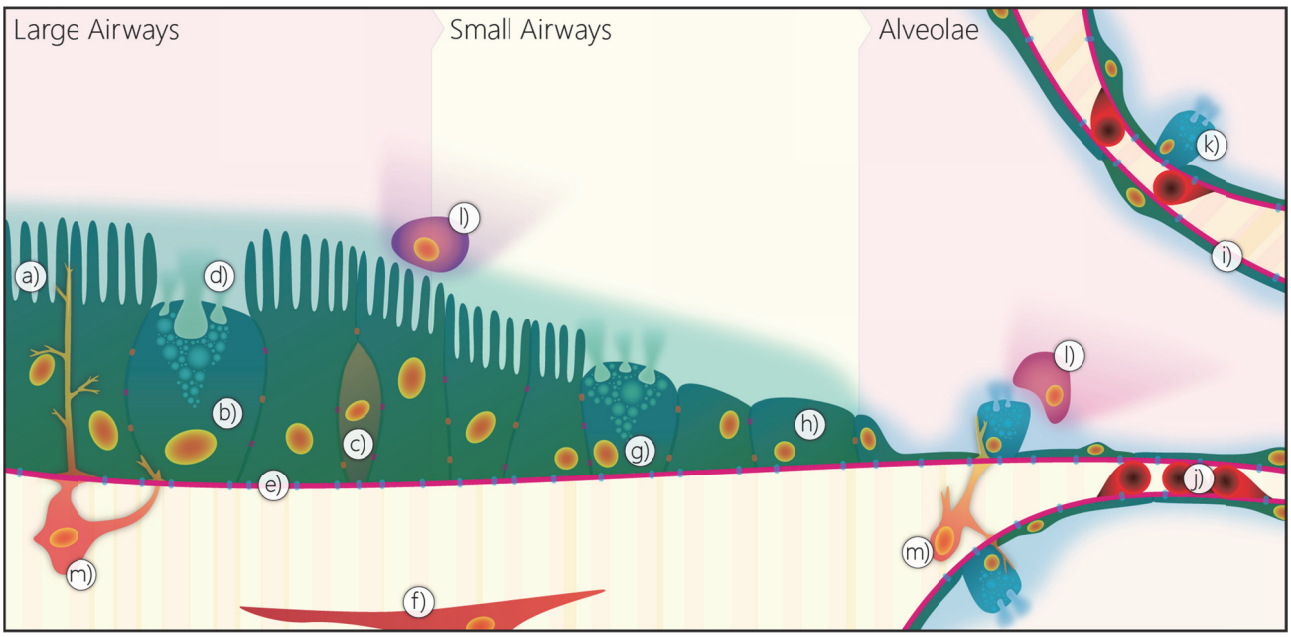

Figure 4 – Progression of the airway epithelium

Moving from left to right the airways progress distally from the bronchus at division 2^0 to the alveoli at 2^{23}. The pseudo-stratified large airways consist of ciliated **a)**, goblet **b)** and basal **c)** cells, bound to each other by tight junction proteins. Basal cells are thought to act as the progenitor cells in the large airway, goblet cells produce mucin **d)** which forms a protective mucus barrier on the surface of the epithelium, which traps harmful objects before being cleared by the action of the ciliated cells. Cells are attached to a basal lamina **e)**, which is secreted by the epithelial cells themselves, which in turn sits on top of a mature and cross-linked collagen I rich supportive matrix, maintained by resident fibroblasts **f)**.

In the small airways there is a reduction in goblet and basal cells, which are replaced by Clara cells **g)**, which act both as the progenitor cell in the small airways and secrete surfactant proteins, which both protect the airways and reduce surface tension in the fluid covering. Ciliated cells are still present although moving distally they become more squat and are eventually replaced by non-ciliated cells **h)**. Most distally the small airways become squamous in nature and transition in the alveoli ducts and sacs.

There are two main cell types in the alveoli, Type I pneumocytes **i)**, which take up the majority of the surface area and are flattened to facilitate efficient gas exchange into the accompanying pulmonary capillaries **j)**. Also present are Type II pneumocytes **k)** which act as the progenitor cell replacing damage Type I pneumocytes and secrete surfactant protein that lowers surface tension in the fluid covering of the alveoli and prevents their collapse.

In both the airway an epithelium patrolling macrophages **l)** are closely associated with the epithelium that inhibits their function in order to prevent an excessive response to non-harmful pathogens, which may damage epithelial cells. Dendritic cells **m)** are also tightly integrated into the epithelium, although the bulk of the cell exists below the basal lamina, they are constantly sampling the airway environment for pathogens, and are also capable of receiving stimulation from the epithelial cells themselves.

1.2 Fibrotic & Inflammatory Lung Disease

The lung is exposed to numerous mechanical and biological insults, and these insults can often lead to the onset and exacerbation of inflammation and fibrosis in the lung. Correspondingly, there is a wide range of lung diseases caused by these insults. The location, cause, progression and outcome of lung disease varies greatly however they are broadly characterized into two classes.

Obstructive airway diseases such as Chronic Obstructive Pulmonary Disease (COPD), asthma and Bronchiolitis Obliterans Syndrome (BOS) result in increased resistance to airflow caused by some form of obstruction, resulting in a decrease in the amount of air that can reach the respiratory zone, decreasing the efficiency of gas exchange. Three main mechanisms can cause this obstruction; a build-up of material in the airway, as in the chronic bronchitis strand of COPD or BOS, a thickening of the airway wall as in asthma or a degradation of the supportive matrix that helps keep the airways open and taut as in the emphysematous strand of COPD. Restrictive lung diseases such as Idiopathic Pulmonary Fibrosis (IPF) inhibit the ability of the lung to expand and contract during respiration. Restrictive diseases are often the result of a change, usually an increase in or thickening of, the supportive ECM. In the case of IPF this can be seen by the thickening of the alveolar walls, which is followed by the loss of epithelial covering within the alveoli. This increase in ECM makes it difficult to breathe, hence the restrictive terminology, whilst also reducing the surface area available for gas exchange.

The lung relies on structural and mechanical means as a first line of defence, however when a harmful object is detected by resident immune cells or the epithelium itself a classic inflammatory response ensues. Resident cells produce a cocktail of inflammatory mediators such as TNFα, IFN-γ and IL-1β/8/17, which act to recruit other immune cells, and modulate the response of cells already present. If the vasculature is breached by injury then factors such as thrombin are also released which are designed to facilitate clotting and quick re-constitution of a barrier between the vasculature and outside world. In more severe cases, non-resident immune cells are recruited to help with clearance and re-constitution of the epithelium.

Under normal circumstances where the stimulus is removed the inflammatory response is short lived due in part to the short lifespan of the released immune mediators and attracted cells , and the release of anti-inflammatory mediators such as IL-10, TGF-β1 (Sanjabi et al., 2009) and proteases capable of cleaving immune mediators (Gueders et al., 2006). In the development of chronic inflammation this clearance does not occur, either as a result of an un-clearable antigen as in allergic responses, a

repeating injurious process as with the majority of diseases relating to particulate mediated damage or some other factor such as a chronic infection or genetic susceptibility.

The inflammatory response can often lead to damage of the lung epithelium; under normal conditions where this may only affect a small region the damage is usually repaired correctly restoring an intact and functional epithelium. However, where inflammation persists one of the common outcomes is the development of fibrotic tissue. The immune mediators released by immune cells recruit fibroblasts resident in the tissue which repair any damage to the ECM caused by the inflammatory response. If the inflammatory response continues then progressively more fibroblasts are activated and encouraged to proliferate (Hetzel et al., 2005), circulating fibrocytes may be recruited from the vasculature (Abe et al., 2001) and induction and survival of myofibroblasts may be increased (Kis et al., 2011). The end result is an excess of mesenchymal cells producing a disorganized matrix of ECM proteins such as collagen III and fibronectin which can quickly over-run the immediate area, destroying the epithelial structure. Not all fibrosis is induced by inflammation as in some instances the causes is unknown, excessive fibroblast recruitment and proliferation can also be induced by factors such as TGF-β1 and FGF, all of which may be linked to genetic pre-dispositions to fibrosis (Riha et al., 2004).

1.2.1 Wound Repair & Chronic Wounding

In a healthy individual epithelial injury should repair effectively in a physiological manner returning it to functional homeostasis. This repair requires a spatially and temporally orchestrated response from the cells of the lung epithelial sheet, the underlying progenitor and supportive cells and resident immune cells, as well as those drawn from the circulatory system. This process can be thought of as occurring in three overlapping phases: an initial response, a recovery of integrity and a final resolution phase. The severity of injury, existing environment and occurrence of prior injury all have a marked effect on the efficacy of recovery and can help explain poor recovery and resolution. It is this poor recovery and resolution that are the pre-cursors to the development of fibrosis, and there are numerous points at which dysregulation can occur.

Upon wounding numerous factors are released into the airway or alveolar space from the epithelial cells themselves, the ECM and the vasculature if breached. These factors recruit non resident immune cells such as neutrophils, eosinophils and basophils migrate to the wound area through chemotaxis (Hudson et al., 1977), and degrade any cellular debris by phagocytosis and/or neutralizing invading pathogens

through an oxidative burst response. The granulocyte count in the wound area peaks rapidly, but is followed by an equally rapid decrease in number due to apoptosis and non-inflammatory phagocytosis by resident macrophages and responding monocytes. Fibroblasts create a temporary ECM composed of factors such as fibronectin and collagen III (Santos et al., 2006) which is more flexible due to a lack of cross linking. Larger wounds are contracted through the activity of myofibroblasts (Hinz, 2007) and nearby epithelial cells loosen their adherence to each other and the basal lamina and creep across the provisional ECM (Farooqui and Fenteany, 2005). This provisional ECM and motile epithelial cells are more susceptible to colonisation from opportunistic pathogens such as *Pseudomonas aeruginosa* (De Bentzmann et al., 1996), an effect which may be exacerbated by immuno-suppression in transplant recipients, or existing physiological conditions.

The few remaining macrophages in the wound are thought to transition from a pro-inflammatory form, often termed the classically activated macrophage, into one with a pro-resolution character often termed the alternatively activated macrophage. These macrophages and monocytes gradually lose their inflammatory nature, and take on a more recovery orientated role before eventually leaving the site (Bellingan et al., 1996; Porcheray et al., 2005). This allows the epithelium to proliferate and re-mature in the best cases regaining full functionality. Alongside this the underlying ECM matures under the control of residing fibroblasts which degrade collagen III and fibronectin replacing it with collagen I which can then be cross linked. A more in-depth coverage of this event process can be found in my review article on the subject (Gardner et al., 2010)

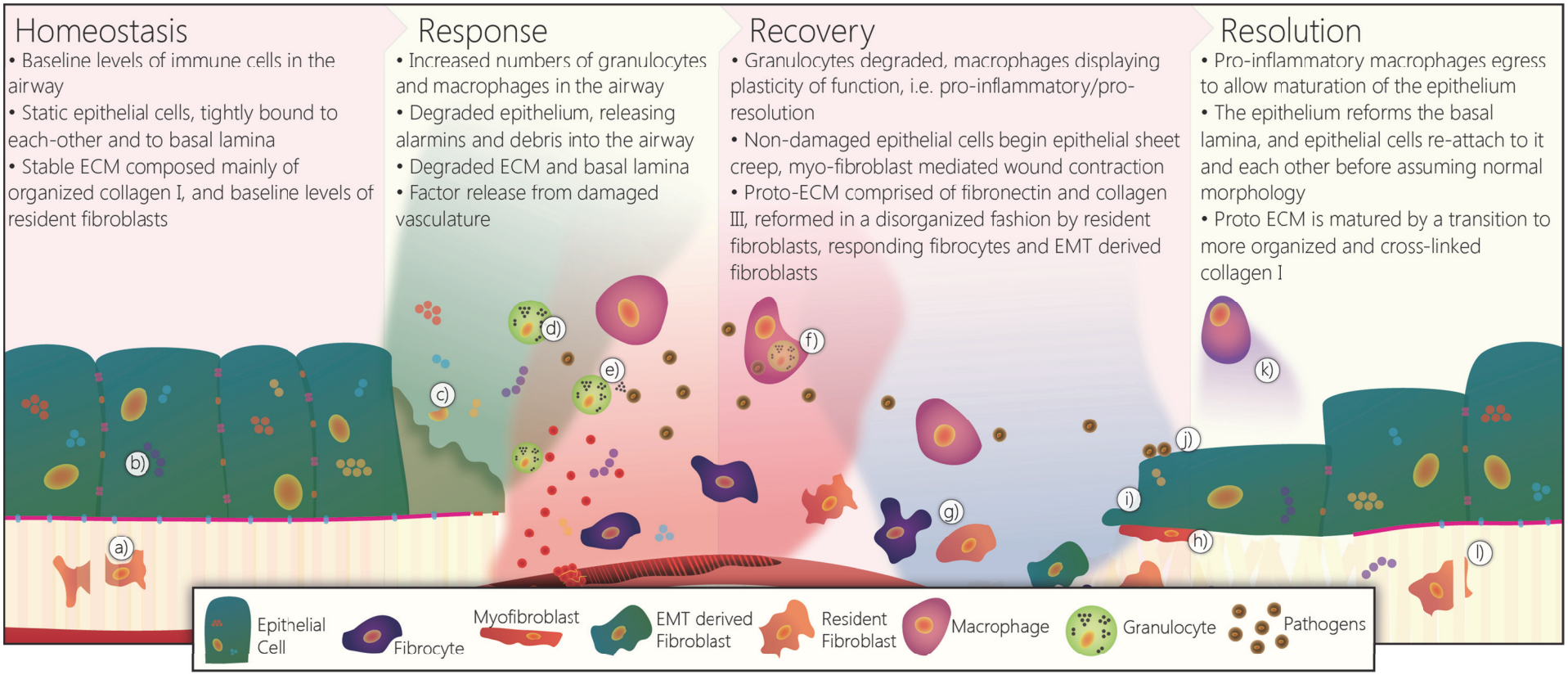

Figure 5 – Epithelial wound repair

Fibroblasts maintain the mature collagen I rich ECM **a)**, upon which the epithelium sits containing potent inflammatory mediators and other factors such as TGF-β1 **b)**. Upon injury debris and the previously described factors are released **c)**, recruiting granulocytes to the wound **d)** which degrade invading pathogens **e)**. The granulocyte count peaks quickly before they are phagocytosed **f)** and replaced by macrophages. Circulating fibrocytes, resident fibroblasts and EMT derived fibroblasts **g)** begin to reform the ECM from fibronectin and collagen III in a disorganized fashion. Contraction of the wound is mediated by myofibroblasts tethered to the ECM **h)**, concurrently non-injured epithelial cells loosen attachments, and creep over the wound area **i)**. This provisional ECM and motile epithelium is susceptible to pathogen colonisation **j)**, however immune cells can inhibit wound closure and so a delicate balance must be maintained. Macrophages are capable of displaying a pro-resolution functionality which aids in closure of the wound **k)**, the bulk of pro-inflammatory macrophages have either transformed or egressed from the wound by this point. The ECM is matured by replacing the disorganized collagen III with collagen I which is tightly cross-linked *via* fibroblasts **l)**, the intact epithelium begins to re-acquire its normal morphology.

Anti-resolution factors	Mechanism
Dysregulation at the Response Stage	
Non-clearance of immune cells, counteracted by overactive anti-inflammatory/pro-fibrotic response.	
Repeated initiation of immune response:	Repeated initiation of the wound healing response which prevents resolution and may lead to the development of fibrosis:
- Allergy	Repeated targeting of non-harmful allergens leads to repeated activation of the immune response. (Holgate et al., 2010)
- Pathogen colonisation	A non-clearable pathogenic colonisation symptomatic of several diseases such as Cystic Fibrosis, or in immuno-compromised individuals, leads to repeated or constant activation of the immune response. (Hafkin and Blumberg, 2009)
- Particulate Matter	Particulate matter that triggers an immune response directly or damages epithelium thus triggering an inflammatory and pro-fibrotic response can be tied to allergy. (Baumgartner et al., 1997)
Non-clearance of granulocytes	Granulocytes are usually only present in the wound site for a short period; longevity in the wound can initiate fibrosis. (Riise et al., 1999)
Dysregulation at the Recovery Stage	
Hyperactive fibrotic response, may. be stimulated by inflammatory mediators	
Fibroblast activity:	Over-recruitment or dysregulation of repair mechanisms leading to the development of fibrosis.
- Overactive resident fibroblasts	Resident fibroblasts proliferate and deposit and re-model ECM in a wound environment. Over activation or over proliferation leads to the development of fibrosis. (Hetzel et al., 2005)
- Excessive fibrocyte recruitment	Circulating fibrocytes can be recruited to assist in wound repair, over-recruitment leads to the development of fibrosis. (Lapar et al., 2011)
- Too many myofibroblasts	Over activation, over recruitment/differentiation or resistance to apoptosis lead to the development of fibrosis. (Kis et al., 2011)
Too 'mesenchymal' epithelium	The transient gain of mesenchymal characteristics by the motile epithelial sheet can become dysregulated, with epithelial cells contributing directly to fibrosis. (Willis and Borok, 2007)
Dysregulation at the Resolution Stage	
Opportunistic colonisation	The motile epithelium and provisional ECM are susceptible to colonisation, which can re-initialize the immune response, leading to further damage in the wound. (De Bentzmann et al., 1996)
Non maturing epithelium	The motile epithelium may not mature correctly, making colonisation more likely, or contributing to fibrosis directly as above.
Non stabilising ECM	The ECM is remodelled to contain cross-linked collagen I, by fibroblasts and factor release, a continuation of this process leads to the development of fibrosis. (Ehrlich and Krummel, 1996)
Other Forms of Dysregulation	
Genetic mutations:	All of the above occurrences may be purely environmental in origin however; there are several fibrotic diseases with a genetic association. This may manifest itself as the over expression, or activity of a pro-inflammatory factor or receptor, the under expression or activity of a repressor of inflammation or fibrosis; or the activation of differential signalling networks in response to 'normal' stimuli. (Riha et al., 2004; Charpidou et al., 2008; Sharma et al., 2008; Rogers et al., 2009)

Table 1 - Potential anti wound resolution mechanisms

The table above outlines several of the mechanisms that can dysregulate a normal wound healing response and lead to a chronic wound with the subsequent development of fibrosis. Whilst correct resolution and progression through all stages of the wound repair process is vital, it is the origin and maintenance of excess or dysregulated fibrogenic cells that is perhaps the most important area to investigate in relation to the development of fibrotic disorders. There are several hypotheses as to the origins of these cells, and the relationship within a chronic wound environment can play a key role in this process.

1.2.2 Origin of Fibrogenic Cells

There are three prominent hypotheses as to the origin of fibrogenic cells in fibrotic disorders, firstly that resident fibroblasts proliferate rapidly and potentially differentiate into myofibroblasts, secondly that circulating fibrocytes are recruited from the vasculature and differentiate into fibroblasts and thirdly that epithelial cells present in the lung trans-differentiate into fibroblasts. None of these processes are innately pathologic, as they all serve important roles in the normal wound healing process so it is likely that hyper-activation of or prolongation of the response is key.

There are many fibroblasts distributed throughout the supportive matrix of the lung and whilst they are required in normal wound resolution their persistence and hyper-activation is a key contributor to fibrosis. The release of several growth factors such as TGF-β1 and FGF as well as other factors such as mechanical stress within the ECM can lead to fibroblast activation. This activation leads to an increase in proliferation and the secretion of less mature ECM products such as fibronectin and collagen III (Hetzel et al., 2005). In more severe wound events these fibroblasts are often induced into the contractile myofibroblast phenotype which associate into foci to facilitate wound closure (Hinz, 2007). These foci contain large amounts of fibrotic material required to facilitate the mechanistic closure of the wound, and dysregulation of this process, or increased proliferation and resistance to apoptosis of myofibroblasts is a hallmark of fibrosis (Kis et al., 2011).

The theory of circulating fibrocytes contributing to repair of lung epithelial wounds is a relatively new concept (Bucala et al., 1994), suggesting that bone marrow-derived fibrocytes can be recruited from the vasculature in response to a chemotactic gradient emanating from the wound. These cells differ from resident fibroblasts in that they express hematopoietic markers such as CD34, CD45 and CD54 (Quan et al., 2004). CD34 was the first marker described for fibrocytes and has therefore been the focus of most

research. Expression of these markers has been shown to decrease *in vitro*, however, it is thought that fibrocytes in the wound environment retain this expression profile (Bucala et al., 1994).

The factors responsible for the chemotactic recruitment of these fibrocytes are not completely understood; however, expression of the CCR3, CCR5, CCR7 and CXCR4 receptors have been shown to play a role (Abe et al., 2001). Once resident in the wound site, the fibrocytes are capable of producing collagen and αSMA, a process that is increased in the presence of TGF-β1 (Abe et al., 2001). While these fibrocytes may play a role in physiological wound repair, over-recruitment is associated with numerous pulmonary disorders. An increased number of fibrocytes is associated with IPF, with an even greater abundance in acute exacerbations (Moeller et al., 2009), although which, if any, of the aforementioned factors is responsible for their recruitment is unknown. In asthma, an increased number of fibrocytes are present in the hyperplasic airway smooth muscle, although it has not yet been determined if they contribute significantly to disease progression or severity, or are attracted by the already hyperplasic tissue (Saunders et al., 2009). In obliterative bronchiolitis (OB) elevated levels of fibrocytes are present in the lung tissue and in the pulmonary vessels running through this tissue, with both displaying evidence of remodelling, although the authors present no evidence about a contribution to obliteration of airways themselves (Andersson-Sjöland et al., 2009).

The third mechanism, trans-differentiation of resident epithelial cells into fibroblasts, termed epithelial to mesenchymal transition is the focus of my project and is discussed below.

1.2.3 Plasticity & Epithelial to Mesenchymal Transition

Epithelial to mesenchymal transition (EMT) describes the loss of epithelial character of a cell, namely tight junction adherence to adjacent cells and a basal lamina forming a continuous epithelial sheet with apical-basal polarity, into a mesenchymal form characterized by increased motility of individual cells and an increase in the ability to secrete ECM proteins. EMT has been demonstrated to play an important role at numerous stages, firstly in early development when mesodermal cells are formed and internalized at the primitive streak. EMT also plays a key role in the wound healing response of the epithelium, in areas where the epithelium has been denuded surrounding basal cells move over the wound site secreting a new basal lamina as they go, displaying several of the characteristics used to define EMT.

EMT is also thought to play a key role in tumorigenesis, with a decrease in E-cadherin expression strongly associated with several cancers, which is thought to facilitate metastasis (Chao et al., 2010; Hou et al., 2011). The role of TGF-β in the development of cancer is poorly understood; initially described as a *pro*-metastatic factor it has now been shown to display both pro (Dalal et al., 1993) and anti-cancer (Zhu et al., 1998) properties in various different models, and even within models (Siegel et al., 2003). This multifunctional response is likely due to the ubiquitous expression of both TGF-β and its receptors and the pleiotropic nature of TGF-β; so whilst TGF-β is important, it is the modulation of upstream activation and downstream effect that is likely to be important as opposed to direct targeting.

The role of dysregulated inflammatory activity in tumorigenesis is much more widely accepted (Lin and Karin, 2007), with factors such as alcoholism and particulate exposure (smoking, asbestos etc.) strongly associated with the development of inflammatory mediated liver and lung cancers respectively. However, the mechanics of this association is again poorly understood; with the multifaceted response of nuclear factor kappa-light-chain-enhancer of activated B cells (NF-κB) the main cause of this lack of clarity. NF-κB was long thought to have purely a tumorigenic role, mediating the expression of anti-apoptotic genes (Barkett and Gilmore, 1999), induction of the cell cycle and cell invasiveness (Pahl, 1999). However a new role as a tumour suppressor is emerging whereby apoptosis of tumour cells is induced by p53 in an NF-κB dependant manner (Rocha et al., 2003). As with TGF-β the multifaceted role of NF-κB means that modulation of function rather than direct targeting may produce better therapeutic targets for EMT.

Since starting my project the consensus view on EMT in fibrosis has shifted considerably. Perhaps due to the over-exuberant claims that were initially made, things now seem to have swung the other way towards general scepticism of the process, at least *in vivo*. Early experiments in the kidney (Iwano et al., 2002), liver (Omenetti et al., 2008) and pancreas (Gershengorn et al., 2004) suggested that EMT may be a key conserved role in the development of fibrosis. However later, more robust lineage tracing experiments in the same systems failed to re-produce these findings; kidney (Humphreys et al., 2010), liver (Scholten et al., 2010) and pancreas (Morton et al., 2007).

Luckily, the one exception to this to date is the lung, as far as I am currently aware no negative lineage tracing studies investigating EMT have been published, although I admit that this alone would not be sufficient evidence. A potential end stage of EMT in the human lung was demonstrated Willis et al whereby tissue segments isolated from patients with advanced IPF showed co-expression of both Type II alveolar epithelial (pro-surfactant protein-B) and myofibroblast (αSMA) markers (Willis et al., 2006). One of the potential driving mechanisms for the induction of this transition is the excessive or continuous

release of cytokines in the lung, with numerous groups showing that treatment with TGF-β1 can induce this change both *in vivo* (Kim et al., 2006; Tanjore et al., 2009) and *ex vivo* in rat cells (Willis et al., 2006) along with human cell lines (Kasai et al., 2005; Borthwick et al., 2011) and primary cultures (Borthwick et al., 2009, 2010; Câmara and Jarai, 2010). The studies by Kim *et al* (Kim et al., 2006) and Tanjore *et al* (Tanjore et al., 2009) are especially powerful as by utilising transgenic mice with labelled epithelial cells they were able to show *in vivo* that these epithelial cells, or their descendants, began expressing mesenchymal markers such as αSMA and vimentin, and a loss of epithelial character in response to stimulation with TGF-β1. Tanjore *et al* went one step further and were able to demonstrate that approximately 30% of resident fibroblasts were derived from the labelled epithelium 2 weeks post bleomycin injury.

Perhaps some of the hostility against EMT arises from the lack of clear definition, does it refer to a complete switch in character or a more gradual transition across a spectrum with the most highly specified cell types at either end, where cells can share display both mesenchymal and epithelial character? By using the second definition, it does not seem too difficult to see how EMT could have a role to play in fibrotic development.

Whilst I am focusing on the process of EMT in this thesis, it is likely that all three described mechanisms play an important role in the development of fibrosis.

1.2.4 Obliterative Bronchiolitis

OB, the pathological correlate of BOS is a progressive scarring disease of the small airways, which, along with a destruction of the epithelium in the local airway often blocks the airway itself with a plug of fibrotic material, mesenchymal and immune cells. There is a strong association of OB in lung transplant recipients with approximately 40% of patients displaying evidence of disease 5 years post-transplant (Christie et al., 2010). Diagnosis is made based upon the decline in FEV_1, a measure of expiratory ability within 1 second as a percentage of the total lung capacity, and is often associated with the development of dyspnoea and a productive cough (Cooper et al., 1993).

There are numerous mechanisms which have been proposed as initiators of disease, prime among them being the occurrence of tissue rejection with the corresponding development of an inflammatory immune reaction (Burton et al., 2009). However other factors such as an increase in acid reflux from the

gut (Vos et al., 2011) or an increase in pathogen load due to immuno-suppression (Vos et al., 2008) as well as non-transplant related causes such as exposure to industrial particles have also been implicated (Akpinar-Elci et al., 2004). However, as there is a large variation in onset, progression and treatment response in BOS it suggests that there is interplay between several factors.

Two distinct forms of OB have been described; a chronic early onset neutrophilic form that displays evidence of a strong inflammatory response, along with an acute late onset version of OB with little to no evidence of increased neutrophil count, and a less acute inflammatory response (Vanaudenaerde, Meyts, et al., 2008). It has been proposed that the neutrophilic OB may occur early after transplant due to the combination of increased reflux and colonisation of the airways with pathogens such as *Pseudomonas aeruginosa* which act in concert to damage the airway epithelium leading to the recruitment of neutrophils to the wound site through chemotaxis. Whereas it is thought that the late onset form of the disease is more dependent on classical acute rejection episodes. The occurrence of these two forms seems to account for the variable response to treatment with azithromycin, which can rescue the decline in FEV_1/FVC in the neutrophilic form of the disease, whereas little effect on FEV_1/FVC is seen in the non-neutrophilic form (Vanaudenaerde, Meyts, et al., 2008; Vos et al., 2010, 2011).

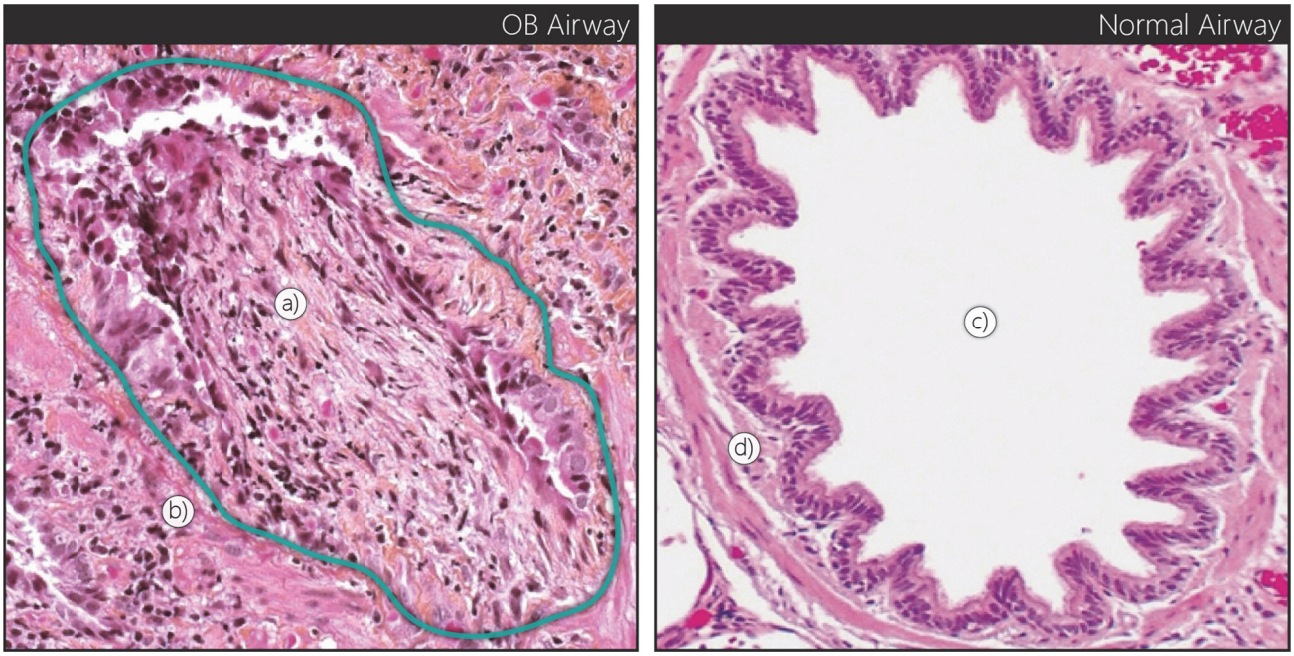

Figure 6 - Histological stain comparing OB to normal tissue

The left photo-micrograph displays an airway from a patient diagnosed with BOS. The airway lumen is almost completely obliterated **a)** with a dense clot of fibrotic material and cells. The majority of epithelial cells lining the lumen have been lost along with the clear boundary separating them from the underlying ECM (which I have attempted to mark in green) **b)**. The right photo-micrograph shows a normal airway, the lumen is clear of any debris **c)** and the epithelium and clear boundary underlying it are intact **d)**.

Images adapted from "Histology for Pathologists, Third Edition by Stacey E. Mills, 2007"

1.3 Signalling Mechanisms

As described in **1.2** an excessive or prolonged release of inflammatory or pro-fibrotic mediators is often a key driver in the development of fibrosis. These factors initiate signalling cascades within receptive epithelial, mesenchymal and immune cells. An understanding the mechanisms at play in these cells may shed light on the development of fibrosis.

In order to respond quickly to stimuli cells need a ready supply of signalling capable proteins, however they also need to exert control over these pathways. Two mechanisms which can regulate these signalling proteins, and that I discuss throughout this thesis are, phosphorylation and ubiquitination. Phosphorylation involves the addition of a phosphate group PO_4^{3-} onto a specific residue within a protein, which can induce a conformational change of the protein structure, usually resulting in the gain or loss of function. This process usually involves a kinase targeting a specific residue, typically serine, threonine or tyrosine and transferring a phosphate group from another molecule such as Adenosine-5'-triphosphate (ATP). Phosphorylation is a reversible procedure, with phosphatases removing phosphate groups from the target protein, which can then either cycle through another phosphorylation de-phosphorylation cycle or be degraded.

Ubiquitination is the process whereby a small ubiquitin protein or proteins are conjugated to a protein in a three step process. The ubiquitin molecule is first activated by an E1 ubiquitin-activating enzyme which, as above, is dependent upon ATP mediated activity. This activated ubiquitin molecule is then conjugated to the lysine residue of the target protein by an E2 ubiquitin-conjugating enzyme, which is then ligated in place by an E3 ubiquitin-ligase enzyme. Again, as above the process is fully reversible under the activity of de-ubiquitinating enzymes. It was traditionally thought that ubiquitination was purely a means for a cell to target unwanted proteins for degradation in the proteasome mediated by the formation of *Lys48*[1] linked chains of ubiquitin molecules on proteins. However more recently the ability of ubiquitin to form *Lys63* linked chains has demonstrated a remarkable capacity to affect numerous cell processes. It is now thought that these chains can play a key role in maintaining protein stability, assisting in protein-protein binding and facilitating conformational changes within target proteins (Adhikari and Chen, 2009).

Throughout this project I have used phosphorylation as a marker of protein activation in response to stimulation. I do not analyze ubiquitination within this system, although its relevance at several key points is discussed. By analyzing the phosphorylation response to stimulation, and by measuring the impact of

[1] *As well as Lys6, 11, 27, 29 and 33.*

signalling protein inhibition I hope to be able to construct a signalling cascade relevant to fibrosis in the lung.

1.3.1 Transforming Growth Factor Beta 1

The cytokine TGF-β1 was first described in 1983, when it was isolated from platelets in its active form (Assoian et al., 1983), and it is now thought that the majority of cells are capable of its expression, including in the lung; epithelial (Xu et al., 2003), mesenchymal and immune cells (Zhang et al., 1995). Encoded by the *TGFB1* gene an initial 75 kDa *pro*-TGF-β1 protein is created which forms a homodimer. This homodimer is then cleaved into an active 48 kDa TGF-β1 dimer, and a 100 kDa latency associated protein (LAP) which immediately binds with and inhibits the function of TGF-β1. This LAP protein then associates with a latent-TGF-β1 binding protein which localizes the LAP and bound TGF-β1 to the cell membrane. The majority of TGF-β1 exists in this form and cleavage from LAP is required before signalling can be induced (Annes, 2003; Shi et al., 2011)

Factors such as MMP-2 and 9 are able to cleave LAP and liberate free TGF-β1 which can then induce the canonical mothers against decapentaplegic (SMAD[2]) signalling response. TGF-β1 binds to a TGF-β Receptor 2 (TGF-R2) dimer inducing a conformational change, which allows for the recruitment of two TGF-β Receptor 1 (TGF-R1) molecules. The binding of TGF-R1 with TGF-R2 activates the innate kinase activity of TGF-R1, and also recruits a chaperone protein such as SMAD anchor for receptor activation (SARA) although others have also been described, which holds SMAD3 inactive in the cytoplasm (Xu et al., 2000). SARA facilitates the phosphorylation of SMAD3 by TGF-R1, the phosphorylated SMAD3 is then released from SARA and is able to form a heterodimer with SMAD4; or a heterotrimer with either SMAD2 or another SMAD3 protein, and SMAD4 (Chacko et al., 2001; Wu et al., 2001). This molecule is transcriptionally active and is able to translocate to the nucleus (Derynck and Zhang, 2003).

[2] *A compression of MAD, the* Drosophila melanogaster *homolog, and SMA, the* Caenorhabditis elegans *homolog.*

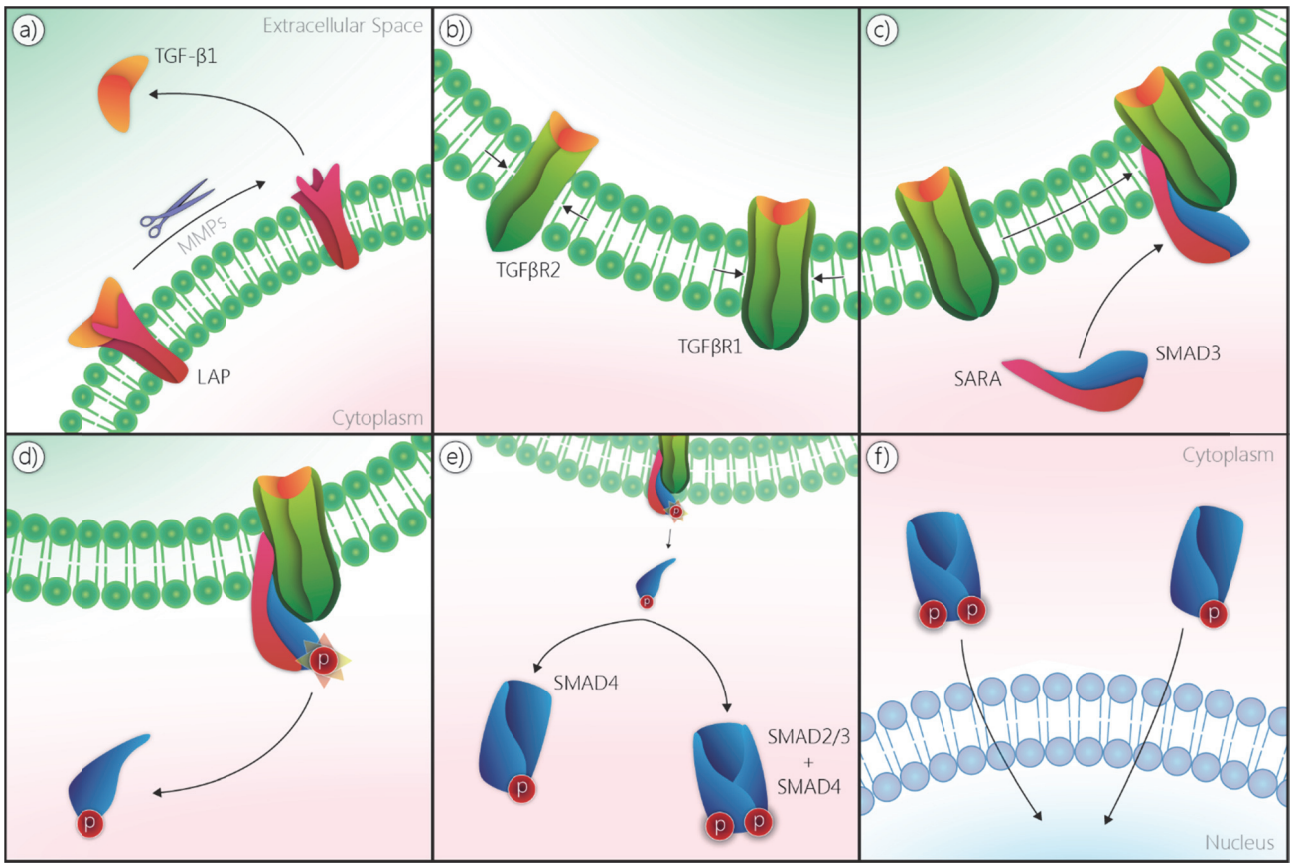

Figure 7 - TGF-β1 signalling mechanism

A TGF-β1 dimer is held inactive at the membrane by LAP **a)** under the action of proteases it is cleaved from LAP becoming signalling competent. TGF-β1 binds to a TGFβR2 dimer **b)** which imitates a conformational change in TGFβR2 allowing TGFβR1 to bind. SARA holds SMAD 3 inactive in the cytoplasm **c)**, upon the formation of a TGFβR1/ TGFβR2 heterotetramer SARA associates with TGFβR1. SARA presents SMAD3 to the kinase site on TGFβR1 **d)**, which phosphorylates SMAD3, which then dissociates from SARA. Phosphorylated SMAD3 is then free to form a heterodimer with SMAD4 **e)** or a heterotrimer with another SMAD2/3 molecule and SMAD4. This association forms a transcriptionally active unit **f)** which can translocate to the nucleus and influence transcription.

In a chronic wound environment, it is believed that constant TGF-β1 expression, combined with the high dissociation constant, a measure of ligand receptor binding efficacy, of TGF-β1 and its receptors, induces fibroproliferation in the wound area, an increased recruitment of fibrocytes and also drives EMT (Frolik et al., 1984).

A major role for TGF-β1 in IPF is now widely accepted, demonstrated through transient expression of TGF-β1 in rat (Sime et al., 1997) and mouse (Gauldie et al., 2007) lungs to produce a severely fibrotic lung, with inhibition of TGF-β1 through SMAD3 knockout blocking this development (Gauldie et al., 2007). Studies of human bronchoalveolar lavage (BAL) have detected elevated levels of TGF-β1 in the IPF lung (Hiwatari et al., 1997).

A similar role for TGF-β1 has been demonstrated in OB as well, with elevated levels of TGF-β detected in the airway and lung tissue associated with, and shown to precede the development of OB (El-Gamel et al., 1999), as well as increased levels detected in the BAL of patients (Elssner et al., 2000). A similar role for SMAD3 has also been described. Using primary fibroblasts isolated from the trachea of either wild-type or SMAD3 deficient mice, SMAD3 deficient fibroblasts did not up-regulate expression of mesenchymal markers in response to TGF-β1 (Ramirez et al., 2006). Previous work performed in our laboratory has also described a similar SMAD3 dependant effect on EMT in primary human bronchial epithelial cells (Borthwick et al., 2009, 2010).

1.3.2 Tumour Necrosis Factor Alpha

The inflammatory cytokine TNFα was first described in 1975 and named for its ability to selectively induce necrosis in transplanted sarcomas in mice (Carswell et al., 1975). The same paper also postulated that the release of TNFα was attributable to macrophages, which was later confirmed in a different paper (Matthews, 1978). Although primarily produced in alveolar macrophages in the lung (Nii et al., 1993) TNFα is also produced by numerous other cells, including resident fibroblasts (Bashir et al., 2009) (only demonstrated in skin fibroblasts) and epithelial cells (Miyazaki et al., 1995).

Encoded by the gene *TNFA* TNFα is produced as a 26 kDa membrane bound protein which associates into homotrimers. This membrane-associated homotrimer can be cleaved by the activity of TNFα converting enzyme (TACE) into a soluble homotrimer composed of 17 kDa molecules. TNFα signals through two distinct trans-membrane receptors, TNF Receptor 1 (TNFR1) and TNF Receptor 2 (TNFR2) (Locksley et al., 2001). TNFR1 is ubiquitously expressed and can respond to both membrane-bound and soluble forms of TNFα whereas TNFR2 is highly regulated in its expression, mainly on immune cells and responds, efficiently, only to membrane bound TNFα (Grell et al., 1995).

The canonical signalling pathway driven by TNFα has been extensively investigated in response to TNF-R1 activation which induces a signalling cascade through NF-κB. TNF-R1 recruits TNF-receptor-associated factor 2 (TRAF2) (Rothe et al., 1994) along with E3 ubiquitin-ligases forming a complex which polyubiquitinates the receptor interacting protein kinase 1 (RIP1) (Ea et al., 2006) as well as TRAF2 itself in a *Lys63* dependant manner. This complex then aids phosphorylation of transforming growth factor beta

activated kinase 1 (TAK1[3]), again through poly-ubiquitination of TAK1 and associated TAK1 associated binding protein (TAB) proteins (Shim et al., 2005; Yang et al., 2011). Activated TAK1 then phosphorylates the kinase components of the IκB kinase (IKK) complex which is composed of three subunits, the regulatory IKKγ and the catalytic IKKα and IKKβ (Wang et al., 2001). The IKK complex binds with Iκ-Bα, a protein which holds NF-κB in the cytoplasm (Jacobs and Harrison, 1998), phosphorylates it and targets it for degradation in the proteasome. The NF-κB dimer, composed from five possible monomers p105[4], p100[5], p65[6], RelB and c-Rel, is then free to translocate to the nucleus and influence transcription. There are numerous levels of processing, activation and regulation that occur throughout this signalling cascade which are covered more elegantly in the following review by Perkins (Perkins, 2007).

[3] *MAP3K7*
[4] *NF-κB1, p105 can be cleaved to p50, but mainly transcribed independently*
[5] *NF-κB2, p100 cleaved to p52*
[6] *RelA*

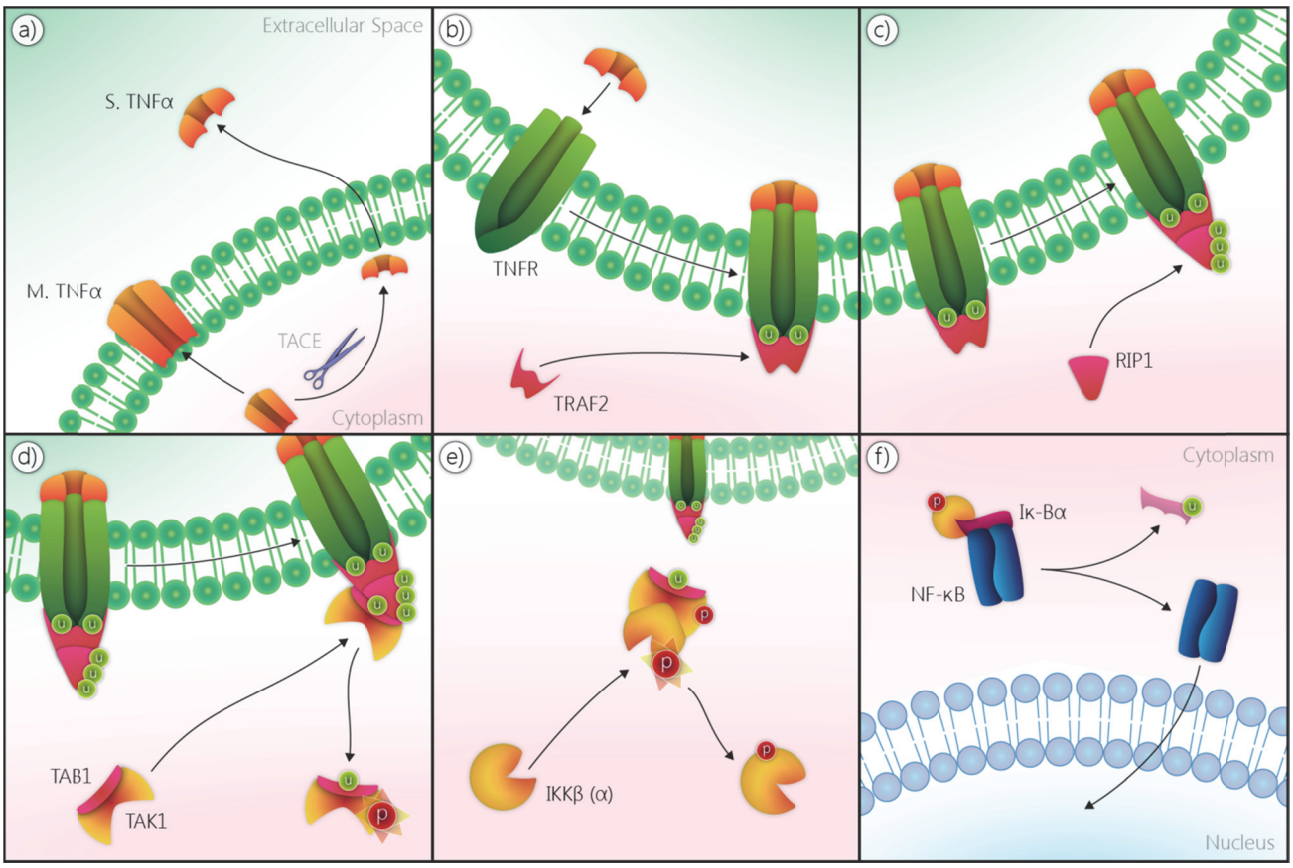

Figure 8 - TNFα signalling mechanism

A TNFα trimer is produced as a membrane associating protein which can interact with both TNFR1 and TNFR2 **a)**, the proteolytic activity of TACE can cleave this TNFα producing a soluble form which interacts efficiently only with TNFR1. Upon binding of TNFα both TNFRs recruit TRAF2 which is polyubiqitinated by E3 ubiquitin ligases **b)**, these polyubiqutin chains facilitate the association of other proteins within the receptor complex. RIP1 is recruited to the receptor complex and is itself polyubiqitinated **c)**. This complex is then capable of recruiting a TAK1-TAB1, TAB1 is polyubiqitinated **d)** and this stimulates the autophosphorylation of TAK1, activating it as a kinase. TAK1 is capable of binding with the IKK group **e)**, and activating its kinase ability, specifically that of IKKβ. IKK binds with Iκ-Bα, holding NF-κB inactive in the cytoplasm, phosphorylating it and thus targeting it for ubiquitin mediated degradation in the proteasome. This frees NF-κB allowing it to translocate to the nucleus and influence transcription **f)**.

It is well recognized in clinical practice that OB is often first diagnosed or progresses more rapidly following a significant episode of acute inflammation or airway injury and that inflammatory cytokine producing T-cells, are elevated in the bronchoalveolar lavage and blood of patients with OB (Hodge et al., 2009). It has been demonstrated in rats that the development of obliterative airway disease is associated with a significant elevation in TGF-β1 and TNFα levels prior to the development of fibrosis and that blockade of TNFα significantly inhibits OB in this model (Farivar et al., 2005). Although it is worth mentioning that neither of these studies address the potential split in OB classification, with both

seeming to refer to the chronic, early onset neutrophilic response, nor provide direct evidence of elevated TNFα in the lungs of patients with OB. An inflammatory response is still associated with the later onset disease but it is less severe.

The contribution of inflammation to the development of IPF is still under debate. On the one hand an increased number of macrophages are often found in the alveoli of IPF patients and from this it was hypothesized that these macrophages were contributing to a non-resolving pro-inflammatory milieu (ATS, 2000). As such the current treatment practice is to deliver anti-inflammatory drugs, such as corticosteroids, cyclophosphamide, cyclosporine or pirfenidone, to the lung (ATS, 2000). This hypothesis was challenged by the lack of strong clinical trials showing a benefit from treatment with any of these drugs, although some slight positive trends were observed (Gharaee-Kermani et al., 2007). As well an inability to detect inflammatory markers themselves *in situ* throughout disease progression. It however is worth noting that the lack of strong clinical trials may be due to the ethical constraints of offering a placebo treatment to patients with a rapidly progressing disease. As such, some people now think of inflammation as an effect of IPF and not a driver as such. Conversely, the TNFA-308G>A polymorphism, which has previously been reported to produce elevated free TNFα levels in sarcoidosis patients (Sharma et al., 2008), was also found to be associated with IPF patients (Riha et al., 2004), suggesting that our understanding of the role of inflammation in IPF is still significantly lacking.

1.3.3 Interleukin-1 Beta

The inflammatory cytokine IL-1β was first described in 1972 (Gery et al., 1972) for its ability to activate lymphocytes , but it was not until later that it was differentiated from IL-1α as a protein secreted from macrophages (March et al., 1985).

Encoded by the gene *IL1B* IL-1β is produced as an inactive 31 kDa protein which is converted into an active 17 kDa molecule by numerous proteinases. Mast cell chymase and tryptase (Black et al., 1989) being the first described although it was later shown IL-1β converting enzyme (ICE) as the primary proteinase (Thornberry et al., 1992). Interestingly whilst many cells, such as fibroblasts, are able to produce the pre-cursor form of IL-1β they lack the ability to produce the proteinases which activates it (Kostura et al., 1989). It is possible for the airway macrophages to secrete proteinases that have been shown to cleave inactive IL-1β extracellularly, albeit in a skin and not lung model. IL-1β binds to IL-1 receptor type 1 (IL-1R1) which recruits IL-1R accessory protein, which is required for transmission of the signal (Wang et al., 2010).

This activation triggers the recruitment of myeloid differentiation primary-response protein 88 (MyD88) to the intracellular portion of the receptor complex, which in turn recruits IL-1R-associated kinase 4 (IRAK4). IRAK4 is then able to recruit and activate ,through phosphorylation, IRAK1; this phosphorylation allows for the recruitment of TRAF6, a homolog of the previously described TRAF2, which interacts with TAK1 in a similar fashion (Akira and Takeda, 2004). At which point the remaining signalling mechanism is conserved with that of TNFα, although evidently there is some form of modulation allowing for the occurrence of different signalling events.

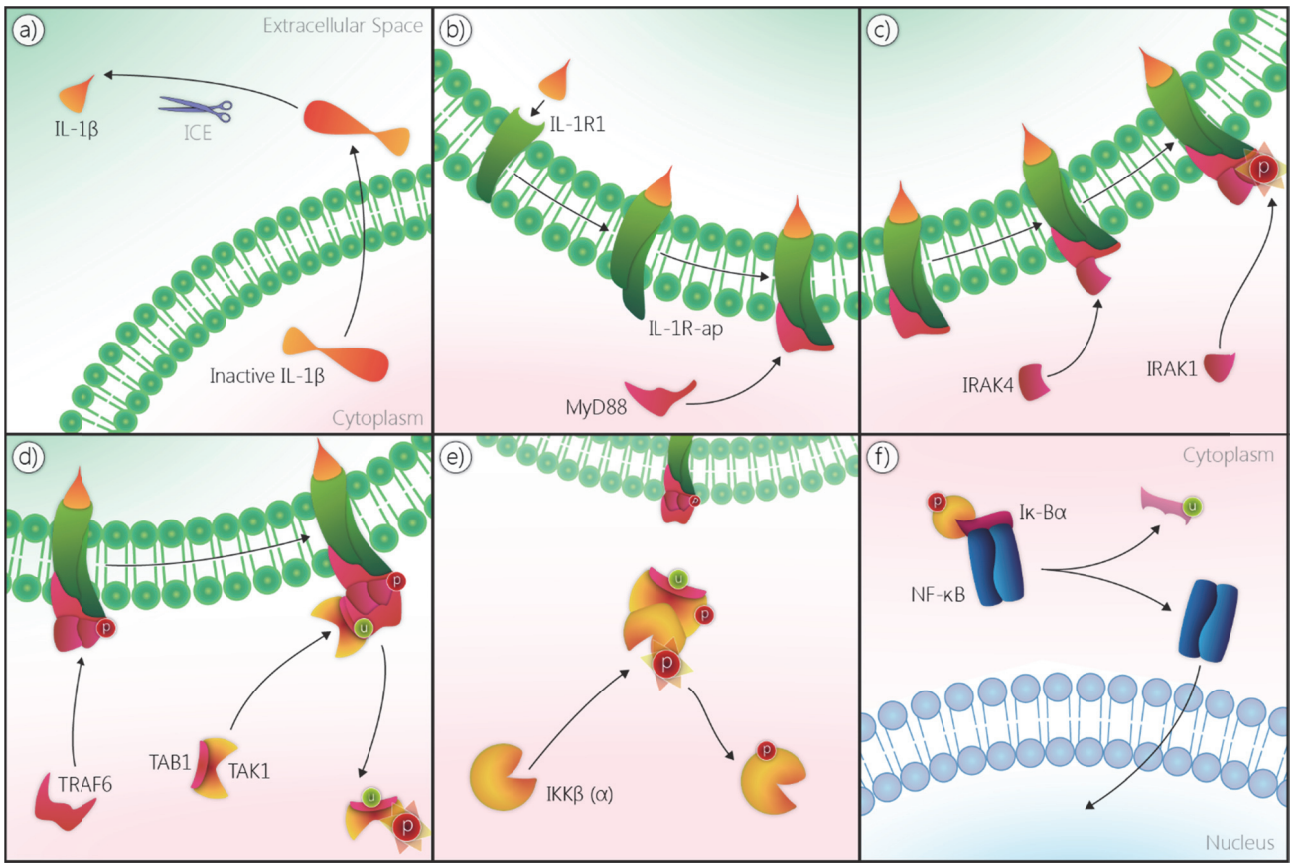

Figure 9 – IL-1β signalling mechanism

IL-1β is produced and can be secreted in an inactive form; it is cleaved by the activity of ICE **a)**, predominately sourced from pulmonary macrophages. IL-1β binds to IL-1R1 which recruits IL-1R accessory protein **b)** in order to facilitate signal transduction within the cell. This receptor complex recruits MyD88 to the intracellular portion of the receptor complex. IRAK4 is recruited to the receptor complex **c)**, which in turn recruits and phosphorylates IRAK1. Phosphorylated IRAK1 recruits TRAF6 **d)**, a homolog of TRAF2 which can recruit TAK1-TAB1, TAB1 is polyubiqitinated and this stimulates the autophosphorylation of TAK1, activating it as a kinase. TAK1 is capable of binding with the IKK group **e)**, and activating its kinase ability, specifically that of IKKβ. IKK binds with Iκ-Bα, holding NF-κB inactive in the cytoplasm, phosphorylating it and thus targeting it for ubiquitin mediated degradation in the proteasome. This frees NF-κB allowing it to translocate to the nucleus and influence transcription **f)**.

As with TNFα the contribution of IL-1β to the development of IPF is poorly understood. Transient expression of IL-1βin the epithelium of rats led to signs of acute inflammation, followed by expression of TGF-β1 and the development of fibrosis (Kolb et al., 2001), with administration of an IL-1R1 antagonist reducing the development of fibrosis in a mouse bleomycin model (Piguet et al., 1993). To my knowledge, no data has been presented showing elevated levels of IL-1β, from any source, in relation to IPF. The only study which seemingly investigates this found no increase, in IL-1β in the BAL of IPF patients, but did demonstrate a reduction in the production of IL-1R1 antagonist (IL-1R1A), which would elevate the inflammatory potential of IL-1β (Mikuniya et al., 1997). It was also shown there was no

variation in receptor expression between IPF and control patients, and there is the aforementioned poor response of IPF to existing anti-inflammatory treatments. More recently, studies have associated polymorphisms within *IL1RN* the gene encoding for IL-1R1A that result in a reduction in mRNA expression with IPF. The authors suggesting that drugs such as anakinra that mimics IL-1R1As activity, and has previously been used in other inflammatory disorders may be of use in IPF (Korthagen et al., 2012).

In OB a significant increase in the levels of IL-1β in the BAL of patients has been described in one study (Vanaudenaerde, De Vleeschauwer, et al., 2008), yet confusingly in another study not only was this effect not replicated, but an increase in the inhibitory IL-1R1A was described instead (Belperio et al., 2002). Although in both cases the authors link their findings with development of disease, in the first instance by hypothesising that the increased inflammation would lead to excessive fibrosis, and in the second by suggesting the anti-fibrotic effects of the inflammatory response were being blocked. Neither of these papers refer to the current debate about the dual forms of OB disease characterisation that may account for their differing findings. One study which investigated this effect, albeit with a small sample size, described an increase in IL-1β detected in the BAL in the early onset neutrophilic form of OB, with no change detected in the late onset form of the disease (Verleden et al., 2011).

1.3.4 Mitogen Activated Protein Kinase Cascade

The previous sections have described the canonical signalling responses of TGF-β1, TNFα and IL-1β, however these molecules also induce other non-canonical signalling responses. One common alternative signalling pathway, which can be activated by all three stimuli, is the mitogen activated protein kinase (MAPK) cascade. Although describing this cascade as common is perhaps a misnomer due both to the breadth of components contained within, and the variety of interactions possible.

There are several families of MAPKs, and of these there are three that are well described. The extracellular signal related kinases (ERK)-1/2 were described first, followed quickly by the c-Jun N-terminal kinases (JNK)-1/2 and p38 families. Each MAPK is activated by dual phosphorylation of a threonine and tyrosine residue separated by a single amino acid. For ERK-1/2 this is glutamate, for JNK-1/2 a proline and p38 gylcine. Once activated these MAPKs can, through the activity of transcription factors such as activating protein 1 (AP-1) or activating transcription factor 1/2 (ATF-1/2), alter gene expression.

The traditional view of MAPK activation is that a signal induces activation of an upstream MAP3K (MAP kinase kinase kinase), which in turn activates a MAP2K and in turn the requisite MAPK. Each MAPK can be activated by several MAP2Ks that can in turn be activated by several MAP3Ks that creates a system with redundancy built in, whilst also facilitating a wide array of outcomes based on the exact signalling input. For example at least four MAP3Ks have been implicated in the activation of JNK-1/2 in response to stimulation by TNFα or IL-1β, with some of these same MAP3Ks being involved in the non-canonical TGF-β1 response. Adding another layer of complexity is that signalling responses are often not conserved between different cell types, for example the MAP3K MEKK1 was required for activation of JNK-1/2 by TNFα in embryonic stem cells (Xia, 2000), but not in fibroblasts (Yujiri, 1998). I cover the specific activities of each MAPK in more detail in the results chapters dealing with each protein, but the review by Rubinfeld *et al* covers the activation and response of each in more detail (Rubinfeld and Seger, 2005).

1.3.5 Synergistic Response

Recently our group and others have shown that TGF-β1 can drive EMT in primary bronchial epithelial cells (PBEC)s (Ward et al., 2005; Hackett et al., 2009), and that inflammatory stimuli such as TNFα and IL-1β can accentuate this effect (Borthwick et al., 2009, 2010; Câmara and Jarai, 2010). However, the signalling mechanisms that underpin this synergistic effect are unknown; and a greater understanding of their interactions is required. TGF-β1, TNFα and IL-1β are all pleiotropic in nature and they often display apparently conflicting effects.

TGF-β1 has strong pro-fibrotic effects and it can also act as a potent suppressor of the immune response, conversely TNFα displays strong inflammatory abilities alongside anti-fibrotic abilities, and yet the presence of both is seen as key in OB and implicated in IPF. Evidently, there is some mechanism that is overriding the conflicting effects of TGF-β1 and TNFα, and by referring back to the chronic wound theory outlined in **1.2.1** it is possible to see how such a mechanism could arise. The immune response usually tails off post clearance of the initiating factor, however if this factor is un-clearable for example in allergic responses, in response to chronic infection or a repeated injury from industrial particulates then this response may be maintained.

Studies have demonstrated that TNFα is capable of increasing the transcription of TGF-β1, as well as stabilising TGF-β1 mRNA *in vitro*, these findings were confirmed *in vivo* in a study whereby transient

over-expression of TNFα induced an increase in detected TGF-β1 and a subsequent development of fibrosis (Sime et al., 1998). However in an alternative study, mice over expressing TNFα in the lung were shown to develop less severe pulmonary fibrosis in response to bleomycin, or when TGF-β1 was also over-expressed (Fujita et al., 2003). It was then postulated that it may be the type of TNFα present that determines whether a fibrotic response is initiated.

Using transgenic mice it was demonstrated that the membrane bound un-processed form of TNFα could generate an inflammatory response *in vivo* but that a subsequent fibrotic response did not occur, whereas the soluble cleaved form of TNFα induced both an in inflammatory and fibrotic response. The same study also demonstrated that the source of this soluble TNFα that drove TGF-β1 and fibrosis was the airway epithelium itself (Oikonomou et al., 2006). It is not known what type of TNFα was predominantly produced in the study which demonstrated TNFα induced bleomycin resistance, as TNFα production was not assessed, however previous studies using the same model measured TNFα in the BAL by ELISA suggesting that at least some soluble TNFα was produced.

Other differences between the models include the uses of a transient TNFα expression with a positive effect on fibrosis, whereas permanent expression inhibited the development of fibrosis. This may indicate that continuous inflammation can inhibit the initiation of fibrosis, whereas pulsed occurrences of TNFα accentuate rather than inhibit the already occurring fibrotic response. The detected levels of TNFα also differed slightly between the two models with the transient model peaking at approximately 150ng/mL, and the permanent model at 90ng/mL of TNFα, although it seems unlikely that such a small variation would produce such a difference in response.

A mechanism whereby TGF-β1 induces the production of TNFα has not been described however, with several studies describing the inhibition of TNFα by TGF-β1 (Vaday et al., 2001; Yu et al., 2009). Together all these studies demonstrate how poorly understood the interplay between TGF-β1 and TNFα is, and demonstrates that a wide variety of other factors play a role in determining what occurs.

1.4 Hypothesis, Aims & Objectives

I propose that the development of fibrosis in OB is at least partially facilitated by a dysregulated wound healing response initiated by a non-resolving, but not continuous, pro-inflammatory milieu within the airway or alveoli which induces a pro-fibrotic response. That this dysregulated wound response manifests itself as EMT, with the airway lining losing its epithelial character and gaining a motile, pro-fibrotic mesenchymal character; an effect which is driven by TGF-β1 and accentuated by inflammatory mediators such as TNFα. That the accentuative effect of TNFα on TGF-β1 driven EMT in the airway epithelium is mediated by a protein (or proteins) which hyper-activates existing signalling pathways or activates a novel signalling cascade.

1.4.1 Aims

- To isolate PBECs from stable lung transplant recipients by bronchial brushing.
- To culture these cells in a submerged system and use this system to model the fibrotic and inflammatory milieu present in OB.
- To observe and quantify the onset and development of EMT within this system.
- To unpick the signalling events involved in the onset and development of EMT.

1.4.2 Objectives

- Utilise previously described PBEC isolation and culture methods to establish sufficient cell stocks.
- Induce EMT within these cultures by the addition of recombinant human TGF-β1 or TNFα; observe the morphological changes and measure the changes in protein expression associated with EMT.
- Disrupt the function of key proteins within the TGF-β1 and TNFα signalling cascades by chemical inhibition and siRNA mediated knockdown, and measure the impact of this disruption on EMT.
- Assess the phosphorylation of proteins within the TGF-β1 and TNFα signalling cascades to determine which if any proteins play a key role.

2 Materials & Methods

All experimental procedures were conducted in compliance with Newcastle University and Institute of Cellular Medicine Safety Policy according to the Control of Substances Hazardous to Health (COSHH) regulations. All tissue culture work was undertaken at Containment Level 2 using standard aseptic techniques.

2.1 Materials

All reagents were sourced directly through the relevant suppliers and COSHH regulations were followed throughout their usage.

2.1.1 Cell Lines

Throughout this project wherever possible I have tried to use primary human cells as due to their un-transformed nature I feel that they are a more relevant model in which to investigate physiological effects. However in some instances due to the requirement for either large cell numbers or a high protein yield it has been necessary to use an alternative cell line population.

2.1.1.1 A549

A549 cells were derived from an explanted lung tumour isolated from a 58 year old male in 1972. They were described as having characteristic multilamellar bodies in the cytoplasm and a high level surfactant protein synthesis from which it was concluded that they are a good model for type II pneumocyte cells. The cell line is predominately hypotriploid with a modal chromosome number of 66 although other frequencies do occur (Giard et al., 1973; Lieber et al., 1976).

2.1.2 Media

Reagent	Supplier	Cat. #	Volume (mL)
Dulbeco's Modified Eagle Medium (DMEM) for A549 Cells			
Dulbeco's Modified Eagle Medium (DMEM)/F-12 Ham	Sigma	D6421	500
Foetal Calf Serum	Sigma	12133C	50
Penicillin (100 units/mL)/Streptomycin (1mg/mL)	Sigma	P4333	5
L-Glutamine	Sigma	G7513	5
Roswell Park Memorial Institute-1640 (RPMI)			
Roswell Park Memorial Institute-1640	Sigma	R0883	500
Foetal Calf Serum	Sigma	12133C	50
Penicillin (100 units/mL)/Streptomycin (1mg/mL)	Sigma	P4333	5
L-glutamine	Sigma	G7513	5
Roswell Park Memorial Institute-1640 (SAGM)			
Small Airway Growth Medium	Lonza	CC-3119	500
Bovine Pituitary Extract			
Hydrocortisone			
Human Epidermal Growth Factor			
Epinephrine			
Insulin			
Triiodothyronine,	Lonza	CC-3118	Kit form
Transferrin			
Gentamicin/Amphotericin-B			
Retinoic Acid			
Bovine Serum Albumin			
Penicillin (100 units/mL)/Streptomycin (1mg/mL)	Sigma	P4333	5

Table 2 - Media Composition

2.1.3 Solutions

Reagent	Supplier	Cat. #	Concentration (M)
TBS-Tween (pH 7.6)			
Trizma Base	Sigma	T1503	0.05
NaCl	Sigma	S3014	0.15
Polysorbate-20 (Tween-20)	Sigma	44112	0.005
-In dH_20			

Table 3 - General Solutions

Reagent	Supplier	Cat. #	Concentration (M)
Denaturing Lysis Buffer			
Sodium Dodecyl Sulphate	Sigma	L3771	0.0034
Ethylenediaminetetraacetic acid	Sigma	EDS	0.005
β-mercaptoethanol (added just prior to use)	Sigma	M3148	0.1
- In dH_20			
Non-denaturing Lysis Buffer			
Trizma HCL	Sigma	T3253	0.02
NaCl	Sigma	S3014	0.140
Glycerol	Sigma	G5516	0.1
Triton X-100	Sigma	T9284	0.01
Ethylenediaminetetraacetic acid	Sigma	EDS	0.002
- In dH_20			

Table 4 - Immuno-precipitation Solutions

Reagent	Supplier	Cat. #	Concentration (M)
Zymography Buffer 1			
Triton-X 100	Sigma	T9284	0.025
Zymography Buffer 2 (ph 7.5)			
Trizma Base	Sigma	T1503	0.05
$CaCl_2$	Sigma	C1016	0.005

Table 5 - Zymography Solutions

Reagent	Supplier	Cat. #	Concentration (M)
Resolving Buffer (pH 8.8)			
Trizma Base	Sigma	T1503	1.5
- In dH_20			
1x Stacking Buffer (ph 6.8)			
Trizma Base	Sigma	T1503	0.5
- In dH_20			
10x Running Buffer (pH 8.3)			
Trizma Base	Sigma	T1503	0.25
Glycine	Sigma	G8898	1.92
Sodium Dodecyl Sulphate	Sigma	L3771	0.034
- In dH_20			
Sample Loading Buffer			
Trizma HCL	Sigma	T3253	0.0625
Glycerol	Sigma	G5516	2
Sodium Dodecyl Sulphate	Sigma	L3771	0.034
Bromophenol Blue	Sigma	114391	0.0005
β-mercaptoethanol (added just prior to use)	Sigma	M3148	0.01
- In dH_20			

Table 6 - SDS-PAGE Solutions

Reagent	Supplier	Cat. #	Concentration (M)
Transfer Buffer			
Trizma Base	Sigma	T1503	0.25
Glycine	Sigma	G8898	1.92
- In dH_20			
Stripping Buffer			
Trizma HCl	Sigma	T3253	0.0625
Sodium Dodecyl Sulphate	Sigma	G8898	0.07
β-mercaptoethanol (added just prior to use)	Sigma	M3148	0.1

Table 7 - Western Blotting Solutions

2.1.4 Antibodies

Target	Supplier	Cat. #	Technique	Dilution
TAK1	Cell-Signalling	4505	Western Blot ICC/IHC Immuno-Precipitation	1:1000 1:100 1:87
*p*TAK1 (*Thr184*)	Cell-Signalling	4537	Western Blot ICC/IHC Indirect ELISA	1:1000 1:100 1:5000
*p*TAK1 (*Thr187*)	Cell-Signalling	4536	Western Blot ICC/IHC Indirect ELISA	1:1000 1:100 1:5000
TAB1	Cell-Signalling	3226	Western Blot	1:1000
TAB2	Cell-Signalling	3745	Western Blot	1:1000
TAB3	Abcam	ab85655	Western Blot	1:1000
SMAD3	Abcam	ab29379	Western Blot ICC/IHC Immuno-Precipitation	1:3000 1:100 1:128
*p*SMAD3 (*Ser423/425*)	Abcam	ab52903	Western Blot ICC/IHC Indirect ELISA	1:1000 1:100 1:10000
JNK-1/2	Cell-Signalling	9252	Western Blot ICC/IHC Immuno-Precipitation	1:1000 1:100 1:69
*p*JNK-1/2 (Both *Thr183/Tyr185*)	Cell-Signalling	4668	Western Blot ICC/IHC Indirect ELISA	1:1000 1:100 1:4000
c-Jun	Cell-Signalling	9165	Western Blot	1:500
*p*c-Jun (*Ser63*)	Cell-Signalling	2361	Western Blot	1:250
p38	Santa-Cruz	sc-7149	Western Blot	1:1000
*p*p38 (*Thr180/Tyr182*)	Santa-Cruz	sc-17852	Western Blot	1:500
ERK-1/2	Cell-Signalling	4695	Western Blot	1:1000
*p*ERK-1/2 (*Thr202/Tyr204 & Thr185 & Tyr187*)	Cell-Signalling	4370	Western Blot	1:500
IKKα/β	Santa-Cruz	sc-7607	Western Blot Immuno-Precipitation	1:2000 1:178
*p*IKKα/β (*Ser176/180 & Ser177/181*)	Cell-signalling	2697	Western Blot Indirect ELISA	1:1000 1:5000
Iκ-Bα	Santa-Cruz	sc-1643	Western Blot	1:1000
*p*Iκ-Bα (*Ser32 & Ser36*)	Cell-Signalling	9246	Western Blot	1:500

Table 8 - Antibodies

Target	Supplier	Cat. #	Technique	Dilution
E-cadherin	BD Bioscience	610181	Western Blot ICC/IHC	1:3000 1:100
ZO-1	Santa-Cruz	sc-10804	Western Blot ICC/IHC	1:1000 1:100
Cytokeratin-14	Santa-Cruz	sc-6278	Western Blot ICC/IHC	1:2000 1:100
Cytokeratin-17	Santa-Cruz	sc-6278	Western Blot ICC/IHC	1:2000 1:100
Cytokeratin-19	Santa-Cruz	sc-6278	Western Blot ICC/IHC	1:2000 1:100
CCSP	Abcam	ab40873	Western Blot ICC/IHC	1:500 1:100
AQP-4	Abcam	ab11026	Western Blot ICC/IHC	1:1000 1:100
SP-B	Abcam	ab3282	Western Blot ICC/IHC	?
αSMA	Abcam	ab32575	Western Blot ICC/IHC	1:2000 1:100
Fibronectin	Sigma	F3648	Western Blot ICC/IHC	1:4000 1:100
Vimentin	Santa-Cruz	sc-6260	Western Blot ICC/IHC	1:500 1:100
β-actin	Sigma	A2228	Western Blot ICC/IHC	1:4000 1:100
Ran	Cell-signalling	4462	Western Blot	1:1000
Pan-IgG	Abcam		Immuno-Precipitation	1:84

Table 8 continued - Antibodies

2.1.5 Cytokines & Growth Factors

Recombinant human cytokines were delivered to cells directly in serum containing media. Effect on EMT was assayed by western blot for endpoint markers at 72 hours post stimulation with phosphorylation response assayed 30 minutes post stimulation. A dose response curve of for each cytokine and pro-fibrotic pro-inflammatory combination was performed in A549 cells assaying for cell viability, growth and morphology and efficacy of inhibition on EMT.

Cytokine	Source	Supplier	Cat. #	Final Concentration (µg/ml of media)
TGF-β1	Chinese Hamster Ovary cells	Peprotech	100-21C	10ng/mL
TNFα	*Escherichia coli*	Invitrogen	PHC3011	20ng/mL
IL-1β	*Escherichia coli*	Invitrogen	PHC0814	20ng/mL

Table 9 - Recombinant Cytokines

2.1.6 Chemical Inhibitors

Chemical inhibitors were delivered to cells 1 hour prior to stimulation. Efficacy of effect was assayed by western blot for EMT endpoint markers at 72 hours post stimulation with phosphorylation response assayed 30 minutes post stimulation. A dose response curve of for each chemical inhibitor was performed in A549 cells assaying for cell viability, growth and morphology and efficacy of inhibition on EMT.

Target	Inhibitor	Supplier	Cat. #	Final Concentration (µM)
SMAD3	Specific Inhibitor of SMAD3	Calbiochem	566405	10
IKKβ	IKK-2 Inhibitor IV	Calbiochem	401481	5
p38	SB 203580	Calbiochem	559389	10
ERK-1/2	FR180204	Calbiochem	328007	5
JNK-1/2	SAPK Inhibitor II	Calbiochem	420119	5
TAK1	(5Z)-7-Oxozeaenol, *Curvularia* sp.	Calbiochem	499610	1

Table 10 - Chemical Inhibitors

2.1.7 Small Interfering RNA

siRNA was delivered to PBECs with HiPerfect lipid transfection reagent (Qiagen: #301705) 24 hours prior to stimulation. Efficacy of siRNA knockdown was assessed by probing for the total form of the protein 24, 48, 72 and 96 hours after transfection, and the impact on detected phosphorylation was also assessed at an appropriate time point after stimulation with TGF-β1 and TNFα.

A scrambled siRNA was used as a negative control in all experiments, the same concentration and dose of transfection reagent of the respective siRNA was used in each instance. A dose response curve of scramble siRNA only, lipid only and scramble siRNA with lipid was performed when first optimising transfection of PBECs assaying for cell viability, growth and morphology.

Target	Sequence	Supplier	Cat. #	Concentration (nM)
SMAD3	ATCAAGGGATTTCCTATGGAA	Qiagen	SI00082481	5
IKKβ	CTGGAGAAGTACAGCGAGCAA	Qiagen	SI02777376	0.1
JNK-1	GTGGAAAGAATTGATATATAA	Qiagen	SI02757209	5
JNK-2	GCCGUCCUUUUCAGAACCAT	Qiagen	SI00300797	10
TAK1	AAGATGGTATATACCAAGTTA	Qiagen	SI02758763	3
Scramble	Proprietary	Qiagen	SI03650318	As per experiment

Table 11 - siRNAs

2.2 Cell Isolation, Culture & Treatment

2.2.1 A549 Cell Line Culture

A549 cells were cultured on un-coated plastic tissue culture vessels or un-coated glass coverslips for immunocytochemistry, in DMEM media. Cells were passaged upon reaching approximately 90% confluence. To passage, cells were washed once with sterile 1x PBS before trypsin (Sigma: #T3924), pre-warmed to 37°C, was added to the culture vessel. Cells were incubated for approximately 5 minutes until the majority had lifted off from the surface, the trypsin was then neutralized with an equal volume of FCS containing DMEM media. Cells were pelleted by centrifugation at 250 x g for 4 minutes and the supernatant was discarded. The cell pellet re-suspended in fresh DMEM and plated according to experimental parameters

2.2.2 Primary Sample Isolation & Culture

All Human Tissue Act regulations and European Union Tissue and Cells Directives were adhered to. I would like to thank Drs Malcolm Brodlie, Laura MacKay, Elizabeth Moisey, Danai Karamanou and Nicola Green, as well as Gail Johnson, Kasim Jiwa and Dr Chris Ward and all the transplant staff at the Freeman Hospital for taking the time out of their already busy days to consent patients, isolate and prepare samples prior to me receiving them.

2.2.2.1 Clinical Definition of BOS

BOS was diagnosed as per International Society of Heart and Lung Transplantation guidelines (Estenne et al., 2002). Briefly, a decrease in FEV1 to between 81 and 90% (averaged over two separate visits) of baseline would highlight the potential development of BOS. Further decreases are classified onto a 3-stage scale with diagnosis confirmed by histological analysis.

2.2.2.2 Primary Sample Isolation Ethics

This study was performed in accordance with approval from the Newcastle and North Tyneside Local Regional Ethics Committee and informed written consent was obtained from all study patients (REC 2001/179).

2.2.2.3 PBEC Isolation

Patient metrics are included in **Appendix 8.1.** PBECs were isolated by bronchial brushing of the sub-segmental bronchi in previously consented lung transplant patients, using a protected specimen single-sheath nylon cytology brush (Olympus: #BC-202D). Cells were dispersed into 5mL of sterile PBS with a further addition of 5mL of RPMI media (Forrest et al., 2005).

2.2.2.4 PBEC Culture

PBECs were cultured on 0.5% collagen I (Nutacon: #5005-B) coated plastic tissue vessels or collagen coated glass coverslips for immunocytochemistry, in SAGM. Cells were passaged upon reaching approximately 90% confluence, and were not taken beyond five passages to ensure epithelial morphology. Very early cultures displayed a morphologically heterogeneous population, however this was lost before first passage with all cells displaying a rounded cobblestone like appearance, at high (>10) passage PBECs became senescent A confluent T25 flask contained approximately 3-400,000 cells and yielded between 100-150µg of total protein. To passage, cells were washed once with sterile 1x PBS before trypsin (Lonza: #CC-5012), pre-warmed to 37°C, was added to the culture vessel. Cells were the incubated for approximately 5 minutes until the majority of cells had lifted off from the surface, the trypsin was then neutralized with an equal volume of trypsin neutralizing solution (Lonza: #CC-5002). Cells were pelleted by centrifugation at 250 x g for 4 minutes and the supernatant was discarded. The cell pellet re-suspended in fresh SAGM and re-plated at a 1:2-1:3 ratio according to experimental parameters. Therefore, from an initial isolation of two T25 flasks it would be possible to generate 8-18 T25 flasks, or equivalent surface area, by P2.

2.2.2.5 Bronchoalveolar Lavage

Bronchoalveolar Lavage was collected as part of the normal screening protocol in post-transplant patients. Where research permission had been previously provided excess BAL samples after clinical diagnostic procedures were carried out were provided for use. Briefly, 60mL aliquots of sterile saline solution are introduced into the lung at the level of the sub-segmental bronchi by a bronchoscope, the aliquot is aspirated then withdrawn under low pressure to minimise airway collapse. This procedure is repeated three times in each patient with the lavage collected as a single sample.

2.2.3 Cell Treatments & Stimulations

All cell treatments were performed using aseptic technique and treatments were made up *en masse* before being aliquoted onto appropriate cells to ensure consistency of treatment.

2.2.3.1 Chemical Inhibition

Experiment appropriate amounts of chemical inhibitors were added to cells in culture 1 hour before stimulation with TGF-β1, TNFα or IL-1β, alongside untreated controls.

2.2.3.2 Small Interfering RNA

siRNA in experiment appropriate amounts was mixed with HiPerfect lipid transfection reagent diluted in sterile 1xPBS for 30 minutes at room temperature. Complexes were added to cell culture 24 hours before stimulation with TGF-β1, TNFα or IL-1β, alongside untreated and sequence scrambled controls.

2.2.3.3 Cytokines

Experiment appropriate doses of TGF-β1, TNFα or IL-1β were added to cells after chemical inhibition or siRNA knockdown. For the assessment of EMT endpoint markers cells were harvested 72 hours post-stimulation. For the assessment of phospho-signalling markers cells were harvested 30 minutes post-stimulation.

2.2.4 Cell Preparation

2.2.4.1 For Immuno-Cytochemistry

Cells cultured on glass coverslips were washed 1 time with 1x PBS before fixation *in situ* with 4% PFA for 1 hour at room temperature or overnight at 4°C. Cells were then washed with 1mM glycine in dH_2O to quench the crosslinking action of PFA for 30 minutes at room temperature. Cells were then stored under 1x PBS at 4°C prior to immuno-staining.

2.2.4.2 For SDS-PAGE & Immuno-Precipitation

Media was harvested and stored at -80°C for gelatin zymography and Sircol assay. Cells were washed 1 time with 1x PBS before being harvested by cell scraping into ice cold 1x PBS. Cells were pelleted by centrifugation at 1000 x g for 5 minutes at 4°C and stored in PhosphoSafe Extraction Reagent (EMD: #71296-3) at -80°C to prevent protease and phosphatase activity.

2.3 Protein Expression & Analysis

2.3.1 Lysate Fractionation

Lysates isolated as per **2.2.4.2** were fractionated by reagent based lysis into nuclear and non-nuclear fractions (Pierce: #78833) as per manufacturer's instructions. Briefly proteins are isolated in a two-step process; firstly the cell membrane is chemically disrupted and the cytoplasm released, the intact nuclei are then pelleted out by centrifugation before being themselves lysed. The cell adhesion protein E-cadherin and Ras-related Nuclear Protein (Ran), a nuclear specific Ras GTPase (Wennerberg et al., 2005), were used as markers to confirm the purity of the respective fractions.

2.3.2 Bicinchoninic Acid Protein Assay

Protein concentration was determined by the Bicinchoninic Acid Protein Assay (BCA – Pierce: #23225). Prior to assay lysates isolated as in **2.2.4.2** were sonicated in a standard fashion, and centrifuged at 500 x g for 1 minute to pellet any remaining cell debris. A standard curve derived from serially diluted 2mg/mL

BSA was also prepared. Samples were loaded onto a 96 well plate as per manufacturer's instruction and incubated at 37°C to improve assay sensitivity (Olson and Markwell, 2007). The plate was read at 570nm.

2.3.3 Immuno-Precipitation

Cells were cultured on 6 well tissue culture plates coated with collagen I, cells were prepared as described in **2.2.4.2** prior to Immuno-precipitation. Samples were well mixed and 10µL was removed for BCA protein assay as described above. The maximum constant protein concentration available was used for all assays, which approximated 20µg.

The harvested cell suspension was centrifuged at 250 x g for 5 minutes at 4°C to pellet the cells. 250µL of ice cold non-denaturing or denaturing lysate buffer mixed with a protease inhibitor cocktail in a 10:1 ratio was added to the cells. When using non-denaturing lysis buffer the cells were agitated for 30 minutes at 4°C before being centrifuged at 1200 x g for 20 minutes, the supernatant was kept and the pellet discarded. For cells lysates which were denatured the samples were boiled for 5 minutes before being quenched with an equal volume of non-denaturing lysis buffer and mechanically agitated through a 20G needle. Samples were spun at 12,000 x g for 10 minutes and re-suspended in 250µL of 1x PBST.

To remove any non-specific IgG binding proteins from the sample 25µL of control IgG antibody was incubated with the sample for 1 hour on ice, 25µL of protein G coated magnetic beads were then added and incubated for 30 minutes under agitation. Beads were isolated through application of a magnetic field and the supernatant collected, beads were re-suspended in 250µL of 1x PBST before being isolated again, this supernatant was added to that previously collected, the beads coated with non-specific IgG binding proteins were discarded.

1µg of antibody was added per 100µg of protein in each sample and incubated overnight at 4°C under agitation. 25µL of protein G coated magnetic beads were added to each sample and incubated for 30 minutes at room temperature under agitation. Beads were isolated through application of a magnetic field and the supernatant collected. Beads were re-suspended in 250µL of 1x PBST before being isolated again, and this supernatant was added to that previously collected. 50µL of sample loading buffer (without bromophenol blue for indirect ELISA experiments) was added to the beads and heated at 80°C for 10 minutes. The beads were isolated and discarded, with the supernatant ready for further analysis.

2.3.4 SDS-PAGE

A standard concentration of protein as used for all samples on a gel, and each sample was mixed with an equal volume of 4x sample loading buffer before being boiled for 5 minutes. This solution was loaded onto either a 4-12% Bis-Tris gradient gel (Invitrogen: #NP0322) and run at 100V in 1x Running Buffer; with a SeeBlue Plus 2 pre-stained ladder (Invitrogen: #LC5925), for 2 hours on ice.

2.3.5 Zymography

An 8% resolving gel was made up as described below and loaded into the casting apparatus; the gel was covered with an appropriate volume of saturated butanol. A stacking gel made up as described below and was layered on top of the resolving gel and left to set at room temperature with an appropriately sized comb in place.

Reagent	Supplier	Cat. #	8% Resolving (mL)	4% Stacking (mL)
Acrylamide	Sigma	A3699	4	1.3
1.5M Tris(hydroxymethyl)aminomethane	Sigma	93349	3.75	2.5
1mg/ml Gelatin in dH_20	Sigma	G2500	6.95	-
dH_20	-	-	-	5.8
10% Sodium Dodecyl Sulfate	Sigma	L4390	0.15	0.1
10% Ammonium Persulfate	Sigma	A5508	0.3	0.1
Tetramethylethylenediamine	Sigma	T9281	0.02	0.02

Table 12 - SDS-PAGE Gel Recipe

The required loading volume of media harvested as per **2.2.4.2** & **2.3.2** is mixed with neat 4x sample loading buffer, without β-mercaptoethanol, in a 3:1 ratio. This solution was loaded into the wells and ran at 100V for approximately 2 hours in 1x Running Buffer. Gels were washed 2 times for 15 minutes in Zymography Buffer 1 prior to 6 quick washes in dH_20; gels were then incubated overnight at 37°C in Zymography Buffer 2. Gels were stained with Coomassie Blue Stain for around 2 hours before being washed in Coomassie destain until distinct bands are visible against the background. Gels were photographed on a SynGene G:Box iChemi XL.

2.3.6 Western Blotting

Proteins separated by SDS-PAGE were transferred onto Polyvinylidene Fluoride (PVDF - GE Healthcare: #RPN303F) membranes at 50mA per membrane overnight on ice. The membranes were then blocked with, either 5% dried milk in 1x TBST; or with 3% BSA for phospho-signalling molecules. Membranes were then incubated overnight at 4°C with a primary antibody diluted in blocking solution. Membranes were washed 3 times for 10 minutes in 1x TBST before being incubated with isotype and species appropriate Horseradish Peroxidase (HRP) conjugated secondary antibodies diluted in blocking solution for 2 hours at room temperature. Membranes were then washed 3 times for 10 minutes in 1x TBST before being covered with Enhanced Chemiluminescence (ECL – Pierce: #32106) substrate for 2 minutes. Membranes were photographed on a SynGene G:Box iChemi XL. For

2.3.7 Band Density Analysis

Band density of western blots and zymograms was analyzed by Image J software (Abramoff et al., 2004). Epithelial marker band intensity was measured relative to controls, with mesenchymal marker expression measured relative to TGF-β1 alone stimulations. All EMT endpoint bands were standardized against β-actin loading controls either co-probed on the same membrane or generated by strip and re-probe of the same membrane. Bands for phospho-signalling protein were standardized against the total form of the protein, which unless otherwise stated was achieved by re-probing the original membrane. Where applicable the mean and Standard Error of the Mean (SEM) were generated and plotted.

2.3.8 Indirect Enzyme Linked Immuno-Sorbent Assay

To perform and indirect Enzyme Linked Immuno-Sorbent Assay (ELISA) 20µL of immuno-precipitated lysate was diluted up to 310µL in 1x PBS, and 100µL of this solution was used to coat 3 wells of a 96 well ELISA plate. The plate was sealed and then incubated overnight at 4°C. The plate was washed 3 times with 1x PBST before being blocked with 100µL of 1% BSA in 1x PBST for 1 hour at room temperature. This was replaced with 100µL of primary antibody diluted in blocking solution and the plate incubated at 4°C overnight. The plate was washed 3 times with 1x PBST before being incubated with 100µL of isotype and species appropriate HRP conjugated secondary antibody diluted in blocking solution for 2 hours at room temperature. The plate was washed 3 times with 1x PBST before 100µL of Tetramethylbenzidine

(TMB) substrate solution was added and the plate stored in the dark for approximately 20 minutes. 50µL of 0.25M sulphuric acid was added to stop the reaction and the plate was read using at 450nm. Patient samples were averaged after samples were standardized with un-stimulated 0 minute samples set at 0.1 relative units.

2.3.9 Bronchoalveolar Lavage Cytokine Assay

Levels of TNFα and IL-1β in the bronchoalveolar lavage (BAL) sampled from a longitudinal population of lung transplant patients were assessed by a Meso Scale Discovery Multi Spot Assay (MSD: #K15025C-2) as per manufacturer's instructions. 20µL of neat BAL per sample was loaded onto the plate in triplicate along with an appropriate standard curve. Briefly, the MSD system is comparable to colourimetric sandwich ELISAs. A capture antibody is bound to a carbon electrode at the bottom of a proprietary 96 well plate, which in this instance bind and hold TNFα and IL-1β present in the BAL. A detection antibody conjugated with a proprietary electrochemi-luminescent then binds to any captured TNFα or IL-1β; which, in the presence of the activated electrode, will emit light at 620nm. Significance was then calculated with a two-tailed Mann-Whitney U Test. Significance was then calculated with a two-tailed Mann-Whitney U Test.

2.3.10 Sircol Assay

Media harvested as per 2.2.4.2 was analyzed for collagen I-IV content by the Sircol collagen assay (Biocolor: # S1000) as per manufacturer's instructions. Briefly the assay relies on the binding, and colourimetric detection of Sirius Red dye to Gly-X-Y repeats (Ramshaw et al., 1998) present in the helixes of acid soluble collagen I-IV in a concentration dependant manner, with concentrations determined against a serially diluted standard curve prepared from 20µg/mL collagen I. Significance was then calculated with a two-tailed Mann-Whitney U Test.

2.3.11 Immuno-Cytochemistry

Cells were prepared as described in **2.2.4.1** prior to staining. Cells were permeabilized with 0.1% Triton X-100 in 1x PBS for 30 minutes at room temperature and washed 3 times, for 5 minutes each, with 1x

PBST. Cells were blocked with 3% BSA in 1x PBST for 1 hour at room temperature prior to incubation with primary antibodies diluted in blocking solution overnight at 4°C. Cells were washed 3 times with 1x PBST prior to incubation with isotype and species appropriate fluorochrome conjugated secondary antibody diluted in blocking solution for 2 hours at room temperature in the dark. Cells were washed 3 times with 1x PBST followed by 1 wash with 1x PBS, a drop of DAPI (4',6-diamidino-2-phenylindole) containing mounting media was placed on a glass slide and the coverslips was gently laid on top. Slides were then left in the dark overnight at 4°C before visualization by confocal microscopy. Blank and secondary only controls were used in all instances.

2.3.12 Immuno-Histochemistry

Formalin fixed tissue was embedded in paraffin blocks before being sectioned and placed on a glass slide. Paraffin was removed from the slide by washing in 98.5% Xylenes for 5 minutes at room temperature followed by 2 washes in 95% ethanol for 5 minutes before being placed in cold dH_20 until ready for antigen retrieval. Ethylenediaminetetraacetic acid (EDTA) at pH 8.0 was pre-boiled in a microwave, slides were placed in a rack then lowered gently into the EDTA which was then boiled for a further 10 minutes, before being left to cool at room temperature for 20 minutes. Slides were removed and excess EDTA removed with a dry cloth and a hydrophobic barrier was drawn around the tissue section with a PAP pen. The staining protocol used is the same as described above for ICC. Blank and secondary only controls were used in all instances.

2.3.13 Confocal Microscopy

All images were acquired on a Leica TCS-SP-2UV confocal microscope at x63 magnification unless otherwise stated. Excitation lasers for fluorescein isothiocyanate (FITC) and tetramethyl rhodamine isothiocyanate (TRITC) dyes were standardized for each experiment, with DAPI dye set by eye for each image as required. Images were taken through the centre of the cell as determined by the presence of the most intense DAPI stain.

2.3.14 Statistical Analysis

Due to the small sample sizes a normal distribution could not be assumed, therefore the non-parametric Mann-Whitney U test was used to test for statistical significance. However, for clarity of presentation data in graphs were displayed as mean + SEM. Western blot band density was not analysed statistically due to their semi-quantitative nature. To allow comparison between blots epithelial markers were standardised to the untreated control, with mesenchymal markers standardised to TGF-β1 stimulated controls. In each case, this value was set at 1 and accordingly lacked error bars when plotted.

2.4 Cell Staining

2.4.1 Haematoxylin & Eosin

Cells were prepared as described in **2.2.4.1** prior to staining. Cells were permeabilized with 0.1% Triton X-100 in 1x PBS for 5 minutes at room temperature, followed by 2 quick washes with dH_20 followed by a 5 minute was in dH_20. Acidified haematoxylin (Thermo Scientific: #6765003) was added to each sample for 4 minutes at room temperature, followed by the above wash protocol. Alcoholized eosin (Thermo Scientific: #6766007) stain was added to each sample for 30 seconds, followed by the above wash protocol. Samples were left inverted to dry before being stored in the dark prior to photography.

2.4.2 Trypan Blue

For trypan blue exclusion cells were culture on 48 well plates. Media for each treatment was harvested, and cells washed once with 1x PBS, which was added to collected media. Cells were then trypsinized, with following trypsin neutralization as per 2.2.2.4, and added to collected media and wash. Samples were centrifuged at 500 x g for 5 minutes at room temperature, supernatant was discarded and cell pellet was re-suspended in 250µL of DMEM media and cells counted. 250µL of 0.4% trypan blue dye was added to each sample, mixed thoroughly and incubated for 3 minutes at room temperature. Two counts of 50 cells from each sample were performed and the percentage of viable cells excluding trypan blue calculated along with the SEM. If the SEM was greater than 5 then a third count of 50 cells was performed.

3 Primary Samples Display Increased Fibrotic and Inflammatory Markers

Throughout this project I have where possible used primary human cells and samples, isolated from lung transplant recipients at the Freeman Hospital in Newcastle-upon-Tyne. The benefits of using these are cells are that they are more physiologically relevant to a living human, and hence the disease models being investigated; and the association of these cells with tissue and BAL samples isolated from the same patients allows for greater integration into a disease model still.

There are however some downsides, the cells are cultured submerged in media on collagen coated glass or plastic, which bears little relationship to their *in vivo* setting. Their proliferative ability is also somewhat limited when compared to a cell line population, although again probably increased over that occurring *in vivo* which means that it is often difficult to generate a sufficient cell number to experiment on. There is also perhaps more of a variation in results between patients, however when an effect that is conserved between distinct patients is described, it is perhaps more striking than reproducibility within a cell line.

3.1 Cytokine Expression in BOS Patients

Throughout this study I will be using recombinant TGF-β1, TNFα and IL-1β to stimulate cells mimicking the environment that is present in the lung during the development of OB. It is routine for post-transplant patients at the Freeman to come in for regular assessments, at which point samples, including the cells I use, tissue sections and BAL fluid are taken. Over time a longitudinal database of patient samples has accrued which in association with clinical notes allows tracking of the environment within a patients lung in respect to disease initiation, progression or escalation post-transplant.

It is well recognized in clinical practice that BOS is often first diagnosed or progresses more rapidly following a significant episode of acute inflammation or airway injury. However that association is based on the observation that immune cells are increased, therefore facilitating a greater release of immune factors, in the lavage and also on histological evidence of inflammation having occurred within the tissue. Therefore, it was decided to directly assay BAL samples isolated from post-transplant patients at recurring check-ups for the presence or absence of both TNFα and IL-1β.

3.1.1 TGF-β1 Expression in BOS Patients

Due to the availability of several studies (Elssner et al., 2000; Ramirez et al., 2008) demonstrating elevated levels of TGF-β1 in the BAL of BOS patients , the scarcity of sample and the expense of custom MSD plates it was decided not to assay for TGF-β1. Below is a figure reproduced from the paper by Elssner *et al.* to demonstrate the levels of TGF-β1 present in the BAL of BOS patients.

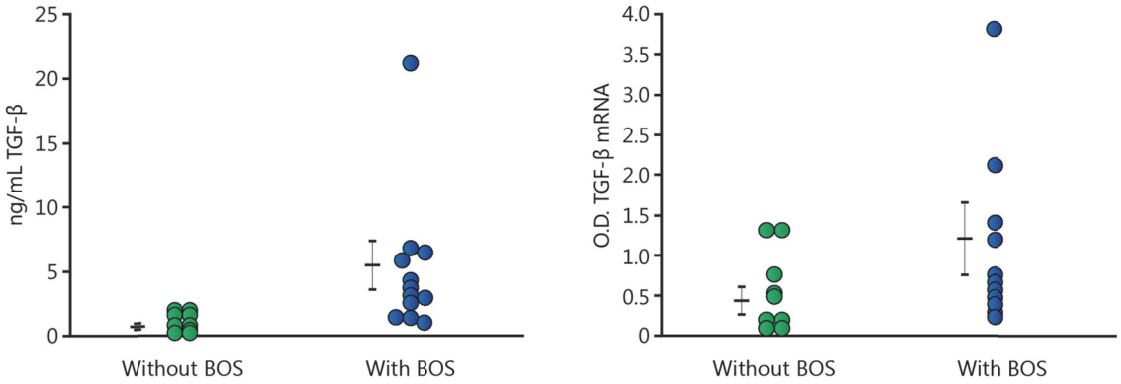

Figure 10 - Adapted, TGF-β1 detected in BAL

TGF-β content in the BAL transplant recipients with and without BOS was detected by sandwich ELISA. There were significantly elevated levels of TGF-β in the BAL of patients diagnosed with BOS compared to those without ($p<0.05$). The levels of TGF-β mRNA in BALF cells isolated from BOS patients whilst elevated was not significantly higher than those without.

Figure adapted from " Elevated levels of interleukin-8 and transforming growth factor-beta in bronchoalveolar lavage fluid from patients with bronchiolitis obliterans syndrome: pro-inflammatory role of bronchial epithelial cells." Elssner et al. Transplantation, 2000.(Elssner et al., 2000)

The BALF samples from BOS patients also showed significantly increased ELF levels of TGF-β (P <0.005). In contrast, TGF-β mRNA expression of bronchial epithelial cells (P =0.62) and BALF cells (P =0.11) was not significantly different between the two groups

3.1.2 TNFα Expression in BOS Patients

BAL samples from patients at the Freeman Hospital in Newcastle-upon-Tyne were assessed for the presence of TNFα using a Meso Scale Discovery Multi Spot Assay as described in 2.3.9. Values were derived from the associated standard curve. In all cases data is presented in two forms, raw and then adjusted (all samples adjusted to 100% BAL return) to account for the variation in percentage of BAL returned from the lung, which in some instances was as low as 5%. I would like to thank Dr Rahul Mahida for collating the clinical samples and linking them with the requisite patient details, and Miss Monika Suwara with whom I jointly performed the MSD assay.

Patients were grouped into those who had a clinical diagnostic of BOS (Stages 1-3 as per ISHLT guidelines) (Estenne et al., 2002)), and those without. The BOS group was then further split into samples occurring up to 6 months before diagnosis of BOS, up to 3 months before diagnosis, at diagnosis, up to 3 months post diagnosis and up to 6 months post diagnosis of BOS. Statistical significance was assessed by two-tailed Mann-Whitney U Test.

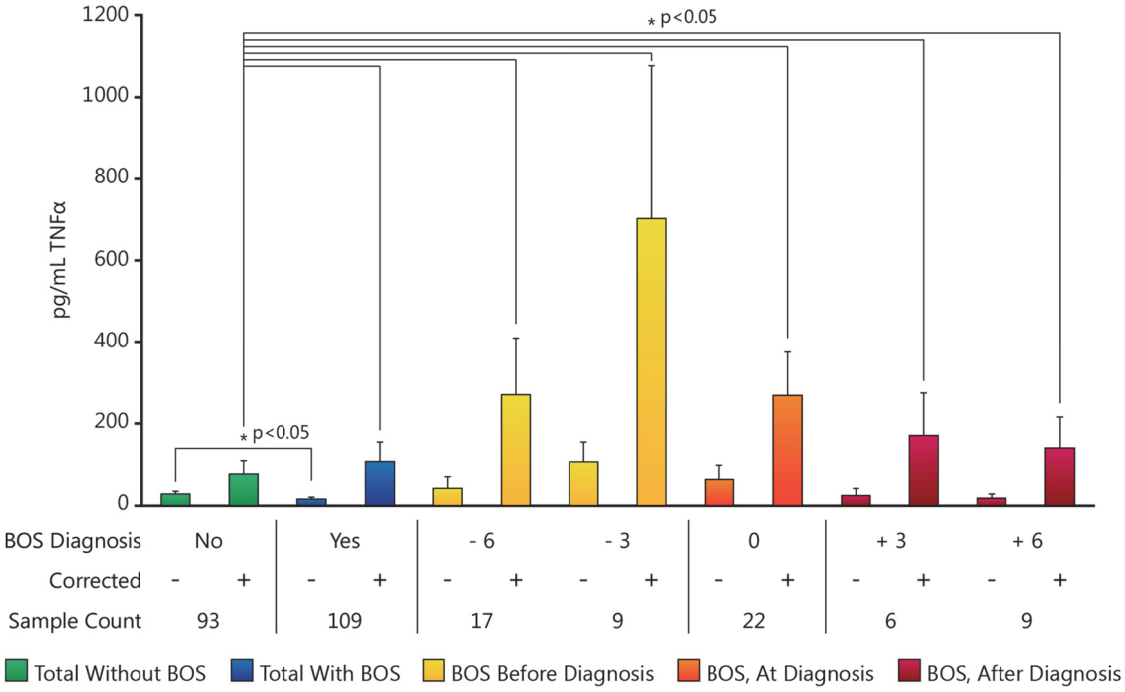

Figure 11 - TNFα detected in BAL

The level of TNFα detected in the total un-corrected group without a diagnosis of BOS was significantly higher than the un-corrected BOS diagnosed group (24±11 *vs.* 16±5 pg/mL, $p<0.05$), however after correction for BAL recovery this was reversed (77±29 *vs.* 108±46 pg/mL, $p<0.05$). For corrected samples all BOS diagnosed subgroups displayed significantly increased levels of TNFα compared to the corrected without BOS group (77±29 *vs.* 271±139, 701±374, 267±108, 171±101, and 129±67 pg/mL, all $p<0.05$). For non-corrected samples 6 months before diagnosis, 3 months before diagnosis and at diagnosis BOS subgroups were significantly higher than the un-corrected without BOS group (see Appendix 8.2 for un-corrected statistics).

3.1.3 IL-1β Expression in BOS Patients

BAL samples from patients at the Freeman Hospital in Newcastle-upon-Tyne were assessed for the presence of IL-1β using a Meso Scale Discovery Multi Spot Assay. Values were derived from the associated standard curve. In all cases data is presented in two forms, raw and then adjusted to account for the percentage of BAL returned from the lung.

Patients were grouped into those who had a clinical diagnostic of BOS (Stages 1-3 as per ISHLT guidelines) (Estenne et al., 2002)), and those without. The BOS group was then further split into samples occurring up to 6 months before diagnosis of BOS, up to 3 months before diagnosis, at diagnosis, up to 3 months post diagnosis and up to 6 months post diagnosis of BOS. Statistical significance was assessed by Mann-Whitney U Test.

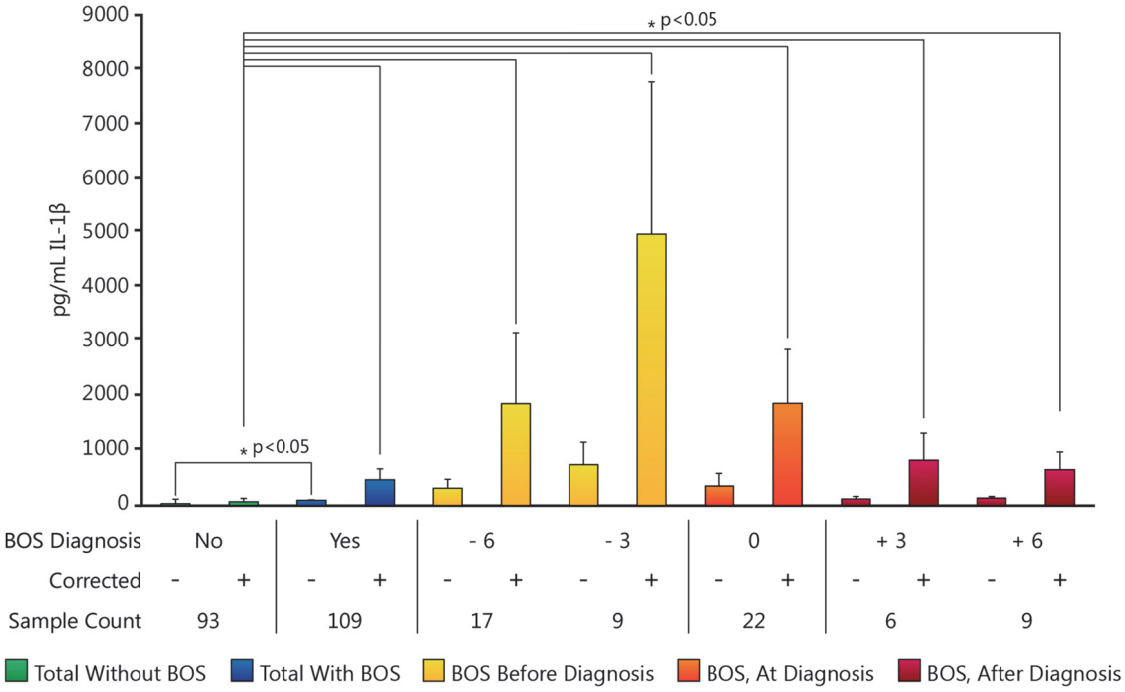

Figure 12 - IL-1β detected in BAL

The level of IL-1β detected in the total corrected and un-corrected BOS diagnosed groups was significantly higher than respective without BOS groups (63±14 *vs.* 483±177 pg/mL, $p<0.0001$ and 14±2 *vs.* 84±23 pg/mL, $p<0.005$). The level of IL-1β in all BOS subgroups, both corrected and un-corrected was also significantly higher than the respective without BOS groups (significance for corrected data shown, 63±14 *vs.* 1853±1294, 4941±3118, 1831±1008, 837±463 and 658±312 pg/mL, all $p<0.05$) (see Appendix 8.2 for un-corrected statistics).

The mean percentage recovery of BAL was lower in BOS patients (24%) than in post-transplant patients without BOS (28%) ($p<0.05$). Looking at TNFα, correcting for recovery increased the level of significance for all groups compared to the without BOS group, induced significance in the 3 and 6 month post diagnosis groups, and increased the detected levels of TNFα in the total BOS group so that it was now significantly elevated, as opposed to lowered when compared to the without BOS groups. Looking at IL-1β both non corrected and corrected data were significant, with correction increasing the level of significance. Anecdotally the recovery of BAL was lowest in BOS patients just after diagnosis (13% - for 3 months post diagnosis) which may account for the gain in statistical significance observed in TNFα for the post diagnosis groups. In the 3 months leading up to diagnosis with BOS recovery was in line with the mean (24%). Unless otherwise specifically mentioned I will be basing my discussions on the corrected data set.

Both TNFα and IL-1β were significantly elevated in the total BOS diagnosed group compared to the without BOS group, suggesting that both TNFα and IL-1β play a key role in the development of BOS and OB. However the total BOS diagnosed group covered all samples from each diagnosed patient, which in some cases could range up to 2 years before diagnosis. To focus on the relevance of TNFα and IL-1β to BOS more closely I split the BOS diagnosis into groups containing all samples 6 months before diagnosis, 3 months before diagnosis, at diagnosis, 3 months post diagnosis and 6 months post diagnosis. Samples in the 3 month groups were also counted in the relevant 6 month group.

Detected TNFα and IL-1β was significantly higher than both the total with BOS and total without BOS groups for all samples. Levels of TNFα and IL-1β at diagnosis of BOS were roughly similar to those 6 months before diagnosis, and there was a drop in levels of both in the 3 and 6 months post diagnosis groups. This drop is likely due to an increase in immuno-suppression post diagnosis. Most interestingly there was a significant peak in both TNFα and IL-1β 3 months before the diagnosis of BOS, which was seemingly not present at or after diagnosis. This acute burst of inflammation may be a key step in the development of BOS driving the increase in OB, potentially by interaction with the elevated levels of TGF-β1 that others have detected.

Poor recovery of BAL from the diseased lung is well recognized but there are few guidelines to help standardize protocol, or explanations as to why recovery is so poor (Löfdahl et al., 2005; Schildge et al., 2007). Looking at the pathology of BOS there are several reasons why recovery may be so poor, firstly obliterated airways may act as sinks for the lavage fluid, preventing it from being retrieved. Secondly, with fibrosis of the airways the count of Clara cell secreting cells may be decreased meaning that the

airways are more liable to collapse trapping lavage fluid, although this is likely only to effect the smaller airways.

This has direct relevance to the process of correction, and BOS, not perhaps for IL-1β where both non-corrected and corrected samples were strongly significant; but for TNFα where significance for the post diagnosis samples was only achieved after correction. Are the cytokine levels detected due to the low volumes recovered being closely associated with a pro-fibrotic and pro-inflammatory airway plug, which when corrected scale upwards significantly, or are they representative of the whole lung? Whilst the paper by Schildge *et al.* attributes no difference in cell and cytokine levels to the recovery rate in various diseases (Schildge et al., 2007) , and yet they are using a cut off value of 30% return, which is higher than mean recovery for both BOS and non BOS groups.

The actual level of TNFα, and perhaps IL-1β, present in the lung is likely higher still as by assessing BAL only the soluble forms of each protein are being measured. TNFα exists as both an active and membrane found trimer and in this assay only the soluble form is being measured, as such any contribution to inflammation by the membrane bound isoform is being missed. Once secreted both cytokines are not necessarily free within the airway or alveolar space, an unknown proportion become bound in the ECM.

Heparan sulphate (Parish, 2006) is a widely studied mediator of this binding, and it can have a diverse role on cytokine mediated signalling. Binding with heparan sulphate can protect cytokines from degradation in the extracellular space by masking proteolytic sites, thus prolonging their lifespan (Sadir et al., 2004) and has also been implicated in facilitating oligomerization of cytokines, a step as previously described which is key for optimal signalling (Hoogewerf et al., 1997). Heparan sulphate in the ECM can also effectively mask cytokines or present them more efficiently to receptors depending on how the cytokine is bound, effectively acting as a reservoir of cytokines within the lung.

There are few studies looking at the role of heparan sulphate in the development of lung disease and non-specifically looking at the development of BOS. However interestingly one study looking at ROS degradation of the ECM mediated by asbestos described a reduced occurrence of inflammation and fibrosis, when heparan sulphate was protected from degradation (Kliment et al., 2008).

There are therefore several ways in which the ECM may be affecting detection of cytokines in the above samples and BOS as a whole. The peaked release 3 months before diagnosis may refer to the activation or release of cytokines from the ECM, either because of its stimulation or degradation. The hypothesis

that soluble TNFα contributes to a more fibrotic and inflammatory response than its membrane bound pre-cursor may fit here (Oikonomou et al., 2006), if a large quantity soluble TNFα was being held inactive in the ECM then it's release could initiate an inflammatory driven fibrosis upon its release, which may correlate with the release seen 3 months before diagnosis. This would require some other factor to induce the activation or cleavage of TNFα from the ECM.

Alternatively cytokines may be being held active and for longer periods within the ECM in BOS patients compared to healthy controls. These are just hypotheses and a more detailed study which encompasses measurements of BAL, cellular and ECM cytokine levels in both diseased and non-diseased patients would be required determine the true physiological levels of cytokines in disease compared to controls.

The raw data and statistical analysis is included in **Appendix 8.2**.

3.2 Primary Bronchial Epithelial Cells

Alongside BAL samples, airway brushings are also conducted post-transplant from which it is possible to derive and culture airway epithelial cells. The protocol for isolation and culture is described in **2.2.2** and in the paper by Forrest *et al.* (Forrest et al., 2005). It has been observed that isolated PBECs change appearance and display a decrease in proliferative ability through passage events. Ideally, upon receipt of brushings, PBECs would be dispersed into the required number of culture vessels, and experimented upon when confluent without passage. However when cells were split too diffusely there was a significant reduction in culture establishment, and those that did establish tended to display excessively mesenchymal phenotypes, either due to resident fibroblasts being able to survive and proliferate, or stress inducing epithelial cells into a more mesenchymal character. Therefore, to achieve the required sample sizes with appropriate cell numbers some passaging must occur.

The following experiments attempt to describe changes within the cells at the protein level throughout culture, and what if any impact this may have on later experiments investigating EMT.

3.2.1 Characterization of Passage Effects in PBECs

When cells arrive in the lab they are pelleted as described in **2.2.2.3** and plated out as P0 in duplicate T25 tissue culture flasks. These cells are then cultured as per **2.2.2.4** until the required number of confluent tissue culture vessels can be achieved. Throughout culture the cell morphology changes as the cells appear to de-differentiate quickly. In order to characterize this change a series of experiments were performed at passage (P) numbers 1 through 4, investigating the expression of various epithelial and mesenchymal markers, hypothesizing that cells would gradually lose specialized epithelial marker expression such as CCSP, retain general epithelial character and possibly gain some mesenchymal or epithelial progenitor characteristics.

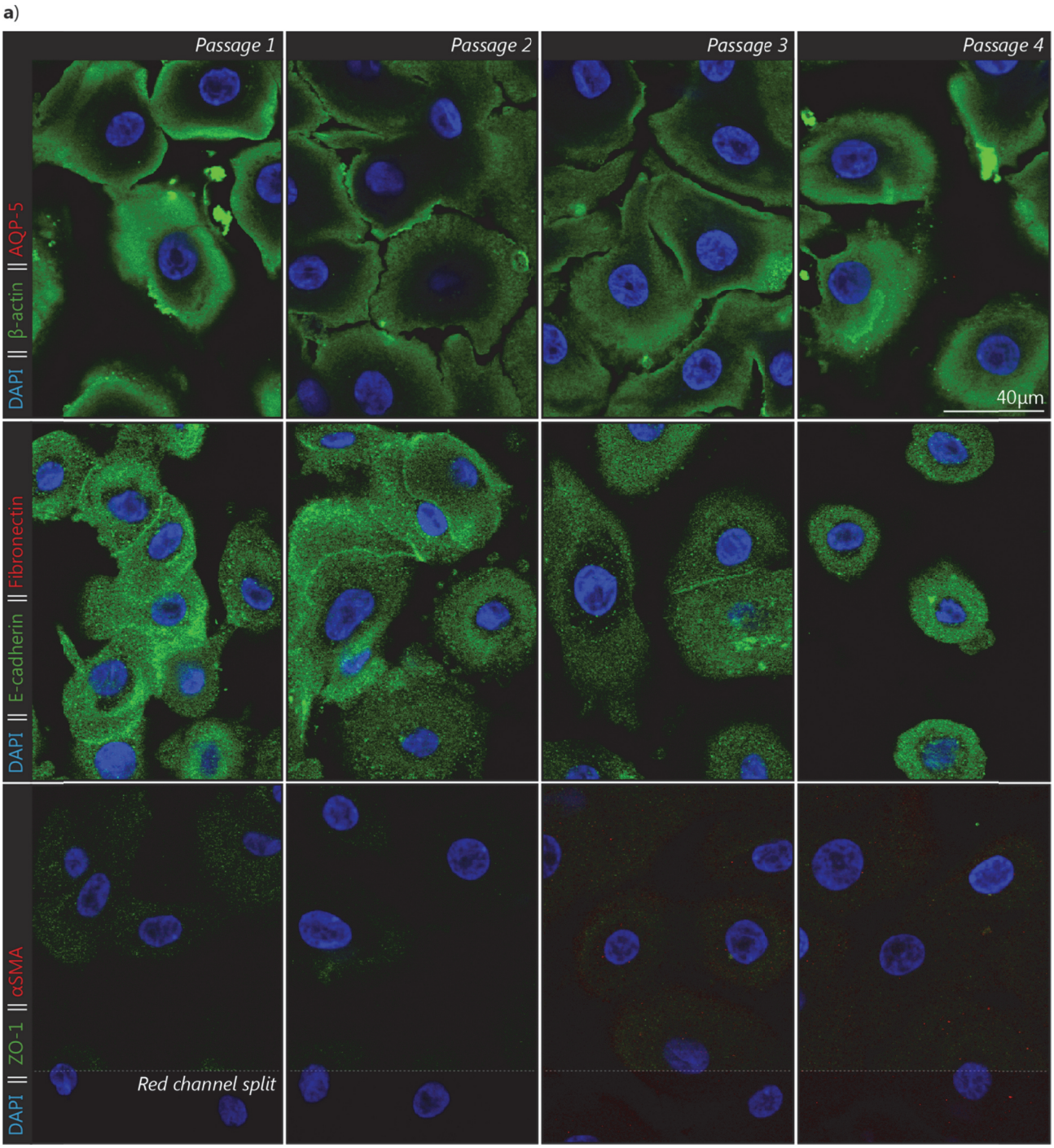

Figure 13 – Characterization of PBECs at passage time-points

a) PBECs at P1 through P4 were assessed for changes in β-actin, E-cadherin and ZO-1 in the FITC (green) channel and AQP-5, fibronectin and αSMA in the TRITC (red) channel. β-actin was consistently detected throughout culture with no change in expression observed, whereas no evidence of AQP-5 was seen at any time-point. E-cadherin expression was also detected at all time-points with no visible change in expression, whereas fibronectin was not detected at any point. ZO-1 expression was consistent at all time-points, whereas αSMA which was not present after P1 or P2 was detected at low levels at both P3 and P4.

b)

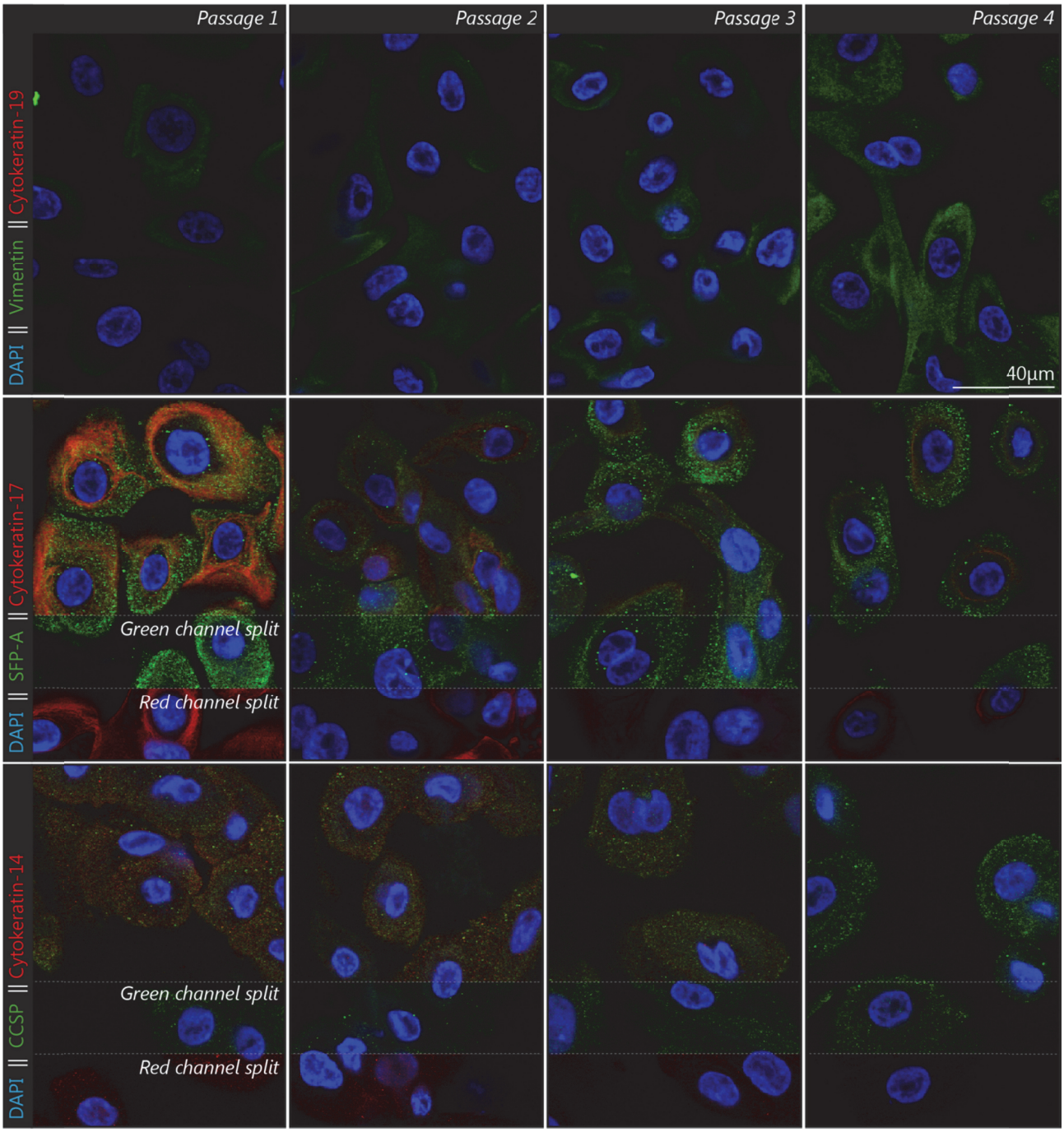

Figure 13 Continued – Characterization of PBECs at passage time-points

b) PBECs at P1 through P4 were assessed for changes in vimentin, SFP-C and CCSP in the FITC channel and cytokeratin-14,17 and 19 in the TRITC channel. Vimentin was consistently detected throughout culture with a slight increase in expression at P4, whereas no cytokeratin-19 was detected at any passage. SFP-A expression was detected at all time-points with a slight decrease in expression after P2 at which point it remained stable. Cytokeratin-17 was strongly detected but this decreased slightly over successive passages. CCSP was present at all time-points with little to no change in expression, cytokeratin-14 was detected at P1 with expression decreasing through to P3, at P4 it was not observed.

c)

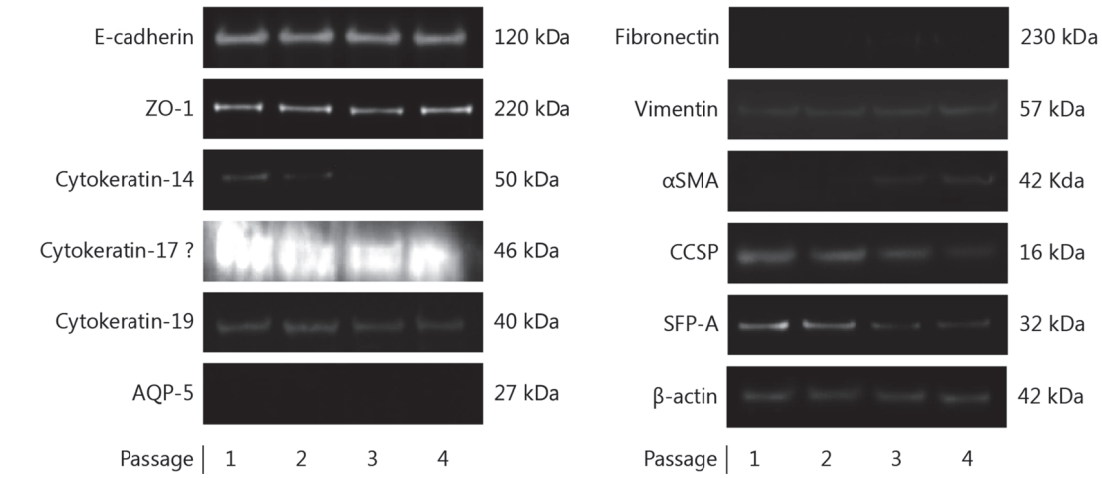

Figure 13 Continued – Characterization of PBECs at passage time-points

c) PBECs were harvested when confluent at P1 through P4. E-cadherin, ZO-1, cytokeratin-19 and vimentin were detected at all time points with no change in expression observed. Expression of CCSP, SFP-A and cytokeratin-14 were initially detected but decreased after each successive passage. In the case of cytokeratin-14 this was lost by P3. Conversely αSMA was not detected until P3 and P4 albeit at low levels, and AQP-5 was not detected and fibronectin was detected at very low levels. Cytokeratin-17 antibody displayed little specificity of binding.

E-cadherin, ZO-1 and fibronectin (5µg), cytokeratin-14 and cytokeratin-19 (10µg), cytokeratin-17, AQP-5, vimentin, αSMA, CCSP and SFP-A (20µg).

Fibronectin is an ECM protein that is often released by fibroblasts during the wound healing process to form a provisional matrix with other quick release factors such as fibrin and hyaluron allowing for extra motility of epithelial and mesenchymal cells to assist resolving the wound (Valenick et al., 2005; Chow et al., 2010). As such its expression is often associated with the development of fibrosis, in these pure un-stimulated epithelial cultures it's low level of expression was to be expected. AQP-5 is typically associated with Type I pneumocytes (Funaki et al., 1998) and so its lack of expression was also to be expected.

E-cadherin (Van Roy and Berx, 2008) and ZO-1 (Fanning and Anderson, 2009) are both tight junction proteins responsible for maintaining epithelial sheet integrity, and are not associated with a particular differentiated form of epithelial cell. Their loss is associated with a transition into a more motile and invasive mesenchymal character as described above. In the wound healing response there is thought to be a reduction but not complete loss of expression, as epithelial cells loosen but do not completely detach their associations with each other. The consistent expression throughout the above expression would suggest that cells are maintaining a generally epithelial character through to at least P4.

Vimentin is an intermediate filamentous protein and is thought to be expressed in mesenchymal cells (Steinert and Roop, 1988). As such it is often used as a marker of EMT (Gilles et al., 1999) for epithelial cells that have gained the more motile invasive phenotype of mesenchymal cells. That it is detected throughout culture suggests that either a baseline level of vimentin is to be expected in epithelial cells, or that in culture PBECs display mesenchymal characteristics, perhaps due to the requirement to move and cover the tissue culture surface or due the culture environment itself. A comparison of a long term confluent culture with a dividing cells, or with air liquid interface (ALI) cultures would be one way of confirming this.

CCSP and SFP-A are both associated with differentiated epithelial cells, Clara cells and Type II pneumocytes respectively. In PBEC cultures I had hypothesized that CCSP would be present and then lost as cells de-differentiated in culture, with no SFP-A detected at all. However both forms were present throughout all passages. Further reading about SFP-A demonstrated that it was often expressed by both Clara cells and, with some evidence of expression in alveolar macrophages (Walker et al., 1986), perhaps accounting for the evidence of SFP-A staining seen. This provides an explanation for the detection of SFP-A however the maintenance of markers of differentiated cells *in vivo* is more puzzling. Once again however with wider reading evidence of expression outside of these specific cells, and even outside of the lung itself has described (Peri et al., 1993; Lacaze-Masmonteil, 1995). This suggests two possibilities, most likely is that this is a baseline expression of SFP-A and CCSP in epithelial cells that have already de-

differentiated, the second being that Clara cells are able to maintain their phenotype within culture and continue expressing CCSP and SFP-A, which is difficult to agree with in light of the expression of other markers discussed below.

Cytokeratins-14 and 17 are thought to be markers specific to basal epithelial cells from all tissues, as such in the lung they would be associated with the larger airways (Troyanovsky et al., 1989; Purkis et al., 1990; Ghosh et al., 2011). Therefore I had hypothesized that their expression may increase throughout culture as epithelial cells revert to a more de-differentiated state. However this was not the case, cytokeratin-14 was initially detected but this detection was lost by western blotting beyond P2, P3 for ICC. All cells seemingly displayed cytokeratin-14 at early passage which suggested that either all PBECs are capable of its expression *in vitro* or that early in culture all surviving cells display basal cell characteristics. The subsequent loss of expression leads me to favour the second explanation, as a loss of basal cells would fit with the concurrent loss of proliferative ability in culture. If attempts were made to immortalize these cells it would be interesting to see if cytokeratin-14 expression was maintained. Cytokeratin-17 mimicked the pattern shown by cytokeratin-14 in ICC, however the quality of the antibody was very poor as can be seen in the western blot, and in Appendix 8.3. Due to the inability to confirm antibody specificity by western blotting the ICC findings should also be discounted.

Cytokeratin-19 is also thought to mark proliferative epithelial cells, but it is not associated specifically with any epithelial sub-population such as SFP-A, CCSP or cytokeratins-14 and 17 (Stasiak et al., 1989; Michel et al., 1996). Whilst not detected by ICC it was detected by western blot at all passage points, with no variation in expression. How this correlates with the drop in cytokeratin-14 and 17 expression is not clear. It is possible by not being expressed in any particular proliferative cell type that cytokeratin-19 may describe an innate proliferative ability, which is maintained in cells throughout culture. A supposition which may be reinforced by the association of cytokertain-19 with the development of several cancers (Alix-Panabières et al., 2009).

The myofibroblast marker αSMA (Hinz, 2007) was included as a negative control as I initially hypothesized that its expression would only be induced under pro-fibrotic conditions. However, faint levels were detected by western blot and ICC in both P3 and P4. This suggests that in culture even when un-stimulated that PBEC cultures are gradually differentiating towards a mesenchymal phenotype. Interestingly αSMA was dropped from the panel of markers I used to assess EMT as there was no detectable variation in expression after any stimulation, with a low baseline level expressed throughout. The stimulants used on cells therefore may not be sufficient to drive epithelial cells towards a

myofibroblast like phenotype in culture, or this change may require a longer time course than for other markers such as fibronectin, vimentin and *pro*-MMP-9, which would fit with the temporal occurrence of myofibroblasts in the wound healing process.

This mixed bag of results demonstrates that measuring EMT can be difficult and that a variety of markers should be assessed. This effect is described in a study by Chai *et al.* who investigated the expression of common epithelial and mesenchymal markers in several epithelial and fibroblast cell lines and found significant crossover of expression, concluding that there is no single reliable marker of either an epithelial or mesenchymal cell (Chai et al., 2010), which fits well with the idea of EMT being a spectrum.

My project is predominantly focused on measuring EMT in PBEC cultures, and the relative importance of key signalling proteins in driving this transition. As such a viable and proliferative population with a strong innate epithelial character would make the ideal point to act as a baseline for EMT experiments. Cells proliferated well up until P4 so any time point before that would be suitable to use for experimentation. Due to the loss of some epithelial marker expression, and the gain of αSMA expression after P2 I chose to not go beyond this passage point with future experiments. Whilst there is still evidence of some mesenchymal protein, vimentin, expression before P2 it was present at a steady baseline, making it possible to measure transitions from this point.

3.2.2 TGF-β1, TNFα & IL-1β dose response

With an appropriate time point that provided sufficient PBECs of epithelial character, and with proliferative ability and evidence of the role of TGF-β1, TNFα and IL-1β expression detected in the BAL of BOS patients. I next investigated the response of PBECs to stimulation with these factors both in isolation and together. There have been several previous studies which have described the interplay between TGF-β1 and TNFα or IL-1β (Borthwick et al., 2010; Câmara and Jarai, 2010; Yamauchi et al., 2010), including from within this research group however I felt that it was important to demonstrate that appropriate dose response experiments had been carried out in relation to this project.

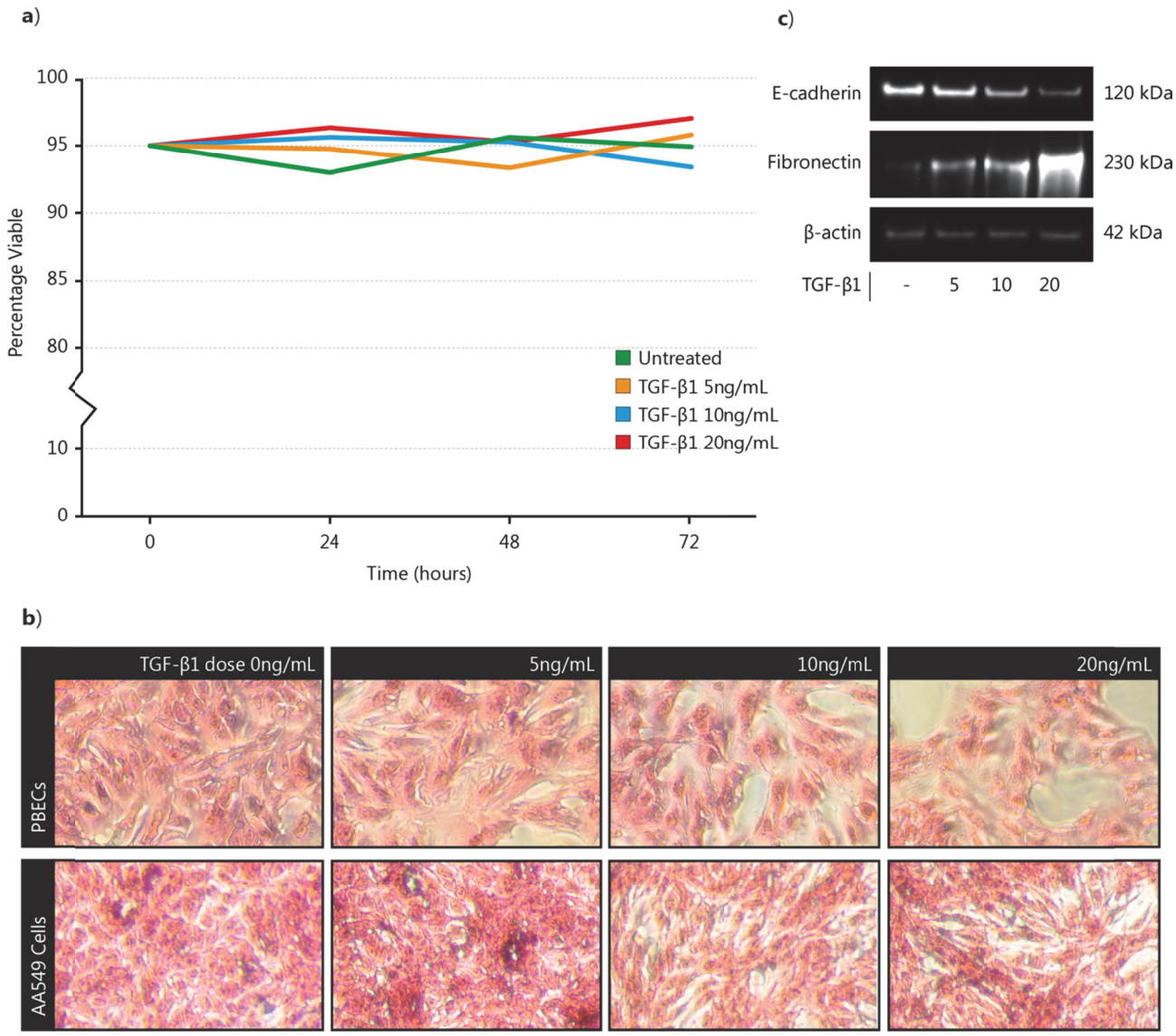

Figure 14 – TGF-β1 dose response time course

a) PBECs were stimulated with TGF-β1 at 5, 10 and 20ng/mL doses for 24, 48 and 72 hours (*n=2*). There was no change in viability at any time point.

b) 72 hours post stimulation with TGF-β1 or TNFα, control cells displayed a uniform cobblestone like appearance, 5ng/mL TGF-β1 induced some breaks between cells but there was generally no change in individual cell morphology, a similar effect was also observed with 10ng/mL. The 20ng/mL dose induced breaks between cells and also induced a slightly more striated appearance compared to un-stimulated controls. In all cases the morphological changes were less severe than those seen in A549 cells, examples of which are also included. E-cadherin and fibronectin (5µg).

c) E-cadherin was present at high levels in un-stimulated cells, expression was reduced in a dose dependant fashion by TGF-β1. Conversely fibronectin expression was up-regulated in a dose dependant manner. β-actin expression was not affected by any stimulation. E-cadherin and fibronectin (5µg).

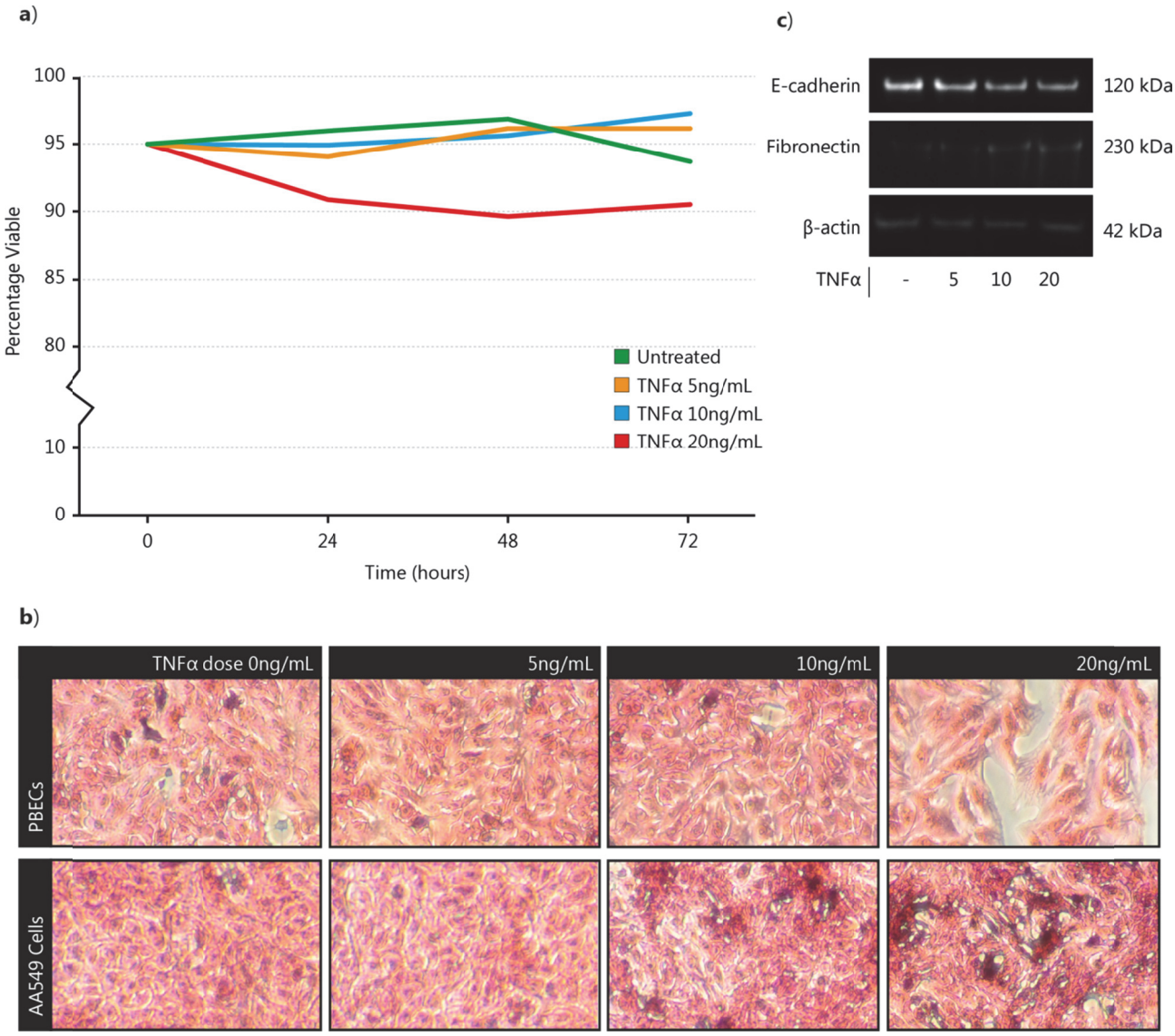

Figure 15 – TNFα dose response time course

a) PBECs were stimulated with TNFα at 5, 10 and 20ng/mL doses for 24, 48 and 72 hours (*n=2*). 5 and 10ng/mL doses of TNFα had no effect on PBEC viability at any time point. A 20ng/mL dose of TNFα induced approximately a 5% drop in viability at 24 hours.

b) 72 hours post stimulation with TGF-β1 or TNFα, control cells displayed a uniform cobblestone like appearance, which was maintained in the presence of 5ng/mL and 10ng/mL TNFα. 20ng/mL TNFα induced a small change in cell morphology to a more striated appearance. In A549 cells neither 5ng/mL or 10ng/mL induced any change in morphology, 20ng/mL however induced some clumping of cells. E-cadherin and fibronectin (5µg).

c) TNFα at 5ng/mL did not reduce E-cadherin expression or increase fibronectin expression, at 10ng/mL there was still no detectable change in E-cadherin expression, but a slight increase in fibronectiin was detected. At 20ng/mL TNFα slightly reduced the levels of E-cadherin detected and induced a slight increase in fibronectin similar to that seen with 10ng/mL. E-cadherin and fibronectin (5µg).

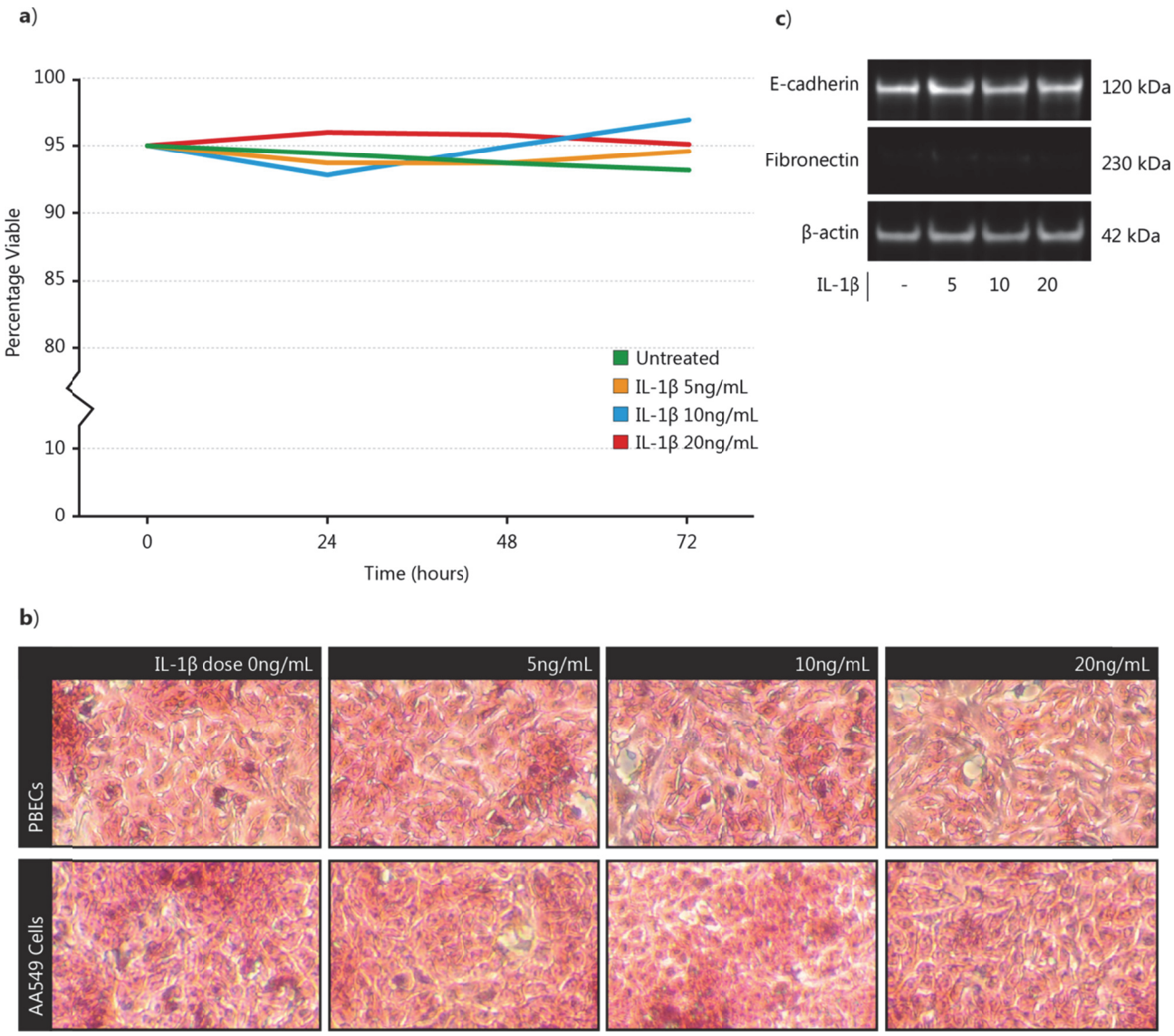

Figure 16 – IL-1β dose response time course

a) PBECs were stimulated with IL-1β at 5, 10 and 20ng/mL doses for 24, 48 and 72 hours (*n=2*). There was no change in viability at any time point.

b) 72 hours post stimulation with TGF-β1 or TNFα, control cells displayed a uniform cobblestone like appearance, all doses of IL-1β had no effect on this morphology, an effect which was replicated in A549 cells. E-cadherin and fibronectin (5µg).

c) All doses of IL-1β had no effect on either E-cadherin or fibronectin expression. E-cadherin and fibronectin (5µg).

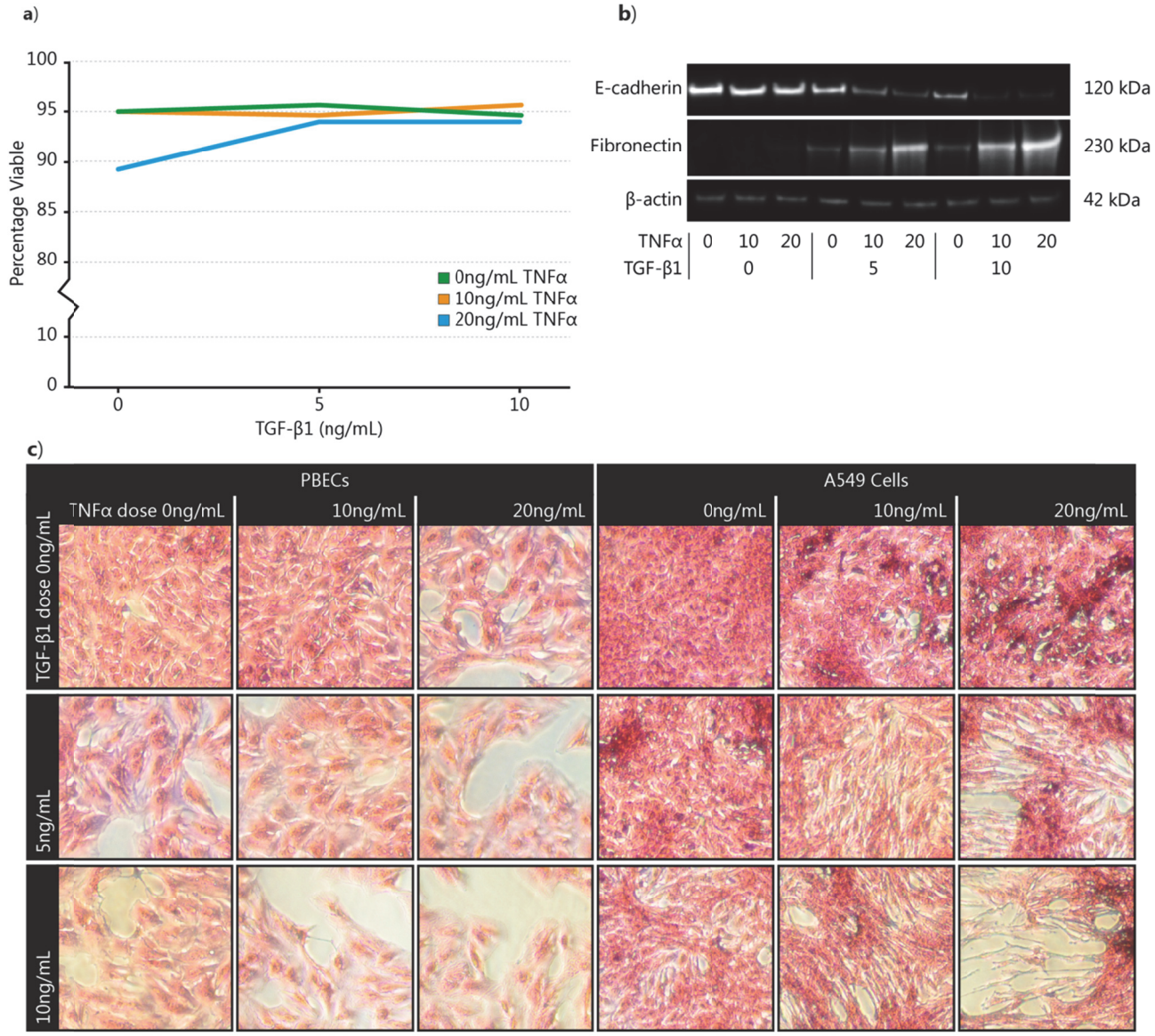

Figure 17– TGF-β1 & TNFα dose response

a) PBECs were stimulated with TGF-β1 at 5 and 10ng/mL or TNFα at 10 and 20ng/mL doses for 72 hours (*n=2*). There was no change in viability for un-stimulated cells, or TGF-β1 alone stimulated cells. A 20ng/mL dose of TNFα induced a small decrease in cell viability. Upon co-stimulation this drop in cell viability was blocked in all instances.

b) 72 hours post stimulation with TGF-β1 or TNFα, control cells displayed a uniform cobblestone like appearance, 5ng/mL and 10ng/mL doses of TGF-β1 induced small breaks between cells. At 10ng/mL TNFα had no effect on cell morphology, at 20ng/mL some cells displayed a more striated appearance. Co-stimulation at the lowest doses of TGF-β1 and TNFα induced a striated appearance and with larger cell breaks than seen with either TGF-β1 or TNFα alone, an effect that was even more apparent at the higher doses. The effect on A549s was more marked still, with the high doses of TGF-β1 and TNFα inducing extremely spindle like cell clusters with large gaps apparent between cell clusters. E-cadherin and fibronectin (5µg).

c) TGF-β1 alone down-regulated E-cadherin expression in a dose-dependent manner and up-regulated fibronectin in a similar fashion. TNFα alone induced a small reduction in E-cadherin expression at 10ng/mL, at 20ng/mL there was again a slight reduction in E-cadherin expression, along with a slight increase in fibronectin. Both 10ng/mL and 20ng/mL doses of TNFα were capable of accentuating the TGF-β1 mediated decrease in E-cadherin and increase in fibronectin expression. E-cadherin and fibronectin (5µg).

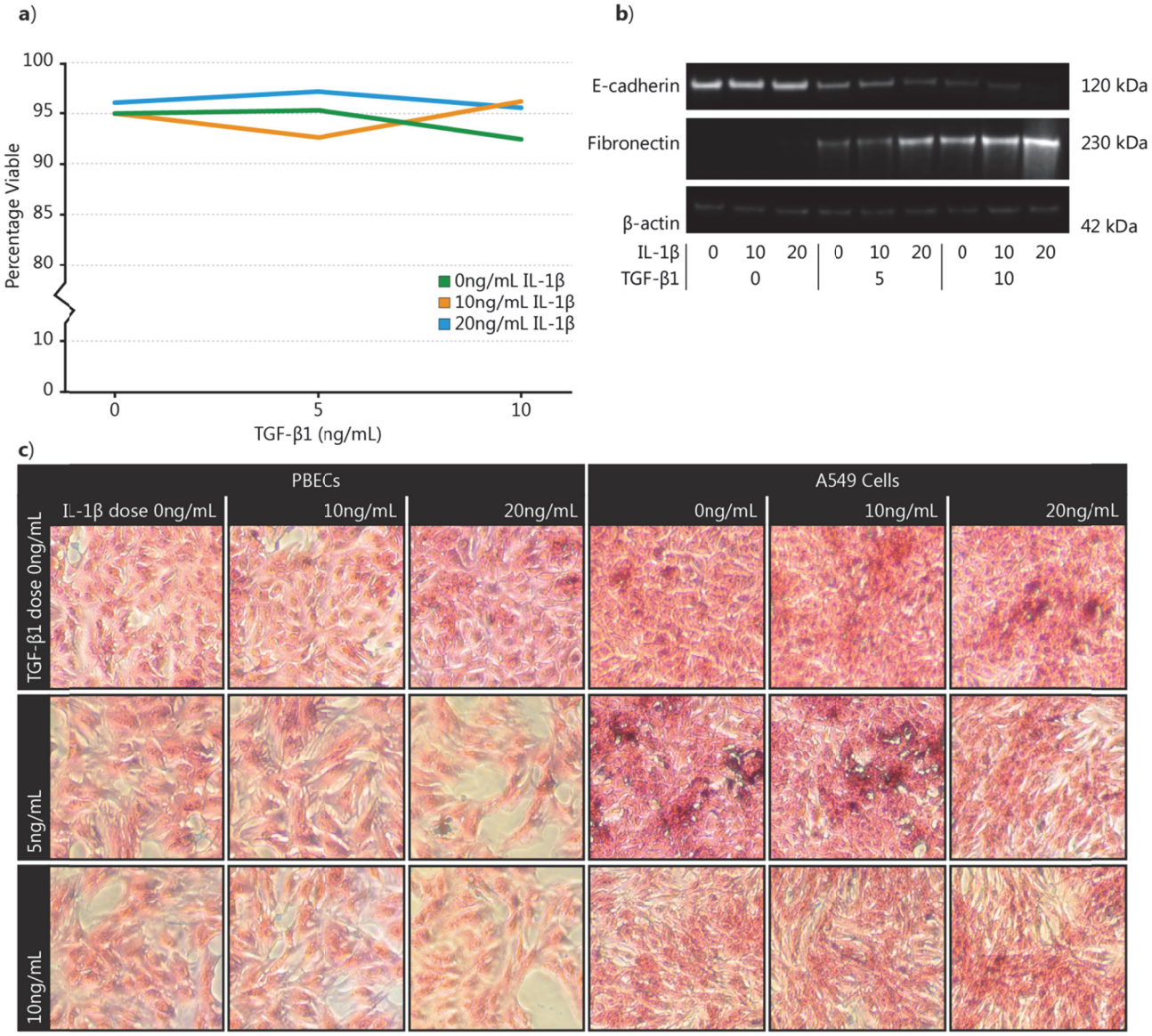

Figure 18 – TGF-β1 & IL-1β dose response

a) PBECs were stimulated with TGF-β1 at 5 and 10ng/mL or IL-1β at 10 and 20ng/mL doses for 72 hours (*n=2*). There was no change in viability for un-stimulated cells, TGF-β1 alone or IL-1β alone stimulated cells. Upon co-stimulation there was a slight decrease in viability in all instances.

b) 72 hours post stimulation with TGF-β1 or TNFα, control cells displayed a uniform cobblestone like appearance, 5ng/mL and 10ng/mL doses of TGF-β1 induced small breaks between cells. IL-1β had no effect on cell morphology. Upon co-stimulation 10ng/mL of IL-1β had no effect on the TGF-β1 mediated change in cell morphology. 20ng/mL IL-1β however induced a more striated phenotype in both instances, although to a lesser degree than was seen with TGF-β1 and TNFα. E-cadherin and fibronectin (5µg).

c) TGF-β1 alone down-regulated E-cadherin expression in a dose-dependent manner and up-regulated fibronectin in a similar fashion. IL-1β alone had no impact on E-cadherin or fibronectin expression at either dose. Co-stimulation with 10ng/mL of IL-1β had no effect on TGF-β1 mediated loss of E-cadherin and gain of fibronectin expression, yet 20ng/mL IL-1β accentuated the effect of both 5 and 10ng/mL TGF-β1 stimulations. E-cadherin and fibronectin (5µg).

These results demonstrate that EMT in PBECs is driven by TGF-β1, was capable of reducing expression of E-cadherin at 5, 10 and 20ng/mL doses whilst simultaneously increasing expression of fibronectin at all doses, without impacting on cell viability. There was a clear increase in effect stepping up from 5ng/mL to 10ng/mL of TGF-β1 but little detectable difference between 10ng/mL and 20ng/mL treatments at the protein level and so it was decided to use a 10ng/mL dose through further experiments. The paper by Elssner *et al.* (see Figure 10) detected a mean of 5ng/mL TGF-β1 in the BAL of BOS patients (Elssner et al., 2000), although as discussed this figure may be higher still if ECM bound TGF-β1 was factored in. Whilst a 5ng/mL dose of TGF-β1 was capable of driving EMT *in vitro* I felt that the stronger effects demonstrated by the 10ng/mL dose would provide a more consistent mesenchymal shift to investigate.

TNFα alone only very slightly induced, fibronectin expression at 10ng/mL with, a slight increase in expression at 20ng/mL and evidence of a decrease in E-cadherin at this same dose, 5ng/mL having no effect on either marker. Cell viability was reduced by approximately 5% 24 hours after stimulation, but remained constant after this initial drop. Interestingly IL-1β had no effect on cell viability, morphology or expression of E-cadherin and fibronectin at any dose. This suggests that neither TNFα or IL-1β are capable of driving fibrosis in our PBEC culture system as the doses use exceed their detected peak in the BAL (0.8ng/mL and 5ng/mL 3 months before BOS diagnosis respectively), this may be because they act over a longer period than TGF-β1 and we are simply missing the effect, although this becomes difficult to assay in cells which are innately losing their epithelial character over time. Another cause may be that EMT is not driven by inflammatory mediators, and such factors induce a pro-fibrotic effect by either inducing or recruiting other cells than drive fibrosis, or act as intermediaries in driving EMT.

When used in conjunction with TGF-β1 however the results were more intriguing. TNFα at both 10ng/mL and 20ng/mL was capable of strongly accentuating the loss of E-cadherin and gain in fibronectin seen in both 5 and 10ng/mL TGF-β1 stimulations. With the largest loss of E-cadherin and gain in fibronectin seen when using the highest doses of each. IL-1β at 10ng/mL did not detectably influence the TGF-β1 driven loss of E-cadherin or gain in fibronectin, yet at 20ng/mL it accentuated the response in both the 5 and 10ng/mL TGF-β1 stimulations, although to a lesser degree than both TNFα stimulations. These results provide clear evidence that inflammatory mediators such as TNFα and IL-1β are capable of acting in synergy with TGF-β1 to drive fibrosis by EMT in PBEC cultures. The doses of required to initiate this effect are higher than those detected in the BAL of BOS patients before diagnosis, but are within an order of magnitude of those figures, and as previously discussed BAL measurements do not account for the bound quantities of cytokines.

Whilst TNFα had a larger accentuative effect on TGF-β1 than IL-1β it is difficult to directly relate these findings to the disease model. Approximately 5 times the amount of IL-1β compared to TNFα was detected in BAL samples, therefore it is possible that a 50ng/mL dose of IL-1β would have a comparative effect, to that of 10ng/mL TNFα. Other factors may also play an important role such as receptor expression, dissociation constant between receptor and ligand, ability of ECM coating to sequester and inhibit or assist with oligomerization. Nevertheless, *in vitro* TNFα produces the largest accentuative effect at a reasonable dose and so it was decided that a 20ng/mL dose would be used in future experiments.

Whilst changes in E-cadherin and fibronectin expression levels were detected by western blotting the changes in PBEC morphology in response to stimulation were, whilst detectable, rather conserved. Comparable A549 photo-micrographs show a much greater morphological shift from a uniform cobblestone appearance to one containing tightly clustered cell foci with a spindle like appearance. This may be due to several factors, most obviously A549 cells are cell line of a different cell type, it may be that the immortalized nature of A549s makes them more susceptible to EMT, or that the Type II cells that they represent are themselves more susceptible. A549 cells also proliferate more rapidly than PBECs, the morphological transition may be linked closely to linked to cell cycle and as such the more rapidly dividing A549 cells undergo this more rapidly.

In the introduction, I discussed whether EMT could be viewed as a discrete occurrence, where an epithelial cell switches completely to a mesenchymal phenotype; or whether a continuous spectrum of marker expression and cell activity was observed. These findings would suggest it is the latter, with isolated epithelial cells capable of expressing both epithelial and mesenchymal proteins, mesenchymal proteins increasing over time and passage in culture. Differing doses of pro-inflammatory and pro-fibrotic stimuli also induced differing severities of EMT in cultured cells, again suggesting that cells were transitioning over a spectrum rather than switching character directly.

In summary in this chapter I have demonstrated the epithelial character of isolated PBECs and decided upon a maximum passage number from which to best assess EMT. The levels of the pro-fibrotic TGF-β1 and the inflammatory TNFα and IL-1β were assessed in the BAL of post-transplant patients. A significant elevation of TNFα and IL-1β was detected in those diagnosed with BOS compared to those without, with a marked increase 3 months before diagnosis. This data was used to determine a suitable dose of TGF-β1 to drive EMT *in vitro* in PBEC cultures, and the accentuative effect of TNFα and IL-1β was confirmed and a suitable dose of TNFα decided upon.

4 TAK-1 Mediates Synergistic Signalling

I decided to investigate the synergistic signalling between TGF-β1 and TNFα at the intracellular signalling level by inhibiting the action of key signalling proteins and observing the effect on EMT and also on the phosphorylation of these same proteins.

In the first instance the function of each protein was chemically inhibited with an appropriate dose determined from experiments in A549 cells. EMT was assessed by observing changes in EMT markers, a decrease in E-cadherin and cytokeratin-19, an increase in fibronectin and vimentin and an increase in the secretion of *pro*-MMP-9 and collagens I-IV. By assessing the impact of inhibition on EMT and also the phosphorylation of signalling proteins it was possible to develop a putative signalling method that described the observed synergy between TGF-β1 and TNFα. These findings were then verified where possible by using siRNA knockdown of the same signalling proteins.

4.1 Mothers against decapentaplegic-3

With TGF-β1 driving EMT it was logical to begin investigation of the signalling mechanisms by investigating the canonical TGF-β signalling pathway. TGF-β1 signalling forms part of the TGF-β super-family signalling group along with other factors such as the bone morphogenic proteins (BMP). The SMAD family of proteins are the major constituents of TGF-β super-family signalling; of which there are 8 isoforms. SMADs are typically split into three categories, receptor (r)SMADs (1, 2, 3, 5 and 8), co-activating (co)SMAD (4) and inhibitory (i)SMADs (6 and 7). All SMADs contain a c-terminal MAD homology domain (MH2) region which regulates the binding of SMAD proteins to each other, as well as other regulatory proteins. The rSMADs and coSMAD also contain an N-terminal MAD homology domain, which facilitates DNA binding and also contains nuclear localization and export signals. The coSMAD and iSMADs are conserved for all arms of the TGF-β super-family, with SMAD2 and SMAD3 acting as the rSMADs for TGF-β1 signalling. SMAD3, 48 kDa, and SMAD2, 55 kDa, were first described in mammalian systems in 1996 (Eppert et al., 1996; Zhang et al., 1996).

In un-stimulated cells SMAD2/3 are inactivated in two ways, firstly by self-binding between their own MH1 and MH2 regions inhibits oligomer formation, nuclear translocation and DNA binding, secondly the un-phosphorylated rSMADs are held in the cell membrane by SARA. SARA displays a higher dissociation constant with un-phosphorylated rSMAD monomers than they do with each other, and so is capable of

limiting random activations. SARA also plays a key role in the activation of SMAD signalling however, upon activation of the TGF-R1 kinase by TGF-β1 binding, SARA presents the un-phosphorylated rSMAD to the receptor, allowing for the phosphorylation of SMAD2/3.

Phosphorylation occurs at the C-terminal of the rSMAD proteins, *Ser465* and *Ser467* for SMAD2 and *Ser423* and *Ser425* for SMAD3, which removes the auto-inhibitory effects of self-binding, and also greatly reduces the affinity between the rSMAD and SARA, freeing SMAD2/3 into the cytoplasm. Once freed these rSMADs are capable of forming heterodimers with SMAD4, or heterotrimers with SMAD4 and another rSMAD molecule, mediated by interactions between the MH2 regions. The mechanisms of dimer or trimer formation, and the differing impacts are not well understood, but evidence of differing transcriptional responses has been described (Inman and Hill, 2002).

The exposed MH2 region of SMAD2/3 also contains a nuclear localization signal which can facilitate a co-SMAD independent localization into the nucleus by associating with importin proteins to pass through nuclear pores, which are then cleaved by the actions of RAs-related Nuclear protein (RAN) a GTPase. Nuclear translocation can also occur in association with SMAD4 , although it is achieved in an importin independent manner through direct interaction with nuclear pore proteins. Although rSMAD complexes can translocate to the nucleus without SMAD4 it is thought that they will remain transcriptionally inactive in its absence, as although SMAD3, but not SMAD2 (Dennler et al., 1999), is capable of binding directly to SMAD binding elements (SBE) within the genome its affinity is low (Shi et al., 1998). Other co-factors such as p300, recruited in the presence of SMAD4 (De Caestecker et al., 2000), are required to stabilise this binding. Activated rSMADs however can form complexes with SMAD4 in the nucleus (Pierreux et al., 2000), suggesting that nuclear import conditions can provide another level of control within the SMAD pathway.

These co-factors can be transcriptionally active in their own right, and upon association with a SMAD oligomer induce an alternative transcriptional event, or they may be transcriptionally inactive and simply facilitate a stronger bond between a SMAD oligomer and a SBE (Feng and Derynck, 2005). Whatever their mechanism a large number of proteins have been implicated in modulation of SMAD DNA binding, and it is this mixture of various SMAD oligomers associated with a wide array of co-factors that allows for a wide range of specific responses to an, initially, rather simple appearing signalling pathway. To my knowledge there is no evidence of activation of the canonical SMAD pathway by either TNFα or IL-1β, although both are capable of indirectly modulating SMAD signalling activity, which I discuss in **1.3.2** and **1.3.3**.

After initiating the desired transcriptional event rSMADs are shuttled back to the cytoplasm, SMAD4 contains a nuclear export signal, however this is masked when in association with rSMADs, and as such is thought to be used to cycle itself back into the cytoplasm (Pierreux et al., 2000). Upon de-phosphorylation by phosphatases such as protein phosphatase 1A (PP1A) rSMADs disassociate from SMAD4, which can then cycle back to the cytoplasm independently, and other co-factors; and are exported from the nucleus (Lin et al., 2006). Un-phosphorylated rSMADs are exported from the nucleus by the same proteins that are capable of importing them (Xu et al., 2002), the exact mechanism that defines direction of transit is unknown although it may be due to the self-masking ability of the rSMADs or the changes within the C-terminal region.

It was initially thought that out of SMAD2 and SMAD3, SMAD2 might be the key factor in response to TGF-β1 stimulation, with SMAD3 acting as a redundant or modulatory protein as knocking out SMAD2 (Heyer et al., 1999) but not SMAD3 (Zhu et al., 1998) resulted in an embryo lethal phenotype in mice. However later work in fibroblast isolated from knockout mouse embryos suggested that the opposite was true, with SMAD3 initiating the response to TGF-β1 stimulation, which could then be modulated by SMAD2 (Yang et al., 2003), which added yet another level of regulation to the canonical signalling pathway. It has also been shown that SMAD3 may play more of a role in the development of the fibrotic response, as in primary hepatic stellate cells SMAD3 overexpression resulted in increased expression of mesenchymal markers such as fibronectin and collagen I, compared to the same cells over-expressing SMAD2 (Uemura et al., 2005). As such it was decided that SMAD3 rather than SMAD2 would be the subject of investigation in our system.

TGF-β1 is a major driver of fibrosis, and of EMT; and therefore understanding the contribution of its canonical signalling pathway to EMT is the logical first step in understanding TGF-β1 driven, TNFα accentuated EMT. The following results outline my attempts to understand SMAD3 phosphorylation in response to TGF-β1 or TNFα stimulation as well as its role, and importance, in the subsequent occurrence of EMT in our OB model system.

4.1.1 Phosphorylation Response of SMAD3

As discussed in **1.3** phosphorylation is often one of the key steps in protein activation. As such understanding of when protein phosphorylation occurs temporally can provide information about order of activation within a signalling cascade. The phosphorylation and subsequent activity of SMAD3 has

been discussed above. SMAD3 is key mediator of TGF-β1 signalling, with no activity in response to TNFα described. I therefore hypothesized that phosphorylation of *Ser423* and *Ser425* in the carboxyl terminal of SMAD3 would occur in response to TGF-β1 alone, with TNFα having no impact either alone or when used in conjunction with TGF-β1.

PBECs were cultured in 6 well collagen coated plates until confluent and stimulated with TGF-β1 or TNFα. Cells were harvested at 0, 0.5, 1, 5, 10, 30 and 60 minute time points. Whole cell PBEC lysate was immuno-precipitated for total SMAD3, under denaturing conditions, with the resulting lysate probed for *p*SMAD3 (*Ser423* and *Ser425*) by indirect ELISA. Neat lysate from the 30 minute stimulation was analyzed by Western blot for both total and phospho forms of SMAD3.

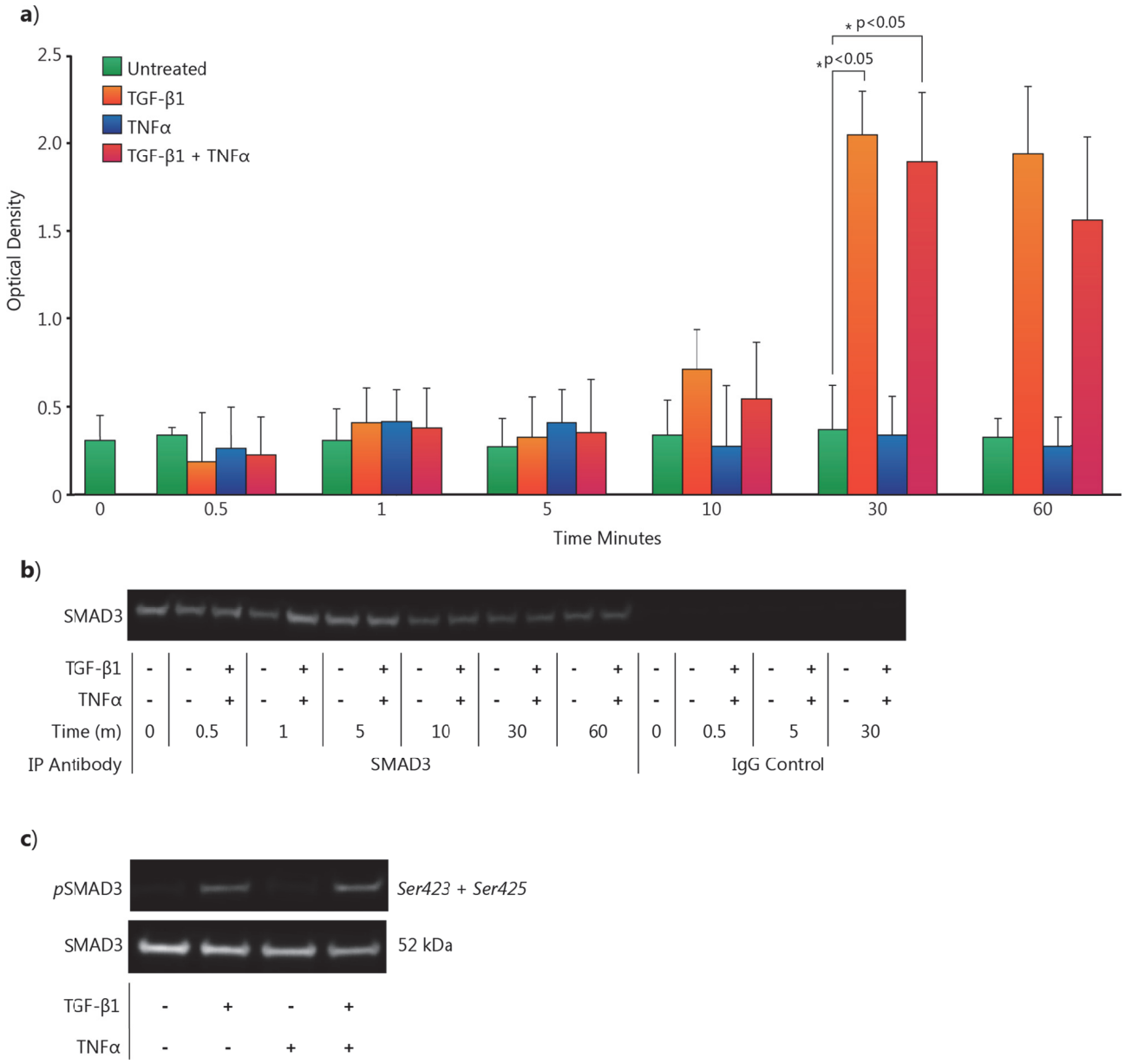

Figure 19 – SMAD3 phosphorylation response

a) TGF-β1 (10ng/mL) stimulation induced significant SMAD3 (*Ser423 + Ser425*) phosphorylation from 30 minutes in PBEC lysates immuno-precipitated against total SMAD3 under denaturing conditions. This significant phosphorylation was maintained through to 60 minutes. TNFα (20ng/mL) alone had no significant impact on SMAD3 phosphorylation at any time point. When used in conjunction with TGF-β1, TNFα had no significant impact on phosphorylation of SMAD3, however there was a trend for reduced levels of phosphorylation, particularly evident at the 60 minute time point. (all $p<0.05$, $n=3$).

b) Detected levels of SMAD3 did not vary significantly across stimulations, and SMAD3 was not present in control IgG lysates. 10µL of output lysate and 20µL wash were analysed.

c) In un-stimulated and TNFα stimulated PBECs phosphorylated SMAD3 was not detected, 30 minutes post stimulation with TGF-β1 there was a large increase in SMAD3 phosphorylation, which was not detectably affected upon co-stimulation with TNFα. *p*SMAD3 (20µg).

TGF-β1 induced a significant phosphorylation of SMAD3 at 30 minutes, which was also the peak phosphorylation value an effect which was maintained at 60 minutes, significance was nearly obtained at 10 minutes (p=0.058). TNFα alone had no impact on SMAD3 phosphorylation at any time point, when used in conjunction with TGF-β1.

These results confirm that in PBECs activation of SMAD3 is purely driven by TGF-β1, with TNFα displaying no role in activation.

4.1.2 Chemical Inhibition of SMAD3

Investigating the phosphorylation of signalling proteins in response to TGF-β1 or TNFα is one means of investigating their role in EMT. However, the previous data demonstrates that SMAD3 was activated in response to TGF-β1, not that it plays a role in EMT. To investigate relevance to EMT SMAD3 activity was chemically inhibited by Specific Inhibitor of SMAD3 (SMAD*i*). SMAD*i* functions by selectively blocking phosphorylation of SMAD3, but not SMAD2, thus inhibiting the formation of a transcriptionally active complex with SMAD4 (Jinnin et al., 2006) with an IC_{50} of 3μM determined in primary human fibroblast cultures.

A dose response curve looking at cell viability, morphology and effect on EMT after pre-treatment with 1, 5, 10 and 20μM doses of SMAD*i* prior to stimulation with TGF-β1 and TNFα for 72 hours was performed in triplicate using A549 cells.

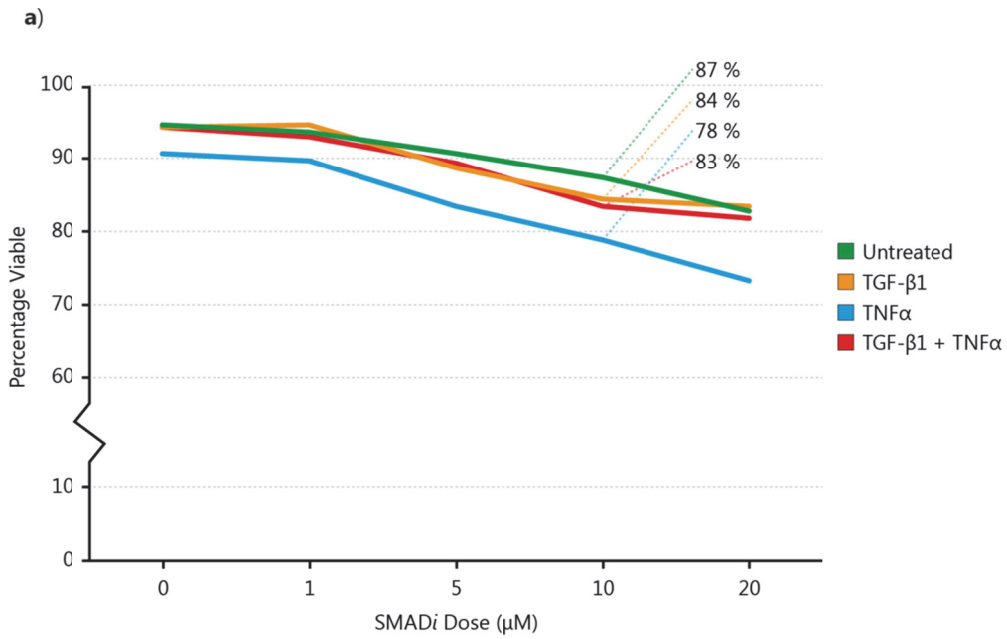

Figure 20 - SMAD*i* dose response

a) A549 cells were stimulated with TGF-β1 (10ng/mL) or TNFα (20ng/mL) for 72 hours after a 1 hour pre-treatment with SMAD*i* at 1, 5, 10 and 20μM doses (*n=3*). There was a general trend of decreased viability with increasing dose of SMAD*i* under all stimulations.

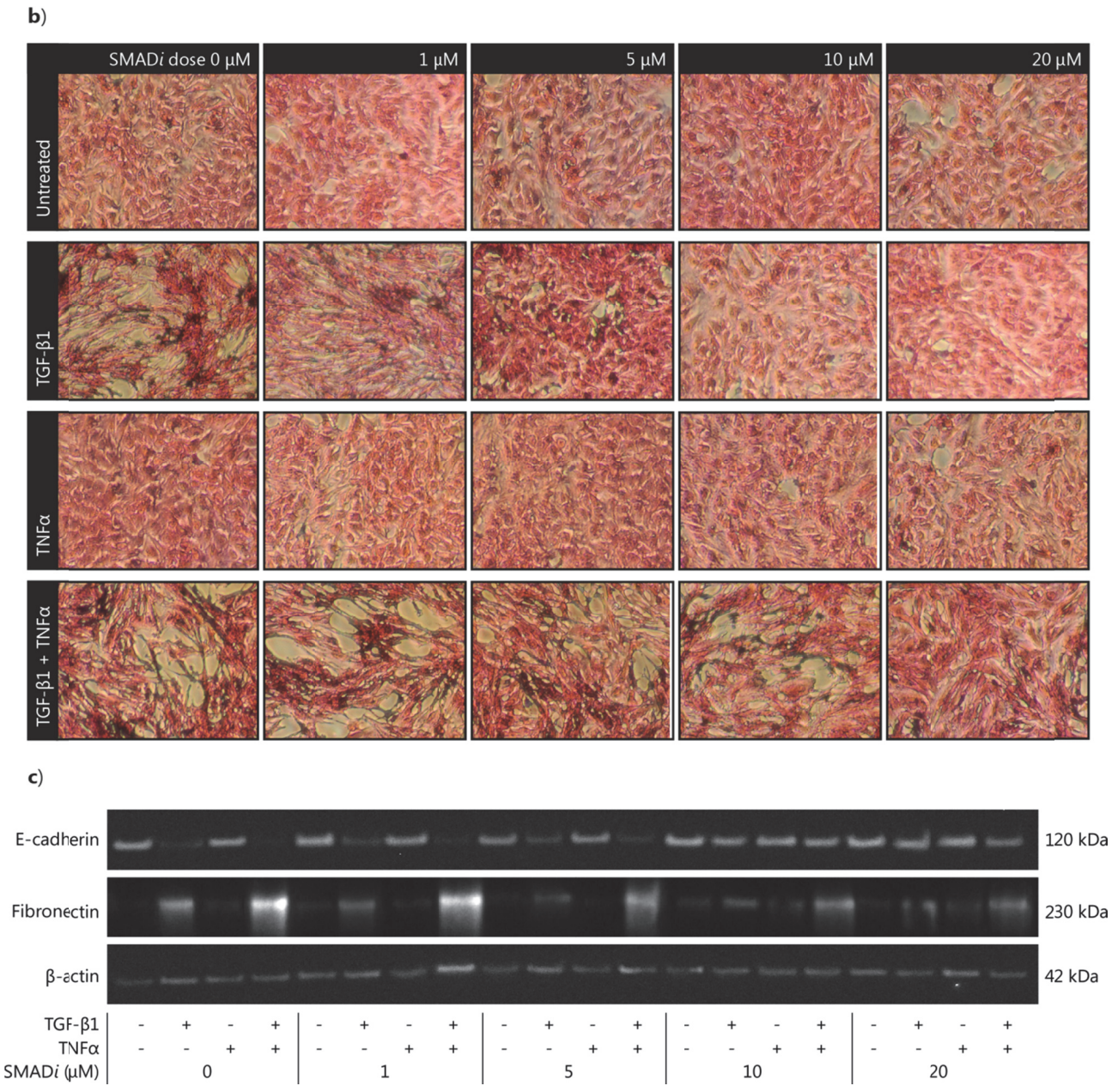

Figure 20 Continued - SMAD*i* dose response

b) 72 hours post stimulation with TGF-β1 there was a marked transition from the cobblestone like epithelial appearance of un-stimulated A549 cells towards a more striated, mesenchymal phenotype. This effect was accentuated by co-stimulation with TNFα, whereas TNFα alone had no effect on cell morphology. Increasing doses of SMAD*i* reduced the morphological shift induced by TGF-β1 or TGF-β1 and TNFα, with normal morphology retained at 10µM for TGF-β1 stimulated cells, and a 20µM dose strongly limiting the morphological transition associated with co-stimulation. E-cadherin and fibronectin (5µg)

c) E-cadherin expression was reduced upon TGF-β1 stimulation with an accentuated reduction upon co-stimulation with TNFα. SMAD*i* reversed this effect in a dose dependant manner with the strongest effect seen at 10µM. Fibronectin expression was increased upon stimulation by TGF-β1 with an accentuated increase upon co-stimulation with TNFα. As above SMAD*i* inhibited this effect in a dose dependant manner with the strongest effect seen at 10µM. The 20µM dose of SMAD*i* conferred no appreciable extra inhibition of TGF-β1 activity. E-cadherin, and fibronectin (5µg).

Inhibition of SMAD3 resulted in a dose dependant decrease in cell viability in all cells, a decrease that was perhaps exacerbated upon TNFα alone stimulation. The higher doses of 10μM and 20μM were the only doses capable of inhibiting EMT, both morphologically and at the protein level. The 20μM dose most strongly inhibited the morphological shift associated with EMT, but did not provide an appreciable inhibition EMT at the protein level over the 10μM dose; therefore a dose of 10μM SMAD*i*, which retained viability at a higher level, was used in all future experiments.

4.1.2.1 Chemical Inhibition of SMAD3, Effect on EMT Endpoint

With an appropriate dose of SMAD*i* decided upon in A549 cells the next step was to observe what effect this would have on EMT in PBECs. *n=4* PBEC cultures from distinct patients were stimulated with TGF-β1 or TNFα for 72 hours after a 1 hour pre-treatment with 10μM SMAD*i*. Cell lysate and culture media was retained and EMT was assessed using a variety of markers.

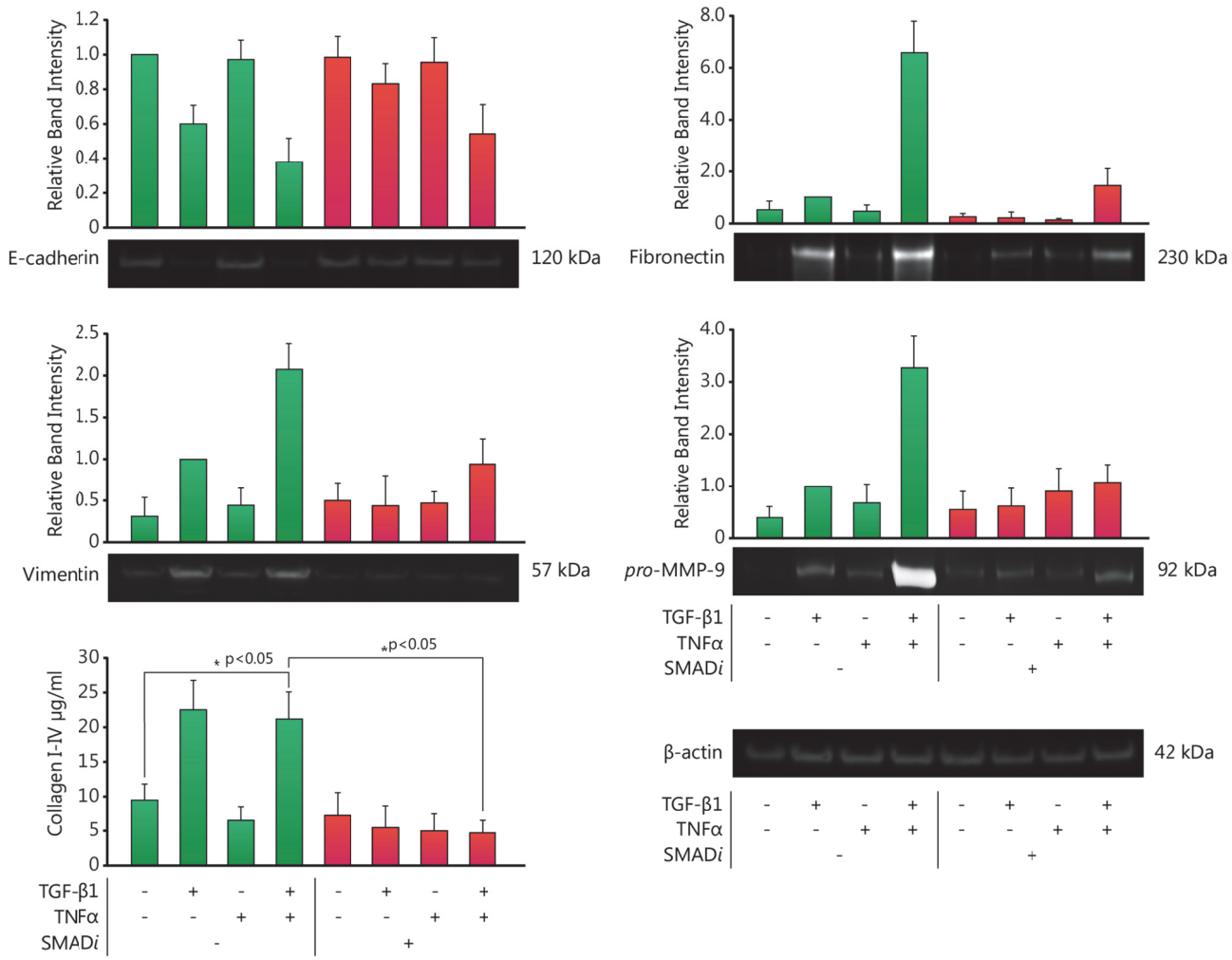

Figure 21 - Effect of SMAD*i* on EMT

Stimulation of PBECs (*n=4*, representative blots from single patient) with TGF-β1 (10ng/mL) for 72 hours down-regulated E-cadherin expression, increased fibronectin and vimentin expression and increased *pro*-MMP-9 secretion. This change in EMT marker expression was accentuated by co-stimulation with TNFα (20ng/mL). Collagen I-IV secretion was significantly up-regulated by stimulation with TGF-β1 ($p<0.05$, *n=4*) however no accentuation was observed upon co-stimulation with TNFα. Pre-treatment with SMAD*i* (10µM) strongly inhibited the TGF-β1 induced down-regulation of E-cadherin expression, the increase in fibronectin expression and, significantly, the increase in collagen I-IV secretion ($p<0.05$, *n=4*), returning levels to near baseline, and slightly reduced vimentin expression and *pro*-MMP-9 secretion. SMAD*i* also reduced EMT in co-stimulated PBECs for all markers when comparing untreated with treated, however an accentuative effect was still apparent for all markers with the exception of collagens I-IV when comparing SMAD*i* treated co-stimulated PBECs with equivalent TGF-β1 alone stimulated PBECs. E-cadherin and fibronectin (5µg), vimentin (20µg), *pro*-MMP-9 (30µL) and collagens I-IV (25µL).

The results described above provide strong evidence, that SMAD3 activation plays a key role in TGF-β1 driven EMT. A 10μM dose of SMAD*i* did not affect viability of PBECs compared to untreated controls. Pre-treatment with SMAD*i* strongly inhibited the loss of E-cadherin expression, gain in fibronectin expression and increase in collagens I-IV secretion in response to TGF-β1, whilst also inducing a small reduction in the expression of vimentin and secretion of *pro*-MMP-9. PBECs pre-treated with SMAD*i* also showed reduced levels of EMT in PBECs stimulated with TGF-β1 and TNFα when compared to untreated controls, however with the exception of collagen an accentuated response was still observed when compared to SMAD*i* treated, TGF-β1 stimulated PBECs. Interestingly SMAD*i* induced a reduction in collagen expression for all stimulations beyond that of untreated, un-stimulated controls.

4.1.2.2 Chemical Inhibition of SMAD3, Effect on Phosphorylation

As seen in **Figure 19** SMAD3 is phosphorylated in response to TGF-β1 alone, with no apparent role for TNFα. However, it is important to understand if SMAD3 phosphorylation is leading to activation of other signalling pathways, therefore I proceeded to investigate the effect of SMAD*i* pre-treatment on the phosphorylation of other key signalling proteins 30 minutes after stimulation with TGF-β1 or TNFα.

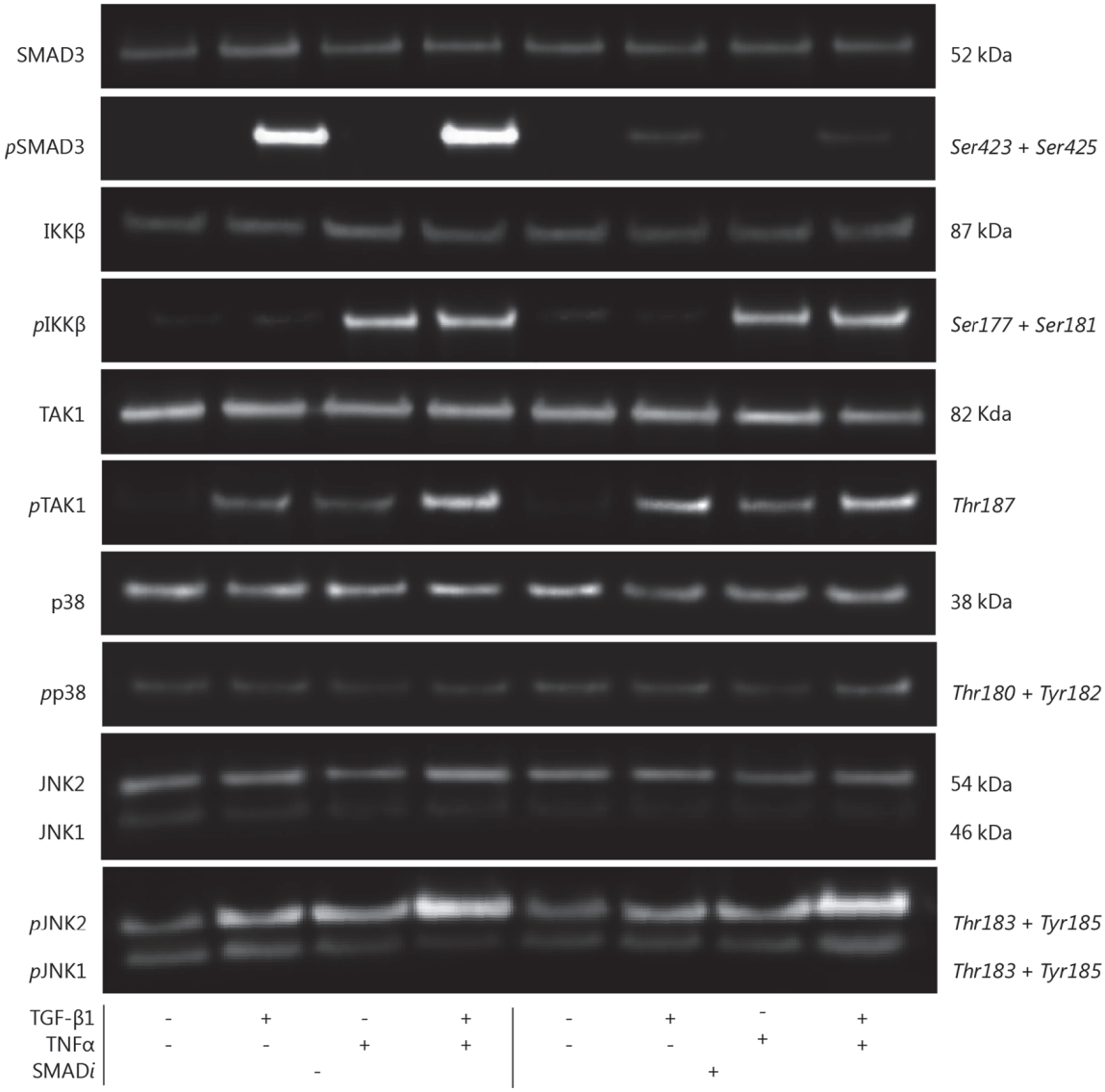

Figure 22 - Effect of SMAD*i* on key signalling proteins

SMAD3 was phosphorylated in PBECs (*n=3*, representative blots from single patient) 30 minutes post stimulation with TGF-β1 (10ng/mL) alone and this was not accentuated by TNFα (20ng/mL). IKKβ was phosphorylated in response to stimulation with TNFα alone and this was accentuated by co-stimulation with TGF-β1. Both TAK1 and JNK-2 were phosphorylated by stimulation with both TGF-β1 and TNFα alone and displayed an accentuated phosphorylation upon co-stimulation. JNK-1 and p38 displayed no increase in phosphorylation in response to stimulation with TGF-β1 or TNFα alone or in combination. Phosphorylation of SMAD3 in response to TGF-β1 stimulation was severely limited upon pre-treatment with SMAD*i* (10μM). After inhibition an increase in phospho-TAK1 was detected in TGF-β1 alone stimulated cells, all other phospho proteins were un-affected. *p*SMAD3 (20μg), *p*IKKβ and *p*p38 (40μg), *p*TAK1, *p*JNK-1/2 and JNK-1/2 (50μg).

SMAD3 was phosphorylated in response to TGF-β1 with no evidence of phosphorylation in response to TNFα alone, or in co-stimulation. There was also no detectable variation in intensity of phosphorylation between TGF-β1 alone and co-stimulated cells. SMAD*i* strongly inhibited the phosphorylation of SMAD3 whilst not affecting total levels. No difference in the phosphorylation of IKKβ, p38 or JNK-1/2 was detected in response to pre-treatment with SMAD*i*, suggesting that these pathways operate independently or upstream of SMAD3. TAK1 however displayed an increase in phosphorylation in response to TGF-β1 alone when PBECs were treated with SMAD*i*.

4.1.3 siRNA Knockdown of SMAD3

SMAD3 targeting siRNA (SMAD*si*) was used to knockdown SMAD3 in order to validate the findings generated using SMAD*i*. A dose response assay; for cell viability, morphology and effect on EMT after a 24 hour pre-treatment with 1, 5, and 10nM doses of SMAD*si* (ATCAAGGGATTTCCTATGGAA), delivered through lipid transfection of adherent cultures prior to stimulation with TGF-β1 and TNFα for 72 hours, was performed in PBECs.

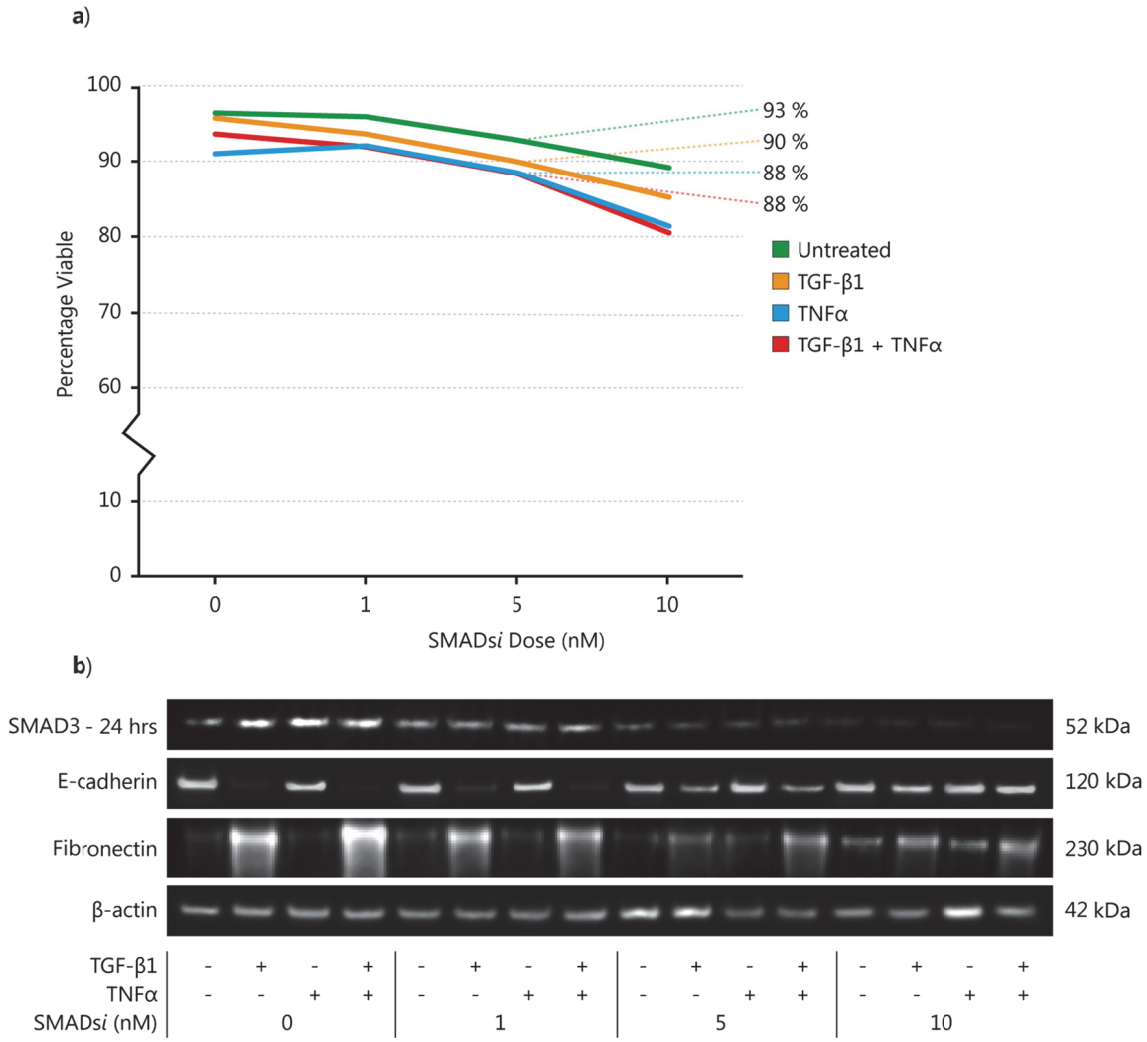

Figure 23 - SMAD*si* dose response

a) PBECs were stimulated with TGF-β1 (10ng/mL) or TNFα (20ng/mL) for 72 hours after a 24 hour pre-treatment with SMADs*i* at 1, 5 and 10nM doses (*n=3*). There was a general trend of decreased viability with increasing dose of SMAD*si* under all stimulations, with little variation between stimulations.

b) SMAD3 was not affected by stimulation by TGF-β1 or TNFα; however, detected levels of SMAD3 were reduced in a dose dependant fashion by treatment with SMAD*si*. A 1nM dose induced approximately a 40% reduction in total SMAD3, with 5nM a 75% drop and 10nM a 90% drop compared to untreated controls.

E-cadherin expression was reduced upon TGF-β1 stimulation with an accentuated reduction upon co-stimulation with TNFα. Fibronectin expression was increased upon stimulation by TGF-β1 with an accentuated increase upon co-stimulation with TNFα. SMAD*si* reversed this effect in a dose dependant manner, with the 1nM dose of SMAD*si* only marginally inhibiting the loss of E-cadherin and gain of Fibronectin under any stimulation. At 5nM EMT was strongly inhibited, with a 10nM dose capable of fully returning E-cadherin expression to baseline levels, but slightly increasing the detected levels of fibronectin in response to all stimulations. E-cadherin, fibronectin and SMAD3 (5µg).

SMAD3 expression was reduced in a dose dependant manner by pre-treatment with SMAD*si*, with a general but shallow decrease in cell viability. The loss of E-cadherin expression in response to TGF-β1 or TNFα stimulation was also inhibited in a dose dependant manner, with a 10nM dose of SMAD*si* capable of returning levels to baseline. The gain of fibronectin in response to TGF-β1 or TNFα stimulation was weakly inhibited by the 1nM dose of SMAD*si*, with a strong effect seen at 5nM. The 10nM dose of SMAD*si* increased the detected levels of fibronectin for all stimulations compared with the 5nM treatment group. Therefore although the 10nM dose induced the strongest recovery of E-cadherin, a 5nM dose which inhibited fibronectin expression more efficiently, and without affecting un-stimulated expression, was used for all future experiments.

4.1.3.1 siRNA Knockdown of SMAD3, Effect on EMT Endpoint

With an appropriate dose of SMAD*si* confirmed for use in PBECs I proceeded to investigate what effect SMAD3 knockdown had on EMT. *n=3* PBEC cultures from distinct patients were stimulated with TGF-β1 or TNFα for 72 hours after a 24 hour pre-treatment with 5nM SMAD*si* or a sequence scrambled control. Cell lysate and culture media was retained and EMT was assessed using a variety of markers.

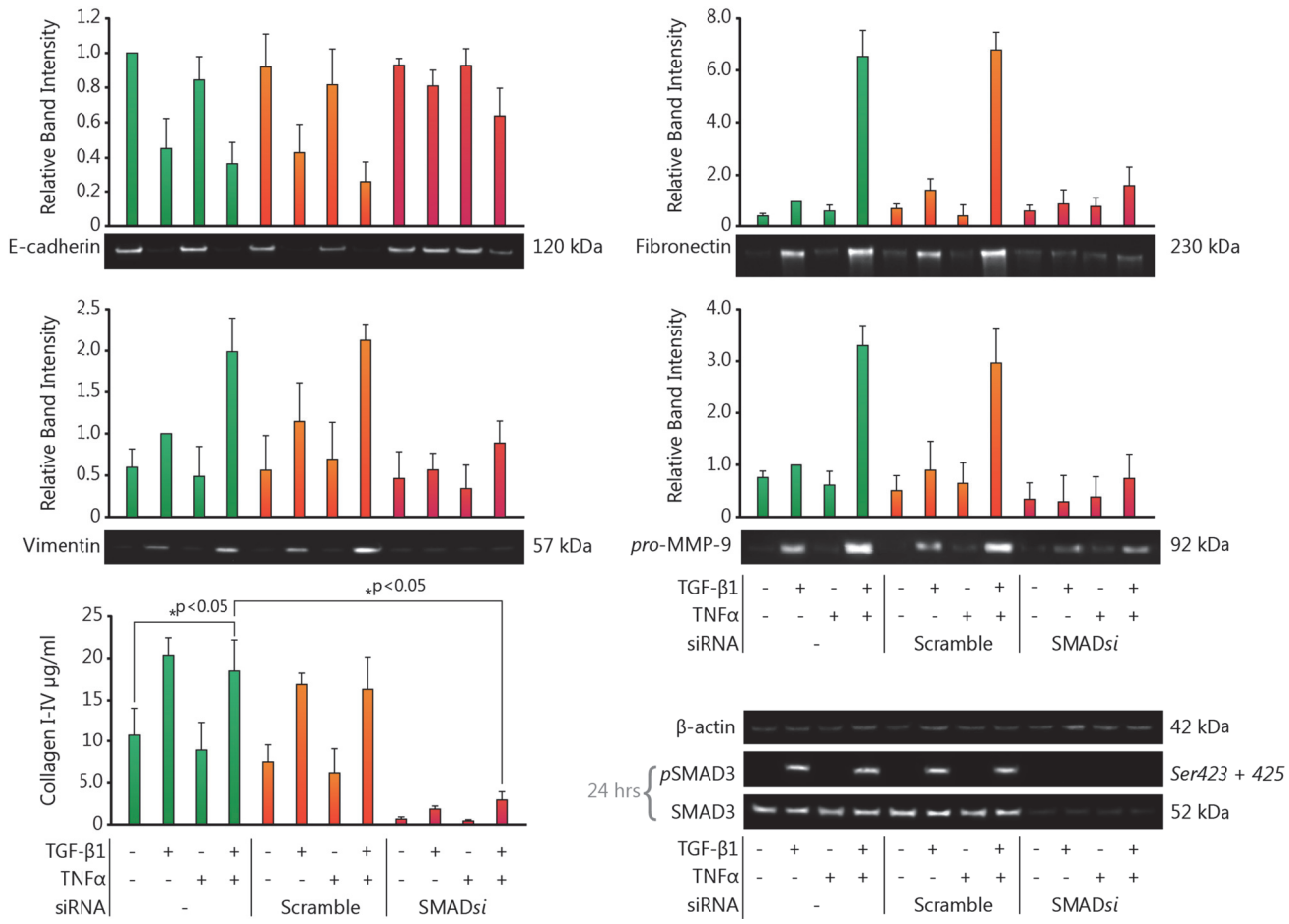

Figure 24 - Effect of SMAD*si* on EMT

Stimulation of PBECs (*n=3*) with TGF-β1 (10ng/mL) for 72 hours down-regulated the expression of E-cadherin, increased the expression of fibronectin and vimentin and increased *pro*-MMP-9 secretion compared to control cells with this effect accentuated by co-stimulation with TNFα (20ng/mL), with the exception of E-cadherin where this effect was more additive in nature. Collagen I-IV secretion was significantly up-regulated by stimulation with TGF-β1 but no accentuation was observed upon co-stimulation with TNFα ($p<0.05$, *n=3*). SMAD*si* (5nM) both the TGF-β1 induced and TNFα accentuated down-regulation of E-cadherin expression, the increase in fibronectin and vimentin expression and the increase in collagen I-IV ($p<0.05$, *n=3*) and *pro*-MMP-9 secretion compared to untreated controls. However an accentuated response was still apparent for all markers with the exception of collagens I-IV when comparing *SMADsi* treated co-stimulated PBECs with equivalent TGF-β1 alone stimulated PBECs. No effect on EMT marker expression was seen using a sequence scramble control.

Approximately 90% knockdown of SMAD3 was achieved by SMAD*si* after 24 hours. Neither a sequence scramble control nor the lipid vector had any effect on SMAD3 knockdown, cell viability or morphology. This reduction in total SMAD3 also led to a complete loss of detected phospho-SMAD3 30 minutes after stimulation with TGF-β1 or TNFα with no effect on SMAD3 phosphorylation seen with either the lipid vector or sequence scramble control. E-cadherin and fibronectin (5µg), vimentin and *p*SMAD3 (20µg), *pro*-MMP-9 (30µL) and collagens I-IV (25µL).

The data presented above validates the findings described with SMAD*i* in **4.1.2**. A 5nM dose of SMAD*si* derived from the screen described in **4.1.3** induced approximately a 75% knockdown in detected total SMAD3, with the subsequent loss of detected phospho-SMAD3 without affecting PBEC viability. Pre-treatment of PBECs with SMAD*si* strongly inhibited the loss of E-cadherin and the gain of fibronectin and vimentin intracellularly, as well as the increase in secretion of *pro*-MMP-9 and collagens I-IV into the media in response to TGF-β1 stimulation, and upon co-stimulation in comparison to untreated controls. However, as with SMAD*i* evidence of a residual accentuation was observed when comparing PBECs pre-treated with SMAD*si* and stimulated with TGF-β1 and TNFα with equivalent TGF-β1 alone stimulated PBECs, confirming that SMAD3 alone does not mediate accentuated EMT. Interestingly SMAD*si* pre-treatment also reduced collagen expression for all stimulations beyond that of untreated, un-stimulated controls, similarly to the effect observed with SMAD*i*.

4.1.4 Localization of SMAD3

Both chemical inhibition and siRNA knockdown of SMAD3 suggested that it plays a key role in EMT, and the phosphorylation assays indicate that solely TGF-β1 alone is capable of driving its phosphorylation. However as discussed above phosphorylation alone does not constitute transcriptional activity as the rSMADs are required to translocate to the nucleus and bind with co-factors to alter transcription. To investigate this further I looked at the localization of both total and phospho-SMAD3 30 minutes post stimulation with TGF-β1 or TNFα in PBECs.

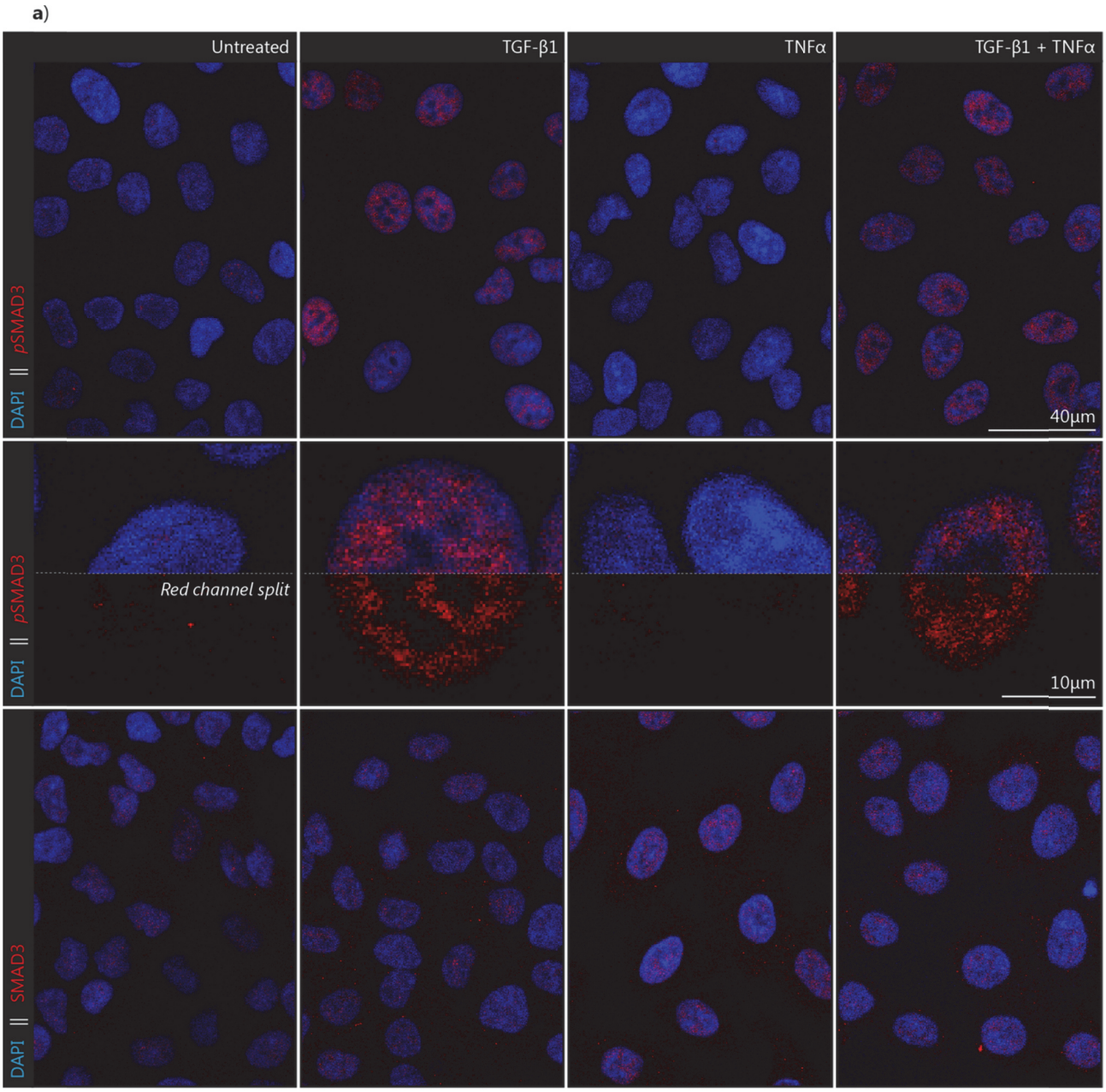

Figure 25 - Localization of SMAD3 and *p*SMAD3

a) PBECs stimulated with TGF-β1 (10ng/mL) or TNFα (20ng/mL) for 30 minutes were assessed for changes in SMAD3 (*Ser423 + Ser425*) phosphorylation displaying in the red (TRITC) channel with DAPI as a nuclear counterstain. Un-stimulated and TNFα alone stimulated PBECs display no evidence of phospho-SMAD3 in the TRITC channel in any cellular compartment. Stimulation with TGF-β1 or co-stimulation with TGF-β1 and TNFα resulted in increased phosphorylation of SMAD3 with a marked localization to the nucleus, with little evidence of phospho-SMAD3 in the cytoplasm. There was no change in total SMAD3 expression or localisation that was detected diffusely in all compartments.

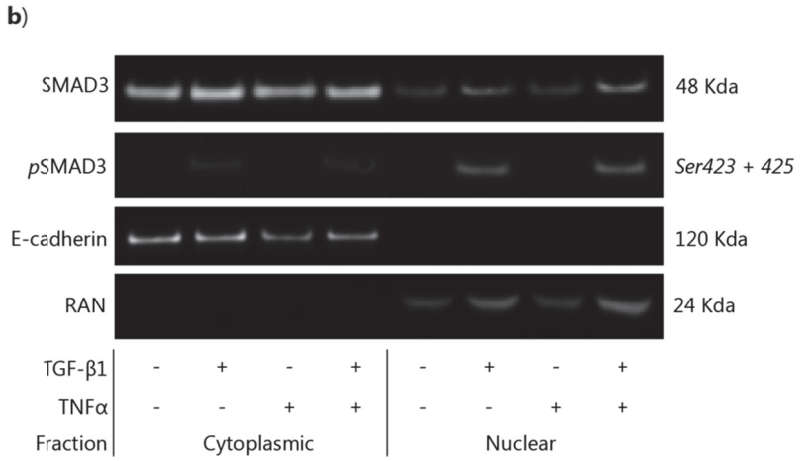

Figure 25 Continued' - Localization of SMAD3 and *p*SMAD3

b) Total PBEC lysates (*n=2*, representative blots from single patient) treated as above were separated into nuclear and non-nuclear fractions, 20µg of non-nuclear lysate and 5µg of nuclear lysate was then separated by SDS-PAGE and probed for SMAD3 and phopho-SMAD3 along with E-cadherin and RAN as fractionation controls. SMAD3 was detected in both the nucleus and the cytoplasm, in the nuclear fraction there was slightly more SMAD3 detected in co-stimulated or TGF-β1 alone stimulated PBECs. Again phospho-SMAD3 was detected only in stimulations containing TGF-β, with a low amount detected in the cytoplasmic fraction; more intense bands were detected in the nuclear fraction, especially considering the relative amounts of protein loaded.

Both ICC and lysate fractionation protocols demonstrated that phospho-SMAD3 localized to the nucleus in response to both TGF-β1 alone and TGF-β1 with TNFα stimulations, unlike in **Figure 19** there was no detectable difference in the level of phosphorylation between TGF-β1 and co-stimulated PBECs. However, the results for the total-SMAD3 were conflicting; ICC showed a diffuse level of total-SMAD-3 throughout the cell, whereas lysate fractionation showed a greater localisation to the cytoplasm. It is possible that proteins present in the nuclear fraction are being degraded due to their longer isolation protocol and hence longer time in detergent solutions, however I can present no data to support this and the protocol is designed to limit protein degradation. Therefore, although the phospho-SMAD3 results correlate with previous findings the lack of reliable total-SMAD3 data means it is not possible to comment on phospho-SMAD3 localization in this system.

4.1.5 SMAD3 Protein Associations

As discussed previously the binding efficiency of SMAD3 to SBEs is low and often requires SMAD4 mediated association with a variety of co-factors (Shi et al., 1998; Dennler et al., 1999). It was therefore decided to investigate the associations of SMAD3 with other selected proteins, after stimulation, assessed as part of this project.

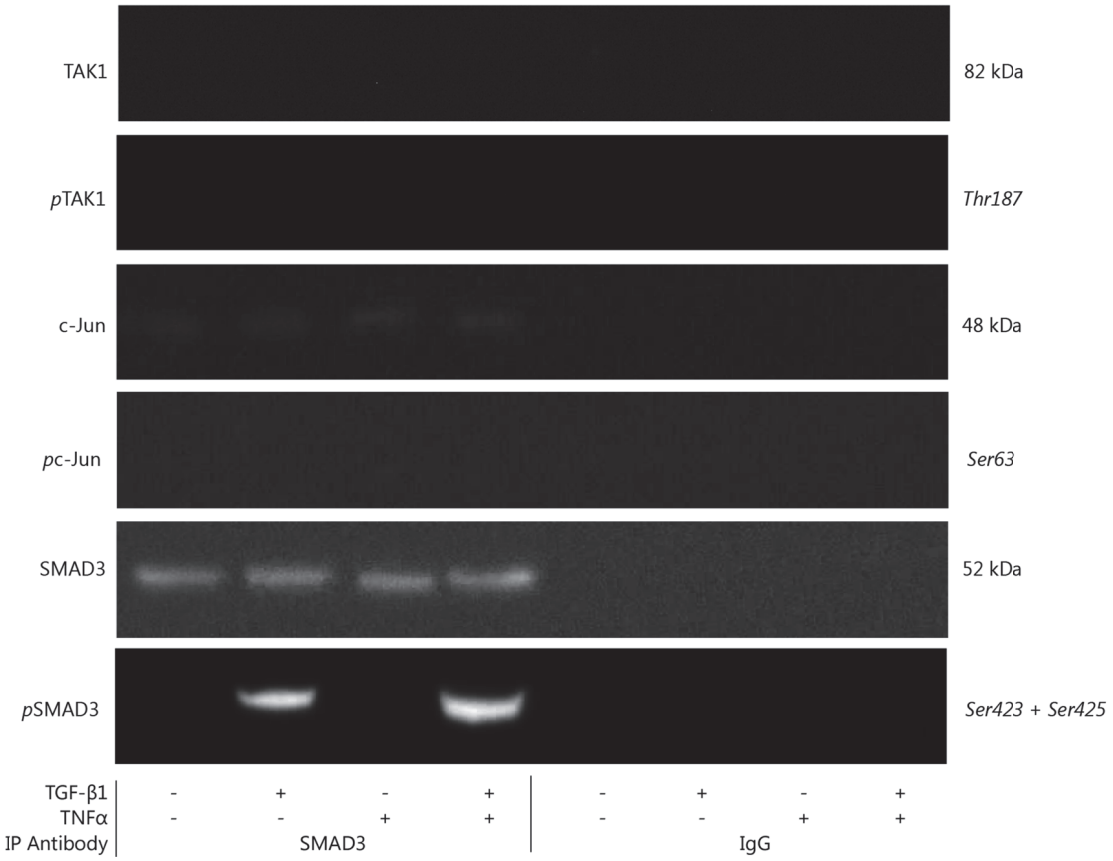

Figure 26 - SMAD3 protein associations

Total PBEC lysates (20µg, *n=2*, representative blots from single patient) stimulated with TGF-β1 (10ng/mL) or TNFα (20ng/mL) for 30 minutes were immuno-precipitated against total SMAD3, or pan-IgG under non-denaturing conditions. Neither total nor phosphorylated TAK1 were associated with SMAD3 at 30 minutes, and similarly no phospho-c-Jun. However a constitutive association of c-Jun with SMAD3 under all stimulations was observed. No bands were detected in the pan-IgG controls.

Neither total nor phosphorylated forms of TAK1 were associated with SMAD3 30 minutes post-stimulation. c-Jun was constitutively associated at this time point, however its phosphorylated form was not.

4.1.6 SMAD3 Discussion

The role of SMAD3 in the accentuation of TGF-β1 driven fibrosis by TNFα was investigated first due to its well described role in canonical TGF-β1 signalling. To summarize the data presented in the preceding sub-chapter: SMAD3 was phosphorylated by TGF-β1 alone peaking towards the later time points of 30 and 60 minutes, TNFα alone had no effect on phosphorylation. Inhibition and knockdown of SMAD3 strongly limited TGF-β1 driven EMT although seemingly did not affect the accentuation of TNFα, although this was difficult to determine due to the very weak EMT driving effect of TNFα alone.

SMAD*si* was also capable of strongly inhibiting TGF-β1 driven EMT, yet in this instance when comparing PBECs within the treated group the effects are less clear with a relative reduction in the accentuated increase in fibronectin and vimentin expression and *pro*-MMP-9 secretion. The continued accentuation of EMT in chemically inhibited cells may be due to residual un-inhibited SMAD3 signalling providing a reduced fibrotic development which TNFα can still accentuate, with a smaller accentuation seen with SMAD*si* due to a stronger inhibitory; based on the lack of detection of any phospho-SMAD3 after SMAD*si*.

This suggested that SMAD3 does not play a direct role in the accentuation of EMT, acting more as the base inducer of fibrosis, with another signalling protein driving the accentuation. However what is not known is if this signalling protein is also stimulated by TGF-β1, which may explain the residual EMT seen in some instances after TGF-β1 alone stimulation, or after co-stimulation. Another interesting finding, was that upon SMAD3 inhibition TAK1 phosphorylation was increased in TGF-β1 alone stimulated PBECs. This may indicate that there is some level of redundancy in TGF-β1 signalling, which may be responsible for the low levels of EMT detected in inhibited PBECs rather than, or in conjunction with, residual SMAD activity. Whilst evidence of redundancy has not previously been described a synergistic mechanism by which rSMADs[7] and TAK1 act co-operatively through ATF-2 to induce transcription (Sano et al., 1999; Monzen et al., 2001). It does however demonstrate the requirement for SMAD3 activity to drive EMT, as

[7] *Used because one paper utilises TGF-β1 and the other a BMP cocktail, hence different rSMADs were investigated.*

even though TAK1 and JNK-2 remained active after SMAD3 inhibition they were not capable of strongly driving EMT, if at all.

The exception to this effect of residual EMT after inhibition was collagen I-IV secretion. In un-treated cells collagen secretion was increased by TGF-β1 but not by TNFα, which also did not accentuate TGF-β1 driven secretion upon co-stimulation; with a very slight decrease in secretion actually observed upon co-stimulation. Both SMAD*i* and SMAD*si* very strongly inhibited the secretion of collagen beyond the baseline levels detected from control cells. These findings would suggest that TGF-β1 canonical signalling is the key mediator of collagen secretion, with TNFα playing no role; and also that some form of constitutive SMAD3 activation is occurring in PBECs to maintain a baseline of secretion.

The requirement for a baseline of SMAD3 activity in maintenance of collagen expression in pulmonary fibroblasts has previously been described (Luzina et al., 2006), whereby stimulation with chemokine CCL18 induced secretion of collagen, but with a requirement for active SMAD3 (Chen et al., 1999, 2000). Several other groups have demonstrated that TNFα is capable of inhibiting collagen secretion either through NF-κB or the MAPK (Armendariz-Borunda et al., 1992; Verrecchia et al., 2002) with one group proposing that p38 may be the key mediator of this effect (Varela-Rey et al., 2002). In their paper Varela-Rey *et al*. demonstrate that TNFα inhibits p38 phosphorylation and by mimicking this effect with an inhibitor of p38 they were able to limit the production of collagen after TGF-β1 stimulation. They do not however directly demonstrate this relationship by co-stimulating cells with TGF-β1 and TNFα (Varela-Rey et al., 2002). The mechanisms of SMAD inhibition by TNFα I describe above would also provide a mechanism by which TNFα could inhibit the primarily TGF-β1 driven secretion of collagen.

It is important to point out however that in another study TNFα induced collagen gene expression through the less common TNFR2, and not TNFR1, in intestinal myofibroblasts (Theiss et al., 2005). A tangential area of research that I performed looked at the role of differing TNFα receptors in accentuating EMT 8.7, which demonstrated that PBECs do not express TNFR2. This may explain why no accentuation in collagen secretion was observed both in this work and in the other referenced studies that do not differentiate between receptor expression.

As a final comment, in hindsight the very strong blocking of SMAD3 activity by chemical inhibition and siRNA knockdown demonstrated its importance as a driver of fibrosis. However, due to the weak effect of TNFα alone on driving EMT, it became difficult to determine the relative contributions of TGF-β1 or

TNFα to EMT in co-stimulated PBECs after inhibition. Using a lower dose of both SMAD*i* and SMAD*si* that inhibited EMT to a lesser extent might have made quantification of contribution easier.

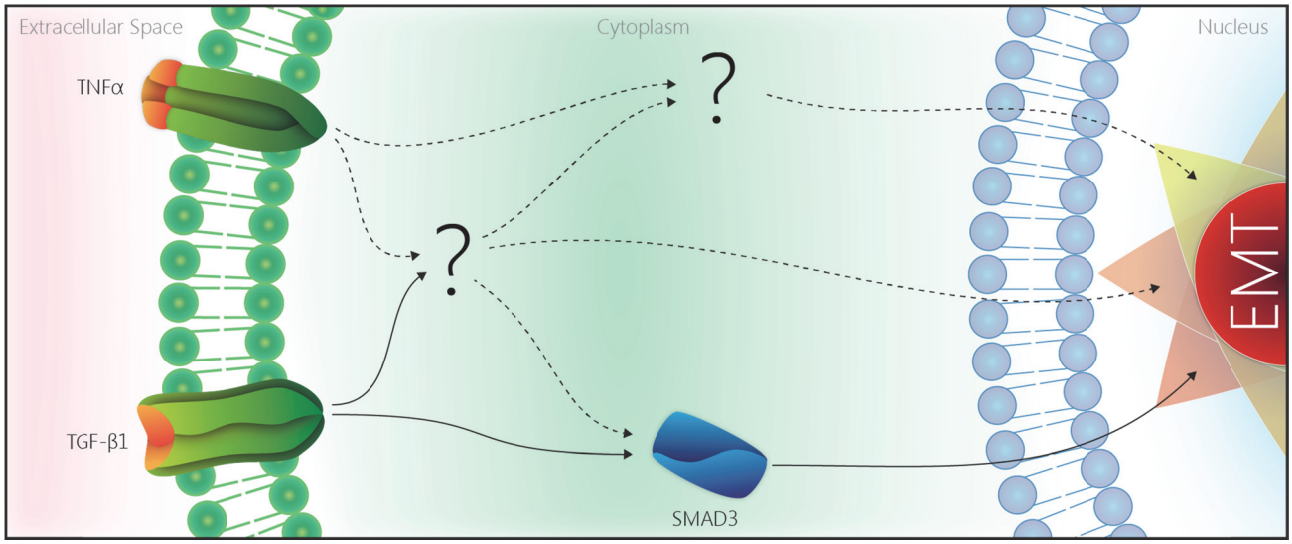

Figure 27 - Proposed Signalling Mechanism I

TGF-β1 signals through the canonical SMAD pathway, utilising SMAD3 and induces EMT, independently of TNFα. SMAD3 is required for TGF-β1 mediated EMT as the un-inhibited activation of TAK1 was not capable of driving EMT strongly, but may provide some slight redundancy. An accentuatory mediator remains unknown, as does the mechanism for TNFα to effect EMT.

By demonstrating that SMAD3 plays a key role in TGF-β1 driven EMT, but not in its accentuation by TNFα the next step is to identify a signalling protein that does. Logically this suggested looking within the canonical TNFα NF-κB pathway.

4.2 IkB kinase Beta

The IKK family of proteins (IKKα/1, IKKβ/IKK2 and IKKγ/NF-κB essential modulator [NEMO]) play a key role in the canonical NF-κB activation pathway by factors such as TNFα and IL-1β. IKKα and β contain kinase sites and are responsible primarily for the phosphorylation of Iκ-Bα and subsequent activation of NF-κB signalling. IKKγ does not contain a kinase site but is required for IKKα/β kinase activity (Yamaoka et al., 1998), recruiting them into a larger IKK complex.

The exact makeup of this complex is not fully understood, and variations likely demonstrate a level of control that is currently not understood. Both IKKα and IKKβ bind to IKKγ through a conserved sequence at their C-terminal, to various N-terminal sequences of IKKγ (May et al., 2000; Tegethoff et al., 2003). Further experiments demonstrated that IKKβ binds to IKKγ with a higher efficiency, although given the conserved C-terminal of IKKα and IKKβ it is not known what mediates this effect (May et al., 2000); although weaker co-bindings have been implicated in this effect (Miller and Zandi, 2001). This is also balanced somewhat by the demonstration that IKKα and IKKβ preferentially form hetrodimers over homodimers *in vivo* before binding with IKKγ (Huynh et al., 2000). It is thought that IKKγ binds with IKKα and IKKβ in a 1:1 ratio, but as mentioned above the exact makeup of the complexes is poorly understood, with hexamer[8] (Agou et al., 2004) and octamer (Tegethoff et al., 2003) forms proposed, with the latter allowing for the binding of two IKKα/β heterodimers.

In un-stimulated cells IKKα and IKKβ are thought to be inactive due to a lack of phosphorylation in their respective activation loops, hiding their kinase site, with activation mediated by activation of IKKγ. Several methods of IKKγ activation have been proposed, phosphorylation at *Ser85* by Ataxia Telangiectasia Mutated (ATM) in the nucleus (Wu et al., 2006), or polyubiquitination of *Lys285* (Abbott et al., 2004) and *Lys399* (Sun et al., 2004) residues by RIP2 and TRAF6 respectively. Whether all these activations are required or just examples of control of function depending on stimuli is not known.

It is thought that the ubiquitination of IKKγ brings the IKK complex into association with other important factors in NF-κB signal modulation such as RIP1 (Ea et al., 2006)which is itself polyubiqitinated, or with TAK1 associated with polyubiqitinated TAB proteins (Wang et al., 2001). This association allows for the phosphorylation of IKKα at *Ser176* and *Ser180* residues and of IKKβ at *Ser177* and *Ser181* (Delhase et al., 1999). The main role of activated IKKβ, over IKKα, is the phosphorylation of Iκ-Bα; which masks the nuclear localization signal of active NF-κB dimers, holding them in the cytoplasm (Jacobs and Harrison,

[8] *Three IKKγ monomers with three IKKα or IKKβ*

1998). Active IKKβ phosphorylates Iκ-Bα at *Ser32* and *Ser36* residues (DiDonato et al., 1996) which recruits an E3 ubiquitin ligase to Iκ-Bα which is phosphorylated in a *Lys48* dependant manner at *Lys21* and *Lys22* (Alkalay, 1995) prior to degradation in the proteasome.

Both IKKα and IKKβ play roles outside of this degradation of Iκ-Bα, with both having roles in NF-κB subunit modification. Both p100 and p105 contain residues that match those of Iκ-Bα, and are thought to act in a similar way, by inactivating their NF-κB dimer partner in the cytoplasm. It was, and often still is, thought that p105 is transcribed from the *NFKB1* gene and subsequently cleaved into its active p50 form. However it was demonstrated that p50 is actually produced alongside p105 by modifications made during translation (Lin et al., 1998). However IKKβ can cleave p105 by phosphorylating *Ser927* and *Ser932* residues of p105 leading to ubiquitination and proteasome processing, which either leads to the complete degradation of p105, or the production of p50 (Cohen et al., 2004). Degradation of p105 can free the inactive dimer, whereas cleavage of p105 to p50 can produce an already formed active dimer pairing, independent of Iκ-Bα activity. Similarly, IKKα is capable of cleaving p100 into its active p52 form, although in this instance the majority of p52 is formed by cleavage of p100. IKKα phosphorylates p100 at *Ser866* and *Ser870* which as above leads to ubiquitination and subsequent cleavage of p100 (Senftleben et al., 2001).

Mechanisms for the termination of IKKβ mediated signalling are poorly understood. One proposed mechanism is auto-inhibition whereby IKKβ phosphorylated in its activation loop phosphorylates its own C-terminal region weakening its association with IKKγ and thus terminate its activation (Delhase et al., 1999; May et al., 2002). Another is the usage of phosphatases such as PP2A, which have been shown to associate with phosphorylated IKK complexes, remove the phosphate groups from the activation loop and decrease their kinase activity (Prajapati et al., 2004); or de-ubiquitinating enzymes such as A20 which remove the ubiquitin scaffolds that mediate the phosphorylation of signalling components (Wertz et al., 2004). Increased production of inhibitory proteins has also been implicated, including Iκ-Bα, transcription of which is regulated by NF-κB dimers in a negative feedback loop (Scott et al., 1993; Hoffmann et al., 2002).

Several studies have demonstrated that of IKKα and IKKβ, IKKβ plays a more important role in canonical NF-κB signalling (Hu et al., 1999; Li et al., 1999) and this is now generally accepted to be the case. As such I focused my attention on IKKβ over IKKα. TNFα is present at elevated levels before the development of BOS, and accentuates TGF-β1 driven EMT in PBECs. As this accentuative activity was not controlled by SMAD3 the next logical pathway to investigate was the canonical TNFα cascade utilising

NF-κB, with IKKβ being a key kinase regulating its transcriptional activity. The following results outline my attempts to understand IKKβ phosphorylation in response to TGF-β1 or TNFα stimulation as well as its role, and importance, in the subsequent occurrence of EMT in our OB model system.

4.2.1 Phosphorylation Response of IKKα/β

PBECs were cultured in 6 well collagen coated plates until confluent and stimulated with TGF-β1 or TNFα. Cells were harvested at 0, 0.5, 1, 5, 10, 30 and 60 minute time points. Whole cell PBEC lysate was immuno-precipitated for total SMAD3, under denaturing conditions, with the resulting lysate probed for *p*IKKβ (*Ser177* and *Ser181*) by indirect ELISA. Neat lysate from the 30 minute stimulation was analyzed by Western blot for both total and phospho forms of IKKβ.

The antibodies used in this protocol targeted both IKKα and IKKβ, although as demonstrated in APPENDIX IKKα was usually only detected via western blots loaded with a very high lysate. Western blotting allows for the differentiation of IKK isoforms based on their different electrophoretic mobility, however the immuno-precipitation and indirect ELISA protocols allow for no such separation. No IKKα was detected by western blotting of the immuno-precipitated lysate, and a single band was observed after Coomassie staining of the agarose gel, nevertheless it is likely that there is some contamination of lysates with IKKα, which may effect this more sensitive assay.

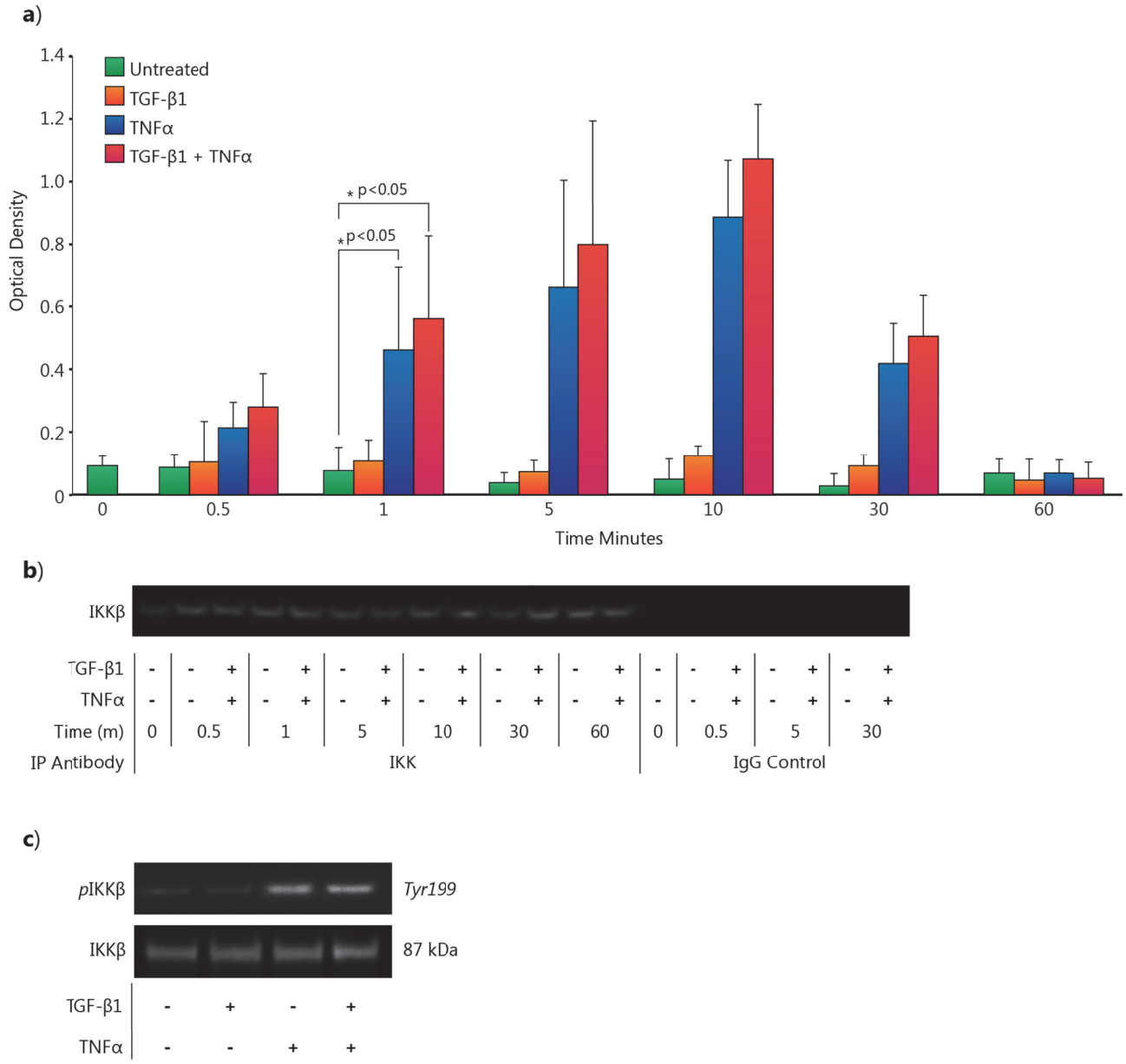

Figure 28 - IKKα/β phosphorylation response

a) TGF-β1 (10ng/mL) stimulation did not induce significant IKKα/β (*Ser177* + *Ser181*) phosphorylation at any time point. in PBEC lysates immuno-precipitated against total IKKα/β under denaturing condition. Stimulation with TNFα (20ng/mL) induced significant phosphorylation from 1 minute, peaking at 10 minutes and maintained this significant phosphorylation through to 30 minutes. Co-stimulation of PBECs with TGF-β1 and TNFα induced a similar pattern to that of TNFα alone (all $p<0.05$, *n=3*).

b) Detected levels of IKKα/β did not vary significantly across stimulations, and was not present in IgG control lysates.

c) TGF-β1 did not increase phosphorylation of IKKβ 30 minutes post-stimulation, whereas TNFα stimulation induced a strong phosphorylation response. Co-stimulation resulted in a strong phosphorylation response similar to that induced by TNFα alone. *p*IKKβ (40µg).

TNFα alone and in combination with TGF-β1 induced significant phosphorylation of IKKα/β from 1 minute, which peaked at 10 minutes and lasted through to 30 minutes, at 60 minutes levels were returned to baseline. Interestingly TGF-β1 alone did not increase phosphorylation at any time-point.

4.2.2 Chemical Inhibition of IKKβ

As previous experiments have demonstrated that TNFα alone had little if any effect on the development of EMT, the focus was on the response to co-stimulation. This was especially true due to the above results demonstrating that co-stimulation with TGF-β1 increased TNFα mediated IKKβ phosphorylation, whilst not phosphorylating IKK itself.

IKK-2 (IKKβ) Inhibitor IV (IKK*i*) is a cell permeable inhibitor of IKKβ isolated from fungi and functions by blocking ATP binding sites, and hence kinase activity responsible for phosphorylation of Iκ-Bα . Due to the wide range of signalling responses that IKKβ is involved in several papers have previously utilised IKK*i* and accordingly described an IC_{50}. In human monocytes a dose of between 170 and 320nM was capable of limiting TNFα production by half (Podolin et al., 2005), whereas in a cell free system, whereby IKKβ was immuno-precipitated from human synovial fibroblast cells and used in a kinase assay, an IC_{50} of 11μM was described (Kishore et al., 2003). A dose response curve looking at cell viability, morphology and effect on EMT after pre-treatment with 1, 5, 10 and 20μM doses of IKK*i* prior to stimulation with TGF-β1 and TNFα for 72 hours was performed in triplicate using A549 cells.

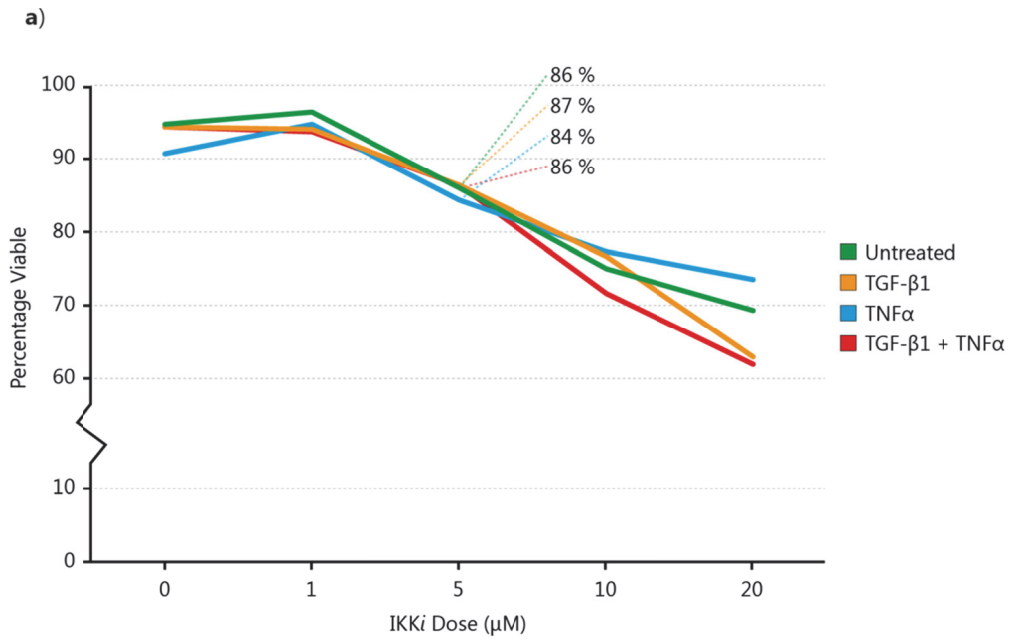

Figure 29 - IKK*i* dose response

a) A549 cells were stimulated with TGF-β1 (10ng/mL) or TNFα (20ng/mL) for 72 hours after a 1 hour pre-treatment with IKK*i* at 1, 5, 10 and 20μM doses (*n=3*). There was a strong trend of decreased viability with increasing dose of IKK*i* under all stimulations with little variation between stimulations, until 20μM where TGF-β1 stimulation induced a greater decrease in viability.

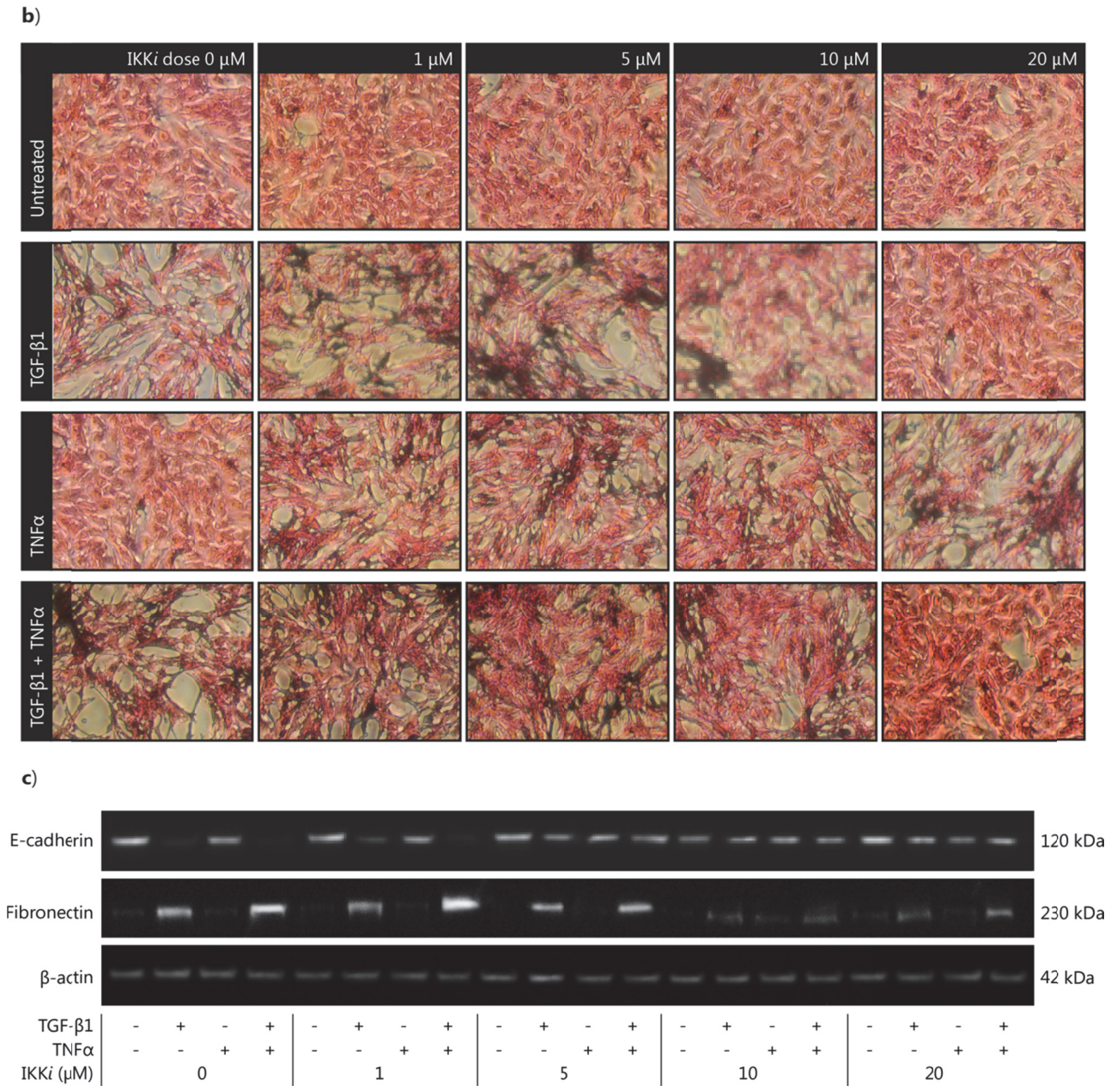

Figure 29Continued - IKK*i* dose response

b) 72 hours post stimulation with TGF-β1 there was a marked transition from the cobblestone like epithelial appearance of un-stimulated A549 cells towards a more striated, mesenchymal phenotype. This effect was accentuated by co-stimulation with TNFα, whereas TNFα alone had no effect on cell morphology. Increasing doses of IKK*i* reduced the morphological shift induced by TGF-β1 or TGF-β1 and TNFα, with normal morphology retained at a 20µM for both. Stimulation with TNFα in the presence of IKK*i* induced a transition to a more striated mesenchymal phenotype in a dose dependant manner.

c) E-cadherin expression was reduced upon TGF-β1 stimulation with an accentuated reduction upon co-stimulation with TNFα. SMAD*i* reversed this effect in a dose dependant manner with the strongest effect seen at 10µM. Fibronectin expression was increased upon stimulation by TGF-β1 with an accentuated increase upon co-stimulation with TNFα. IKK*i* reversed this effect in a dose dependant manner with the strongest effect seen at 20µM, although there was an appreciable difference at 5 and 10µM doses. E-cadherin and fibronectin (5µg).

IKK*i* at doses of 5μM and above was capable of strongly inhibiting the loss of E-cadherin expression in response to stimulation with TGF-β1 or TNFα with no benefit observed at the higher 10 and 20 μM doses. A 5μM dose of IKK*i* was also capable of inhibiting the gain of fibronectin expression, but to a lesser extent than the 10 and 20μM doses. Morphologically only the 20μM dose of IKK*i* was capable of inhibiting EMT, maintaining cells cobblestone like appearance, with the lower doses displaying little if any benefit compared to controls. Interestingly all doses of IKK*i* were, when used in association with TNFα alone, capable of inducing a striated mesenchymal like appearance. Based purely on ability to inhibit EMT a 20μM dose of IKK*i* would be used, however at this and the 10μM dose there was a large decrease in viability for all stimulations. Therefore in all future experiments a 5μM dose of IKK*i* was used which was capable of inhibiting EMT to a lesser degree but maintained cell viability at more normal levels.

4.2.2.1 Chemical Inhibition of IKKβ, Effect on EMT Endpoint

With an appropriate dose of IKK*i* decided upon in A549 cells the next step was to observe what effect this would have on EMT in PBECs. *n=4* PBEC cultures from distinct patients were stimulated with TGF-β1 or TNFα for 72 hours after a 1 hour pre-treatment with 5μM IKK*i*. Cell lysate and culture media was retained and EMT was assessed using a variety of markers.

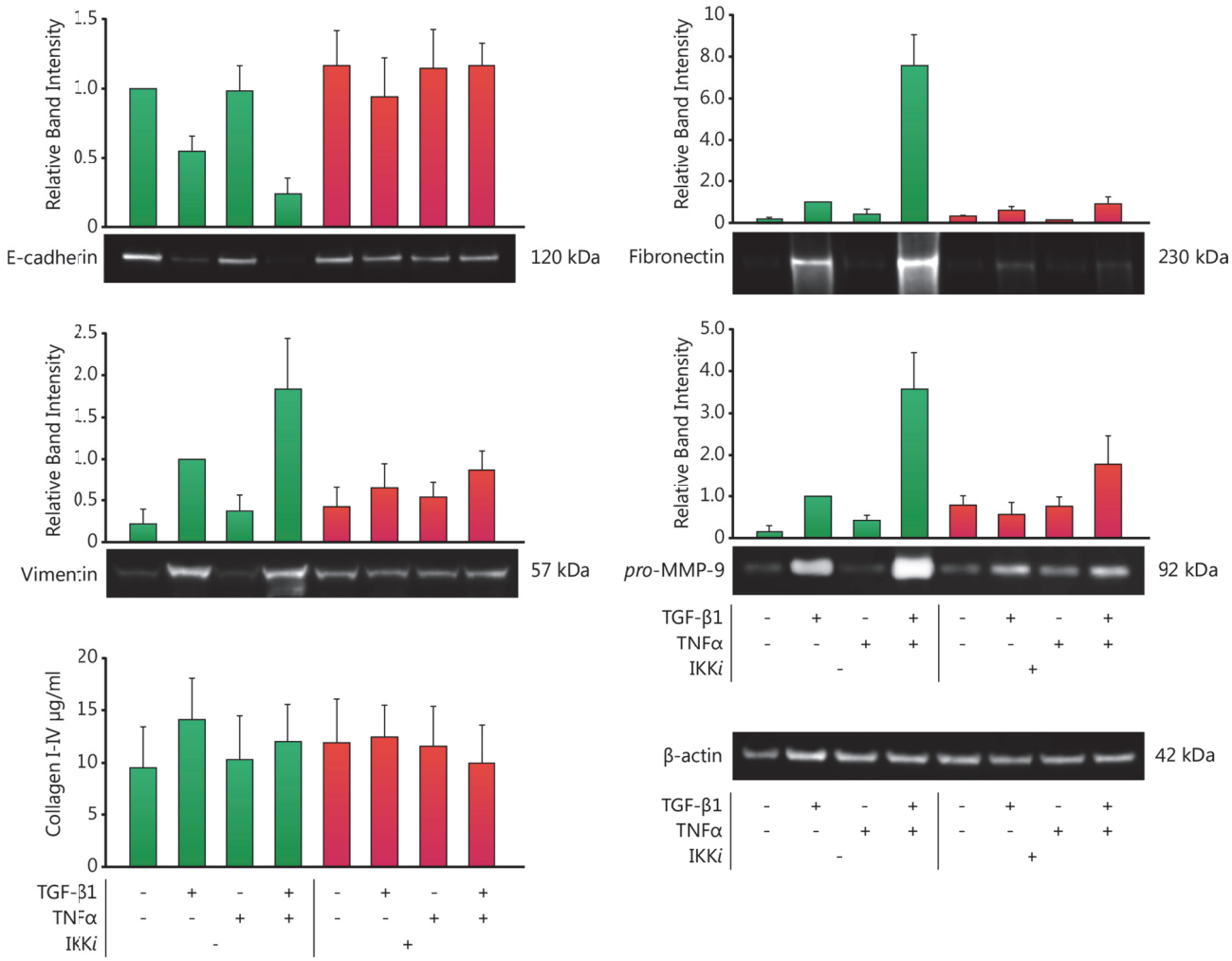

Figure 30 - Effect of IKK*i* on EMT

Stimulation of PBECs (*n=4*, representative blots from single patient) with TGF-β1 (10ng/mL) for 72 hours down-regulated E-cadherin expression, increased fibronectin and vimentin expression and increased *pro*-MMP-9 secretion. This change in EMT marker expression was accentuated by co-stimulation with TNFα (20ng/mL). Collagen I-IV secretion was significantly up-regulated by stimulation with TGF-β1 ($p<0.05$, *n=4*) however no accentuation was observed upon co-stimulation with TNFα. Pre-treatment with IKK*i* (5μM) inhibited the TGF-β1 induced down-regulation of E-cadherin expression, the increase in fibronectin and vimentin expression and, slightly, the increase in collagen I-IV and *pro*-MMP-9 secretion. IKK*i* strongly reduced the accentuating effect of TNFα on TGF-β1 driven EMT marker expression, in the instance of E-cadherin restoring levels to baseline, and above those of TGF-β1 alone stimulated PBECs. E-cadherin and fibronectin (5μg), vimentin (20μg), *pro*-MMP-9 (30μL) and collagens I-IV (25μL).

The results above suggest that IKK plays a role in the TNFα mediated accentuation of TGF-β1 driven EMT. A 5μM dose of IKK*i* induced a small decrease in PBEC viability compare to untreated controls, with pre-treatment strongly inhibiting the accentuated loss of E-cadherin, gain in fibronectin and vimentin, and a slight decrease in the accentuated secretion of *pro*-MMP-9. As collagen I-IV secretion does not display an accentuated response normally no reduction in this effect was observed. Interestingly pre-treatment with IKK*i* also inhibited the TGF-β1 driven EMT, albeit relatively weakly for all markers, excepting collagen.

Collagen I-IV secretion which was usually significantly elevated in response to TGF-β1 stimulation was in this instance non-significantly elevated, and it is difficult to discern if IKK*i* had any impact on this elevation. This lack of significance may be due to a degradation of samples which were stored for a longer period of time before assay than other experimental groups, however as the baseline level of secretion from the un-stimulated cells was similar to that of other experimental groups it seems unlikely to be the case.

4.2.2.2 Chemical Inhibition of IKKβ, Effect on Phosphorylation

As seen in **Figure 28** IKKβ is phosphorylated in response to TNFα, displaying a slight increase upon co-stimulation with TGF-β1, with no effect seen with TGF-β1 alone. To investigate possible mechanisms that may explain how IKKβ may be phosphorylated differentially upon co-stimulation, I investigated the effect of IKK*i* pre-treatment on the phosphorylation of other key signalling proteins, in this instance with Iκ-Bα as a substrate for IKKβ, 30 minutes after stimulation with TGF-β1 or TNFα.

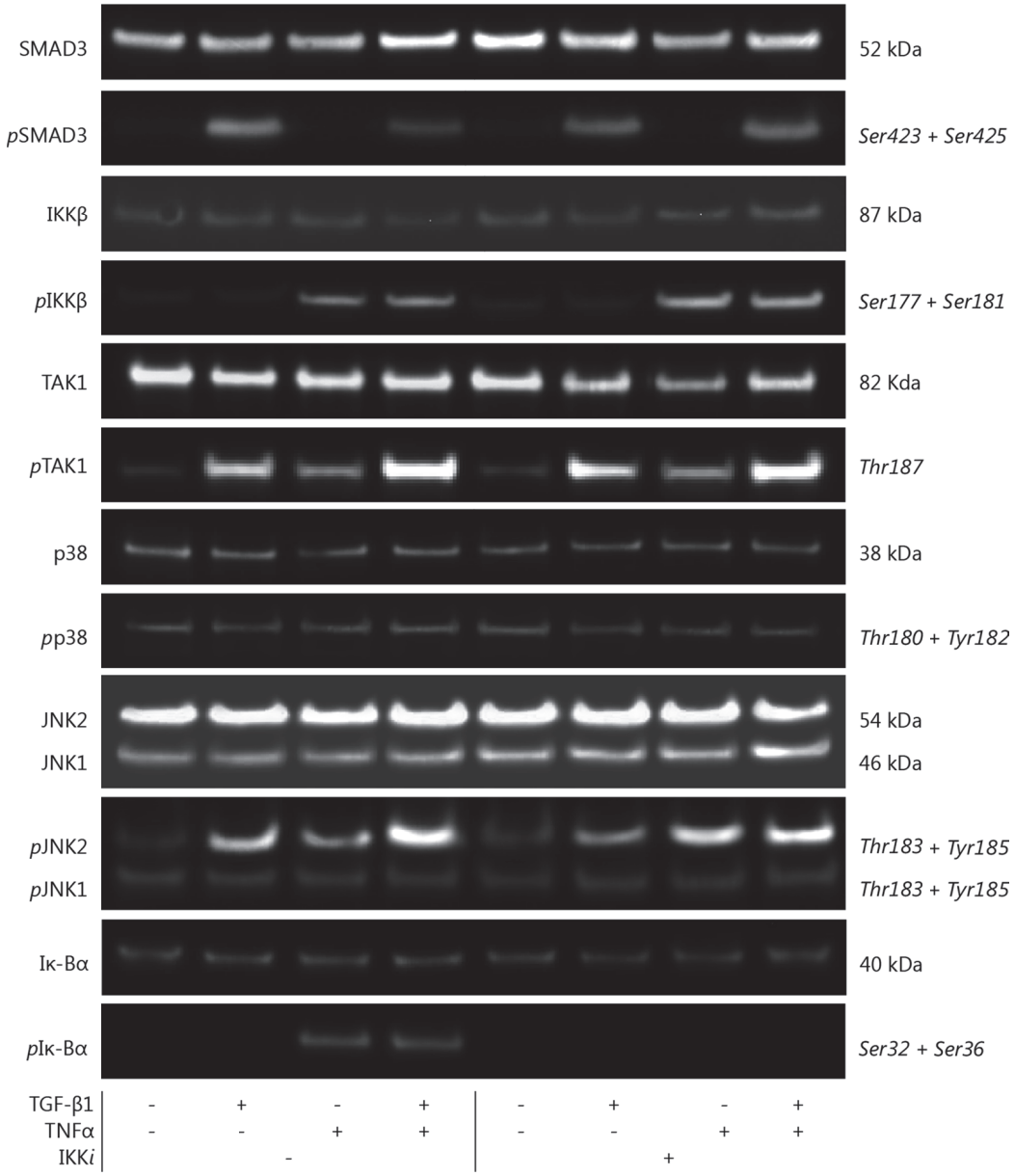

Figure 31 - Effect of IKK*i* on key signalling proteins

SMAD3 was phosphorylated in PBECs (*n=2*, representative blots from single patient) 30 minutes post stimulation with TGF-β1 (10ng/mL) with co-stimulation with TNFα (20ng/mL) having no effect on detected phosphorylation. IKKβ was phosphorylated in response to stimulation with TNFα with co-stimulation having no impact. Both TAK1 and JNK-2 were phosphorylated by stimulation with both TGF-β1 and TNFα alone and displayed an accentuated phosphorylation upon co-stimulation. JNK-1 and p38 displayed no increase in phosphorylation in response to stimulation with TGF-β1 or TNFα alone or in combination. IKK*i* (5μM) had no impact on the phosphorylation of the standard panel of signalling proteins assessed including that of IKKβ. Iκ-Bα was phosphorylated in response to TNFα alone, TGF-β1 alone had no effect and co-stimulation mediated phosphorylation was the same as that of TNFα alone. Upon pre-treatment with IKK*i* all phosphorylation was completely inhibited. *p*SMAD3 (20μg), *p*Iκ-Bα (30g), *p*IKKβ and *p*p38 (40μg), *p*TAK1, *p*JNK-1/2 and JNK-1/2 (50μg).

IKKβ was phosphorylated in response to TNFα with no evidence TGF-β1 having an impact either alone, or in co-stimulation. IKK*i* did not inhibit the phosphorylation of IKKβ due to its method of action, which is to block kinase activity in an ATP competitive manner, but not its activation. To investigate IKK*i* activity understanding of the kinase activity of IKKβ was required. Iκ-Bα, which is phosphorylated by activated IKKβ, is one such substrate. In uninhibited PBECs the pattern of Iκ-Bα phosphorylation was the same as that of IKKβ, however upon pre-treatment with IKK*i* this phosphorylation was completely blocked, suggesting that IKKβ kinase activity was being inhibited. Interestingly Iκ-Bα was not degraded, as previously discussed, post stimulation.

4.2.3 siRNA Knockdown of IKKβ

IKKβ targeting siRNA (IKK*si*) was used to knockdown IKKβ in order to validate the findings generated using IKK*i*. A dose response assay for cell viability, morphology and effect on EMT after a 24 hour pre-treatment with 0.1, 0.5, and 1nM doses of IKK*si* (CTGGAGAAGTACAGCGAGCAA), delivered through lipid transfection of adherent cultures, prior to stimulation with TGF-β1 and TNFα for 72 hours was performed in PBECs.

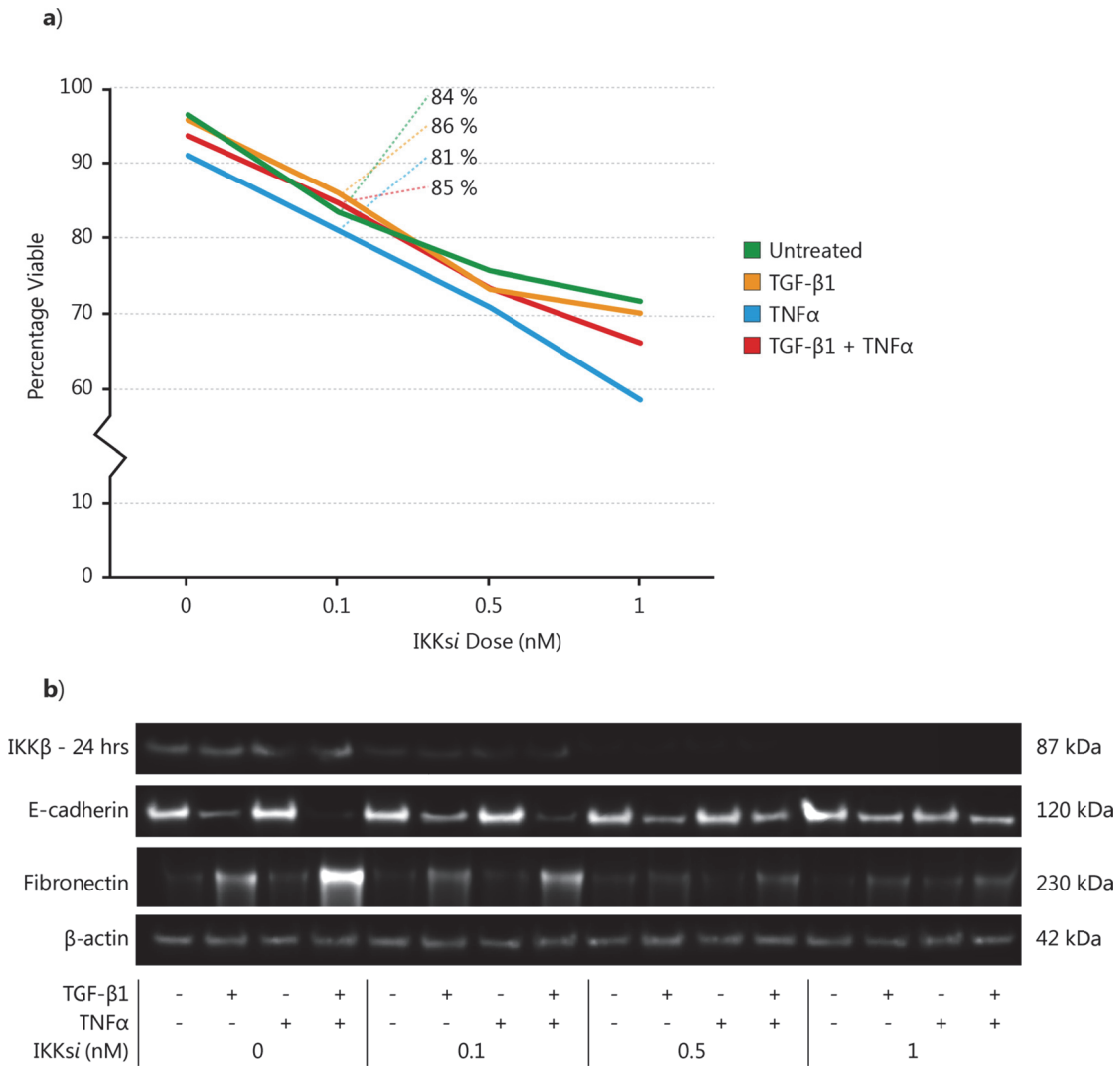

Figure 32 - IKK*si* dose response

a) PBECs were stimulated with TGF-β1 (10ng/mL) or TNFα (20ng/mL) for 72 hours after a 24 hour pre-treatment with IKK*si* at 0.1, 0.5 and 1nM doses (*n*=2). There was a strong trend of decreased viability with increasing dose of IKK*si* under all stimulations. There was little variation between stimulations, with the exception of TNFα alone, with a 5nM dose of IKK*si* which induced a strong decrease in cell viability.

b) IKKβ was not affected by stimulation by TGF-β1 or TNFα; however, detected levels of IKKβ were reduced in a dose dependant fashion by treatment with IKK*si*. Knockdown was so strong that beyond 0.1nM doses (90% knockdown, although weak IKKβ staining makes accurate quantification difficult) it was not possible to quantify this. E-cadherin expression was reduced upon TGF-β1 stimulation with an accentuated reduction upon co-stimulation with TGF-β1. Fibronectin expression was increased upon stimulation by TGF-β1 with an accentuated increase upon co-stimulation with TNFα. IKK*si* reversed these effects in a dose dependant manner, with the strongest effect seen at 1nM. E-cadherin and fibronectin (5µg) and IKKβ (40µg).

IKKβ expression was reduced in a dose dependant manner by pre-treatment with IKK*si;* with a strong decrease in cell viability. The loss of E-cadherin expression and gain of fibronectin expression in response to TGF-β1 or TNFα stimulation was also inhibited in a dose dependant manner, with a 5nM dose of IKK*si* producing the strongest effect. Interestingly at the highest dose of IKK*si* along with TNFα stimulation induced a larger loss of cell viability, especially evident at the highest dose of 5nM than the other stimulations. Therefore although the 1 and 5nM doses most strongly inhibited EMT, a 0.1nM dose which still limited EMT, but did not significantly reduce cell viability was used for all future experiments.

4.2.3.1 siRNA Knockdown of IKKβ, Effect on EMT Endpoint

With an appropriate dose of IKK*si* confirmed for use in PBECs I proceeded to investigate what effect IKKβ knockdown had on EMT. *n=3* PBEC cultures from distinct patients were stimulated with TGF-β1 or TNFα for 72 hours after a 24 hour pre-treatment with 0.1nM IKK*si* or a sequence scrambled control. Cell lysate and culture media was retained and EMT was assessed using a variety of markers.

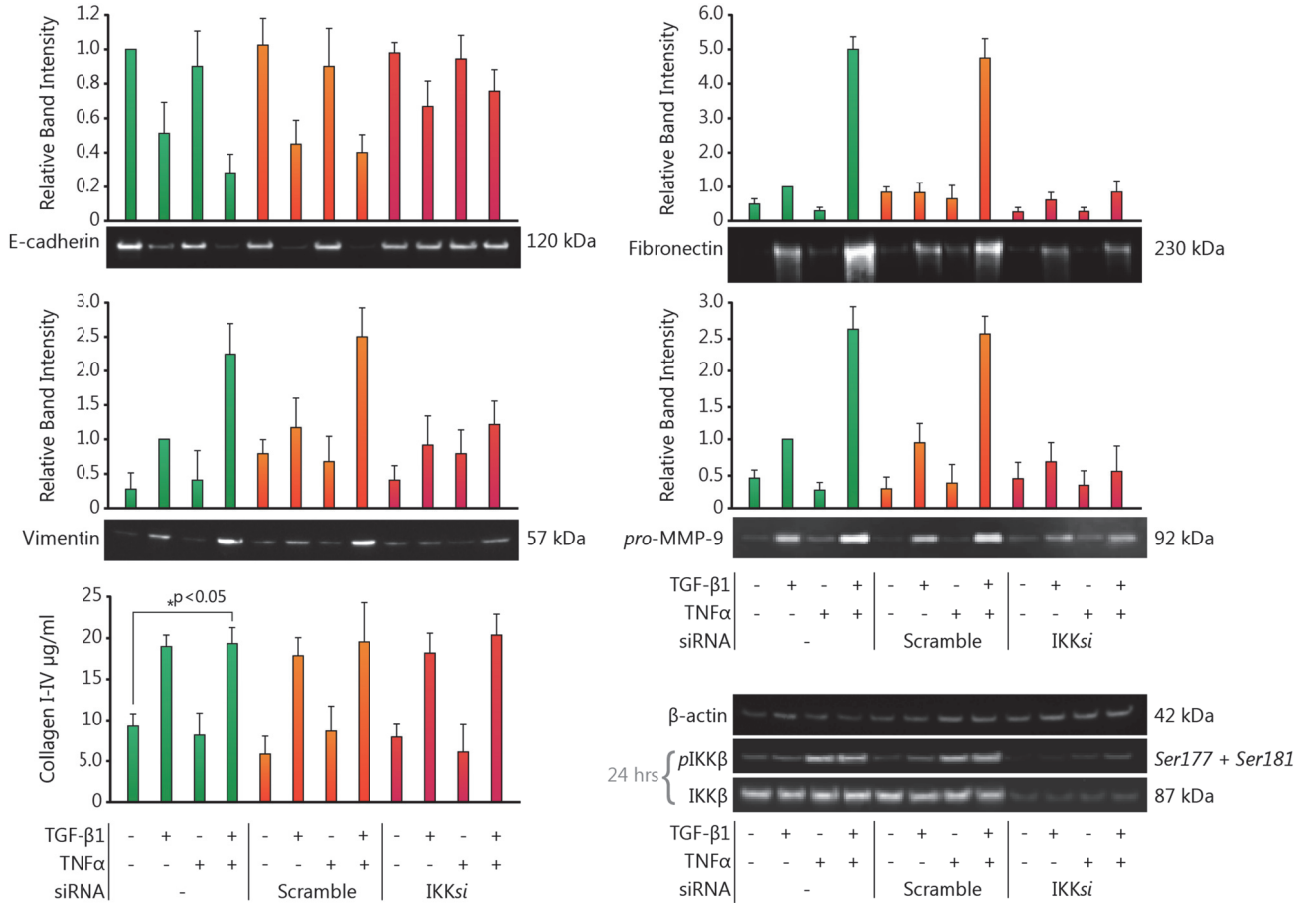

Figure 33 - Effect of IKK*si* on EMT

Stimulation of PBECs (*n=3*) with TGF-β1 (10ng/mL) down-regulated the expression of E-cadherin, increased the expression of fibronectin and vimentin and increased *pro*-MMP-9 secretion compared to control cells with this effect accentuated by co-stimulation with TNFα (20ng/mL), with the exception of E-cadherin where this effect was more additive in nature. Collagen I-IV secretion was significantly up-regulated by stimulation with TGF-β1 but no accentuation was observed upon co-stimulation with TNFα ($p<0.05$, *n=3*). IKK*si* (0.1nM) weakly inhibited the TGF-β1 mediated loss of E-cadherin, and gain if other markers of EMT. However, knockdown did strongly inhibit the TNFα mediated accentuation of TGF-β1 driven EMT for all markers with the exception of collagens I-IV. No effect on EMT marker expression was seen using a sequence scramble control.

Approximately 90% knockdown of IKKβ was achieved by IKK*si* (0.1nM) after 24 hours. Neither a sequence scramble control nor the lipid vector had any effect on IKKβ knockdown, cell viability or morphology. This reduction in total IKKβ also led to a reduction in the detected levels of phospho-IKKβ 30 minutes after stimulation with TGF-β1 or TNFα with no effect on IKKβ phosphorylation seen with either the lipid vector or sequence scramble control. E-cadherin and fibronectin (5µg), vimentin (20µg), *p*IKKβ (40µg), *pro*-MMP-9 (30µL) and collagens I-IV (25µL).

The results described above suggest that IKKβ plays a role in the accentuation of TGF-β1 driven EMT. A 0.1nM dose of IKK*si* strongly knocked down levels of IKKβ with the subsequent reduction in detection of phosphorylated IKKβ, and reduced the accentuative effect of TNFα in the TGF-β1 driven loss of E-cadherin, gain of fibronectin and vimentin expression and increase in *pro*-MMP-9 secretion. IKK*si* also weakly inhibited the TGF-β1 alone driven loss of E-cadherin with a similar weak effect on other markers of EMT. The one exception was the secretion of collagens I-IV that displayed no accentuated response in untreated cells with IKK*si* not significantly reducing the TGF-β1 driven increase.

4.2.4 IKKβ Discussion

By previously demonstrating that SMAD3 mediates either all or the majority of TGF-β1 signalling that drives EMT, with no evidence of accentuatory activity, if anything a slight inhibitory effect was demonstrated, it was next decided to investigate IKKβ, part of the canonical TNFα NF-κB cascade. To summarize the data presented in the preceding sub-chapter: IKKβ was phosphorylated by TNFα but not TGF-β1 alone, with TGF-β1 having no effect on TNFα driven IKKβ phosphorylation in co-stimulated samples. Inhibition and knockdown of IKKβ inhibited the accentuation of EMT by TNFα and in some instances inhibited TGF-β1 driven EMT as well, more so after chemical inhibition than siRNA knockdown. Inhibition of IKKβ inhibited its phosphorylation of Iκ-Bα and this its functionality. However TAK1 and JNK-2 were still phosphorylated in response to TNFα stimulation, but did not accentuate EMT suggesting that IKKβ is crucial in this role, with TAK1 playing an activating role and JNK-2 either no role or a modulatory one.

The indirect ELISA assays for both IKKα and IKKβ, however IKKα was not usually detected by western blot. By looking at later figures such as Figure 53 where a sufficient quantity of lysate was used for IKKα to be detected it is possible to see that IKKα follows a similar pattern to IKKβ. However by looking at another example blot in this case Figure 39 it is possible in this instance to observe a difference between the TNFα alone, and co-stimulated samples. This suggests that TGF-β1 can accentuate IKKβ phosphorylation but only to a small degree, a mechanism to facilitate this phosphorylation has been described, using the MAPK TAK1 to induce IKK NF-κB signalling (Mao et al., 2011).

This effect is perhaps more apparent when looking at the effect of inhibiting IKKβ; as was hypothesized inhibition reduced TNFα accentuation of TGF-β1 driven EMT. However, there was also a slight inhibition of TGF-β1 driven EMT, which was most evident when using E-cadherin as a marker for both IKK*i* and

IKK*si*. In general, the effect was more apparent when using IKK*i*, which raises the possibility of a non-specific effect, the question being where this non-specific inhibition is occurring. In the studies initially describing the effects of IKK*i* a screen of effect on other signalling proteins was also performed. In one instance the next most inhibited molecule was IKKα demonstrating a 20 fold difference between the respective IC_{50} amounts (Podolin et al., 2005); in the other study a 200 fold difference was observed, with in this instance the next most inhibited molecule after IKKβ being p38 (Kishore et al., 2003). Interestingly the latter paper demonstrated that IKK*i* had a 5 fold stronger inhibitory effect on an IKKα/IKKβ heterodimer than on IKKβ alone. As discussed in 4.2 IKKα and IKKβ preferentially form this heterodimer *in vivo* (Huynh et al., 2000), from this it is possible to speculate that I underestimated the role of IKKα in the accentuation of TGF-β1 driven EMT. However, it is also possible that the chemical inhibitor could be inhibiting some other signalling protein.

In the SMAD3 discussion I talk about the seemingly SMAD3 dependant, non-TNFα accentuated up-regulation of collagen and the findings outlined above would seem to confirm this effect. I hypothesized that the production of collagen was mediated purely through SMAD3 and did not involve the as yet unknown accentuatory protein, thus preventing TNFα from playing a role. When using the chemical inhibitor a significant increase in response to TGF-β1 was not obtained and it was difficult to discern if IKK*i* had any impact, I can present no explanation for this lack off effect as in all other samples tested significance was obtained. However, in the IKK*si* experiment where a clear significant increase in collagen secretion was demonstrated IKK*si* had no inhibitory effect, which would lend credence to this hypothesis.

One interesting observation not linked directly to the study at hand was that IKK*i* and IKK*si* both seemed to have a greater effect on PBEC viability than the other chemical inhibitors, most evident with IKK*si*. The siRNA used to knock down IKKβ was very effacious, able to knockdown approximately 90% of detected IKKβ after 24 hours with a 0.1nM dose. At doses beyond this where 100% inhibition, or near to, was achieved there was a very rapid decrease in viability. TNFR1 is capable of inducing cell death by recruiting alternative proteins into the receptor complex. Instead of the TRAF mediated NF-κB activation, Fas-Associated protein with Death Domain (FADD) can be recruited and initiate cell death through the caspase cascade; although it is thought that this effect is usually masked by the inhibitory effects of NF-κB signalling on FADD (Micheau and Tschopp, 2003). By chemically inhibiting IKKβ activity, it is possible that I am inducing a block in this protective NF-κB signalling, with a resultant increase in death signalling. Looking more specifically at the role of IKKα and IKKβ a similar inhibitory effect was described, in one paper siRNA knockdown of IKKα and IKKβ significantly decreased cell viability (Jiang et al., 2010), with

another using a transgenic cell line expressing dominant negative IKKα and IKKβ showing a similar effect (Kim et al., 2002).

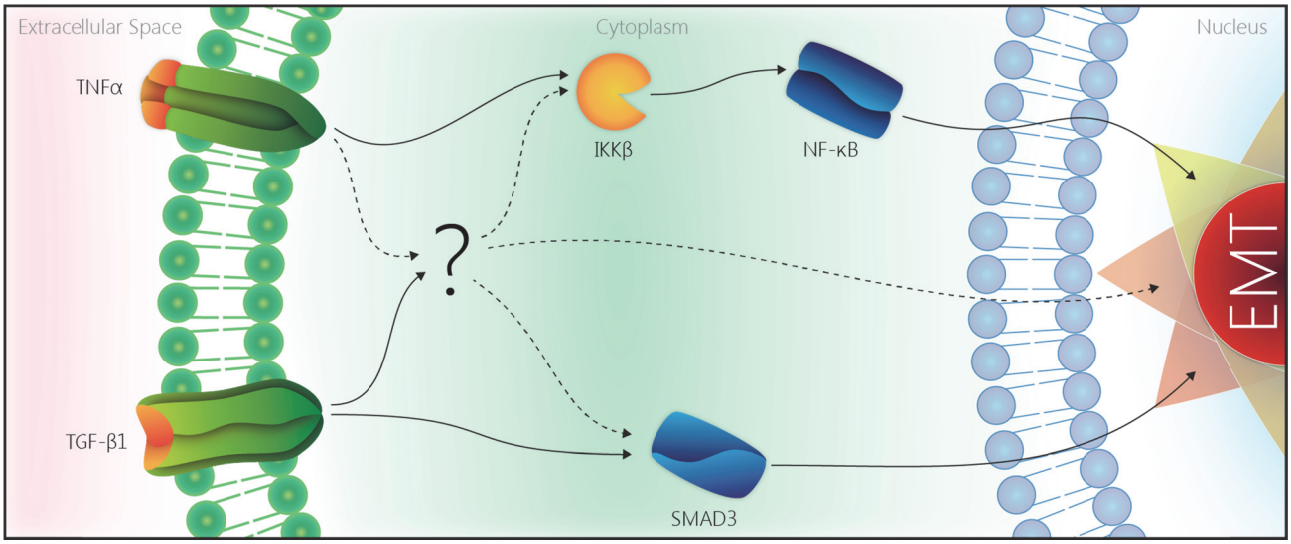

Figure 34 - Proposed Signalling Mechanism II

TGF-β1 signals through the canonical SMAD pathway, utilising SMAD3 and induces EMT, independently of TNFα. SMAD3 is required for TGF-β1 mediated EMT as un-inhibited activation of TAK1 was not capable of driving EMT strongly, but may provide some slight redundancy. TNFα signals through IKKβ, and possibly IKKα, to NF-κB, mediated by the phosphorylation of Iκ-Bα. IKKβ activity may be required to accentuate EMT as again the un-inhibited activation of TAK-1 and JNK-2 were not capable of accentuating EMT alone.

These results suggest that IKKβ, and potentially IKKα activity are involved in accentuating EMT, driven by TGF-β1. As such, the next step was to find a protein that is capable of responding to both stimuli and that was capable of signalling through IKKβ, with the briefly mentioned and clearly involved TAK1 seemingly the ideal candidate.

4.3 TGF-β activated kinase 1

As shown in **4.2.2** and **4.2.3** inhibition and siRNA knockdown of IKKβ limited the TNFα mediated accentuation of EMT, whilst also slightly inhibiting TGF-β1 driven EMT. A mechanism or protein, which facilitated the transference of TGF-β1 signalling through the IKK complex, may therefore be a key player in the accentuative process. One potential protein that is receiving much interest is TAK1; a 67 kDa serine-threonine kinase which can both activate and is activated by a diverse range of signalling proteins. First described as a mediator of non-canonical TGF-β signalling (Yamaguchi et al., 1995) it has now been shown that TAK1 can be stimulated by TLR family ligands such as lipopolysaccharide (Ear et al., 2010), and other factors such as IL-1β (Fan, Yu, Mao, et al., 2010) and TNFα (Ea et al., 2006). However, the mechanisms that facilitate TAK1 activation and its downstream effects remain poorly understood and results described in the literature are often conflicting.

Prior to stimulation with TGF-β1 it is thought that TAK1 exists bound to a TRAF6-TAB2 or TAB3 complex, which is itself associated with TGFβR1 (Sorrentino et al., 2008). Upon stimulation with TGF-β1 the hetero-tetramer complex of TGFβR1 and TGFβR2 proteins as described in **1.3.1** is formed, which facilitates the auto-poly-ubiquitination of TRAF6 (Xia et al., 2009) in a *Lys63* dependant manner, without the use of TGF-R1 kinase activity. This auto-poly-ubiquitination results in the activation of TRAFs E3 ubiquitin ligase ability, poly-ubiquitinating TAK1 at the *Lys158* (Mao et al., 2011) and *Lys34* (Sorrentino et al., 2008) residues of which only *Lys158* was shown to be required for subsequent activity. Upon ubiquitination TAK1 is released from its association with TRAF6, it is unknown if TAB2 or 3 remain associated with TAK1 at this point, and forms a new complex with TAB1 (Kim et al., 2009). An alternative hypothesis is that TAK1-TAB1 interactions and TAK1-TAB2/3 interactions are independent, with TAB2/3 requiring other cellular apparatus to induce the auto-phosphorylation of TAK1, whereas TAB1 is capable of achieving this effect alone (Scholz et al., 2010).

Upon binding with TAK1, TAB1 is itself auto-phosphorylated, which in turn facilitates the auto-phosphorylation of key residues within the hypothesized activation loop of TAK1 such as *Thr178, Thr184* and *Thr187* (Singhirunnusorn et al., 2005). Phosphorylation of these key resides is thought to occur sequentially, starting with *Thr178* which augments auto-phosphorylation followed by phosphorylation of *Thr184* and *Thr187* thought to be required for TAK1 kinase activity. It is thought that constitutive TAB1 binding is required for maintenance of this activation (Kishimoto et al., 2000). Phosphorylation of *Ser192* has been shown to be required to facilitate TAB1 binding to TAK1, with the subsequent phosphorylation

of the other described residues (Scholz et al., 2010). Phosphorylation of other sites not within this activation loop have been described during large scale phosphorylation analysis by mass spectrometry (Dephoure et al., 2008) but no details of their activity are described in the literature. It is not known whether specific phosphorylation events are associated with a particular stimulus, TAB protein, or indeed, if co-phosphorylation is required, or improves, kinase activity.

Activation of TAK1 by TNFα occurs in a similar manner to activation by TGF-β1 albeit with different receptor scaffold proteins involved in the recruitment and polyubiquitination of TAK1. As TAK1 is now thought to be key in mediating IKK-NF-κB activity I have already described the mechanism of its activation in 1.3.2. The same is true of activation by IL-1β stimulation as TAK1 is once again a key factor in its downstream signalling; details of this activation are described in 1.3.3.

It is worth mentioning that as TRAF6 plays an important role in the ubiquitination of TAK1 in both TGFβR and IL-1βR signalling that it may itself play an important synergistic role. This is especially true in light of its ability to polyubiquitinate different residues of TAK1 depending on which receptor complex it is associated with *Lys34* (Sorrentino et al., 2008) with TGFβR, *Lys209* (Fan, Yu, Mao, et al., 2010) with IL-1βR and a seemingly conserved *Lys158*. As above, it is not known if the varying ubiquitination responses are specific to a certain upstream stimuli or interactions with TAB proteins.

Once activated TAK1 is able to mediate downstream signalling events by its kinase activity. TAK1 has been shown to directly phosphorylate both IKKα, IKKβ (4.2) and JNK-1/2 and is also required for the activation of p38, ERK, NLK and has been shown to modulate the function of IKKγ (Ohkawara et al., 2004; Fan, Yu, Mao, et al., 2010; Fan, Yu, Shi, et al., 2010; Mao et al., 2011; Yang et al., 2011). There is currently no evidence in the literature describing any non-kinase activities by TAK1, and TAK1 is thought to be localized solely within the cytoplasm. The duration of phosphorylation has also not been described, and likely varies depending on stimulation, however at some point TAK1 is de-phosphorylated by the phosphatase PP2A. In addition, no data is presented as to whether TAK1 is subsequently degraded or if it cycles back into an association with TRAF and TAB proteins, ready for a new signalling event.

As mentioned in the opening paragraph of this section TAK1 is the very definition of a pleiotropic molecule with its ability to respond to a wide variety of stimuli and interact with an equally wide range of signalling mediators. From the brief description above it is possible to see several distinct levels where modulation of signalling response can occur, namely TAB association, residue ubiquitination and phosphorylation and downstream interaction among others, and because of this it is easy to understand

why findings are often conflicting and difficult to interpret. However, it also presents a large and interesting area to research, and greater understanding of the control mechanisms and outcomes relating to TAK1 stimulation, may in the short-term explain the synergy between TGF-β1 and TNFα that I am investigating, and in the long-term describe potential therapeutic targets. The following results outline my attempts to understand TAK1 phosphorylation in response to TGF-β1 or TNFα as well as its role, and importance, in the subsequent occurrence of EMT in our OB model system.

4.3.1 Phosphorylation Response of TAK1

As with SMAD3 and IKKβ, I investigated the phosphorylation of TAK1 in response to stimulation with TGF-β1 or TNFα as an assay for TAK1 activation. In this instance though I attempted to investigate three distinct phosphorylation sites located within the activation loop of TAK1 *Ser192, Thr184* and *Thr187*, to describe which, if any, responded to stimulation, if there was a differing response between the residues or if co-stimulation resulted in accentuated or prolonged activation. Unfortunately, the phospho-TAK1 (*Ser192*) antibody failed to demonstrate reproducible results and therefore no assays are shown for this residue.

PBECs were cultured in 6 well collagen coated plates until confluent and stimulated with TGF-β1 or TNFα. Cells were harvested at 0, 0.5, 1, 5, 10, 30 and 60 minute time points. Whole cell PBEC lysate was immuno-precipitated for total TAK1, under denaturing conditions, with the resulting lysate probed for phospho-TAK1 (*Thr184 or Thr187*) by indirect ELISA. Neat lysate from the 30 minute stimulation was analyzed by Western blot for both total and phospho forms of TAK1.

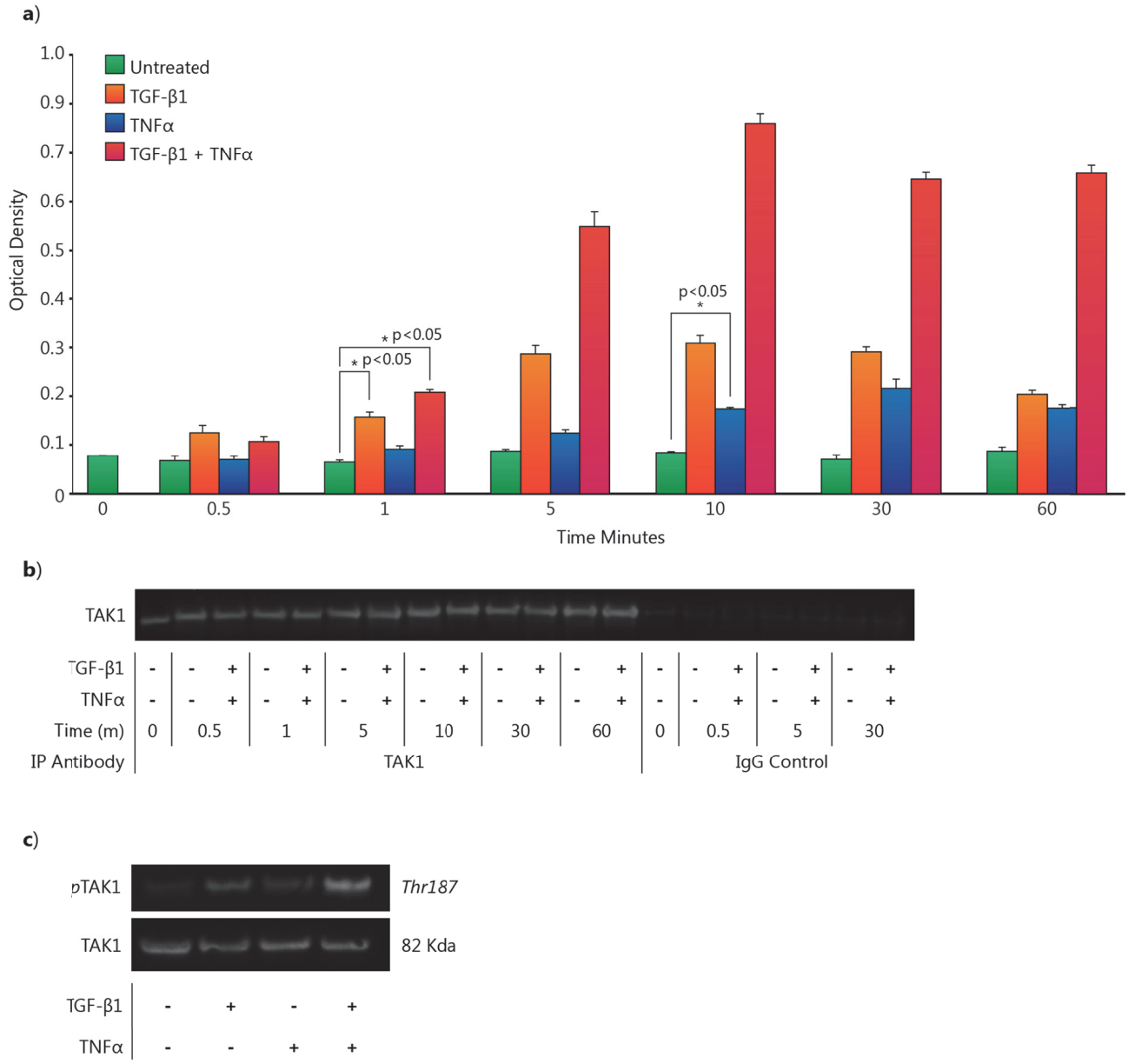

Figure 35 - TAK1 (*Thr187*) phosphorylation response

a) TGF-β1 (10ng/mL) stimulation induced significant TAK1 (*Thr187*) phosphorylation from 1 minute in PBEC lysates immuno-precipitated against total TAK1 under denaturing conditions. This significant phosphorylation of TAK1 peaked at 10 minutes and lasted beyond 60 minutes. Stimulation with TNFα (20ng/mL) induced significant phosphorylation of TAK1 from 10 minutes, peaking at 30 minutes and lasting beyond 60 minutes, although the amount of phosphorylation was lower than that seen with TGF-β1 alone. Co-stimulation of PBECs with TGF-β1 and TNFα induced significant phosphorylation of TAK1 from 1 minute, peaking at 10 minutes and again lasting beyond 60 minutes. A significant accentuative effect was observed from 5 minutes onwards in co-treated cells compared to cells treated with TGF-β1 or TNFα alone (all $p<0.05$, $n=3$).

b) Detected levels of TAK1 did not vary significantly across stimulations, and was present only at very low levels in IgG lysates.

c) Both TGF-β1 and TNFα alone induced phosphorylation of TAK1 30 minutes post stimulation; upon co-stimulation an accentuated phosphorylation was observed. *p*TAK1 (50µg).

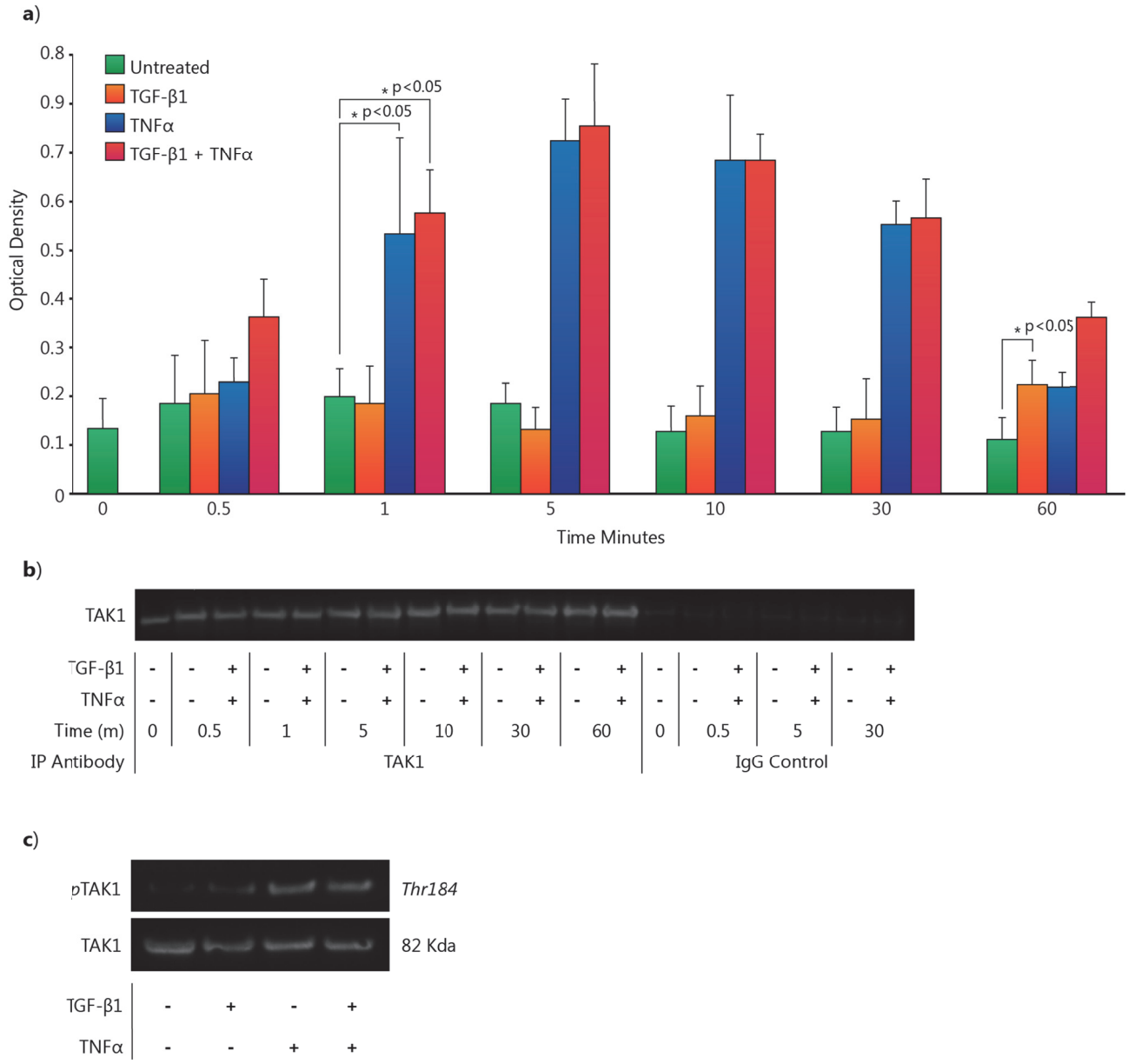

Figure 36 - TAK1 (*Thr184*) phosphorylation response

a) TGF-β1 (10ng/mL) stimulation did not induce significant TAK1 (*Thr184*) phosphorylation until 60 minutes post stimulation, in PBEC lysates immuno-precipitate against total TAK1 under denaturing conditions. Stimulation with TNFα (20ng/mL) induced significant phosphorylation of TAK1 from 1 minute, peaking at 5 minutes and returning to near baseline, although still significant, at 60 minutes. Co-stimulation of PBECs with TGF-β1 and TNFα induced significant phosphorylation of TAK1 from 1 minute, peaking at 5 minutes and again lasting beyond 60 minutes, although again at this point response was beginning to tail off (all $p<0.05$, $n=3$).

b) Detected levels of TAK1 did not vary significantly across stimulations, and was present only at very low levels in IgG lysates.

c) TGF-β1 did not increase phosphorylation 30 minutes post-stimulation, whereas TNFα stimulation induced a strong phosphorylation response. Co-stimulation resulted in a strong phosphorylation response similar to that induced by TNFα alone. *p*TAK1 (50µg).

The phosphorylation response of the *Thr187* residue seems to provide strong evidence for the role of TAK1 in the described accentuation of TGF-β1 EMT by TNFα. TGF-β1 stimulation induced a significant increase in phosphorylation from 1 minute onwards with a peak at 10 minutes, whereas TNFα induced a significant increase in phosphorylation from 10 minutes onwards peaking at 30 minutes. In general, TNFα seemed to induce a smaller and delayed increase in phosphorylation of TAK1. Co-stimulation resulted in a significant increase in phosphorylation, compared to un-stimulated controls, from 1 minute onwards, again peaking at 10 minutes. An accentuative effect was seen from 5 minutes onwards, ascertained by simply combining the individual TGF-β1 and TNFα amounts. This accentuation was strongly maintained even out to 60 minutes where the individual stimulations were trending back towards baseline.

In contrast, phosphorylation of *Thr184* seemed dependant on TNFα alone. However, it is worth considering that TGF-β1 is able to induce a delayed phosphorylation of this residue. TNFα induced significant phosphorylation from 1 minute, peaking at 5 minutes and returning to near baseline by 60 minutes. An accentuative response was only observed at 60 minutes, this seems to be due to the declining level of phosphorylation induced by TNFα stimulation alone in comparison to the maintenance of phosphorylation due to co-stimulation.

Whilst these experiments look at the phosphorylation of certain TAK1 residues, they do not describe whether co-phosphorylation was occurring on single TAK1 molecules. A better understanding of this might describe a mechanism that allows for specificity of function from such a pleiotropic molecule, especially in light of the multiple sites of poly-ubiquitination described in the literature. Attempts to assay this are described in **4.3.6**. However, the findings do confirm that TAK1 *Thr187* can respond to TGF-β1 and TNFα co-stimulation in an accentuated fashion, therefore I next decided to inhibit TAK1 function to evaluate its role in EMT, and to elucidate downstream signalling mechanisms.

4.3.2 Chemical Inhibition of TAK1

5*Z*-7-Oxozeaenol (TAK*i*) is a cell permeable inhibitor of TAK1 isolated from fungi and functions by blocking ATP binding sites, and hence kinase activity, in an irreversible fashion. The initial paper describing the effects of TAK*i* determined that the IC_{50} in 293-IL-1R1[9] and mouse embryonic fibroblast cells was 8nM (Ninomiya-Tsuji et al., 2003). A dose response curve looking at cell viability, morphology and effect on EMT after pre-treatment with 0.1, 0.5, 1 and 5μM doses of TAK*i* prior to stimulation with TGF-β1 and TNFα for 72 hours was performed in triplicate using A549 cells.

[9] *Human embryonic kidney cell line over-expressing IL-1 receptor 1*

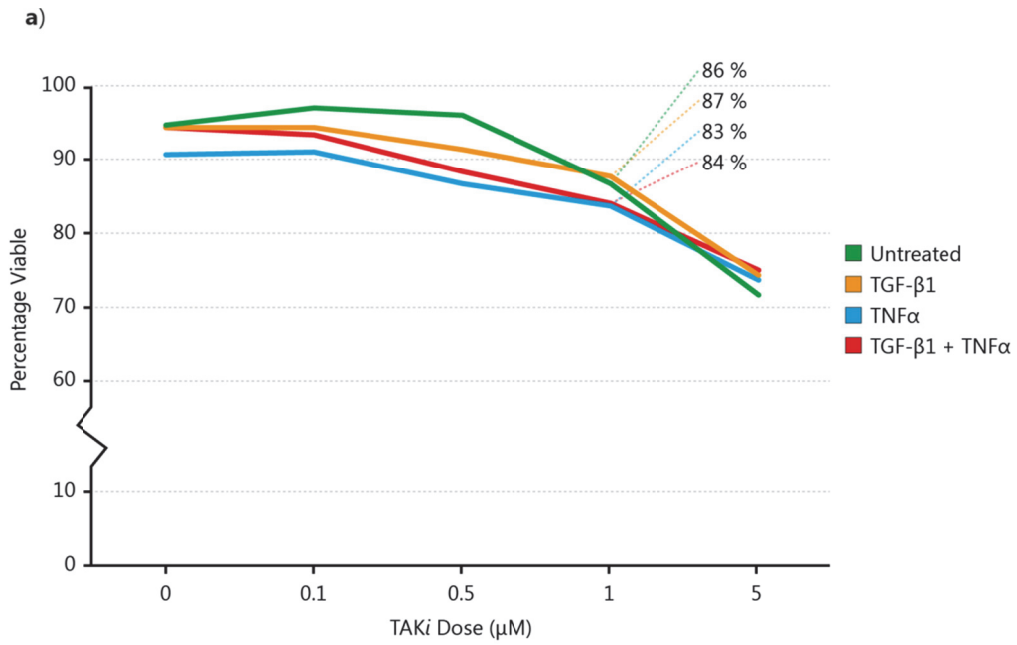

Figure 37 - TAK*i* dose response

a) A549 cells were stimulated with TGF-β1 (10ng/mL) or TNFα (20ng/mL) for 72 hours after a 1 hour pre-treatment with TAK*i* at 0.1, 0.5, 1 and 5µM doses. There was a general trend of decreased viability with increasing dose of TAK*i* under all stimulations with little variation between stimulations.

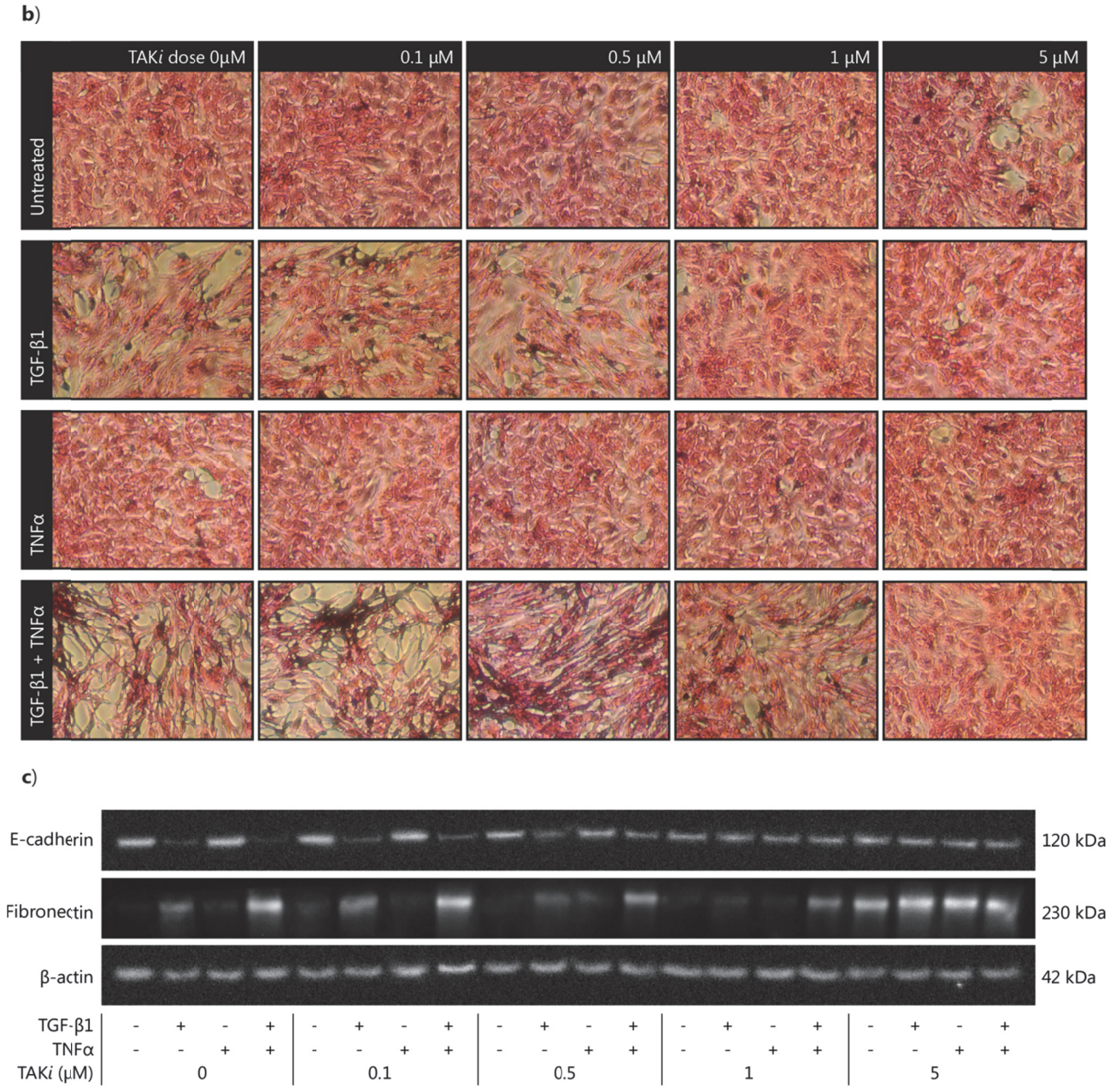

Figure 37 Continued - TAK*i* dose response

b) 72 hours post stimulation with TGF-β1 (10ng/mL) there was a marked transition from the cobblestone like epithelial appearance of un-stimulated A549 cells towards a more striated, mesenchymal phenotype. This effect was accentuated by co-stimulation with TNFα (20ng/mL), whereas TNFα alone had no effect on cell morphology. Increasing doses of TAK*i* reduced the morphological shift induced by TGF-β1 or TGF-β1 and TNFα, with normal morphology retained at a 1µM for TGF-β1 stimulated cells, and at a 5µM dose for co-stimulated cells. TAK*i* seemingly had no impact on cell morphology at the tested doses.

c) E-cadherin expression was reduced upon TGF-β1 stimulation with an accentuated reduction upon co-stimulation with TNFα. TAK*i* reversed this effect in a dose dependant manner with the strongest effect seen at 1µM and 5µM. Fibronectin expression was increased upon stimulation by TGF-β1 with an accentuated increase upon co-stimulation with TNFα. As above TAK*i* inhibited this effect in a dose dependant manner up to the 1µM dose, however the 5µM strongly increased the expression of fibronectin which may indicate a stress response from the cells due to the high dose. E-cadherin and fibronectin (5µg).

At a 1μM dose of TAK*i*, cell viability was maintained at approximately 85% for all stimulations. A 1μM dose was also capable of strongly inhibiting the morphological shift from a cobblestone like epithelial appearance towards a striated mesenchymal phenotype, and inhibited the concurrent decrease in E-cadherin and increase in fibronectin expression at the protein level without influencing baseline expression as seen with the 5μM dose. Therefore, a dose of 1μM TAK*i* was used in all future experiments.

4.3.2.1 Chemical Inhibition of TAK1, Effect on EMT Endpoint

With an appropriate dose of TAK*i* decided upon in A549 cells the next step was to observe what effect this would have on EMT in PBECs. *n=6* PBEC cultures from distinct patients were stimulated with TGF-β1 or TNFα for 72 hours after a 1 hour pre-treatment with 1μM TAK*i*. Cell lysate and culture media was retained and EMT was assessed using a variety of markers.

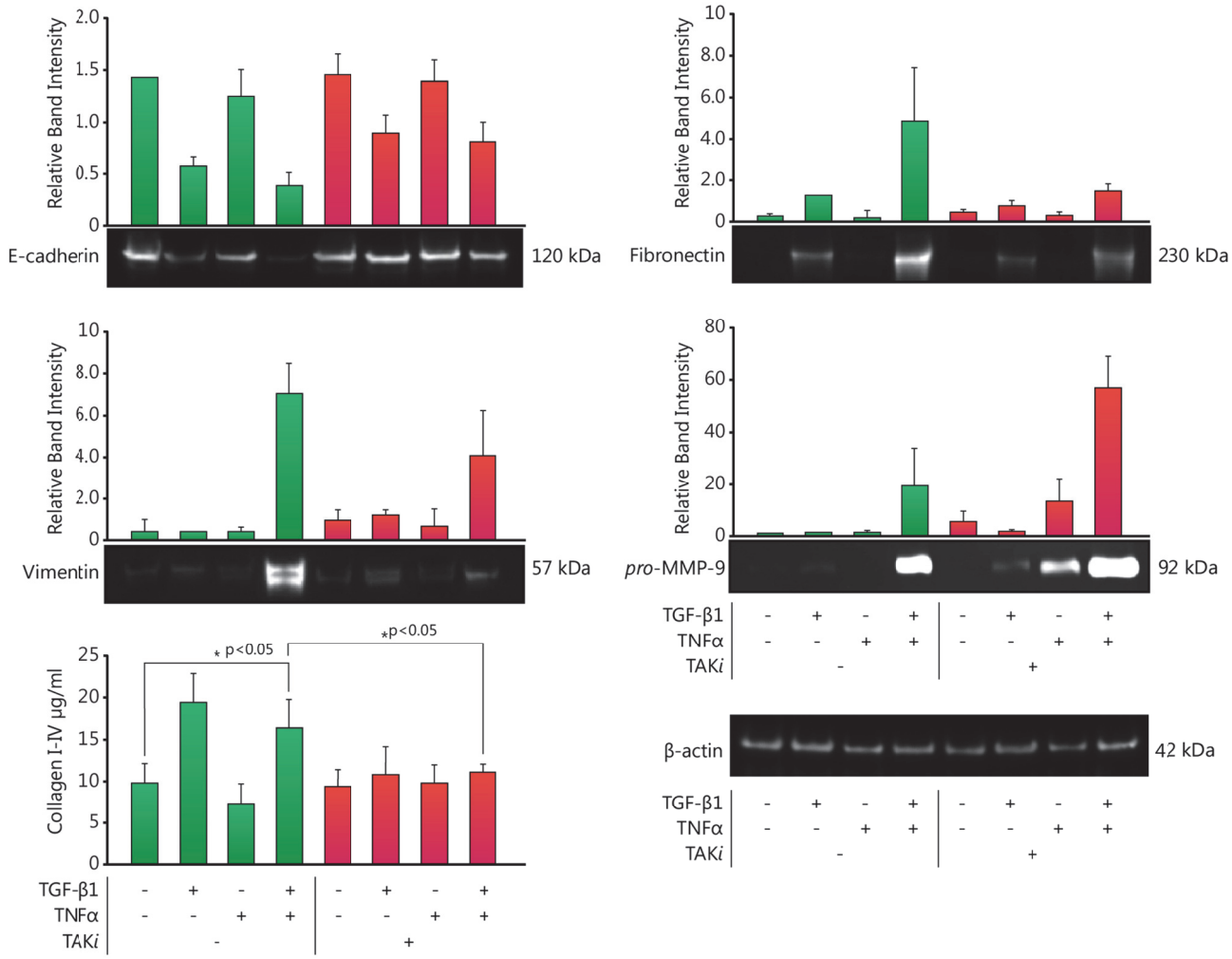

Figure 38 - Effect of TAK*i* on EMT

Stimulation of PBECs (*n=6*, representative blots from single patient) with TGF-β1 down-regulated E-cadherin expression, increased fibronectin and vimentin expression and increased *pro*-MMP-9 secretion. This change in EMT marker expression was accentuated by co-stimulation with TNFα, with the exception of E-cadherin where this effect was more additive in nature. Collagen I-IV secretion was significantly up-regulated by stimulation with TGF-β1 ($p<0.05$, *n=6*) however no accentuation was observed upon co-stimulation with TNFα. Pre-treatment with TAK*i* (1µM) inhibited the TGF-β1 induced down-regulation of E-cadherin expression, the increase in fibronectin and vimentin expression and, significantly, the increase in collagen I-IV secretion ($p<0.05$, *n=6*), returning levels to near baseline. TAK*i* also reduced the accentuating effect of TNFα on TGF-β1 driven EMT marker expression. TAK*i* reduced TGF-β1 induced secretion of *pro*-MMP-9; however, TAK*i* increased secretion of *pro*-MMP-9 from PBECs treated with TNFα alone or in combination with TGF-β1. E-cadherin and fibronectin (5µg), vimentin (20µg), *pro*-MMP-9 (30µL) and collagens I-IV (25µL).

The results described above provide evidence, that TAK1 activation plays a key role in the subsequent occurrence of EMT. Pre-treatment of PBECs with a 1μM dose of TAK*i* strongly inhibited the loss of E-cadherin expression and the gain of fibronectin and vimentin expression, as well as the increase in secretion of collagens I-IV into the media in response to TGF-β1 stimulation. TAK*i* also strongly inhibited the accentuation of EMT in response to TGF-β1 and TNFα co-stimulation for the markers described above. Interestingly TAK*i* consistently increased the secretion of *pro*-MMP-9 into the media, with the results most apparent in the media from cells treated with TNFα.

4.3.2.2 Chemical Inhibition of TAK1, Effect on Phosphorylation

As seen in **Figure 35** TAK1 displays an accentuated phosphorylation of its Thr187 residue in response to co-stimulation with TGF-β1 and TNFα. I therefore proceeded to investigate the effect of TAK*i* pre-treatment on the phosphorylation of other key signalling proteins 30 minutes after stimulation with TGF-β1 or TNFα, to determine where and how TAK1 mediated signalling activity was being transferred.

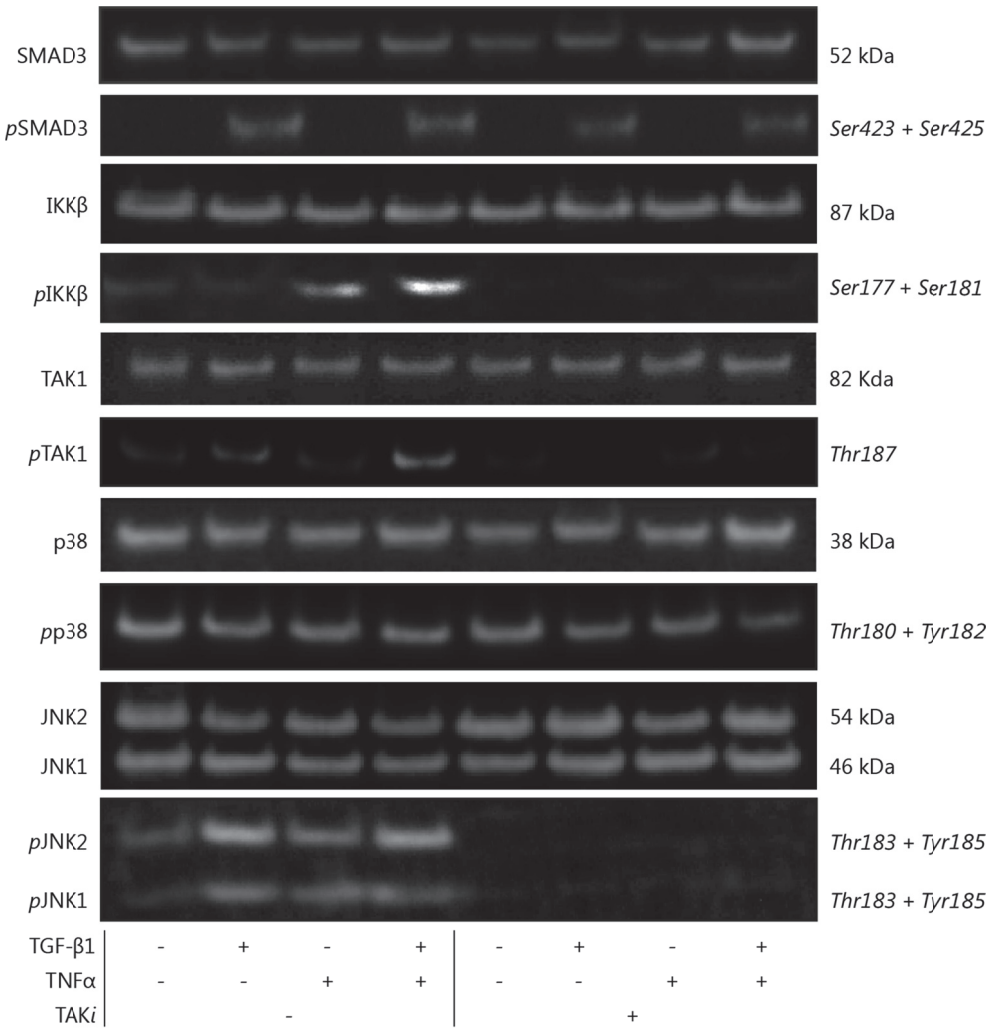

Figure 39 - Effect of TAK*i* on key signalling proteins

SMAD3 was phosphorylated in PBECs (*n=3*, representative blots from single patient) response to stimulation with TGF-β1 (10ng/mL) alone and this was not accentuated by TNFα (20ng/mL). IKKβ was phosphorylated in response to stimulation with TNFα alone and this was accentuated by co-stimulation with TGF-β1. Both TAK1 and JNK-2 were phosphorylated by stimulation with TGF-β1 alone with TAK1 showing an accentuation in response to co-stimulation. JNK-1 and p38 displayed no increase in phosphorylation in response to stimulation with TGF-β1 or TNFα alone or in combination. SMAD3 and p38 phosphorylation was not affected by pre-treatment with TAK*i* (1μM). However, detected levels of phosphorylated TAK1, JNK-1/2 and IKKβ were decreased for all stimulations by pre-treatment with TAK*i*. *p*SMAD3 (20μg), *p*IKKβ and *p*p38 (40μg), *p*TAK1, *p*JNK-1/2 and JNK-1/2 (50μg).

No difference in the phosphorylation of SMAD3 or p38 following stimulation with TGF-β1 or TNFα in the presence of TAK*i* was demonstrated; however TAK1 phosphorylation was completely inhibited. Interestingly phosphorylation of IKKβ and JNK-1/2 in response to stimulation was strongly inhibited, suggesting that TAK1 plays a key role in the activation of these proteins, and provides further evidence for the potential role of TAK1 as a convergence point for the accentuative effect of TNFα on TGF-β1 driven EMT. Surprisingly, TAK*i* inhibited TAK1 phosphorylation, even though its described activity was to inhibit ATP binding and hence kinase activity. It is possible that this inhibition of phosphorylation is an un-described effect of TAK*i* or that TAK1 phosphorylation is unstable if not in a complex in a similar fashion to that described SMAD3, or inhibits itself in a similar fashion to IKKβ.

4.3.3 siRNA Knockdown of TAK1

TAK1 targeting siRNA (TAK*si*) was used to knockdown TAK1 in order to validate the findings generated using TAK*i*. A dose response assay for cell viability, morphology and effect on EMT after a 24 hour pre-treatment with 1, 5, and 10nM doses of TAK*si* (AAGATGGTATATACCAAGTTA), delivered through lipid transfection of adherent cultures, prior to stimulation with TGF-β1 and TNFα for 72 hours was performed in PBECs.

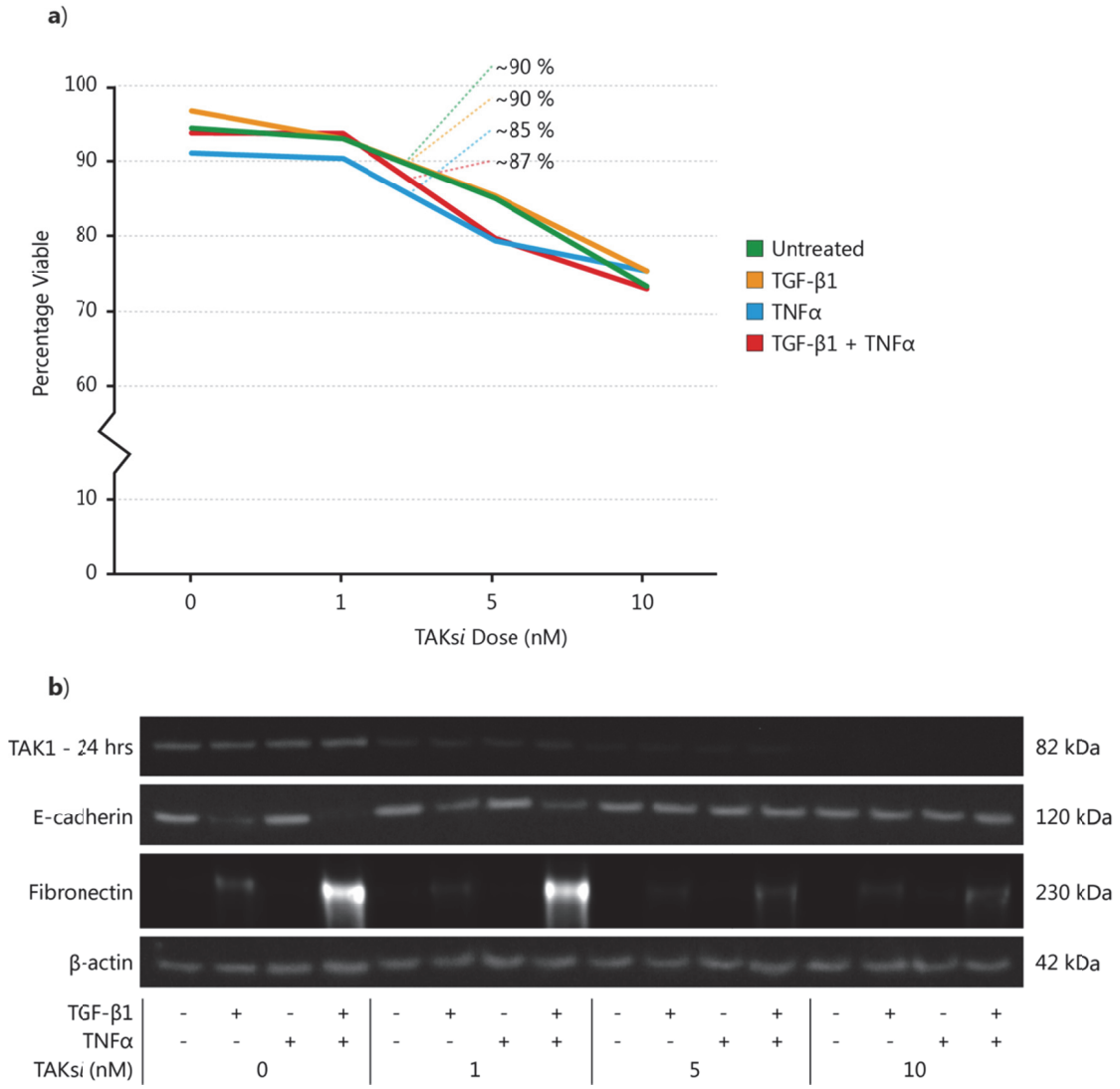

Figure 40 - TAK*si* dose response

a) Percentage PBEC viability was assessed by trypan blue exclusion assay (*n=2*). Cells were stimulated with TGF-β1 (10ng/mL) or TNFα (20ng/mL) for 72 hours after a 24 hour pre-treatment with TAK*si* at 1, 5 and 10nM doses. There was a general trend of decreased viability with increasing dose of TAK*si* under all stimulations. At the 5nM dose there was a more severe drop in viability observed in cells stimulated with either TNFα or both TGF-β1 and TNFα, however this effect was corrected at the 10nM dose

b) The efficacy of TAK*si* was assessed by Western blotting, probing for total TAK1, E-cadherin and Fibronectin. TAK1 was not affected by stimulation by TGF-β1 or TNFα; however, detected levels of TAK1 were reduced in a dose dependant fashion by treatment with TAK*si*. A 1nM dose induced approximately a 25% reduction in total protein, with no TAK1 detected after the 5nM and 10nM pre-treatments. E-cadherin expression was reduced upon TGF-β1 stimulation with an accentuated reduction upon co-stimulation with TNFα. Fibronectin expression was increased upon stimulation by TGF-β1 with an accentuated increase upon co-stimulation with TNFα. TAK*si* reversed this effect in a dose dependant manner, with the 1nM dose of TAK*si* only marginally inhibiting the loss of E-cadherin and gain of Fibronectin under any stimulation. At 5nM the EMT was strongly inhibited with no appreciable difference observed between the 5nM and 10nM doses. E-cadherin and fibronectin (5µg) and TAK1 (30µg).

TAK1 expression was reduced in a dose dependant manner by pre-treatment with TAK*si*, with an associated decrease in cell viability. The loss of E-cadherin and gain in fibronectin expression in response to TGF-β1 or TNFα stimulation was also inhibited in a dose dependant manner up to a 5nM dose, beyond which there was no appreciable benefit. Anecdotally it was observed that the higher doses of TAK*si*, or the requisite higher dose of lipid transfection reagent[10], caused large numbers of cells to detach from the culture surface. With a 5nM dose this effect was observe at around 72 hours post knockdown, whereas with the 10nM dose this was seen at 24 hours. These cells were counted as part of the viability assay, and separate counts of the attached and detached populations showed no variation in viability. However, their innate characteristics and response may differ from the normal adherent PBEC cultures. Therefore, an intermediate dose, which did not induce cell detachment, of 3nM TAK*si* was used in all future experiments.

4.3.3.1 siRNA Knockdown of TAK1, Effect on EMT Endpoint

With an appropriate dose of TAK*si* confirmed for use in PBECs, I proceeded to investigate what effect TAK1 knockdown had on EMT. *n=5* PBEC cultures from distinct patients were stimulated with TGF-β1 or TNFα for 72 hours after a 24 hour pre-treatment with 3nM TAK*si* or a sequence scrambled control. Cell lysate and culture media was retained and EMT was assessed using a variety of markers.

[10] *Although this effect was not seen with an equivalent doses in other siRNA knockdown experiments*

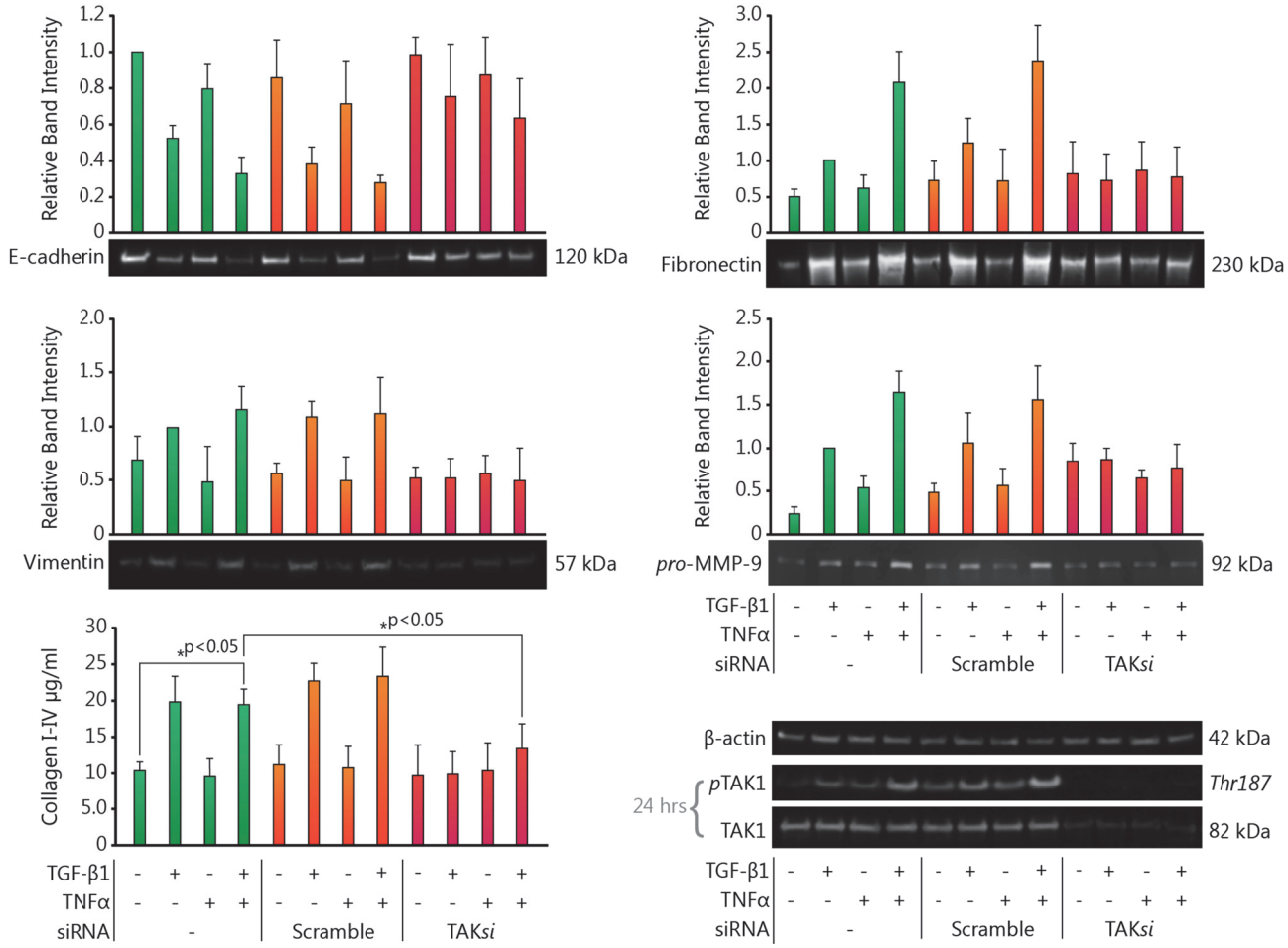

Figure 41 - Effect of TAK*si* on EMT

Stimulation of PBECs (*n=5*) with TGF-β1 (10ng/mL) for 72 hours down-regulated the expression of E-cadherin, increased the expression of fibronectin and vimentin and increased *pro*-MMP-9 secretion compared to control cells with this effect accentuated by co-stimulation with TNFα (20ng/mL), with the exception of E-cadherin where this effect was more additive in nature. Collagen I-IV secretion was significantly up-regulated by stimulation with TGF-β1 but no accentuation was observed upon co-stimulation with TNFα ($p<0.05$, *n=5*). TAK*si* (3nM) inhibited both the TGF-β1 induced and TNFα accentuated down-regulation of E-cadherin expression, the increase in fibronectin and vimentin expression and the increase in collagen I-IV ($p<0.05$, *n=5*) and *pro*-MMP-9 secretion, returning levels to near baseline. No effect on EMT marker expression was seen using a sequence scramble control.

Approximately 80% knockdown of TAK1 was achieved by TAK*si* after 24 hours. Neither a sequence scramble control nor the lipid vector had any effect on TAK1 knockdown, cell viability or morphology. This reduction in total TAK1 also led to a reduction in the detected levels of phospho-TAK1 30 minutes after stimulation with TGF-β1 or TNFα with no effect on TAK1 phosphorylation seen with either the lipid vector or sequence scramble control. E-cadherin and fibronectin (5µg), vimentin (20µg), *p*TAK1 (50µg), *pro*-MMP-9 (30µL) and collagens I-IV (25µL).

The data presented above validates the findings described with TAK*i* in **4.3.2**, with the inhibitory effect on EMT being even more striking. The 3nM dose of TAK*si* derived from the screen outlined in figure **4.3.3** induced an approximately 80% knockdown in detected TAK1 protein, without significantly affecting cell viability. This dose also did not result in a large number of cells detaching from the culture surface, as mentioned above, suggesting that the culture as a whole was retaining its "normal" PBEC character. Pre-treatment of PBECs with TAK*si* strongly inhibited the loss of E-cadherin and the gain of fibronectin and vimentin intracellularly, as well as the increase in secretion of *pro*-MMP-9 and collagens I-IV into the media in response to TGF-β1 stimulation. TAK*si* also strongly inhibited the accentuation of EMT in response to TGF-β1 and TNFα co-stimulation for the markers described above. Unlike the TAK*i* results described in figure **4.3.2.1** blocking TAK1 knockdown did not result in increased secretion of *pro*-MMP-9.

4.3.4 Localization of TAK1

Both chemical inhibition and siRNA knockdown of TAK1 suggested that it plays a key role in EMT. When observing the phosphorylation cascade of key signalling proteins TAK1 displayed an accentuative response to co-stimulation with TGF-β1 and TNFα, whilst phosphorylating to a lesser degree upon stimulation by either factor. It was also observed that TAK1 might transmit its signal downstream by JNK-1/2 or IKKβ. To investigate this further I looked at the localization of both total and phospho-TAK1 30 minutes post stimulation with TGF-β1 or TNFα in PBECs.

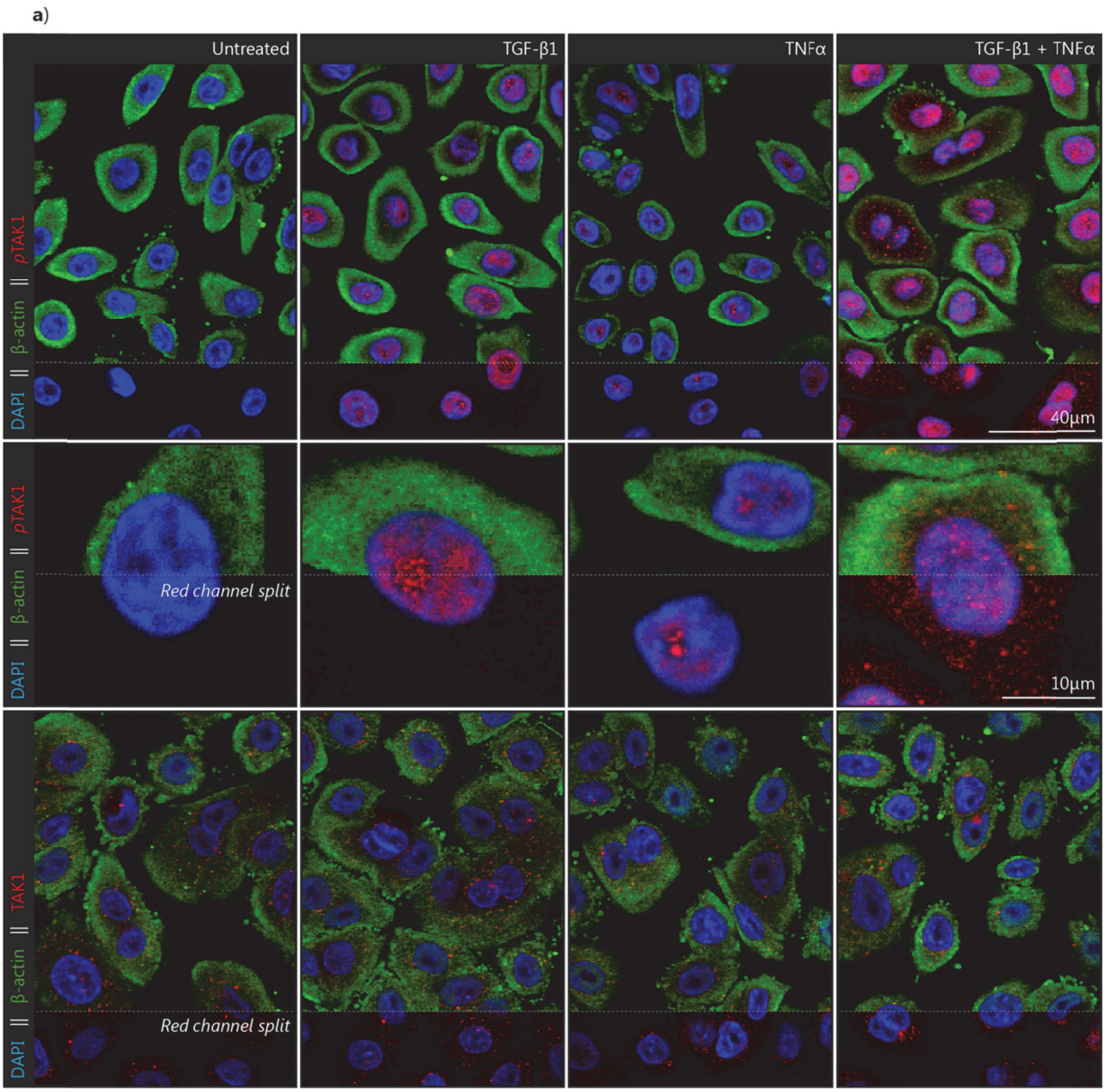

Figure 42 - Localization of TAK1 and phospho-TAK1

a) PBECs stimulated with TGF-β1 (10ng/mL) or TNFα (20ng/mL) for 30 minutes were assessed for changes in TAK1 (*Thr187*) phosphorylation displaying in the red (TRITC) channel, with DAPI as a nuclear counterstain. Un-stimulated PBECs display little to no evidence of phospho-TAK1 in the TRITC channel, with only a very small amount detected in the nuclei of some cells. Stimulation with TGF-β1 resulted in increased phosphorylation of TAK1 with a marked localization to the nucleus, with little evidence of phospho-TAK1 in the cytoplasm. Stimulation with TNFα resulted in an increase in TAK1 phosphorylation located in the nucleus of cells, but not to the same extent as TGF-β1stimulated cells. Upon co-stimulation, an accentuated level of phospho-TAK1 was detected in the nucleus of cells, as well as in the cytoplasm. Total TAK1 levels remained consistent under all stimulations. There was no change in intensity or localisation of total TAK1 that was detected throughout the cell.

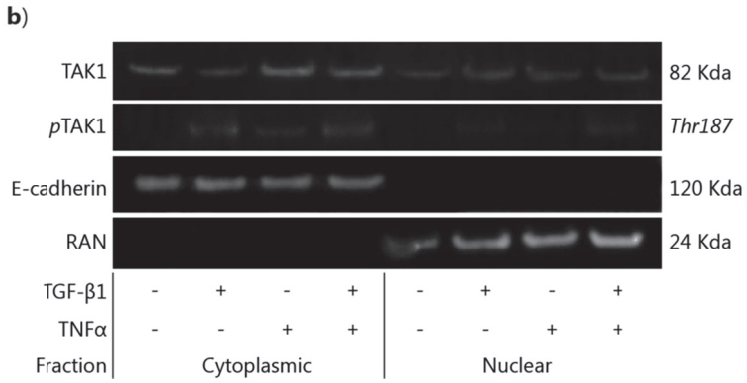

Figure 42 Continued - Localization of TAK1 and phospho-TAK1

b) Total PBEC lysates (*n=3*, representative blots from single patient) treated as above were separated into nuclear and non-nuclear fractions, 25µg of non-nuclear lysate and 8µg of nuclear lysate was then separated by SDS-PAGE and probed for TAK1 and phopho-TAK1 along with E-cadherin and RAN as fractionation controls. TAK1 was detected in both the nuclear and cytoplasmic fractions; a very faint phospho-TAK1 signal was also detected in the nuclear fraction.

When assessed by ICC total-TAK1 localization was unchanged under all conditions, maintaining a diffuse cytoplasmic stain. However, nuclear localization of phospho-TAK1 was increased following stimulation with both TGF-β1 and, to a lesser extent, TNFα compared to control cells. Co-stimulation with TGF-β1 and TNFα resulted in an accentuated nuclear localisation of phospho-TAK1 compared to either stimulation alone. To confirm the observed nuclear translocation of TAK1, nuclear and non-nuclear fractions were prepared from PBECs treated with TGF-β1 or TNFα for 30mins. As with SMAD3 attempts to confirm these findings using lysate fractionation again generated conflicting results, however, in this instance it was with the phosphorylated as opposed to total form of the protein. ICC showed a clear preference for TAK1 nuclear localisation with little if any phospho-TAK1 appearing in the cytoplasm (with the exception of co-stimulated cells). However, after protein fractionation phospho-TAK1 was detected only in the cytoplasm for all stimulations. Therefore, once again it is not possible to comment on TAK1 localization without further investigations.

4.3.5 TAK1 Tissue Staining

With TAK1 playing a key role in EMT in my post-transplant cell culture model I next proceeded to assay for TAK1 activation and localisation in fibrotic and normal lung sequential tissue sections, isolated from patients at the Freeman Hospital.

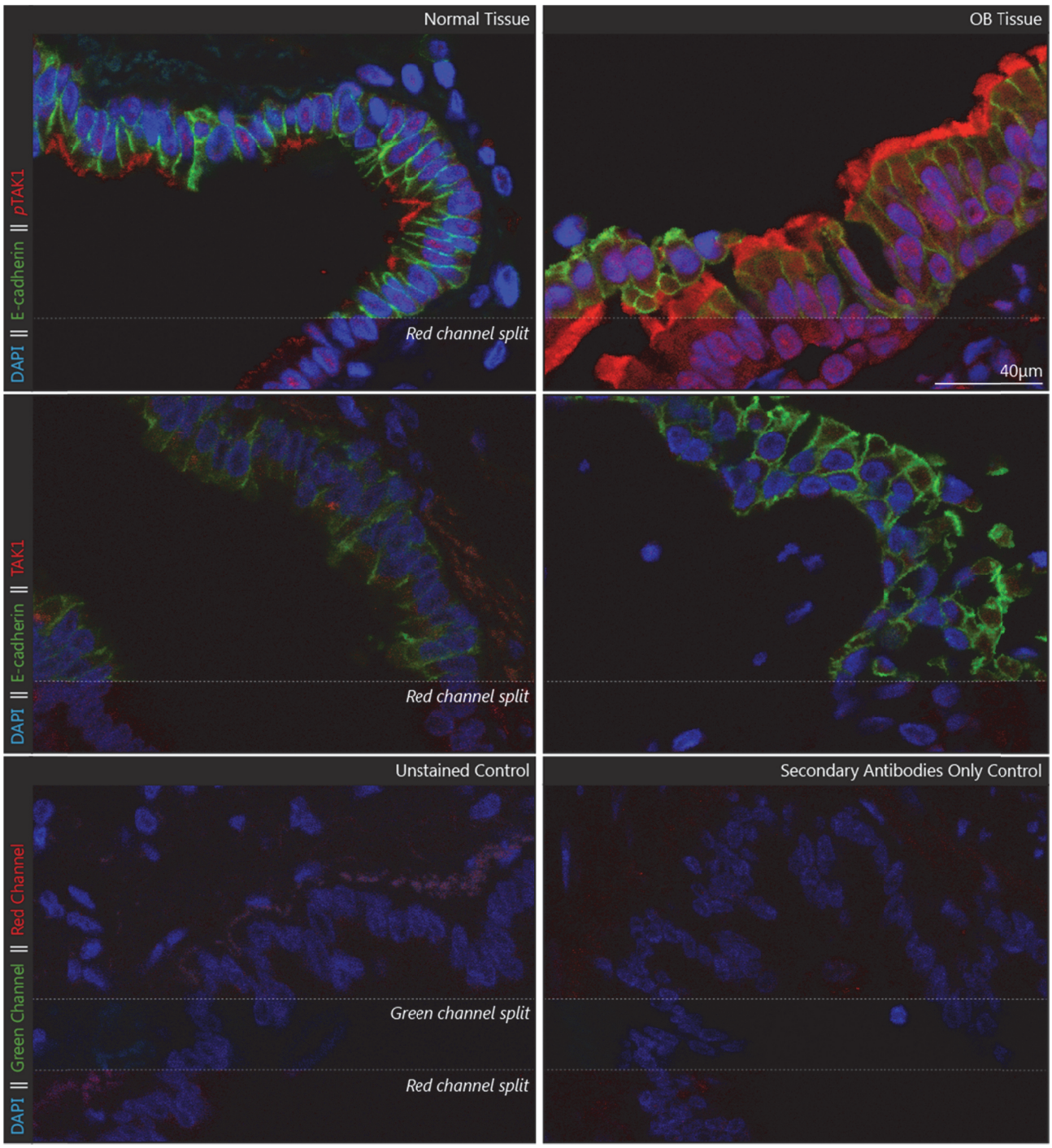

Figure 43 - OB and normal tissue stained for TAK1 and phospho-TAK1

Sequential sections taken from normal and OB lung were assessed for changes in TAK1 (*Thr187*) phosphorylation displaying in the red (TRITC) channel. E-cadherin in the green (FITC) channel was used to outline cell shape, and identify epithelial cells, with DAPI as a nuclear counterstain. In the normal airway epithelium phospho-TAK1 was located throughout the cell with evidence of nuclear translocation. In OB tissue TAK1 phosphorylation was increased in both the cytoplasm and nuclei of the epithelium. Significant non-specific binding of antibodies to the airway epithelium was observed in both normal and OB sections. A diffuse and faint level of total TAK1 was detected in both normal and OB sections with no discernible difference in intensity. The mature extra cellular matrix underneath the epithelium auto-fluoresced in the red channel. Secondary only controls showed no increase in the intensity of expression in the red or green channels suggesting little non-specific effects were mediated by auto-fluorescence and primary antibody specificity.

Total TAK1 was located throughout all airway cells and there was no detectable difference in the intensity of expression between normal and OB lung tissue. In contrast, levels of phospho-TAK1 were higher in epithelial cells in OB tissue compared to normal. It was also noted that phospho-TAK1 displayed evidence of nuclear localization that was more pronounced in OB tissue. However, there was significant non-specific staining of the ciliated regions of the airway by the anti phospho-TAK1 antibody making it difficult to conclude that TAK1 phosphorylation is increased in OB tissue. Attempts were made to nullify this effect by blocking samples with antibodies against microtubule proteins such as α and β-tubulin and other structural proteins such as β-actin to no avail.

4.3.6 Further Investigations into TAK1 Activity

In light of the potential nuclear localisation of TAK1 described in **Figure 42** and **Figure 43** along with the fact that TAK1 contains no described nuclear localization signal, but interacts with a wide variety of proteins, it was thought that investigating TAK1-protein interactions might help explain this localization effect. As discussed above the TAB family of proteins are known to have a strong association with TAK1 and appear to help modulate its function. As described in previously TAK1 is also capable of inducing phosphorylation of other signalling proteins such as JNK-2 and IKKβ, potentially by direct kinase activity.

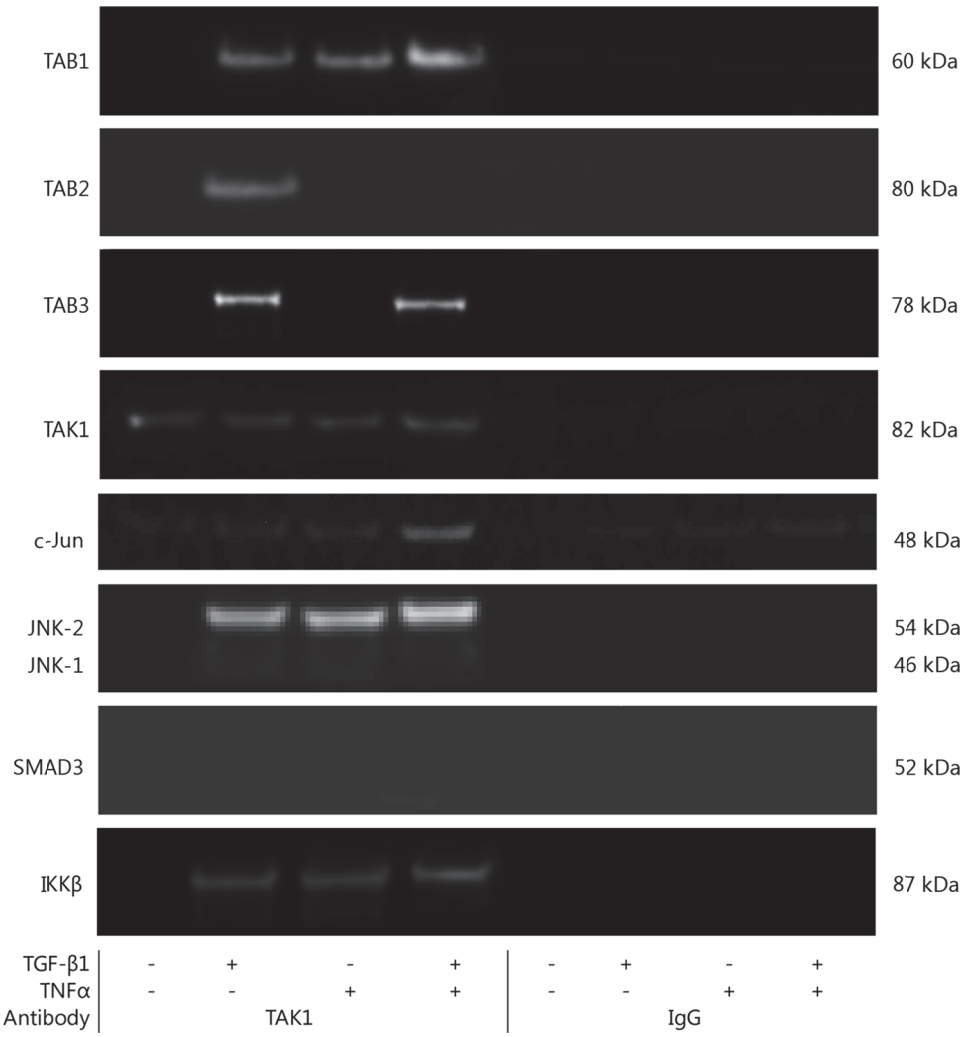

Figure 44 - TAK1 protein associations

PBEC lysates (20µg, *n=3*, representative blots from single patient) from cells treated with TGF-β1 (10ng/mL) or TNFα (20ng/mL) for 30 minutes were immuno-precipitated for total TAK1, or pan-IgG under non-denaturing conditions. TAB1 was associated with TAK1 at 30 minutes when stimulated with TGF-β1 or TNFα, with potentially an accentuated association upon co-stimulation. Both TAB2 and TAB3 were found to associate with TAK1 upon stimulation with TGF-β1, but not TNFα. Upon co-stimulation there was no change in TAB3 association when compared to TGF-β1, but TAB2 association with TAK1 was completely lost. SMAD3 did not associate with TAK1 at 30 minutes after any stimulation. However IKKβ and JNK-2 but not JNK-1 were associated with TAK1 at 30 minutes after stimulation, but there was no detectable difference in association between stimulations, c-Jun associated with TAK1 only after co-stimulation with both TGF-β1 and TNFα. No bands were detected in the pan-IgG controls.

At 30 minutes TAB1 was associated with TAK1 under all stimulations, TAB2 and TAB3 were associated only in the presence of TGF-β1. Upon co-stimulation TAK1-TAB2 association was lost. SMAD3 and JNK-1 did not associate with TAK1 however; JNK-2 and IKKβ were associated under all stimulations. c-Jun was detected only upon co-stimulation with TGF-β1 and TNFα. However, this experiment was limited to a single time point due to the volume of cells required for immuno-precipitation.

Attempts were also made to immuno-precipitate proteins using the various anti phospho-TAK1 antibodies with the aim of investigating the resulting lysates for specific protein associations and the occurrence of co-phosphorylation. However, probing neat lysate with phospho-TAK1 antibodies resulted in yields greater than that achieved by precipitating with the total form, which suggested that the phospho-TAK1 was pulling out non-specific proteins; confirmed by Coomassie staining of SDS-PAGE separated lysates, and potentially explain the non-specific effects seen in **Figure 43**. Performing a two-step immune-precipitation using total-TAK1 followed by phospho-TAK1 antibodies resulted in a lysate so dilute that no bands were detectable by Coomassie staining.

4.3.7 TAK1 Discussion

Prior investigation had shown that TGF-β1 but not TNFα was capable of inducing the canonical SMAD signalling response; with inhibition of SMAD3 limiting TGF-β1 driven EMT, with an unknown activity in relation to the accentuative effect of TNFα. Inhibition of IKKβ not only limited the accentuative effect of TNFα on EMT but also inhibited the driving effect of TGF-β1, which in conjunction with previously detected accentuated TAK1 phosphorylation was the catalyst to look at TAK1 as a potential mediator of this signalling crosstalk.

To summarize the data presented in the preceding sub-chapter: the *Thr187* residue of TAK1 is phosphorylated in response to both TGF-β1 and TNFα alone, with an accentuated response upon co-stimulation, whereas *Thr184* is phosphorylated only in response to TNFα. Inhibition and knockdown of TAK1 limited both TGF-β1 driven EMT and its accentuation by TNFα; and also inhibited the phosphorylation of IKKβ and JNK-2 but not SMAD3 further developing the putative signalling mechanism. As well as the increased phosphorylation of the *Thr187* residue in response to stimulation TAK1 phosphorylated potentially translocated to the nucleus, although results were conflicting, an effect not previously described. A similar effect was also observed in sequential sections taken from normal and OB lung, where increased phosphorylation of TAK1 (*Thr187*) and nuclear localization were observed in OB

sections compared to normal lung, although there was strong non-specific binding of the phospho-TAK1 antibody. TAB1 was shown to associate with TAK1 under all stimulations with a potentially accentuated association upon co-stimulation, TAB2 and TAB3 bound only in the presence of TGF-β1 with TAB2 binding lost upon co-stimulation with TNFα. IKKβ and JNK-2 associated with TAK1 at 30 minutes after stimulation with TGF-β1 or TNFα, c-Jun was associated only upon co-stimulation.

The inhibition of TGF-β1 driven EMT by TAK*i* and TAK*si* suggests that TAK1 may play a key role in driving EMT. However in 4.1.2.2 it was demonstrated that activated TAK1 was not capable of driving EMT alone, as SMAD3 phosphorylation was not inhibited by TAK*i* this suggests that TAK1 activity is required for TGF-β1 driven EMT, but is not the actual driver; instead suggesting that TAK1, or its downstream mediators, are in some way assisting the activity of SMAD3, possibly by co-factor recruitment or through synergistic activity as already discussed in 4.1.6 (Sano et al., 1999; Monzen et al., 2001). As IKKβ is key to the accentuation of EMT and is a substrate of TAK1, the lack of IKKβ mediated accentuation after TAK1 inhibition is un-surprising. From these results, it is possible to hypothesize that TGF-β1 activation of TAK1 is able to modulate its response to TNFα thus inducing a different, pro-fibrotic, NF-κB transcriptional activity leading to the observed accentuation of effect.

In the introduction to this section I highlighted the multiple levels of control apparent during the activation of TAK1, and how these may help describe the accentuative response seen upon co-stimulation with TGF-β1 and TNFα. I hypothesized that these residues may phosphorylate independently, possibly in response to different stimuli, with co-stimulation perhaps inducing pro-longed or accentuated phosphorylation. Comparing the intensity of phosphorylation between the residues is not possible using with the techniques used as a host of conflicting factors come into play, so any comparison can be based only on the trends of response.

That *Thr184* and *Thr187* are activated differentially in response to stimuli is very interesting and does provide evidence that modulation of TAK1 function may be possible in response to co-stimulation. The most elegant way in which to investigate this would be to generate *Thr184* or *Thr187* mutants and then assess TAK1 kinase activity across a range of substrates, along with other downstream markers. This may help identify if *Thr184* or *Thr187* had a preferred substrate or downstream effectors. I attempted to investigate this by immuno-precipitating using anti phospho-TAK1 antibodies but as described in **4.3.6** these attempts were unsuccessful. I also hypothesized that co-phosphorylation may also help explain the synergy between TGF-β1 and TNFα but again was unable to develop an assay to investigate this properly.

The above effect was interesting in relation to understanding underlying cell signalling methods, however my project was also firmly based in translating these findings into a disease model. As such the accentuated and prolonged phosphorylation of the *Thr187* residue upon co-stimulation with TGF-β1 and TNFα is perhaps more interesting. With heightened TGF-β1 and TNFα detected in the BAL of OB patients, it is possible to see how the *Thr187* residue of TAK1 could become hyper or constitutively activated. Combined with the later inhibitory experiments that showed the importance of TAK1 in EMT, and the presence of phosphorylated TAK1 in OB epithelial cells it is possible to construct a clinically relevant hypothesis, whereby increased or altered TAK1 activity is mediating the fibrotic development of disease, through alteration of downstream signalling.

To my knowledge there is no data that associates a particular mutation of TAK1 or any of the TAB proteins with a disease, which suggests that whilst TAK1 may mediate disease progression, it is not in itself an initiating factor, although of course it is possible that this has simply not been looked at. The only result in the literature demonstrates no association of mutated TAK1 with several different cancers (Kondo et al., 1998).

Whilst no data linking mutations of TAK1 or the TAB family have been described, there are numerous examples where TAK1 is identified as playing a key role in the development of disease. We have described a role for a TAK1 mediated synergy between TGF-β1 and TNFα in OB, however the *pro*-fibrotic, *pro*-inflammatory milieu found in the disease and mimicked in our culture models is not specific to just OB. Taken alongside the seemingly ubiquitous expression of TAK1 we propose that this method of action may be conserved in other disease states. IPF a disease of unknown aetiology is characterized by a progressive, chronic fibrosing of the alveolae. TGF-β1 driven EMT of the resident type II pneumocyte progenitor cell population is thought to play a key role in this process (Kim et al., 2006). There is some debate as to the role of inflammation in IPF (Behr et al., 2009), which may fit nicely with our hypothesis that whilst inflammatory markers are present, they require the *pro*-fibrotic effects of TGF-β1 to have a profound impact.

Other organ and disease models suggest a possible role for our TAK1 mediated synergistic hypothesis; in the kidney TGF-β1 has been shown to play an important role in the development of fibrosis by EMT (Liu, 2010), alongside this a role for inflammatory mediators secreted from leukocytes has also been described (Lange-Sperandio et al., 2007). Similarly within the development of liver fibrosis, a potential TGF-β1 driven EMT (Zeisberg et al., 2007) exists within an inflammatory milieu (Connolly et al., 2009), although in this instance there is no link between inflammation and EMT.

Whilst mutations of TAK1 itself do not seem to associate with the development of lung cancer (Kondo et al., 1998), the synergistic phosphorylation in response to TGF-β1 and TNFα may play a key role in tumorigenesis. Numerous papers link TAK1 with the development of cancer however, the suggested role varies widely. Suppression of TAK1 has demonstrated a ROS driven tumour cell specific apoptotic effect (Omori et al., 2010), also activation of TAK1 has been shown to induce NF-κB activation resulting in increased production of Iκ-Bα which in turn limited the anti-apotopic effects of NF-κB (Arsura et al., 2003). Conflictingly TAK1 mRNA levels analyzed from head and neck squamous cell cancer patients were reduced in relapsing patients (Honorato et al., 2008). TAK1 has also been shown to have tumour suppressive capabilities, mediated by the suppression of IKKγ (Bettermann et al., 2010), in an NF-κB independent fashion. As mentioned previously the role NF-κB in tumorigenesis and cancer maintenance is poorly understood; so it seems reasonable that the role of TAK1 as an upstream modulator of NF-κB and canonical TGF-β1 signalling may also lack clarity.

The previously mentioned SnoN has also been described as an important oncogenic protein, up-regulated in several different cancer cells in that it acts to inhibit the anti-proliferative action of TGF-β signalling (dysregulation of which is a key characteristic of certain cancers), facilitating oncogenic transformation of effected cells. A non-functional mutant failed to inhibit SMAD transcriptional activity and hence blocked this oncogenic transformation. An interaction between TAK1 and the oncogenic Ski-related novel protein N (SnoN), an inhibitor of SMAD transcriptional activity, would seem to fit well with a hyper-activated model whereby TAK1 accentuates EMT leading to cancer progression, however it appears that there is currently only a single paper investigating the activity of SnoN and TAK1 in a cancer setting; which suggests that whilst SnoN plays a key role in autophagic resistance to anti-cancer treatment it did so in a TAK1 independent manner (Smith et al., 2010).

The potential localization of TAK1 to the nucleus was not expected. Initially I hypothesized that TAK1 would function in the cytoplasm, modulating other proteins, such as JNK-2 or its downstream effectors, which would translocate to the nucleus. However, it became apparent that the nuclear translocation of TAK1 has been described previously. TAK1 itself does not contain a described nuclear translocation signal, although this does not necessarily mean that it is unable to translocate on its own; also no evidence of direct action with the genome has been presented, but this may be because it has not been investigated previously. In comparison the localization of ERK-1/2 remained poorly explained until a novel translocation method was discovered (Chuderland et al., 2008), and so it is possible that such a mechanism may subsequently be described for TAK1. Although the conflicting results raised in **Figure 42,**

and non-specific binding of phospho-TAK1 antibodies in **Figure 43** mean further investigations into TAK1 localisation are required.

To my knowledge three papers describe a nuclear localization of TAK1; the first describes localization in response to IL6 treatment with an increased kinase activity in both cellular compartments (Kojima et al., 2005). Secondly a more recent paper described the translocation of TAK1 into the nucleus in association with the previously mentioned SnoN (Kajino et al., 2007). In this instance, TAK1 is required for the TGF-β mediated degradation of SnoN and therefore the activation of SMAD transcriptional activity. In this system it is possible that our accentuated activation of TAK1 may result in an even greater inhibition of SnoN activity and an increase in resultant SMAD transcriptional activity, facilitating an even stronger fibrotic response.

The final paper has looked at this effect in the most detail and describes TAK1 as existing within both the cytoplasm and the nucleus in its un-phosphorylated state, the paper does not look at phosphorylation of TAK1 itself. Stimulation with TNFα or LPS had no effect on cellular distribution, nor did blocking nuclear export either, suggesting that TAK1 was not being trafficked (Ear et al., 2010). In my system total TAK1 and phospho-TAK1 were detected in both the nuclear and non-nuclear fractions, in agreement with the paper, however I did not block nuclear-trafficking. This raises the important question of how TAK1, if it does not traffic between the cytoplasm and the nucleus can become activated in the nucleus? The three described papers and my work contribute partially to the understanding of this process; however a more in-depth investigation is required to fully understand the mechanism behind, either how translocation is achieved or how activation in the nucleus occurs, and the subsequent activity of TAK1 in the nucleus. A ChIP assay for TAK1 would be able to describe a DNA binding role for TAK1, however in practice the required number of PBECs to perform this assay satisfactorily was prohibitive. In light of the modulatory role for TAK1 in SMAD3 driven EMT I hypothesized that TAK1 may be translocating to the nucleus with SMAD3 acting as a co-factor to induce or sustain its transcriptional activity.

By immuno-precipitating TAK1 under non-denaturing conditions I hoped to investigate which if any TAB proteins were associated with TAK1 under varying stimulations, as well as identifying downstream TAK1-protein interactions, such as the above mentioned TAK1-SMAD3 interaction. Confirming its description in the literature, TAB1 was constitutively associated with TAK1 at 30 minutes, when stimulated with TGF-β1 or TNFα, with a potentially accentuative association upon co-stimulation, although a more accurate outcome measurement is desirable. Both TAB2 and TAB3 were found to be associated with TAK1 at 30 minutes after stimulation with TGF-β1, with TNFα alone inducing no association. Upon co-stimulation

however the TGF-β1 mediated binding of TAB2 to TAK1 was inhibited, with no effect upon TAB3 binding observed. The TGF-β1 mediated association of TAB3 with TAK1, which was maintained under co-stimulation, may provide a mechanism for the hypothesized alteration of IKKβ and NF-κB transcriptional activity in response to co-stimulation although no evidence of altered transcription in response to differential TAB binding has been described in the literature.

It is difficult to draw conclusions from these findings due to the limited time-points sampled, again an product of limited cell populations, nevertheless the TAB2 findings in particular demonstrate the interplay between TGF-β1 and TNFα. For example after stimulation with TNFα alone TAB1 may be more free to induce phosphorylation of the *Thr184* residue of TAK1. Does the accentuated association of TAB1 directly lead to the accentuated phosphorylation of TAK1 *Thr187*. To understand this more fully a wider array of time-points would need to be studied, and most importantly an understanding of whether there is competition for binding of TAK1 between the TABs, and if so what affect the absence of a particular TAB can have on phosphorylation and downstream signalling.

The downstream associations of TAK1 are again interesting. TAK1 was not shown to associate with SMAD3 at a 30 minute time-point, which suggests that TAK1 is not acting as a co-factor with SMAD3. Both IKKβ and JNK-2, but seemingly not JNK-1 are associated with TAK1 at this time point after stimulation, although there was no noticeable variation between stimulations. Whilst it is unknown if TAK1 is directly binding to IKKβ or JNK-2, as this assay just shows an association it does provide clear evidence that TAK1 is in some way inducing their subsequent phosphorylation. Perhaps more interestingly is the association of c-Jun with TAK1 only upon co-stimulation. As a component of the AP-1 transcription factor c-Jun is important in regulating genes involved in many different cell responses, including but not limited to cellular differentiation. By displaying an association with TAK1 only upon co-stimulation this may describe the mechanism whereby the accentuated signalling response is interacting with the genome initiating the EMT.

This binding may also help describe the nuclear localization of TAK1 as IKKβ, JNK-2 and c-Jun are known to be able to translocate to the nucleus, and TAK1 may be piggybacking in association with these factors. The obvious way to investigate this effect would be to immuno-precipitate the nuclear and cytoplasmic fractions, however as with a ChIP assay the number of PBECs required to generate a suitably sized nuclear fraction was prohibitive. Once again the above discussion must be couched with the understanding that only a single time-point was observed, and results may differ accordingly.

In the discussion sections for SMAD3 and IKKβ I constructed a hypothesis of collagen I-IV secretion being independent of the then unknown accentuatory protein. With TAK1 potentially filling this role, and due to the strong inhibitory effect of both TAK*i* and TAK*si* it is necessary to reconsider this hypothesis. The only hypothesis I can construct to fit these new findings is that TAK1 plays some form of modulatory role in relation to SMAD3 activity, although not directly due to the lack of detected association, possibly by activating co-activating transcription factors in a way which is not affected by TNFα stimulation although I can present no data to support this supposition either directly or from the literature.

TAK*i*, but not TAK*si*, pre-treatment consistently induced an increase in *pro*-MMP-9 secretion, seemingly magnifying the normal response to stimulation with TGF-β1 or TNFα. My initial thoughts were either that; in our cell system TAK1 is more involved in the production of TIMPs and hence the suppression of *pro*-MMP-9 secretion, or that I was observing an off target effect of the chemical inhibitor. However the only references linking TAK1 and *pro*-MMP-9 secretion in the literature describe a mechanism which follows the expected hypothesis, namely that TNFα (Srivastava et al., 2007) and TGF-β1 are capable of increasing secretion, with several papers postulating that TAK1 is required for this to occur.

As discussed in 4.1.6 I investigated the role of the different TNFα receptors in accentuating EMT 8.7, to investigate this receptor specific isoforms of TNFα were used, at the same dose for the generic recombinant TNFα used throughout my project. As PBECs only expressed TNFαR1 accentuation of EMT was only observed with TNFαR1 specific TNFα. Pre-treatment with TAK*i* strongly reduced this accentuation, which then suggested that it was the generic TNFα that was driving the increased secretion of *pro*-MMP-9, as opposed to TAK*i*.

The only hypothesis that I can propose to explain this effect presumes non-specific effects from both TAK*i* and TNFα. If the non-receptor specific isoform of TNFα is binding to a receptor other than TNFR1, potentially due to the relatively high concentrations used, it may induce a signalling response utilising unknown signalling proteins. If we then hypothesized that this unknown pathway was responsible for the maintenance of TIMP production, and also contained a protein which was effected by off target effects of TAK*i*, or itself modulated by TAK1, then it is possible to see a mechanism where de-regulated and increased *pro*-MMP-9 secretion could occur. However, I present no evidence to support this supposition.

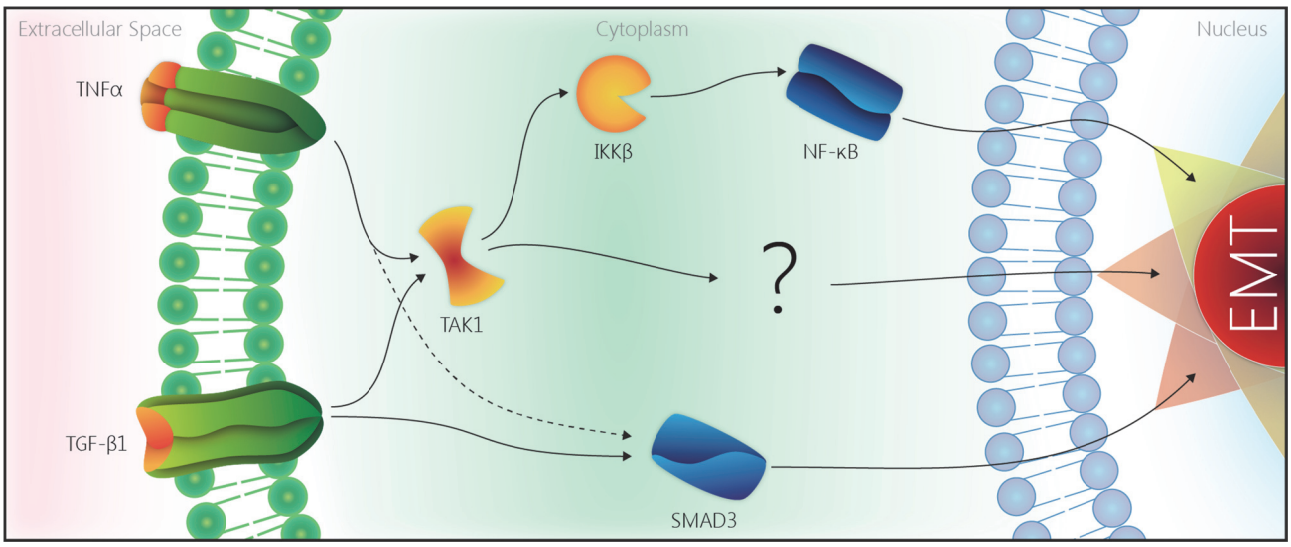

Figure 45 - Proposed Signalling Mechanism III

TGF-β1 signals through the canonical SMAD pathway, utilising SMAD3 and induces EMT, independently of TNFα. TAK1 whilst not capable of driving EMT alone is required to facilitate SMAD3 driven EMT. TNFα signals through TAK1 which activates IKKβ signalling required to accentuated EMT upon co-stimulation. This raises the possibility that TGF-β1 stimulation of TAK1 in some way alters the IKKβ response inducing a more fibrotic NF-κB transcriptional response, or through downstream effectors such as the MAPK family, particularly JNK-1/2.

These findings help identify TAK1 as a potential controller of the fibrogenic synergy between TGF-β1 and TNFα, although the mechanism of its control is unknown. It was demonstrated that TAK1 and SMAD3 do not directly associate and so modulation of SMAD3 activity likely requires use of downstream mediators, potentially acting as co-factors. The associations of TAB proteins, especially TAB3 with TAK1 in response to co-stimulation, and the differing phosphorylation responses highlight how TAK1 interaction with IKKβ, and subsequent NF-κB activity may be altered to be more fibrogenic. However, work investigating other potential effectors, namely the MAPK constituents P38, ERK-1/2 and JNK-1/2 is required to describe a complete signalling cascade.

5 JNK-2 Modulates TAK-1 Activity

5.1 MAPK p38

The MAPK p38 family of 38kDa proteins consists of four members p38α, β, γ and δ displaying approximately 60% sequence homology, of which p38α was the first described (Han et al., 1994) responding to LPS stimulation. It is now thought that the main role of p38 signalling is to respond to stress stimuli. As well as being the first discovered p38, p38α is also the most widely studied in part due to its ubiquitous expression with the other family members displaying a more tissue specific expression (Cuenda and Rousseau, 2007). p38 and the other MAPKs which I will discuss later share a similar structure, consisting of two distinct lobes between which the kinase site sits, with co-phosphorylation of threonine and tyrosine residues separated by a single amino acid, which in the case of p38 is *Thr180-Gly-Tyr182*, of the activation loop required to allow substrate binding.

p38 activation sits at the bottom of a multifaceted cascade, directly activated by MAP2Ks which are in turn activated by MAP3Ks activation of which is usually receptor coupled but may be as a result of intracellular activation. p38 has been shown to be phosphorylated by the following MAP2Ks, MKK3,4 and 6. MKK3 and 6 are thought to be very selective for p38 over ERK-1/2 and JNK-/1 (Dérijard et al., 1995; Raingeaud et al., 1996; Terada et al., 1999) and are also thought to be the main activators of p38, with MKK4, which can also activate JNK-1/2, required only in response to certain stresses (Brancho et al., 2003). The use of MKK3 and MKK6 is itself likely to be cell and stimulus dependant, although with some demonstrated overlap (Enslen, 1998), with one study demonstrating that CD4 T cells utilized MKK3 to a greater extent than MKK6, whilst T cell progenitors preferentially used MKK6 (Tanaka et al., 2002).

These MAP2Ks require activation themselves, again by co-phosphorylation of their activation loop, by MAP3Ks, at this level there is much greater overlap of function, again covered in more detail in the review by Rubinfeld *et al* (Rubinfeld and Seger, 2005), including ASK1, TAK1, MLK2 and MEKK3 among others. Whilst these activations and those of the MAPKs themselves can occur as direct kinase interactions, as with the other signalling mechanisms already described the role of scaffold proteins is now widely being investigated. The scaffold protein osomosensing scaffold for MEKK3 (OSM) forms a scaffold that recruits and facilitates the activation of MEKK3, MKK3 and p38 in a cascade in response to osmotic stress (Uhlik et al., 2003), although no mechanism for this recruitment was or has been described, so the usage of poly-ubiquitin chains in this system is unknown.

This wide variety of activating proteins means that p38 can be activated by numerous different stimuli, of direct importance to my study however is its response to TGF-β1 and TNFα, and response to both has been demonstrated (Wysk, 1999; Wang et al., 2002). TGF-β1 activation of p38 utilizes the non-canonical pathway described in **1.3.4** utilising TRAF6 and TAK1 (Yamashita et al., 2008), although p38 can subsequently activate this canonical arm (Furukawa et al., 2003); with TNFα and IL-1β also utilising this activatory mechanism (McDermott and O'Neill, 2002; Royuela et al., 2008), although other activating pathways are used as well depending on stimuli. The localization and activity of p38 in response to stimuli is poorly understood; p38 is thought to reside in the cytoplasm in its un-stimulated state with some reports stating that nuclear localization is specifically mediated by DNA damage signals (Wood et al., 2009) although others describe phosphorylated p38 in the nucleus in un-stimulated cells (Lu et al., 2006; Gorog et al., 2009).

When nuclear localized, the export of p38 is mediated by its downstream substrates such as MAPK activated protein kinase (APK)-2 and 5 which both contain nuclear localization and nuclear export signals, upon binding with these substrates in the nucleus the localization signal is masked and the complex exported (Seternes et al., 2002; Gorog et al., 2009). This led to the hypothesis that mitogen activated protein kinase activated protein kinase (MAPKAPK)-2/5 may be responsible for p38 nuclear localization as well with signals masked depending on other stimuli, however MAPKAPK-2 knockout experiments demonstrated an elevated nuclear localisation of p38 (Gorog et al., 2009). Interestingly TAB1 is capable of binding and phosphorylating p38, which leads to a reduction p38 signalling activity and also decreases nuclear localization (Lu et al., 2006), from which it is possible to hypothesize that p38 activating factors such as MKK3 may also act as mediators of localisation, although to date this has not been described.

p38 interacts with a huge variety of substrates including the MAPKAPKs mentioned above as well as other factors such as ATF-1, p65, FADD inhibitors and p53, for a more in depth coverage see the review by Cargnello *et al* (Cargnello and Roux, 2011). This wide range of substrates allows p38 to modulate several other signalling pathways either directly or indirectly, for example p38 through its substrate mitogen and stress activated protein kinase 1 (MSK1) is capable of phosphorylating p65, which important in p65 transcriptional activity in response to TNFα (Vermeulen et al., 2003). Alternatively, as well as being phosphorylated by TAB1, p38 is itself capable of phosphorylating TAB1 inhibiting it's activation of TAK1 and the subsequent downstream signalling that it mediates (Cheung et al., 2003).

As with all the other areas of this introduction, inactivation of p38 is also poorly understood. Inhibitory methods such as those described already through TAB1 mediated inactivation (Lu et al., 2006), and potential negative feedback through inhibition of TAK1 activity (Cheung et al., 2003). De-phosphorylation of p38 has also been shown to play a key role in the regulation of p38 activity, traditional phosphatases such as the previously discussed PP2A which removes singular phosphate groups from the p38 activation loop. Interestingly de-phosphorylation of *Thr180* completely inhibits p38 activity, whereas de-phosphorylation of *Tyr182* leads to a 20 fold reduction in kinase activity (Zhang et al., 2008), which may provide a means of tuning p38 response. As well as these more generic phosphatases special MAPK phosphatases (MKP)s which can de-phosphorylate both residues of MAPK have been described with MKP-1, 4 and 5 having been shown to de-phosphorylate p38 (Owens and Keyse, 2007).

5.1.1 Chemical Inhibition of p38

Previous assays of phosphorylation in PBECs 4.1.2.2, 4.2.2.2 and 4.3.2.2 had demonstrated that p38 was not phosphorylated in response to TGF-β1 or TNFα, but displayed a constant level of phosphorylation after stimulations, which was not affected by any inhibitory treatment used so far. Prior to assessing phosphorylation across a time course I decided to chemically inhibit its function. SB 203580 (p38*i*) is a well characterized cell-permeable inhibitor of p38 that blocks ATP binding required for kinase function (Tong et al., 1997). As with the inhibitor of IKKβ a variety of IC_{50} doses have been described, with a 50-100nM dose inhibiting TNFα production in the THP-1 human monocyte cell line, or mechanistically a 1μM inhibiting platelet aggregation initiated by collagen (Saklatvala et al., 1996).

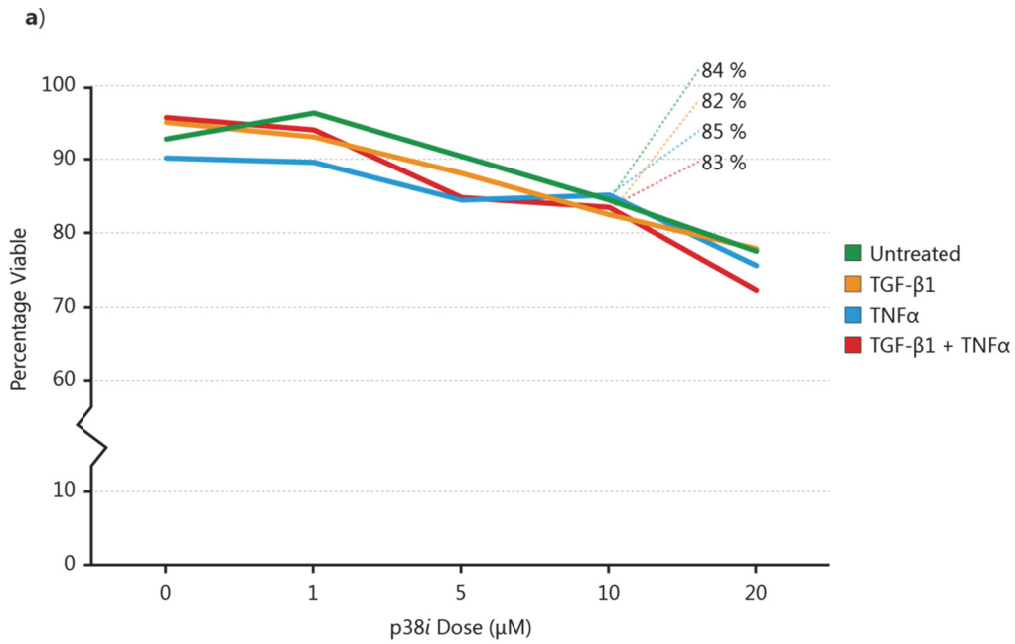

Figure 46 - p38*i* dose response

a) A549 cells were stimulated with TGF-β1 (10ng/mL) or TNFα (20ng/mL) for 72 hours after a 1 hour pre-treatment with p38*i* at 1, 5, 10 and 20µM doses (*n=3*). There was a trend of decreased viability with increasing dose of p38*i* under all stimulations with little variation between stimulations.

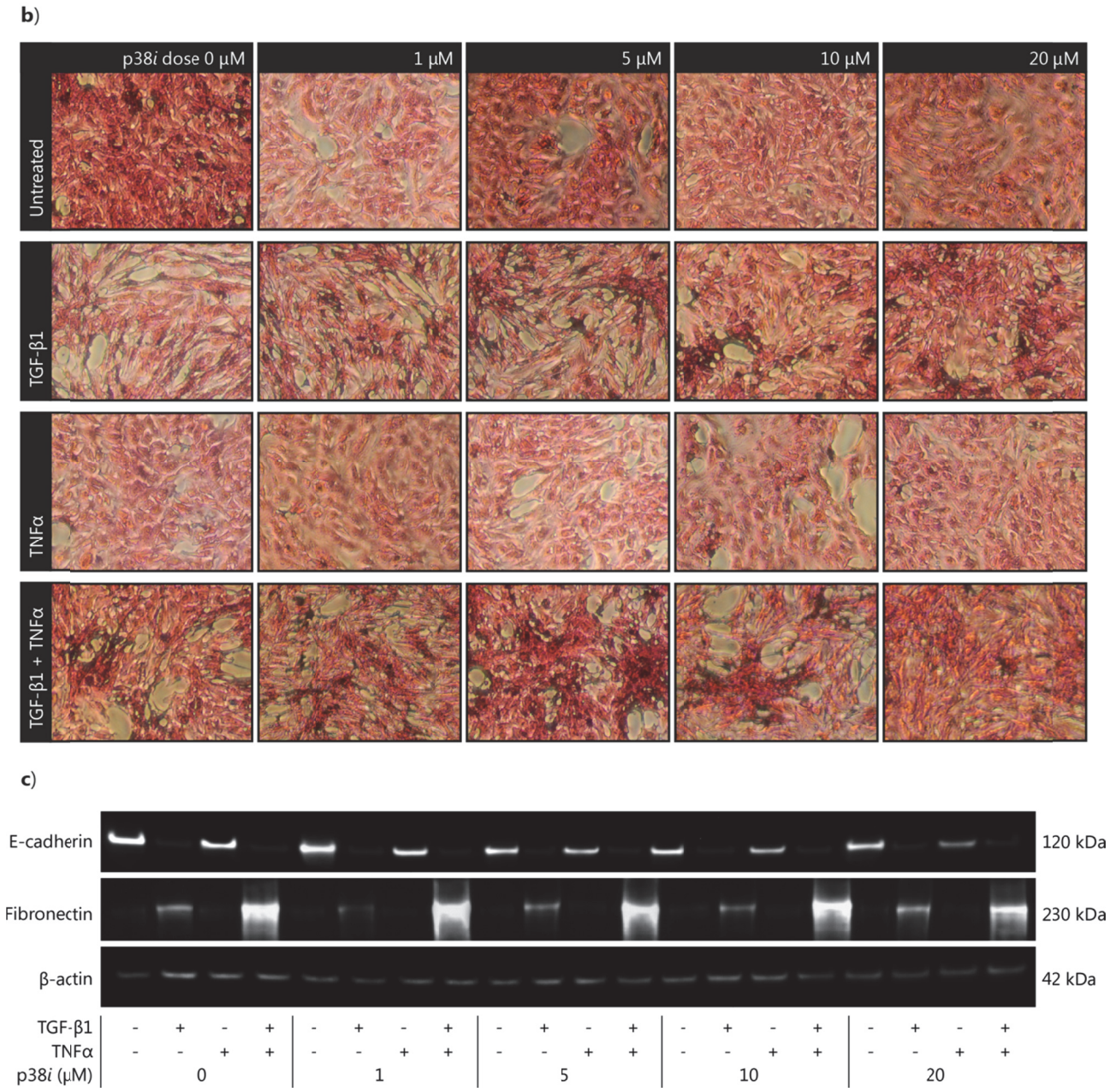

Figure 46 Continued - p38*i* dose response

b) 72 hours post stimulation with TGF-β1 there was a transition from the cobblestone like epithelial appearance of un-stimulated A549 cells towards a more striated, mesenchymal phenotype. This effect was accentuated by co-stimulation with TNFα, whereas TNFα alone had no effect on cell morphology. No dose of p38*i* strongly inhibited TGF-β1 driven EMT or its accentuation by TNFα, although a weak inhibitory effect was seen at and beyond a 10µM dose.

c) E-cadherin expression was reduced upon TGF-β1 stimulation. A 20µM dose of p38*i* slightly inhibited the TNFα accentuation of TGF-β1 driven fibronectin expression, but offered no protection against the loss of E-cadherin expression, which even in un-stimulated cells was reduced compared to controls. E-cadherin and fibronectin (5µg).

A 10μM dose of p38*i* was, at the morphological level, capable of slightly inhibiting EMT in response to TGF-β1 or TNFα, however the effect was very mild. No dose of p38*i* inhibited the TGF-β1 driven and TNFα accentuated loss of E-cadherin and gain in fibronectin expression significantly. A slight inhibition of the accentuated production of fibronectin was observed at 20μM, but conversely this high dose was also down-regulating E-cadherin expression in its own right when comparing un-stimulated cells. Due to the lack of inhibitory effect, choosing a dose of p38*i* for future experiments was difficult; nevertheless, a 10μM dose was chosen and used over the 20μM dose due to its reduced effect on cell viability and weaker impact on baseline levels of E-cadherin.

5.1.1.1 Chemical Inhibition of p38, Effect on EMT Endpoint

With an appropriate dose of p38*i* decided upon in A549 cells the next step was to observe what effect this would have on EMT in PBECs. *n=3* PBEC cultures from distinct patients were stimulated with TGF-β1 or TNFα for 72 hours after a 1 hour pre-treatment with 10μM p38*i*. Cell lysate and culture media was retained and EMT was assessed using a variety of markers.

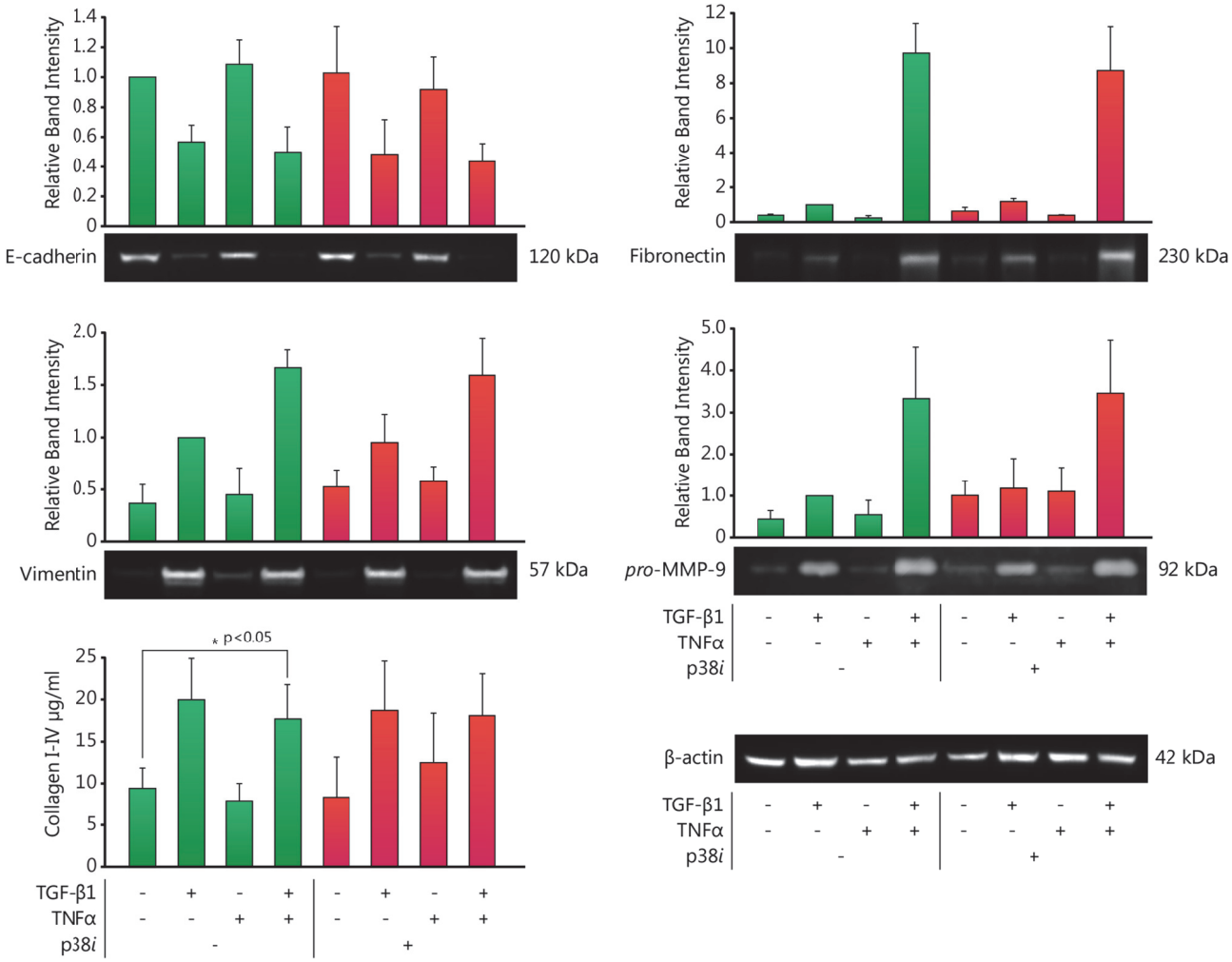

Figure 47 - Effect of p38*i* on EMT

Stimulation of PBECs (*n=3*, representative blots from single patient) with TGF-β1 (10ng/mL) for 72 hours down-regulated E-cadherin expression, increased fibronectin and vimentin expression and increased *pro*-MMP-9 secretion. This change in EMT marker expression was accentuated by co-stimulation with TNFα (20ng/mL). Collagen I-IV secretion was significantly up-regulated by stimulation with TGF-β1 ($p<0.05$, *n=3*) however no accentuation was observed upon co-stimulation with TNFα. Pre-treatment with p38*i* (10µM) did not inhibit either TGF-β1 driven EMT, or its accentuation by TNFα for any marker assessed. E-cadherin and fibronectin (5µg), vimentin (20µg), *pro*-MMP-9 (30µL) and collagens I-IV (25µL).

The above results demonstrate that along with not phosphorylating in response to TGF-β1 or TNFα stimulation, p38 does not appear to play a role in EMT for the assessed markers. Due to this surprising outcome it was decided to not investigate the role of p38 further, and to focus on other potential downstream mediators of TAK1.

5.1.2 p38 Discussion

Stimulation with TGF-β1 or TNFα had not induced phosphorylation of p38 in previous experiments, therefore I moved straight into chemical inhibition of p38 to confirm this lack of role before initiating other more involved experiments. p38*i* did not limit either TGF-β1 driven EMT or its accentuation by TNFα, confirming in our system that it did not play a direct role.

This finding was somewhat surprising as numerous studies have demonstrated p38 activation in response to TGF-β1 (Varela-Rey et al., 2002; Yamashita et al., 2008; Kolosova et al., 2010) and TNF (Varela-Rey et al., 2002; Royuela et al., 2008), has been strongly implicated in the development of EMT (Kolosova et al., 2010; Lv et al., 2011) and also in OB (Ramirez et al., 2006) with a p38δ inhibitor[11] recently approved for use in treatment of IPF (Moran, 2011). However with the data to hand it is only possible to conclude that p38 does not play a role in our system; interestingly our group has previously demonstrated this effect in A549 cells, whereby p38 phosphorylation was increased by TNFα stimulation, but played no role in the subsequent development of EMT (Borthwick et al., 2011).

One possibility is that the chemical inhibitor used is not blocking p38 activity, or all p38 activity. It has been demonstrated that p38*i* inhibits p38α and β more strongly than p38γ or δ (Davies et al., 2000). It is therefore possible, especially in light of a p38δ inhibitor entering clinical use (Moran, 2011) that we are not inhibiting the correct isoform. However in a study investigating the role of p38 in the development of EMT in a pulmonary epithelial cell line used half the dose of p38*i* and strongly inhibited the expression of fibronectin and secretion of collagen I (Kolosova et al., 2010). Similarly this does not account for the lack of change in phosphorylation seen upon stimulation, using an antibody that can detect all isoforms of p38 (Avitzour et al., 2007); also in a previous paper our group has demonstrated a change of p38 phosphorylation using the same antibodies (Borthwick et al., 2011). Whilst not displaying a lack of effect, p38 phosphorylation has been shown to inhibit TGF-β1 driven EMT, protecting against the loss of E-

[11] *Esbriet (Pirfenidone), InterMune*

cadherin, and gain of vimentin expression by inhibiting TAK1 activity (Strippoli et al., 2010) suggesting that the role of p38 may be cell type dependant.

As with IKK*i,* p38*i* does not block the phosphorylation of p38, but rather its kinase activity, as such to investigate efficacy of inhibitor a specific p38 substrate is required; due to the often overlapping roles for MAPKs it can be difficult to isolate such a substrate. There are several kits available that facilitate a cell free kinase/substrate assay using antibodies raised against p38, and other groups have modified p38 to allow for a more specific pull down (Szafranska et al., 2005). The transcription factor myocyte-enhancer factor 2C is phosphorylated selectively by p38 but not ERK2 or JNK1 (Han et al., 1997), and as such may have served as a good target for a cell based system. However, due to the lack of phosphorylation seen in previous PBEC experiments, and the poor effect of the inhibitor at doses higher than those described in other positive studies (Kolosova et al., 2010; Lv et al., 2011) it was decided to halt investigations into p38 at this point.

5.2 Extracellular signal-regulated-1/2

The MAPK ERK family of proteins are encoded for by two genes, *MAPK1* and *MAPK3* which encode the ubiquitously expressed 42 kDa ERK-2 and 44 kDa ERK-1 proteins respectively, and were the first MAPKs to be discovered (Boulton et al., 1990) and display approximately 85% sequence homology (Boulton et al., 1991). As with p38 both ERK-1 and ERK-2 are formed of two lobes with a catalytic groove running between which is activated by co-phosphorylation of threonine and tyrosine residues in the activation loop; separated by glutamate in a *Thr202-Glu-Tyr204* arrangement for ERK-1 and *Thr185-Glu-Tyr187* for ERK-2, with tyrosine phosphorylation occurring before threonine (Ferrell Jr., 1997). Some evidence of redundancy between ERK-1 and ERK-2 has been demonstrated (Voisin et al., 2010) however several non-redundant functions have also been described (Hatano et al., 2003; Li and Johnson, 2006).

ERK-1/2 signalling follows a broadly similar pattern to that of p38 utilising a similar cascade but with different key components. Receptor stimulation, and both TGF-β1 (Lee et al., 2007) and TNFα[12] (Kakiashvili et al., 2011) have been shown to be able to activate ERK-1/2. This leads to the activation of small GTPases such as Ras and Rap which are capable of activating MAP3Ks; with the rapidly accelerated fibrosarcoma (RAF) family of proteins specifically associated with ERK-1/2 activation (Hagemann and Rapp, 1999) and other less specific MAP3Ks such as MEKK1 (Karandikar et al., 2000), also associated with JNK activation (Xia, 2000). Downstream of this the MAP2Ks MEK1 and 2 specifically activate ERK-1/2 by phosphorylation of its activation loop (Catalanotti et al., 2009). Efficient signal transduction is thought to mediated by association of the various components with the scaffold protein kinase suppressor of Ras-1 (KSR1) (Therrien et al., 1996).

ERK-1/2 reside in the cytoplasm in their un-stimulated state held in place by several scaffold proteins (Tanoue et al., 2000; Perlson et al., 2006), upon phosphorylation within the activation loop they are released into the cytoplasm. In this state ERK-1/2 is not capable of nuclear translocation and requires further phosphorylation, by unknown means, in a region outside of the activation loop, which allows ERK-1/2 to associate with nuclear import proteins and translocate to the nucleus, however it was shown that this phosphorylation and not just nuclear import protein association was required for this transition (Chuderland et al., 2008). Within the nucleus ERK-1/2 are capable of activating numerous different transcription factors including c-Jun[13] (Morton et al., 2003), c-Fos (Murphy et al., 2002), NF-κB (Peng et

[12] *TNFα is proposed to act through epidermal growth factor receptor (EFGR) rather than TNFR.*
[13] *Differentially to JNK-1/2 mediated phosphorylation.*

al., 2010) and more exclusively for ERK-1/2 the E twenty-six-like transcription factor 1 (ELK1) (Gille et al., 1995).

Although the majority of activated ERK-1/2 translocates to the nucleus a fraction remains in the cytoplasm where it is capable of interacting with numerous factors including MAPK-interacting kinase-1/2 (MNK1, 2) (Waskiewicz et al., 1997) and the ribosomal S6 kinase (RSK) family of proteins (Chen et al., 1992), although these are also often located in the nucleus as well. In both instances these kinases are capable of interacting with other transcription factors for example the RSK2 is capable of phosphorylating Iκ-Bα initiating NF-κB signalling in an IKK independent manner (Peng et al., 2010)

As with p38 deactivation of ERK-1/2 signalling can be achieved through generic phosphatases such as PP2A (Kins et al., 2003), with the dual de-phosphorylating MKP-3 showing strong associations with ERK-1/2 (Kim et al., 2003).

5.2.1 Chemical Inhibition of ERK-1/2

A reliable phospho-ERK-1/2 antibody was never worked up, hence why it was not used in other phosphorylation panels. Example blots are included with the chemical inhibitor data. Due to this lack of reliable assay, and with the limited results acquired suggesting that it ERK-1/2 was not phosphorylated by TGF-β1 or TNFα it was decided that, as with p38, prior to assessing phosphorylation across a time course I would chemically inhibit ERK-1/2 activity.

FR180204 (ERK*i*) is a cell-permeable inhibitor of ERK-1/2 which blocks ATP binding required for kinase function (Ohori et al., 2005) with the same paper describing an IC_{50} of 500nM when analyzing the phosphorylation of myelin basic protein, a substrate of ERK-1/2 in a cell free system, and a dose of 3.1μM inhibiting the activation of AP-1 by half in Mv1Lu cells[14].

[14] *Mink lung epithelial cell line*

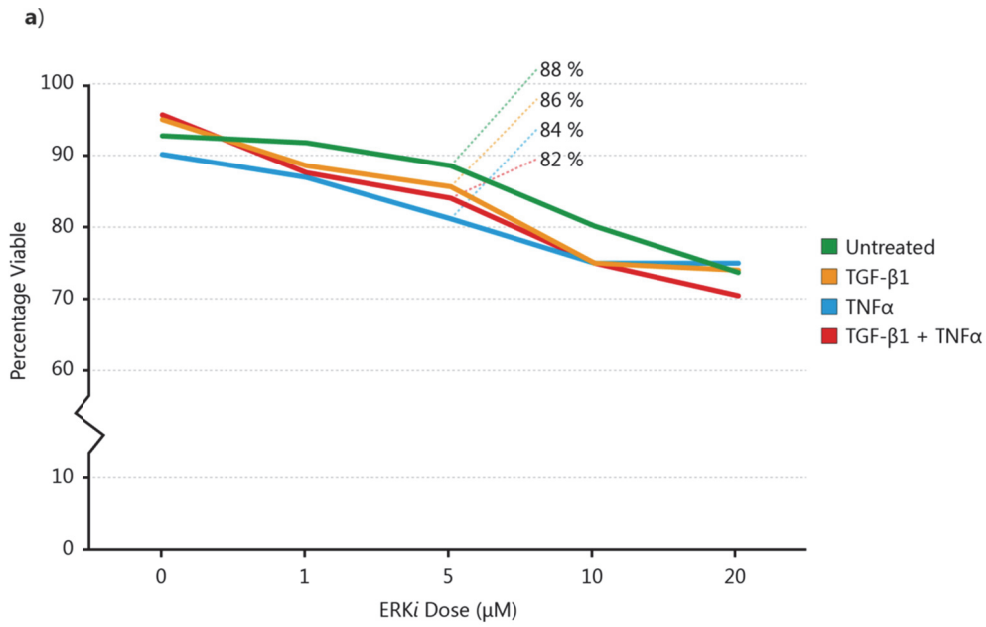

Figure 48 - ERK*i* dose response

a) A549 cells were stimulated with TGF-β1 (10ng/mL) or TNFα (20ng/mL) for 72 hours after a 1 hour pre-treatment with ERK*i* at 1, 5, 10 and 20µM doses. There was a trend of decreased viability with increasing dose of ERK*i* under all stimulations with little variation seen between stimulations.

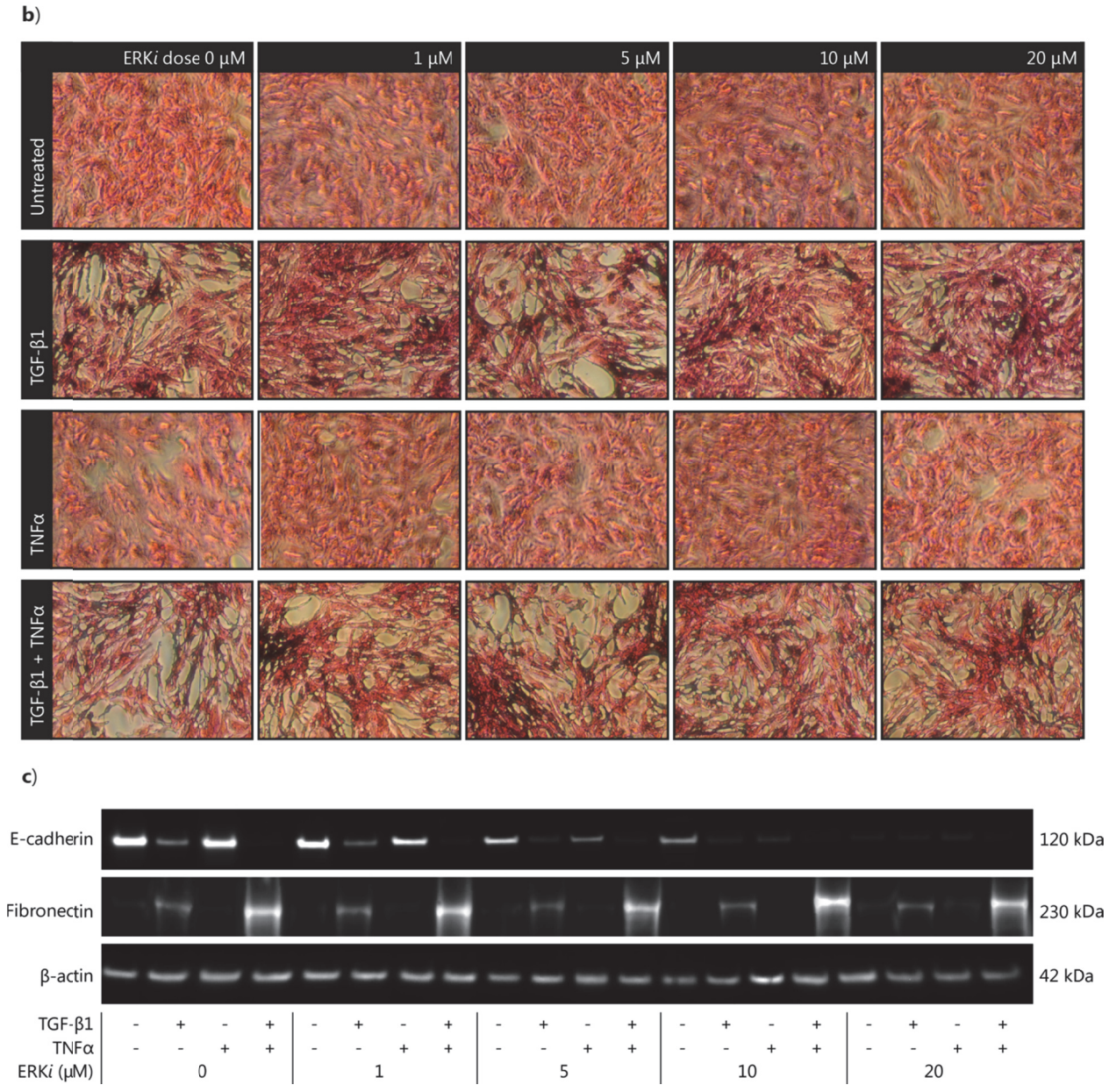

Figure 48 Continued - ERK*i* dose response

b) 72 hours post stimulation with TGF-β1 there was a marked transition from the cobblestone like epithelial appearance of un-stimulated A549 cells towards a more striated, mesenchymal phenotype. This effect was accentuated by co-stimulation with TNFα, whereas TNFα alone had no effect on cell morphology. ERK*i* had no inhibitory effect on morphological EMT at any dose.

c) E-cadherin expression was reduced upon TGF-β1 stimulation with an accentuated reduction upon co-stimulation with TNFα. ERK*i* had no inhibitory effect on EMT at the protein level at any dose, with E-cadherin expression strongly decreased even in un-stimulated cells at doses above 5µM. E-cadherin and fibronectin (5µg).

ERK*i* was not capable of inhibiting EMT either morphologically or at the protein level at any dose, with higher doses of 10 and 20μM decreasing the baseline level of E-cadherin expression. To verify this lack of role in EMT I decided to use a 5μM dose of ERK*i* and perform the standard screen in PBECs to determine if other markers of EMT were also unaffected.

5.2.1.1 Chemical Inhibition of ERK-1/2, Effect on EMT Endpoint

With an appropriate dose of ERK*i* decided upon in A549 cells the next step was to observe what effect this would have on EMT in PBECs. *n=3* PBEC cultures from distinct patients were stimulated with TGF-β1 or TNFα for 72 hours after a 1 hour pre-treatment with 5μM ERK*i*. Cell lysate and culture media was retained and EMT was assessed using a variety of markers.

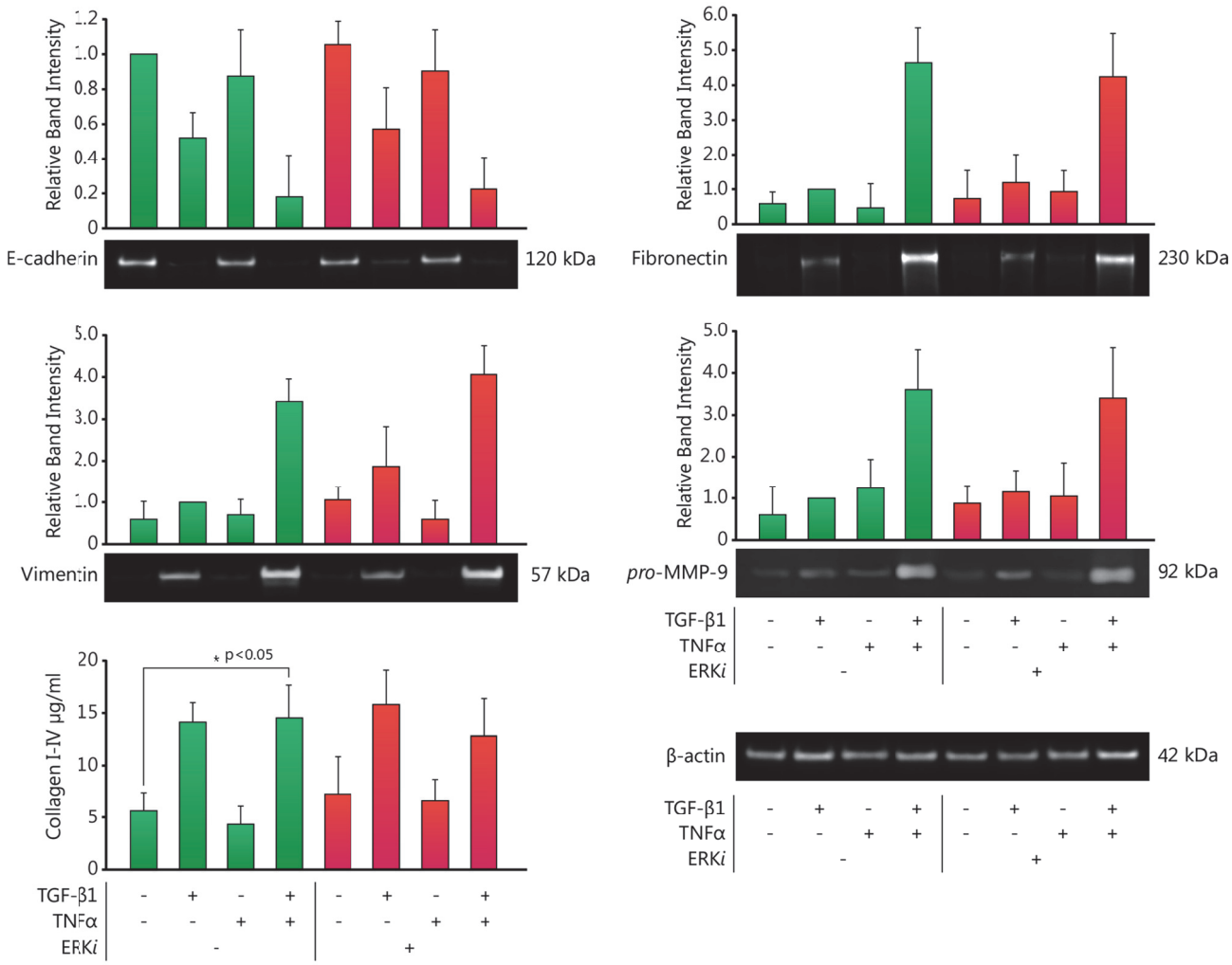

Figure 49 - Effect of ERK*i* EMT

Stimulation of PBECs (*n=3*, representative blots from single patient) with TGF-β1 (10ng/mL) for 72 hours down-regulated E-cadherin expression, increased fibronectin and vimentin expression and increased *pro*-MMP-9 secretion. This change in EMT marker expression was accentuated by co-stimulation with TNFα (20ng/mL). Collagen I-IV secretion was significantly up-regulated by stimulation with TGF-β1 ($p<0.05$, *n=3*) however no accentuation was observed upon co-stimulation with TNFα. Pre-treatment with ERK*i* (5µM) did not inhibit either TGF-β1 driven EMT, or its accentuation by TNFα for any marker assessed. E-cadherin and fibronectin (5µg), vimentin (20µg), *pro*-MMP-9 (30µL) and collagens I-IV (25µL).

As with p38 the above results demonstrate that ERK-1/2 does not play a role in either TGF-β1 driven EMT, or its accentuation by TNFα for the assessed markers, in the case of vimentin ERK*i* was increased EMT compared to untreated controls. ERK*i* phosphorylation was difficult to assay, but displayed no change upon stimulation, and was not inhibited by ERK*i*.

5.2.2 ERK-1/2 Discussion

Stimulation with TGF-β1 or TNFα had not induced phosphorylation of ERK-1/2 in the limited experiments where a signal was detected, therefore I moved straight into chemical inhibition of ERK-1/2 to confirm this lack of role before initiating other more involved experiments. Similarly to p38*i*, ERK*i* did not limit either TGF-β1 driven EMT or its accentuation by TNFα, confirming in our system that it did not play a direct role. Whilst detection of total ERK-1/2 was feasible and did not vary upon stimulation or inhibition detection of the phosphorylated form required the use of excessively high lysate concentrations, although again when detectable there was no variation in the level of phosphorylation.

These results were again surprising as ERK-1/2 has been implicated in EMT (Lee et al., 2007; Strippoli et al., 2008; Kakiashvili et al., 2011) and is capable of being activated by TAK1 (Nishimura et al., 2009) although it is thought that p38 and JNK-1/2 are more strongly activated by the typical MAP2Ks activated TAK1. Alternative splice variants are produced from *MAPK1* and *MAPK3* (Strausberg et al., 2002) and a novel effect from one of these splice variants has been described (Shaul et al., 2009). However this splice variant produces a smaller ERK-1 protein which is detectable as a distinct band under the normal ERK-1 and ERK-2 bands (Aebersold et al., 2004), and was not observed, and there is no data to suggest that ERK*i* would have less of an effect on these variants due to the high degree of homology.

Therefore the only conclusion to draw is that in this system ERK-1/2 and p38 play little role in the development of EMT. The lack of change in phosphorylation upon stimulation or after TAK1 inhibition suggests both that TGF-β1 or TNFα are not utilising these pathways in PBECs, and also that activation of each is not mediated by TAK1. As discussed in the various introductory sections there are numerous other stimuli and MAP3K/MAP2Ks that are capable of activating p38 and ERK-1/2 and it may be that these are their preferred cascades in PBECs. The final MAPK I investigated was JNK-1/2 which already displayed a phosphorylation response to simulation which was effected by inhibition of TAK1 its upstream mediator.

5.3 c-Jun N-terminal kinase-1/2

The JNK family of MAPK proteins consists of three members JNK-1, 2 and 3 encoded for by the *JNK1,2* and *3* genes respectively, with several variants of each capable of being produced. JNK-1 and 2 are thought to ubiquitously expressed (Kallunki et al., 1994) whereas JNK-3 (Mohit et al., 1995) is thought to be specific to neuronal cells. The main target of JNK-1, 46 kDa, and JNK-2, 55 kDa, is control the AP-1 transcription factor especially through activation of c-Jun one of its components with JNK-2 displaying a higher affinity (Kallunki et al., 1994); although redundancy has been demonstrated in relation to other substrates (Kosters et al., 2009). Activation of JNK-1/2 is mediated by the co-phosphorylation of *Thr183-Pro-Tyr185* within the activation loop of each form, which facilitates substrate binding.

Initiation of JNK-1/2 signalling is thought to be mediated by the usage of GTPases such as RAC-1 and RAC-2 when signalling in response to growth factor receptors such as EGFR (Minden et al., 1995); with these factors being less important on TNFR and IL-1R mediated JNK-1/2 activation (Minden et al., 1995), suggesting that upstream kinases, sometimes termed MAP4Ks, such as the archetypal MAP4K (Su et al., 1997) playing more of a role. Whatever the means of activation a wide variety of MAP3Ks are capable of responding to stimulation including MEKK1 (Xia, 2000) and importantly TAK1 (Wang et al., 2001; Mao et al., 2011). At the MAP2K level MKK4 and 7 have been shown to be key non-redundant regulators of JNK-1/2 co-phosphorylation required for its efficient activation. MKK4 has been shown to preferentially phosphorylate the *Tyr185* residue, whereas MKK7 targets *Thr183* (Lawler et al., 1998). Phosphorylation of *Thr183* alone leads to a 10 fold reduction in kinase activity, whereas phosphorylation of *Tyr185* alone leads to complete inhibition of activity (Khokhlatchev et al., 1997). Activation of JNK-1/2 is once again thought to be mediated by associated scaffold proteins such as the JNK-interacting protein (JIP) family of proteins which can recruit and activate JNK-1/2 along with its upstream effectors (Matsuguchi et al., 2003).

Once activated the main and first described function of JNK-1/2 is to activate the AP-1 transcription factor component c-Jun (Hibi et al., 1993), which when dimerized with other AP-1 components such as c-Fos can rapidly alter transcription with the dimer composition controlling specificity of interaction with DNA (Angel and Karin, 1991), and also interactions with other transcription factors such as SMAD3 (Verrecchia et al., 2000) and NF-κB (Shyu et al., 2008). Activation of c-Jun is achieved by phosphorylation of *Ser63* and *Ser73* specifically by JNK-1/2 with other proteins such as ERK capable of phosphorylating different residues. Phosphorylation of *Ser63* and *Ser73* is thought to control activation of c-Jun with alternative phosphorylation determining its associations (Hibi et al., 1993; Minden et al., 1995).

As with previous MAPKs discussed JNK-1/2 signalling can be de-activated through generic phosphatases such as PP2A, which can decrease as opposed to completely inhibit activity (Khokhlatchev et al., 1997) as well as dual de-phosphorylating MKPs such as MKP1 (Mizuno et al., 2004) and MKP7 (Tanoue et al., 2001).

5.3.1 Phosphorylation Response of JNK-1/2

In previous work JNK-1/2 was phosphorylated by both TGF-β1 or TNFα with a possibly accentuated response seen upon co-stimulation. To verify this, and also investigate the initiation and duration of phosphorylation a time course experiment was performed.

PBECs were cultured in 6 well collagen coated plates until confluent and stimulated with TGF-β1 or TNFα. Cells were harvested at 0, 0.5, 1, 5, 10, 30 and 60 minute time points. Whole cell PBEC lysate was immuno-precipitated for total SMAD3, under denaturing conditions, with the resulting lysate probed for *p*JNK-1/2 (both *Thr183* and *Tyr185*) by indirect ELISA. Neat lysate from the 30 minute stimulation was analyzed by Western blot for both total and phospho forms of JNK-1/2.

As with the IKKα/β phospho-time course the antibodies used in this protocol targeted both isoforms of JNK. Unlike IKKα/β both isoforms of JNK were strongly detected in total and phosphorylated forms, and although JNK-1 phosphorylation was not affected by TGF-β1 or TNFα stimulation its phosphorylation was blocked by chemical inhibition of TAK1, therefore separating the relative contributions of JNK-1 or JNK-2 to the results below is not possible, although western blots at a 30 minute time point would suggest that variation between stimulations was due to JNK-2.

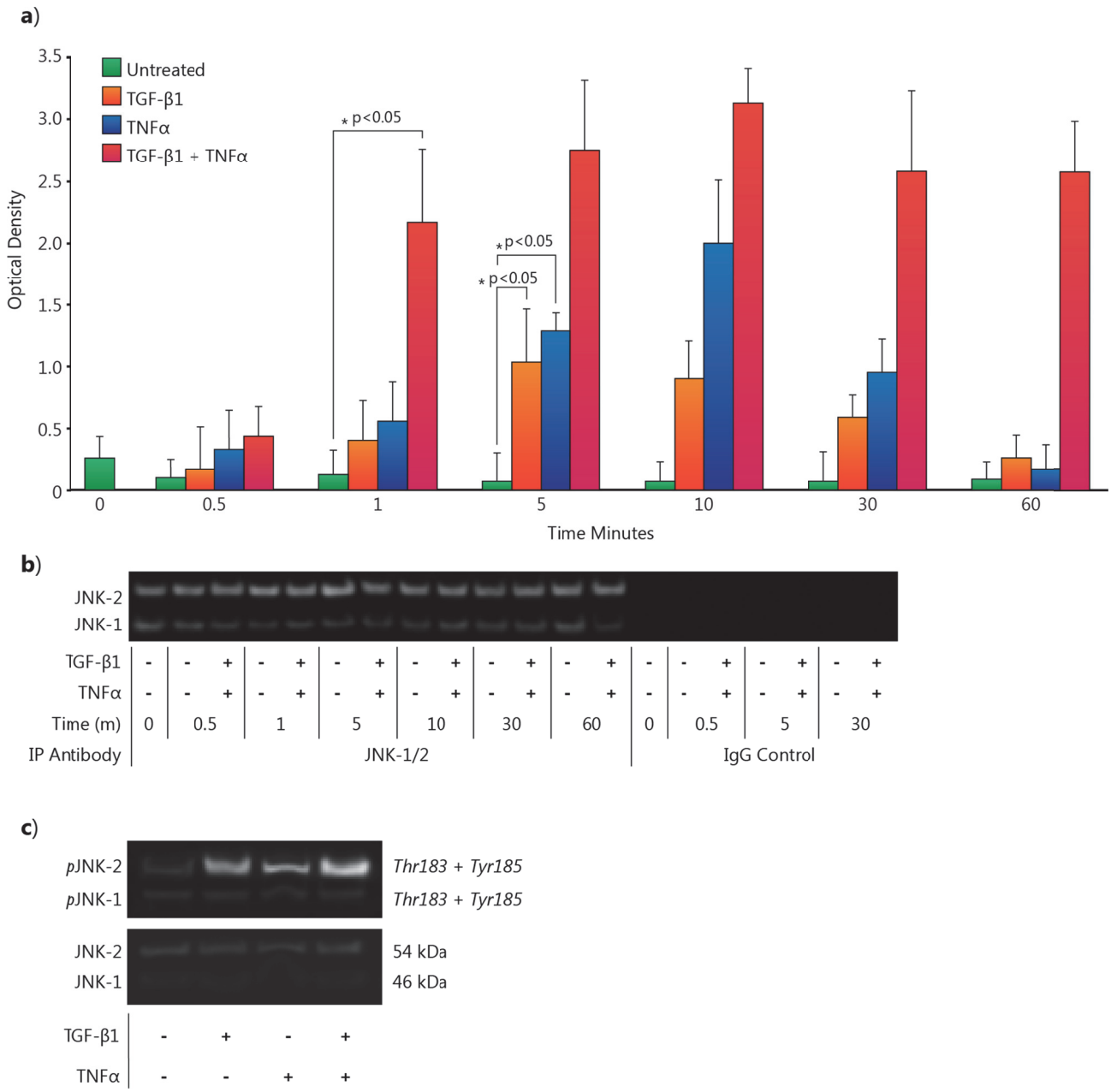

Figure 50 - JNK-1/2 phosphorylation response

a) TGF-β1 (10ng/mL) stimulation induced significant phosphorylation of JNK-1/2 (*Thr183* + *Tyr185*) from 5 minutes, which was also the peak lasting through to 30 minutes. A similar effect was seen with TNFα (20ng/mL) although the level of phosphorylation was generally higher, significantly so at 10 minutes. Co-stimulation of PBECs with TGF-β1 and TNFα induced significant phosphorylation from 1 minute onwards which peaked at 10 minutes. A significant accentuated response was seen at 1 and 60 minute time points, with those between being more additive in nature (all $p<0.05$, $n=3$).

b) Detected levels of JNK-1/2 did not vary significantly across stimulations, and was not present in IgG control lysates.

c) TGF-β1 and TNFα alone induced phosphorylation of JNK-1/2 30 minutes post stimulation, with an increased phosphorylation seen upon co-stimulation. *p*JNK-1/2 and JNK-1/2 (50µg).

Both TGF-β1 and TNFα induced significant phosphorylation of JNK-1/2 from 5 minutes up until 30 minutes, at 60 minutes levels were returned to near baseline. Co-stimulation however induced a significant increase in phosphorylation from 1 minute, which lasted beyond 60 minutes. Most interestingly, however was the nature of the response to co-stimulation, an accentuative phosphorylation occurred at both 1 and 60 minute time points, with the level of phosphorylation remaining high at all time points.

5.3.2 Chemical Inhibition of JNK-1/2

With previous results demonstrating that TAK1 may phosphorylate JNK-1/2 as a downstream mediator, and with JNK-1/2 phosphorylating in response to both TGF-β1 and TNFα investigations into its role in EMT were required.

JNK Inhibitor II (JNK*i*) is a cell permeable inhibitor of JNK-1/2 and 3 that acts by blocking ATP binding sites required for kinase activity. In a cell free kinase assay an of JNK mediated phosphorylation of the transcription factor c-Jun an IC_{50} of 50nM was described with the same paper describing an *in vitro* IC_{50} of 5-10μM when looking at c-Jun phosphorylation in Jurkat cells[15] (Bennett et al., 2001).

A dose response curve looking at cell viability, morphology and effect on EMT after pre-treatment with 1, 5, 10 and 20μM doses of JNK*i* prior to stimulation with TGF-β1 and TNFα for 72 hours was performed in triplicate using A549 cells.

[15] *T-lymphocyte cell line*

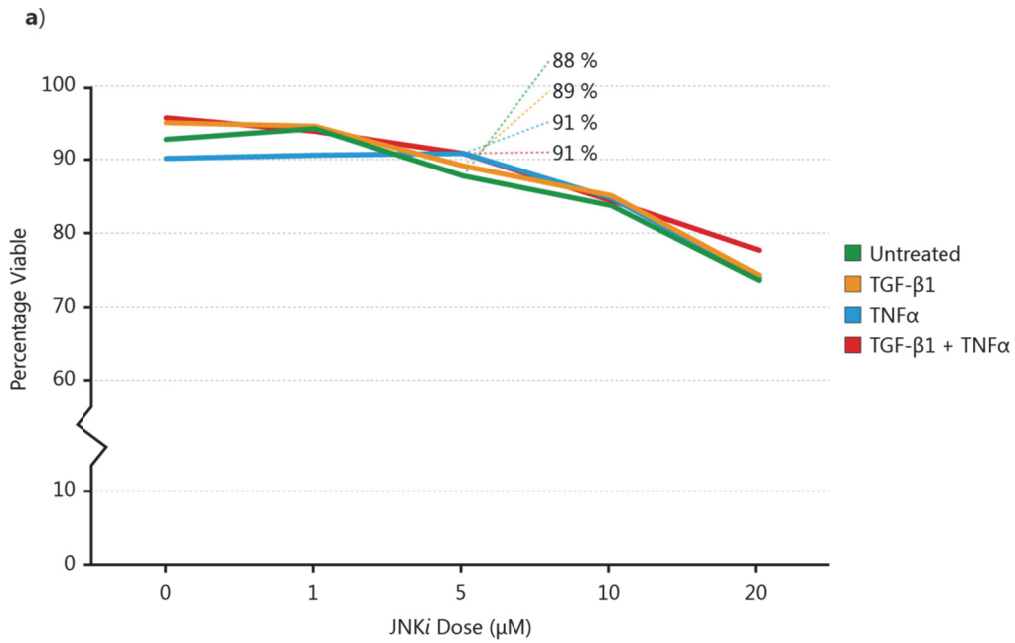

Figure 51 - JNK*i* dose response

a) A549 cells were stimulated with TGF-β1 (10ng/mL) or TNFα (20ng/mL) for 72 hours after a 1 hour pre-treatment with SMAD*i* at 1, 5, 10 and 20µM doses (*n=3*). There was a general trend of decreased viability with increasing dose of JNK*i* under all stimulations.

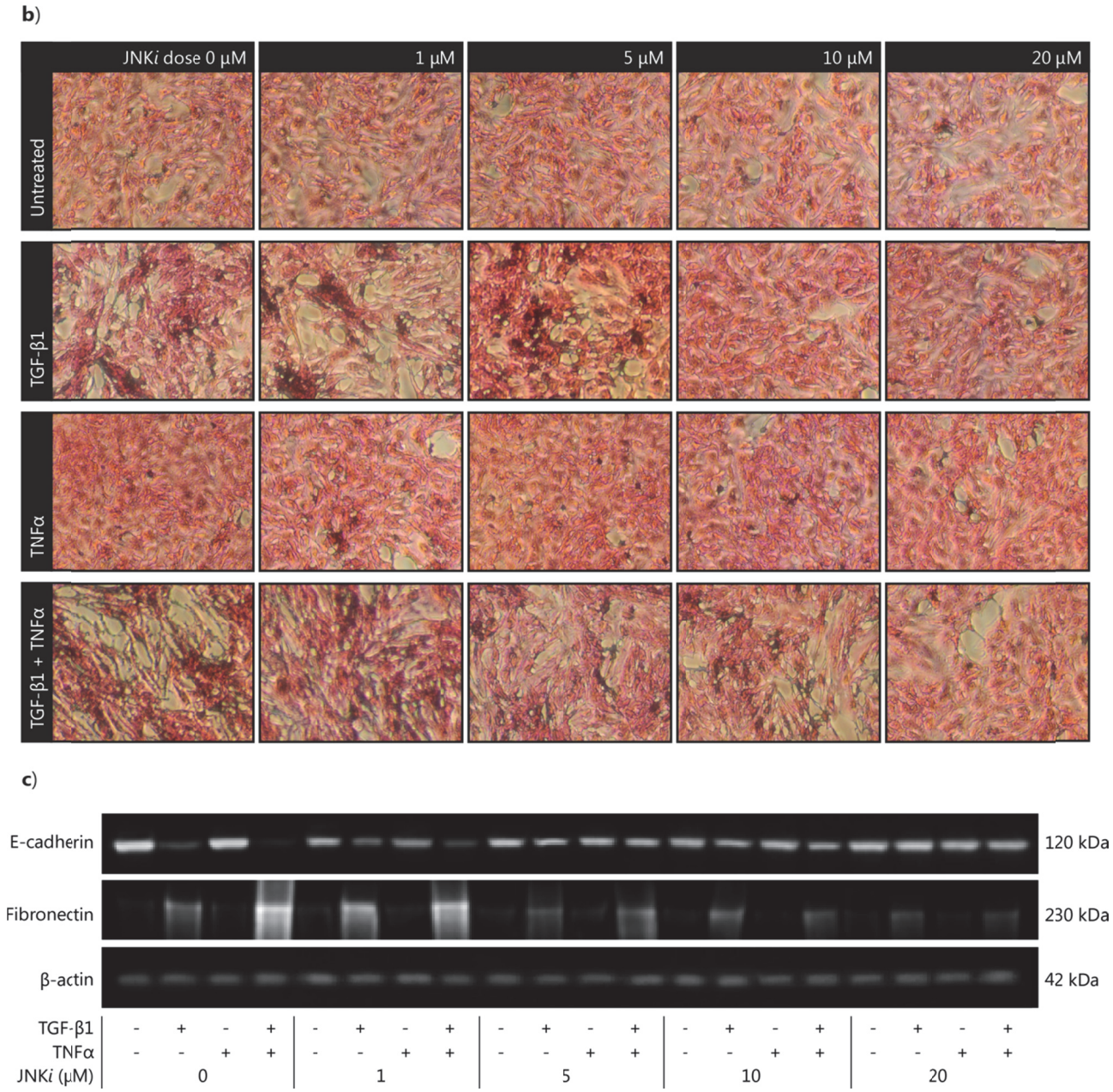

Figure 51 Continued - JNK*i* dose response

b) 72 hours post stimulation with TGF-β1 there was a marked transition from the cobblestone like epithelial appearance of un-stimulated A549 cells towards a more striated, mesenchymal phenotype. This effect was accentuated by co-stimulation with TNFα, whereas TNFα alone had no effect on cell morphology. Increasing doses of JNK*i* limited both TGF-β1 driven and TNFα accentuated EMT at the morphological level in a dose dependant manner; with a 10µM dose of JNK*i* most strongly inhibiting the driving effect of TGF-β1 and a 20µM dose the TNFα accentuation.

c) E-cadherin expression was reduced upon TGF-β1 stimulation with an accentuated reduction upon co-stimulation with TNFα. A strong inhibition of EMT was observed from 1µM onwards, with a 5µM dose of JNK*i* returning E-cadherin expression to baseline levels with no subsequent improvement at higher doses. For fibronectin the strongest effect was observed at 10µM JNK*i* with no improvement at 20µM. E-cadherin and fibronectin (5µg).

JNK*i* strongly inhibits both TGF-β1 driven EMT and its accentuation by TNFα morphologically and at the protein level. A 20μM dose inhibited all facets of EMT most efficiently yet induced a large decrease in cell viability compared to untreated controls. At the protein level, there was no added benefit at using a 20μM dose over 10μM, and looking at E-cadherin alone 5μM JNK*i* inhibited its loss to the same degree as 10 and 20μM doses of JNK*i*. In future experiments a 5μM dose of JNK*i* was used which was capable of strongly inhibiting EMT at the protein level with very little reduction in cell viability.

5.3.2.1 Chemical Inhibition of JNK-1/2, Effect on EMT Endpoint

With an appropriate dose of JNK*i* decided upon in A549 cells the next step was to observe what effect this would have on EMT in PBECs. *n=4* PBEC cultures from distinct patients were stimulated with TGF-β1 or TNFα for 72 hours after a 1 hour pre-treatment with 5μM JNK*i*. Cell lysate and culture media was retained and EMT was assessed using a variety of markers.

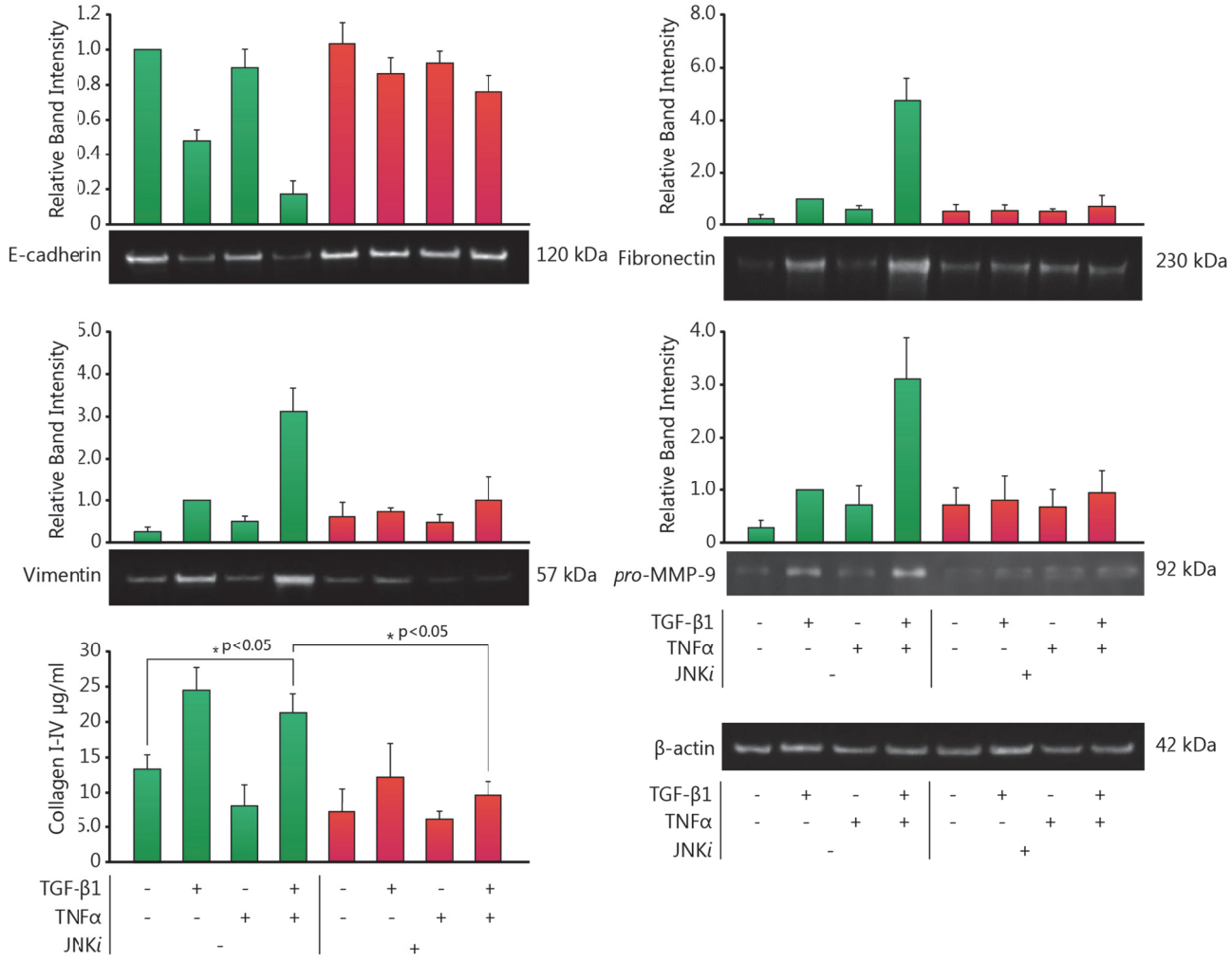

Figure 52 - Effect of JNK*i* on EMT

Stimulation of PBECs (*n=5*, representative blots from single patient) with TGF-β1 (10ng/mL) for 72 hours down-regulated E-cadherin expression, increased fibronectin and vimentin expression and increased *pro*-MMP-9 secretion. This change in EMT marker expression was accentuated by co-stimulation with TNFα (20ng/mL). Collagen I-IV secretion was significantly up-regulated by stimulation with TGF-β1 ($p<0.05$, *n=5*) however no accentuation was observed upon co-stimulation with TNFα. Pre-treatment with JNK*i* (5µM) inhibited the TGF-β1 induced down-regulation of E-cadherin expression, the increase in fibronectin and vimentin expression, the increase in *pro*-MMP-9 secretion and, significantly, the increase in collagen I-IV secretion ($p<0.05$, *n=5*), returning levels to near baseline. JNK*i* also reduced the accentuating effect of TNFα on TGF-β1 driven EMT marker expression in all instances. E-cadherin and fibronectin (5µg), vimentin (20µg), *pro*-MMP-9 (30µL) and collagens I-IV (25µL).

The results described above provide strong evidence, that JNK-1/2 activation plays a key role in the subsequent occurrence of EMT. Pre-treatment of PBECs with a 5μM dose of JNK*i* strongly inhibited the loss of E-cadherin expression and the gain of fibronectin and vimentin expression, as well as the increase in secretion of collagens I-IV and *pro*-MMP-9 into the media in response to TGF-β1 stimulation. JNK*i* also strongly limited the accentuative effect of TNFα for all markers of EMT.

5.3.2.2 Chemical Inhibition of JNK-1/2, Effect on Phosphorylation

JNK-2 has previously been shown to phosphorylate in response to both TGF-β1 and TNFα, with an accentuated and extended phosphorylation of JNK-1/2 in response to co-stimulation. It was also demonstrated that JNK-1/2 phosphorylation could be inhibited, by the upstream inhibition of TAK1. To verify the proposed location of JNK-1/2 in this signalling cascade I investigated the effect of JNK*i* pre-treatment on the phosphorylation of other key signalling proteins, in this instance with the addition of c-Jun as a substrate of JNK-1/2, 30 minutes after stimulation with TGF-β1 or TNFα.

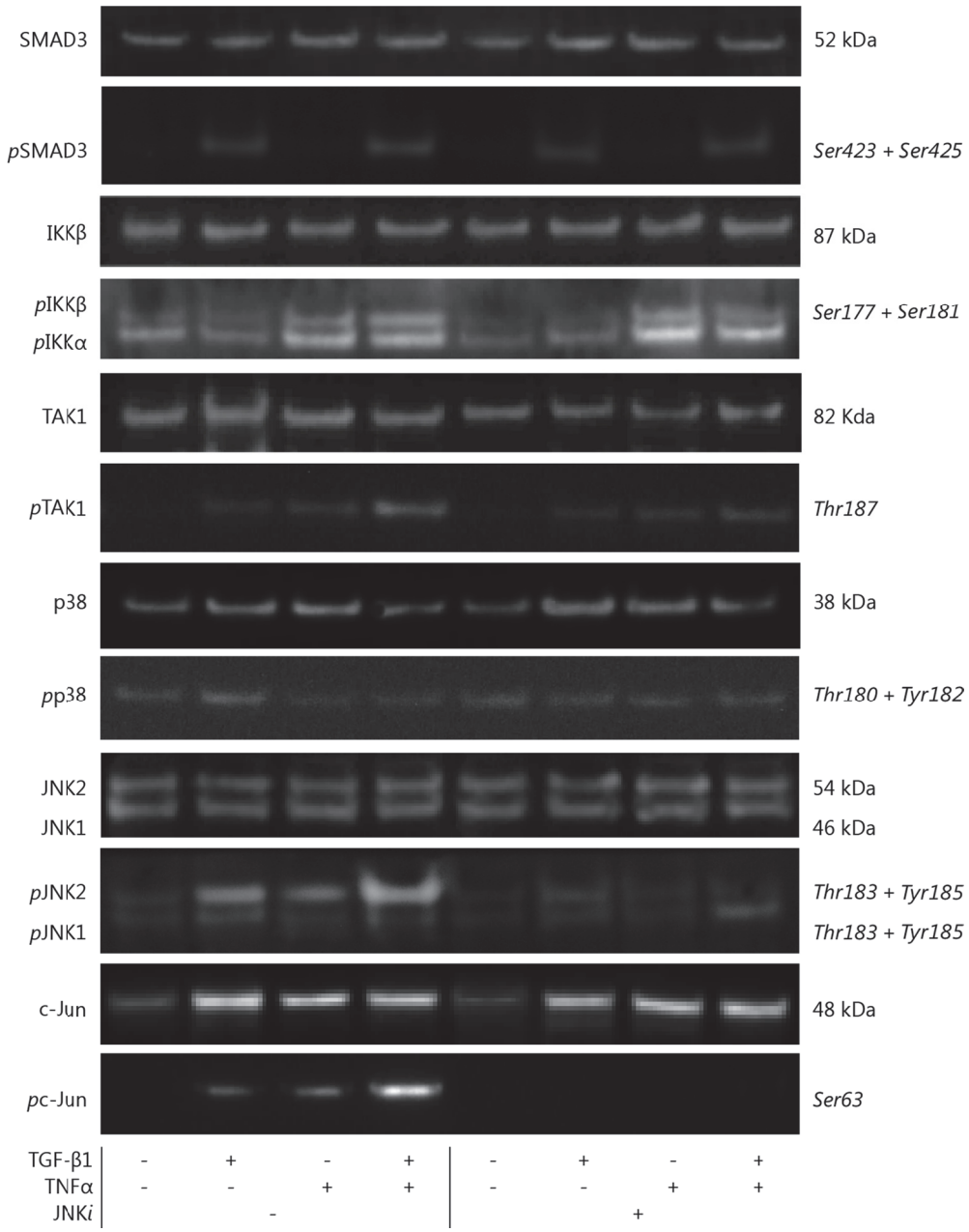

Figure 53 - Effect of JNK*i* on key signalling proteins

SMAD3 was phosphorylated in PBECs (*n=3*, representative blots from single patient) 30 minutes post stimulation TGF-β1 (10ng/mL) alone and this was not accentuated by TNFα (20ng/mL). IKKα/β were phosphorylated in response to stimulation with TNFα alone and this was accentuated by co-stimulation with TGF-β1. Both TAK1 and JNK-2 were phosphorylated by stimulation with both TGF-β1 and TNFα alone and displayed an accentuated phosphorylation upon co-stimulation. JNK-1 and p38 displayed no increase in phosphorylation in response to stimulation with TGF-β1 or TNFα alone or in combination. JNK*i* (5μM) inhibited the phosphorylation of both JNK-1 and JNK-2 without affecting the phosphorylation status of other signalling proteins,, or the total protein level of any marker. To check for JNK*i* efficacy phosphorylation of c-Jun, a substrate of JNK-1/2, was used as a marker of JNK-1/2 kinase activity. c-Jun was phosphorylated by both TGF-β1 and TNFα with an accentuated phosphorylation upon co-stimulation, this was completely blocked upon pre-treatment with JNK*i*. *p*SMAD3 and *p*c-Jun (20μg), *p*IKKβ and *p*p38 (40μg), *p*TAK1, *p*JNK-1/2 and JNK-1/2 (50μg).

JNK-2 was phosphorylated in response to TGF-β1 or TNFα alone and displayed an accentuated phosphorylation upon co-stimulation, phospho-JNK1 was detected in all stimulations with no variation between. Due to the described inhibitory activity of JNK*i* it was thought that phosphorylation would not be affected, however surprisingly phosphorylation of both JNK-1 and JNK-2 was blocked by pre-treatment with JNK*i*, possibly due to similar mechanisms discussed for TAK*i*. c-Jun, a substrate of JNK-1/2, was phosphorylated by both TGF-β1 or TNFα alone, with an accentuative phosphorylation upon co-stimulation; upon pre-treatment with JNK*i* this phosphorylation was completely blocked. This confirms that JNK-1/2 sit below TAK1 and with IKKβ and SMAD3 acting independently.

5.3.3 siRNA Knockdown of JNK-1/2

JNK*i* inhibited both JNK-1 and JNK-2 phosphorylation, siRNA knockdown of each isoform would help better understand the relative importance of JNK-1 and JNK-2 in EMT, whilst also confirming the work performed with JNK*i*. siRNA targeting JNK-1 (JNK1*si* - GTGGAAAGAATTGATATATAA) or JNK-2 (JNK2*si* - GCCGUCCUUUUCAGAACCAT) were used in a dose response assay for cell viability, morphology and effect on EMT after a 24 hour pre-treatment with 1, 5, and 10nM doses of siRNA delivered through lipid transfection of adherent cultures, prior to stimulation with TGF-β1 and TNFα for 72 hours.

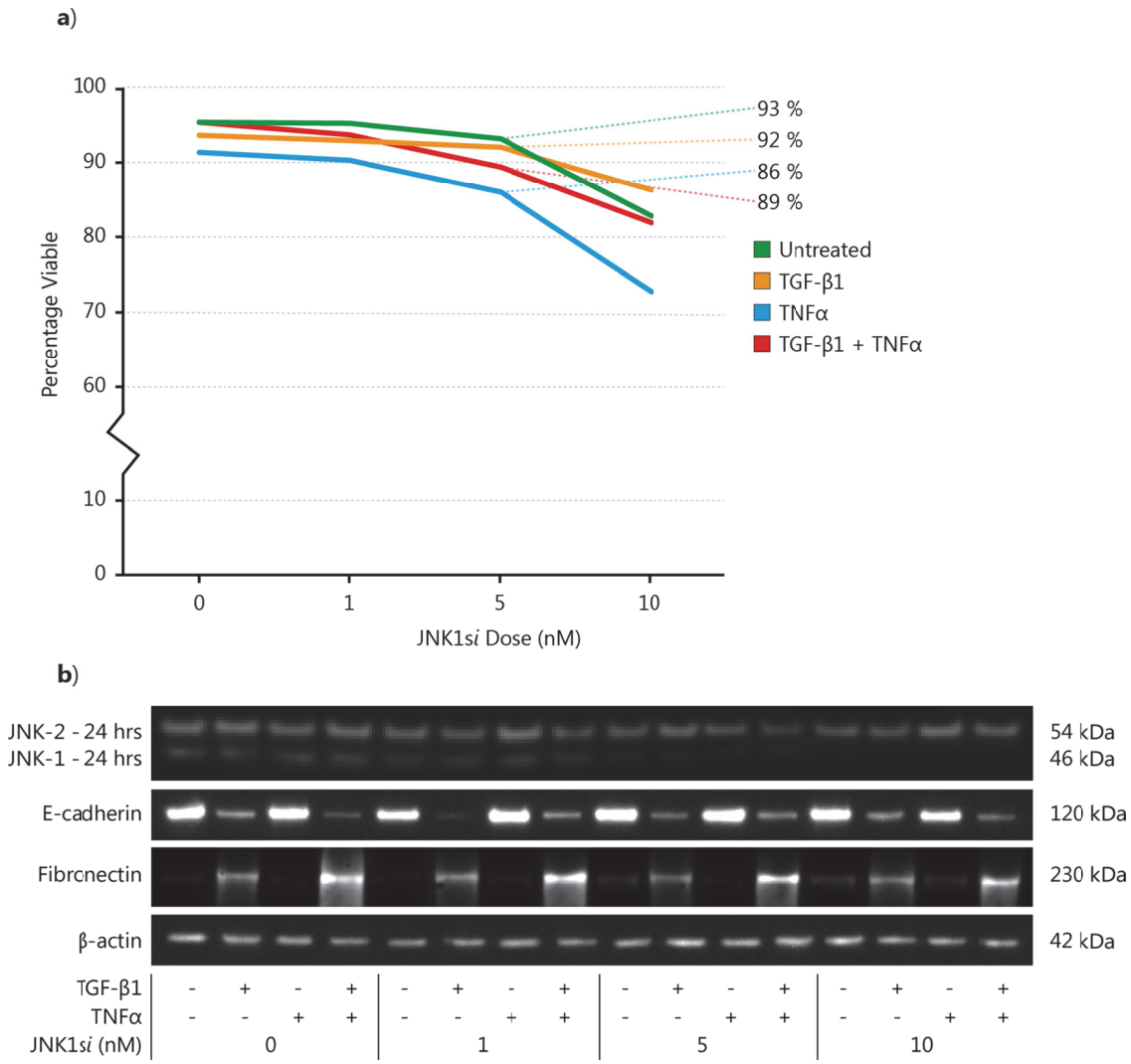

Figure 54 - JNK1*si* dose response

a) PBECs were stimulated with TGF-β1 (10ng/mL) or TNFα (20ng/mL) for 72 hours after a 24 hour pre-treatment with JNK1s*i* at 1, 5 and 10nM doses (*n=2*). There was a trend of decreased viability with increasing dose of JNK1*si*, with a larger decrease in viability observed in TNFα stimulated cells.

b) JNK-1 and JNK-2 were not affected by stimulation by TGF-β1 or TNFα; JNK-1 but not JNK-2, was reduced in a dose dependant fashion by treatment with JNK1*si*. At 1nM there was approximately a 60% knockdown of JNK-1, beyond this level no JNK-1 was detected. JNK1*si* at any dose did not inhibit the TGF-β1 driven loss of E-cadherin or gain in fibronectin expression, or the accentuation of this effect by TNFα. E-cadherin and fibronectin (5µg) and JNK-1/2 (50µg).

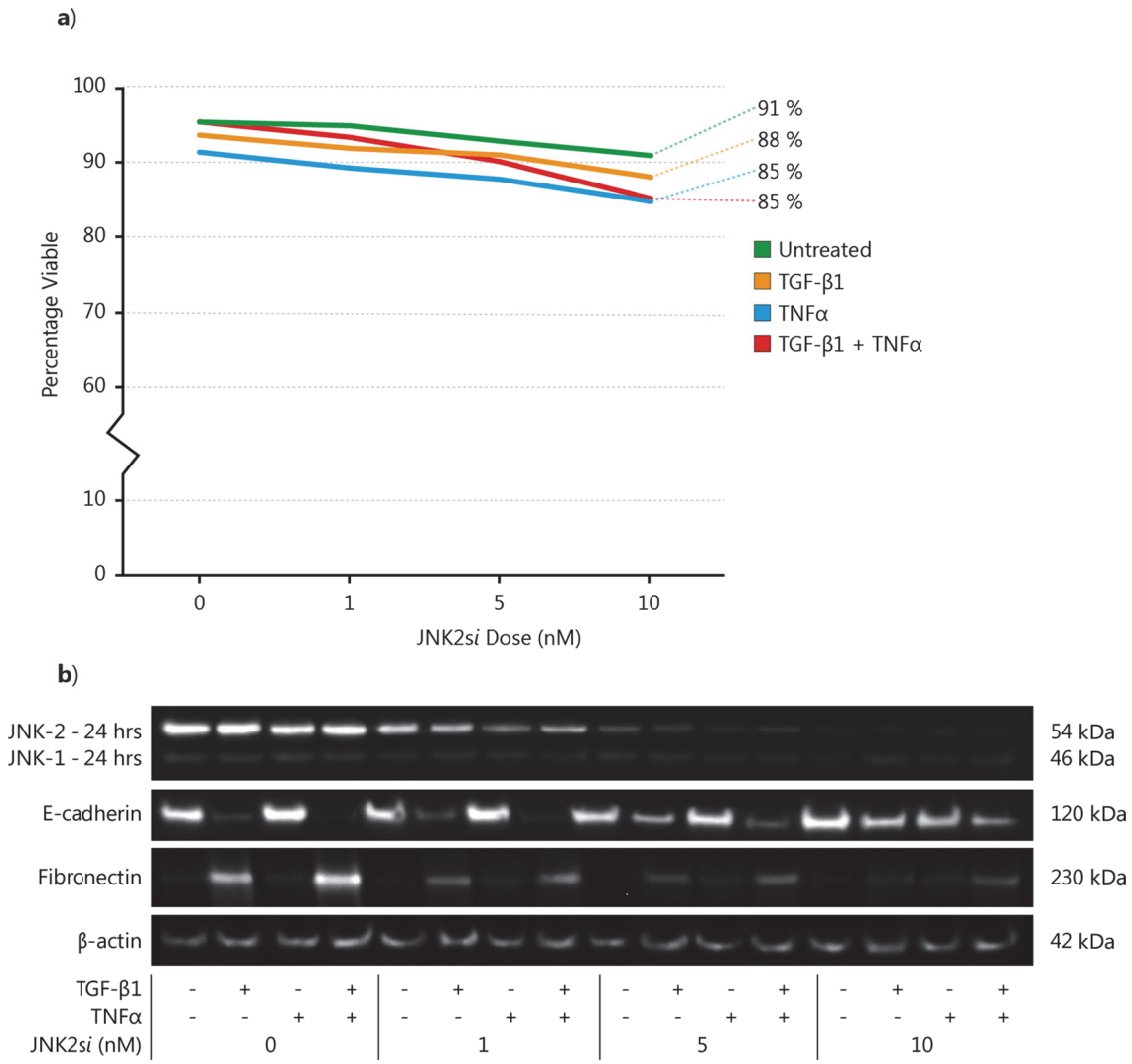

Figure 55 - JNK2*si* dose response

a) PBECs were stimulated with TGF-β1 (10ng/mL) or TNFα (20ng/mL) for 72 hours after a 24 hour pre-treatment with JNK2s*i* at 1, 5 and 10nM doses (*n=2*). There was a very slight trend of decreased viability with increasing dose of JNK2*si*.

b) JNK-1 and JNK-2 were not affected by stimulation by TGF-β1 or TNFα; JNK-2 but not JNK-1, was reduced in a dose dependant fashion by treatment with JNK2*si*. At 1nM there was approximately a 40% knockdown of JNK-2, an 80% knockdown at 5nM and a 95% knockdown at 10nM. JNK2*si* inhibited the TGF-β1 driven loss of E-cadherin and gain in fibronectin expression, and the accentuation of this effect by TNFα in a dose dependant fashion, with the greatest inhibition seen at 10nM. E-cadherin and fibronectin (5µg) and JNK-1/2 (50µg).

JNK1*si* knocked down JNK-1 in a dose dependant manner without affecting expression of JNK-2, however knockdown of JNK-1 did not inhibit the TGF-β1 driven loss of E-cadherin or gain of fibronectin, or the accentuation of this effect by TNFα. There was a trend for decreased viability upon increased dose, which was amplified in TNFα alone treated cells especially at the 10nM dose, therefore a dose of 5nM JNK1*si* was used in future experiments.

JNK2*si* knocked down JNK-2 in a dose dependant manner without affecting expression of JNK-1. JNK2*si* also inhibited TGF-β1 driven loss of E-cadherin or gain of fibronectin, or the accentuation of this effect by TNFα in a dose dependant manner with the greatest effect seen with the 10nM dose. There was a very slight trend for decreased viability upon increased dose, and therefore a 10nM dose was used in further experiments.

5.3.3.1 siRNA Knockdown of JNK-1/2, Effect on EMT Endpoint

With appropriate doses of JNK*si* confirmed for use in PBECs I proceeded to investigate what effect knockdown of JNK-1 or JNK-2 had on EMT. *n=3* PBEC cultures from distinct patients were stimulated with TGF-β1 or TNFα for 72 hours after a 24 hour pre-treatment with 5nM JNK1*si*, 10nM JNK2*si* or a sequence scrambled control. Cell lysate and culture media was retained and EMT was assessed using a variety of markers.

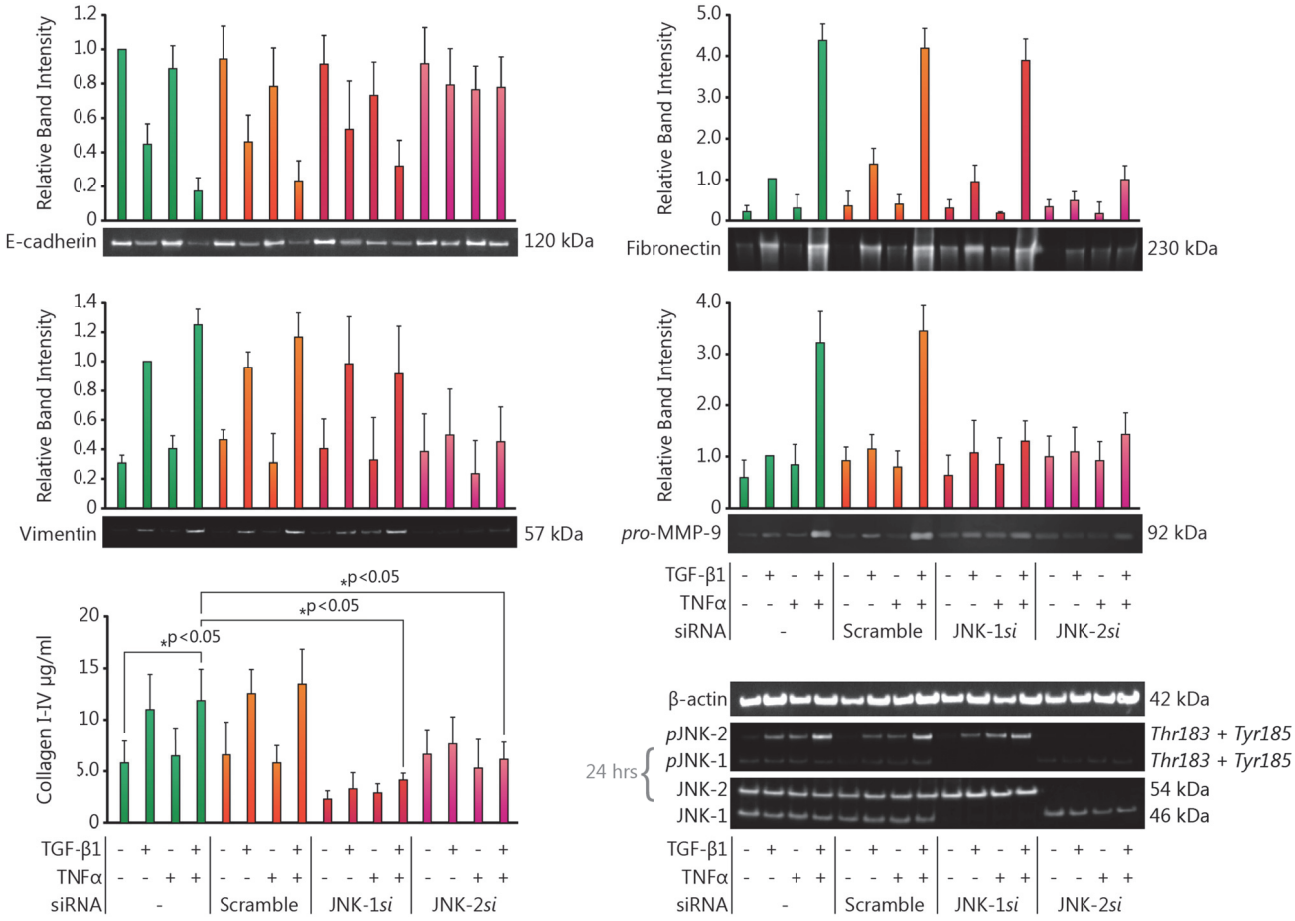

Figure 56 - Effect of JNK1*si* and JNK2*si* on EMT

Stimulation of PBECs (*n=3*) with TGF-β1 (10ng/mL) for 72 hours down-regulated the expression of E-cadherin, increased the expression of fibronectin and vimentin and increased *pro*-MMP-9 secretion compared to control cells with this effect accentuated by co-stimulation with TNFα (20ng/mL), with the exception of E-cadherin where this effect was more additive in nature. Collagen I-IV secretion was significantly up-regulated by stimulation with TGF-β1 but no accentuation was observed upon co-stimulation with TNFα ($p<0.05$, *n=3*). siRNA knockdown of JNK-2 but not JNK-1 strongly inhibited the TGF-β1 mediated loss of E-cadherin and gain of vimentin and fibronectin, and also strongly inhibited the accentuative effect of TNFα on these markers. Both JNK1*si* and JNK2*si* strongly inhibited the secretion of *pro*-MMP-9 in response to both TGF-β1, and both also inhibited the accentuative effect of TNFα. Again both JNK1*si* and JNK2*si* significantly inhibited the TGF-β1 mediated increase in collagens I-IV with JNK-1*si* demonstrating a stronger effect.

Approximately 100% knockdown of JNK-1 was achieved by JNK-1 targeting siRNA (5nM) after 24 hours, with JNK-2 targeting siRNA (10nM) mediating a similar knockdown of JNK-2, neither siRNA demonstrated non-specific knockdown. Neither a sequence scramble control nor the lipid vector had any effect on JNK-1/2 knockdown, cell viability or morphology. This reduction in total JNK-1 or JNK-2 also led to a reduction in the respective levels of phospho-JNK-1/2 30 minutes after stimulation with TGF-β1 or TNFα with no effect on JNK-1/2 phosphorylation seen with either the lipid vector or sequence scramble control. E-cadherin and fibronectin (5µg), vimentin (20µg), *p*JNK-1/2 and JNK-1/2 (50µM), *pro*-MMP-9 (30µL) and collagens I-IV (25µL).

The results above confirm that JNK-2 plays a key role in EMT for all of the markers assayed, with knockdown of total protein inhibiting the loss of E-cadherin expression, gain in vimentin and fibronectin expression and increase in *pro*-MMP-9 and collagens I-IV secretion. Interestingly knockdown of JNK-1, which is not phosphorylated by either TGF-β1 or TNFα, and plays no role in controlling the expression of E-cadherin, fibronectin or vimentin was able to strongly inhibit the secretion of *pro*-MMP-9 and collagens I-IV. In the case of collagen secretion JNK1*si* was actually more effective than JNK2*si* at reducing collagen secretion, increasing levels to below that of baseline un-stimulated cells.

5.3.4 Localization of JNK-1/2

Both chemical inhibition and siRNA knockdown of JNK-2 suggest that it plays a key role in EMT, and siRNA knockdown of JNK-1 implicated it in the control of collagen and protease secretion. JNK-1/2 is also known to interact with the c-Jun transcription factor which can translocate to the nucleus, and TAK1 which we have demonstrated localizes to the nucleus by unknown means. I therefore hypothesized that JNK-1/2 may be mediating this localization of TAK1 in association with a transcription factor such as c-Jun, to investigate this I first looked at localization of both total and phospho-JNK-1/2 30 minutes post stimulation with TGF-β1 or TNFα in PBECs.

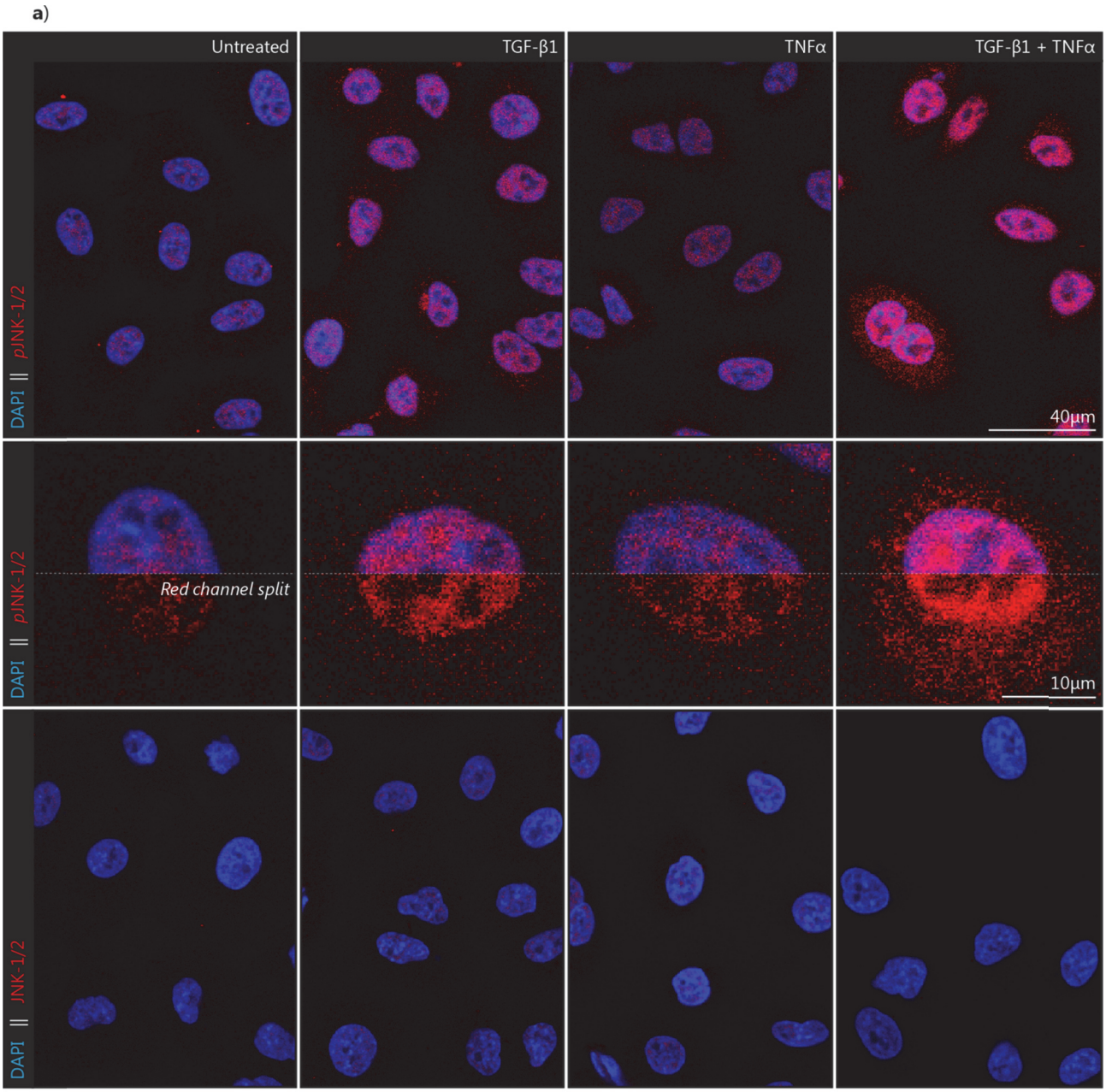

Figure 57 - Localization of JNK-1/2, *p*JNK-1/2 and c-Jun

a) PBECs cultured on collagen coated coverslips stimulated with TGF-β1 (10ng/mL) or TNFα (20ng/mL) for 30 minutes were assessed for changes in JNK-1/2 (*Thr183* + *Tyr185*) phosphorylation displaying in the red (TRITC) channel with DAPI as a nuclear counterstain. Phospho-JNK-1/2 was detected under all stimulations in both the cytoplasm and the nucleus. Upon stimulation with TGF-β1 or TNFα alone the intensity of phospho-JNK-1/2 in the nucleus increased, which was potentially accentuated upon co-stimulation, with greater levels of phospho-JNK-1/2 detected in the cytoplasm of co-stimulated cells. Total JNK-1/2 levels remained consistent under all stimulations, although very little was detected by ICC.

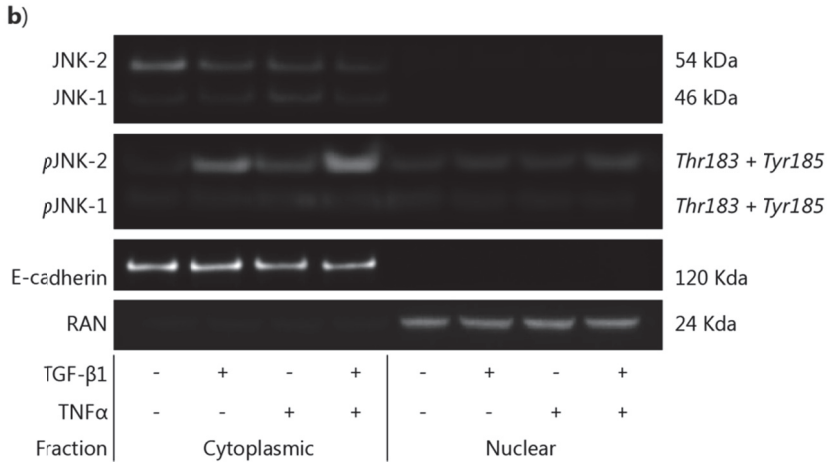

Figure 57 Continued - Localization of JNK-1/2, *p*JNK-1/2 and c-Jun

b) Total PBEC lysates (*n=2*, representative blots from single patient) treated as above were separated into nuclear and non-nuclear fractions, 27µg of non-nuclear lysate and 6µg of nuclear lysate was then separated by SDS-PAGE and probed for JNK-1/2, phopho-JNK-1/2 and c-Jun along with E-cadherin and RAN as fractionation controls. Total JNK-1/2 were detected in cytoplasmic and very weakly in the nuclear fraction of PBECs, phospho-JNK-1/2 were detected in the nucleus but the activated pattern of JNK-2 which was seen in the cytoplasm was not detected. c-Jun was detected in both the cytoplasmic and nuclear fractions and in both fractions an increase in phosphorylation was observed upon treatment with TGF-β1 or TNFα alone, possibly accentuated upon co-stimulation.

Total-JNK-1/2 localization was unchanged under all conditions as assessed by western blot, located most strongly in the cytoplasm with some evidence of nuclear localization. Conflicting results for phospho-JNK-1/2 were described; ICC demonstrated a pronounced increase in phosphorylation and nuclear localization in response to TGF-β1 or TNFα alone, with a potentially accentuated effect upon co-stimulation. However, western blotting showed that whilst phospho-JNK-1/2 was activated in the cytoplasm in the aforementioned pattern, phospho-JNK-1/2 levels in the nucleus did not vary upon stimulation, and detected levels were greatly reduced.

5.3.5 Further JNK-1/2 Work

To validate previous work that showed JNK-1/2 associating with TAK1 and potentially c-Jun, and also to demonstrate if c-Jun is indeed activated by JNK-1/2, an investigation into JNK-1/2 protein interactions was required.

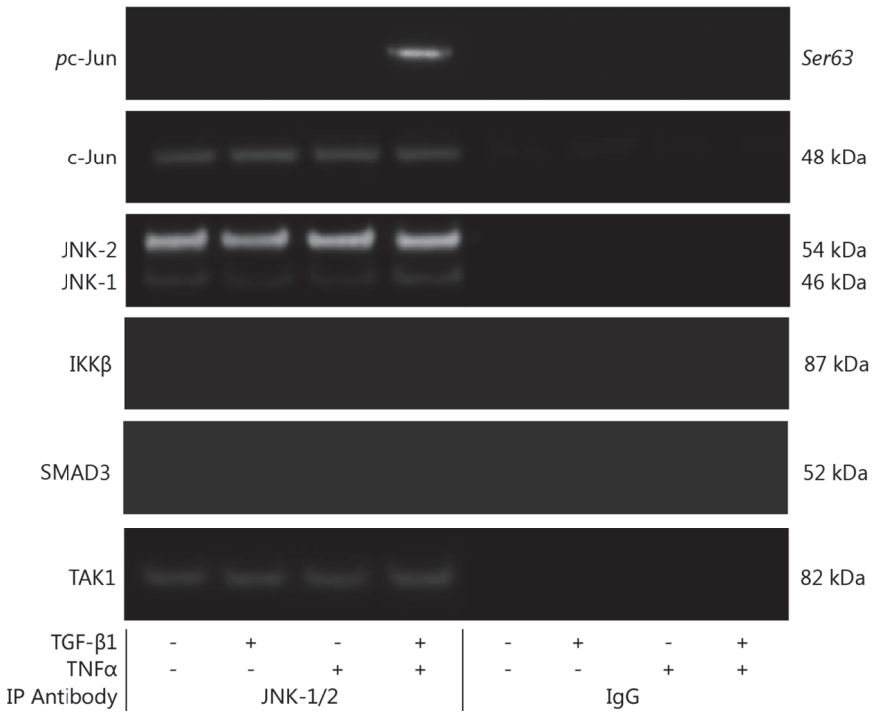

Figure 58 - JNK-1/2 protein associations

Total PBEC lysates (20µg, *n=2*, representative blots from single patient) stimulated with TGF-β1 (10ng/mL) or TNFα (20ng/mL) for 30 minutes were immuno-precipitated against total JNK-1/2, or pan-IgG under non-denaturing conditions. Neither SMAD3 nor IKKβ was associated with JNK-1/2 at 30 minutes under any stimulation. TAK1 and total c-Jun were constitutively associated with JNK-1/2 with no variation under any stimulations. Phospho-c-Jun was associated only upon co-stimulation with TGF-β1 and TNFα. No bands were detected in the pan-IgG controls.

At 30 minutes neither SMAD3 nor IKKβ were associated with JNK-1/2 under any stimulation, c-Jun and TAK1 were both associated but there was no variation in strength of association between stimulations. Phospho-c-Jun was not associated with JNK-1/2 after stimulation with TGF-β1 or TNFα alone, however upon co-stimulation an association was detected. As with the TAK1 investigation before it this experiment was limited to a single time-point so it is possible that associations may have varied outside of this.

5.3.6 JNK-1/2 Discussion

Prior investigation had shown that TGF-β1 but not TNFα was capable of inducing the canonical SMAD signalling response; with inhibition of SMAD3 limiting TGF-β1 driven EMT, with an unknown activity in relation to the accentuative effect of TNFα. Inhibition of IKKβ not only limited the accentuative effect of TNFα on EMT but also inhibited the driving effect of TGF-β1, which in conjunction with previously detected accentuated TAK1 phosphorylation was the catalyst to look at TAK1 as a potential mediator of this signalling crosstalk.

To summarize the data presented in the preceding sub-chapter: TGF-β1 or TNFα phosphorylate JNK-1/2 with an accentuated and prolonged phosphorylation upon co-stimulation, with c-Jun displaying a similar pattern. Western blots suggested that JNK-2 was being phosphorylated preferentially to JNK-1. Chemical inhibition of JNK-1/2 strongly inhibited TGF-β1 driven EMT and its accentuation by TNFα for all markers, siRNA knockdown of JNK-2 had a similar effect, whereas knockdown of JNK-1 only inhibited the secretion of *pro*-MMP-9 and collagens I-IV. JNK*i* inhibited the phosphorylation of JNK-2 and c-Jun without altering the phosphorylation of other signalling proteins. JNK-2 displayed some evidence of nuclear localisation on phosphorylation but significant levels were also detected in the cytoplasm. TAK1 and c-Jun were constitutively associated with JNK-1/2, phospho-c-Jun was associated only upon co-stimulation.

In **4.2.4** I proposed that IKKβ activity was driving the TNFα mediated accentuation of EMT, with TAK1 purely playing an activating role, and JNK-2 no role even though activated. In **4.3.7** I revised this hypothesis to describe a potential modulation of IKKβ NF-κB activity by TAK1 as a result of differential protein associations, and with TAK1 and JNK-2 modulating SMAD3 activity. However in light of the fact that inhibition of JNK-1/2 strongly blocks TGF-β1 driven EMT and its accentuation it is now apparent that JNK-1/2 most likely through the action of c-Jun is modulating both SMAD3 (Sano et al., 1999; Verrecchia

et al., 2001) and NF-κB (Liu et al., 2000; Wang and Sonenshein, 2005) transcriptional activity inducing EMT and its accentuation upon co-stimulation.

JNK*i* targeted both JNK-1 and JNK-2 and strongly blocked EMT development in all markers, when using JNK-1 or JNK-2 specific siRNA JNK-2 was confirmed as playing the key role in this development. JNK1*si* however whilst not affecting E-cadherin, fibronectin or vimentin expression strongly inhibited the secretion of *pro*-MMP-9 and collagens I-IV for all stimulations. That JNK2*si* was also capable of strongly inhibiting this secretion suggests that JNK-1 and JNK-2 are working co-operatively; as far as I am aware a single paper has demonstrated a similar effect, whereby JNK-1 phosphorylates JNK-2 before both phosphorylating p53 at different activation residues (Oleinik et al., 2007) . However in this instance JNK-1 displays increased phosphorylation whereas in my results only a basal level was detected, suggesting that it is the presence of JNK-1 rather than it's activation that is required. Another group working in primary tracheal cells has demonstrated an important role for JNK-1 in mediating TGF-β1 SMAD3 driven EMT, especially when looking at collagen I expression (Alcorn et al., 2008; Velden et al., 2011), interestingly their results suggested that EMT was independent of JNK-2. Due to the higher efficiencies of JNK-2 binding with c-Jun (Kallunki et al., 1994) this may suggest than an alternative transcriptional component is being activated, although downstream mechanisms were not discussed.

Total c-Jun was detected at lower levels than in stimulated cells, between which there was no variation, this may be explained by the fact that JNK-1/2 activated c-Jun is capable of inducing its own transcription in a positive feedback loop (Angel et al., 1988; Minden et al., 1994). With accentuated activation of TAK1 and JNK-2, c-Jun phosphorylation is itself accentuated; in an environment whereby TAK1 and JNK-2 are constitutively activated, such as that present in OB continued activation of c-Jun could lead to excessive activation of *JUN*, with this excess c-Jun perhaps capable of interacting with NF-κB and inducing accentuated EMT.

In our model a I have described a distinct MAPK cascade through TAK1, JNK-2 and c-Jun with no evidence of p38 or ERK-1/2 involvement, in the following section I attempt to outline my final signalling hypothesis, and areas where I feel further work is required.

6 Final Remarks

I have discussed specific results in their relevant chapters, so this final section is an attempt to briefly outline the findings which I think are most important, to discuss areas of the work which, with the benefit of hindsight, may have been better undertaken and to briefly discuss where I envisage this work could lead.

Firstly the work performed with Dr Rahul Mahida and Monika Suwara, which is still ongoing, provides strong evidence that both TNFα and IL-1β are present in the airway space of the lung, with their occurrence appearing to peak before the diagnosis of BO, which complements previous studies looking at TGF-β1 (Elssner et al., 2000) in the BAL and inflammatory mediators released from BAL immune cells (Hodge et al., 2009). The results I present represent analysis of my contribution to the work, further analysis and characterisation of patient samples is underway, which may assist with the debate over neutrophilic or non-neutrophilic BOS (Vanaudenaerde, Meyts, et al., 2008), as well as to the treatment of lung transplant recipients.

Secondly I have demonstrated a mechanism by which the accentuation of TGF-β1 driven EMT by TNFα may occur. TGF-β1 signals through the canonical SMAD pathway, utilising SMAD3 but requiring TAK1 and JNK-2 activation, although TAK1 and JNK-2 are not capable of driving EMT themselves. Neither TAK1 nor JNK-2 is directly associating with SMAD3 but downstream mediators may be influencing its transcriptional efficacy. TNFα signals through TAK1 and activates IKKβ and JNK-2, which without TGF-β1 stimulation does not strongly induce EMT. IKKβ activation is directly required for the accentuation of TGF-β1 driven EMT with JNK-2 modulating this effect.

Upon co-stimulation TGF-β1 drives EMT through SMAD3 and TNFα accentuates this effect through IKKβ. TAK1 and JNK-2 do not directly drive either effect but are required by both, TAK1 and JNK-2 may be modulating SMAD3 activity possibly through c-Jun. TAK-1 activates IKKβ and upon co-stimulation with TGF-β1 may be initiating a more pro-fibrotic IKKβ NF-κB transcriptional activity, possibly through differential phosphorylation or TAB association. Alternatively, as JNK-2 was shown to also facilitate this accentuation and c-Jun was shown to be more strongly activated after co-stimulation modulation of NF-κB activity may also be occurring at this level.

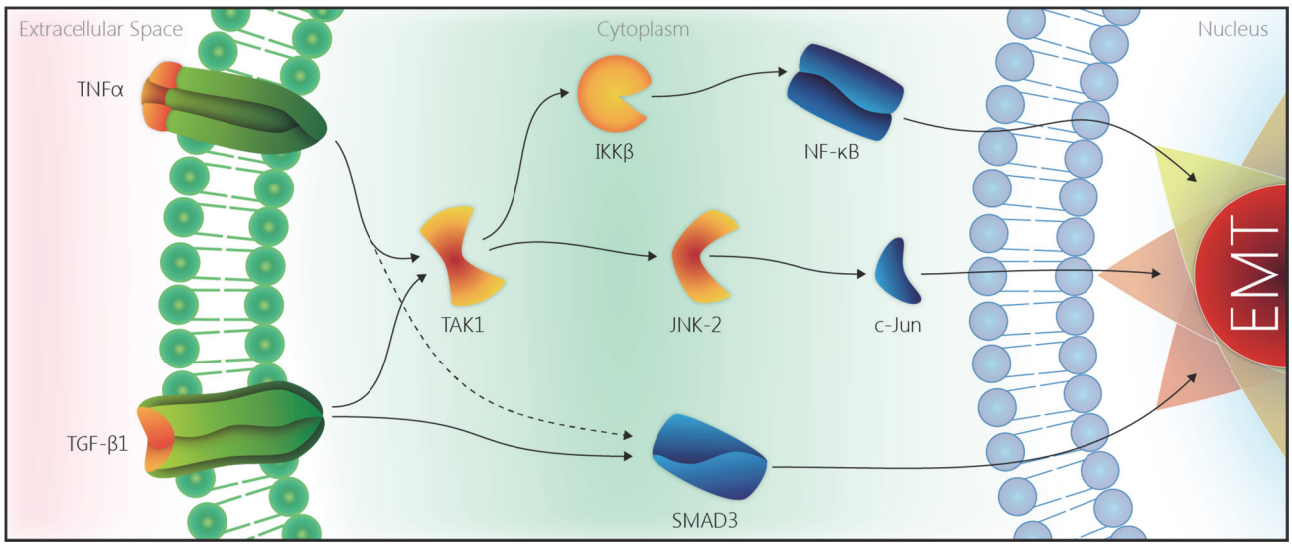

Figure 59 - Proposed Signalling Mechanism IV

TGF-β1 signals through the canonical SMAD pathway, utilising SMAD3 but with a requirement of TAK1 and JNK-2 activity to induce EMT. TNFα activates TAK1 and subsequently IKKβ and JNK-2 although without TGF-β1 EMT is not induced. Co-stimulation with both TGF-β1 and TNFα leads to an accentuated activation of TAK1, JNK-2 and c-Jun, whilst SMAD3 and IKKβ phosphorylation remains unchanged. TAK1 is required for both TGF-β1 driven EMT and its TNFα mediated accentuation but it's action remains unknown.

The third and final key finding from my PhD arose from studies into the mechanisms of activation for the pathway described above. The phosphorylation time course for SMAD3 followed a generally similar pattern to others described. The response of IKKβ whereby TGF-β1 induced a non-significant increase in IKKβ phosphorylation when used in conjunction with TNFα, over TNFα alone, without having any impact alone was interesting and provided evidence that synergy may be occurring at the level of intracellular signalling. However, for me personally the most interesting finding, and perhaps the one that may become of most clinical relevance is the accentuated and prolonged phosphorylation of TAK1 (*Thr187*) and JNK-1/2, most likely JNK-2, in response to co-stimulation. In both instances upon co-stimulation there was a more rapid phosphorylation, which was larger than that of either stimulation alone, and was significantly elevated at the 60 minute time point; at which point individual stimulations had returned to near baseline levels. This prolonged activation may be the factor that is inducing accentuation of EMT, perhaps as discussed above by producing excessive quantities of c-Jun, or through maintenance of SMAD3 and NF-κB activity. Also interesting in this effect was the differential response of TAK1 *Thr184* and *Thr187* phosphorylation, and the different associations of TAB proteins under various stimulations, particularly TAB3; which provide a potential mechanism for the co-activation of TAK1 and hence its, and perhaps JNK-1/2s accentuated and prolonged phosphorylation.

If I was to carry on this investigation there are two key points that I would focus in on. Firstly by manipulating the phosphorylation of specific TAK1 residues (potentially through the use of blocking antibodies or selective mutations within a cell line), as well as TAB protein association and observing the effect on NF-κB transcriptional activity it would be possible to demonstrate if the synergistic effect was modulated at this level. Similar techniques have been already used to describe the activation mechanism of TAK1 (Sakurai et al., 2002; Singhirunnusorn et al., 2005; Yu et al., 2008), by using these techniques it may be possible to describe how TAK1 can mediate so many differing outcomes. Secondly I would investigate the role of c-Jun on AP-1 (through further IP experiments, ChIP and the use of selective mutation of c-Jun), particularly its own transcriptional ability and how its activation can alter SMAD3 (Sano et al., 1999; Verrecchia et al., 2001) and NF-κB activity (Liu et al., 2000; Wang and Sonenshein, 2005) in relation to EMT.

Due to the key role of TAK1, JNK-1 and c-Jun in numerous cell signalling events blanket inhibition of their function *in vivo* would likely do more harm them good. However targeted inhibition, both temporally and spatially, of the accentuated phosphorylation in response to pro-fibrotic and pro-inflammatory factors may help limit the development of fibrosis in OB, and due to the ubiquitous nature of these proteins, potentially other disorders with a similar pathophysiology, for example a recent study in a mouse kidney fibrosis has described a similar key role for TAK1 in regulation both inflammation and fibrosis (Ma et al., 2011)

6.1 Critiques

Looking back at the work I have performed for this thesis perhaps the greatest criticism I can make is that it alternated between trying to be a basic science project whilst at the same time attempting to directly tie findings in with a disease model; and as such may not be as strong as if I had focused specifically on one arm. The use of PBECs provided a strong link to diseased tissue, and when used in association with other samples isolated from the same patients at the same time point can be very powerful, however the only true instance where I leveraged this in my thesis was by observing the phosphorylation of TAK1 in lung epithelium of patients with BOS. At the same time, the use of PBECs in several instances limited further experiments into the more molecular side of my project, such as ChIP assays, and large-scale screens of phospho proteins that would have been more feasible in a cell line.

As such, I may have been better served to more robustly investigate the mechanistic action in a cell line population, before attempting to replicate key findings in PBECs, and then taking this further by linking in

with the longitudinal catalogue of patient samples. However following the path that I did necessitated me to think laterally and develop alternative assays to cope with limited cell numbers. The immuno-precipitation and indirect ELISA protocol being the prime example of this, rather cobbled together because of trial and error it provided perhaps the most interesting results of my project.

As well as the A549 (Lieber et al., 1976) cell line that I have discussed there are several other widely used human lung epithelial cell lines such as the 16HBE (Viallet et al., 1994) and BEAS-2B (Reddel et al., 1988) lines. Both of these lines would have born more resemblance to the primary cells used as they were both initially derived from the bronchus as opposed to cultured adenocarcinoma cells. However, as with A549 cells both display significant abnormalities in chromosome number and in both instances were virally immortalized with human papilloma virus E6 and E7, and simian virus 40 early region oncogenes respectively.

It has been postulated that chromosome abnormalities in cells immortalized in this fashion arise due to the stresses put on cells by the conflicting actions of natural telomeric shortening, and senescence against the virally induced oncogenes maintaining proliferation. Co-expression of telomerase reverse transcriptase (TRT) during the generation of cell lines is thought to reduce these stresses and thus the generation of cytogenetic abnormalities (Vogelstein and Kinzler, 2004). In order to generate a more physiologically relevant population human bronchial cell lines have been generated using the addition of TRT and alternative oncogenes that maintain a normal chromosome number, and displayed maintenance of pseudo-stratified morphology. However, whilst this technique did extend cell life span it was not to the same extent as seen after traditional viral immortalization (Fulcher et al., 2009).

These attempts to improve the physiological relevance of cells used for investigations could and should be carried over into primary cell work, as the culture of PBECs as a submerged monolayer monoculture is very removed from their *in vivo* setting. For example, current PBEC culture protocol stipulates the use of collagen I, which as I have discussed in the introduction is often laid down as a provisional matrix after wound healing; as opposed to collagen IV that is associated with homeostasis. It is therefore possible that epithelial cells cultured on a collagen I matrix are more likely respond to remodelling stimuli and that after initial establishment of culture a collagen IV matrix should be introduced.

Secondly the techniques that I used to pick apart signalling events were rather blunt, by looking at the phosphorylation of signalling proteins it was possible to tell that they responded to stimulation and may be involved in EMT, with inhibition of these same proteins confirming this involvement. However, what

was not demonstrated was the relevant importance of each signalling arm in the contribution to EMT, or what if any interplay or redundancy existed between them, such as that discussed for SMAD3 and TAK1. Although this process is required to identify proteins that are important, perhaps it would have been better to focus in on one specific protein such as TAK1, perhaps carrying out the work outlined in **6**, rather than attempting to investigate all components equally.

The temporal activation of the various signalling proteins is an area of particular further interest. Activation of specific residues of key proteins was assessed at multiple time points in response to the standard panel of TGF-β1 or TNFα (up to 60 minutes); however, their responses to chemical and siRNA-mediated inhibition were investigated only at 30 minutes. As such, important activations of proteins not assessed in detail such as p38 or ERK-1/2 may have been missed. Temporal phosphorylation data in inhibited cells would allow stronger conclusions to be drawn about the order of the signalling cascade leading to the development of EMT, highlighting areas of particular interest. For example, why is SMAD3, identified as key in TAK1 activation, phosphorylated at a later time point? Does the earlier co-activation of proteins such as TAK1 (*Thr187*) prime SMAD3 to respond in a different manner to TGF-β1 leading to EMT? How long is activation of proteins such as JNK-1/2 upon co-stimulation maintained for, and is this the mechanism that is inducing EMT?

Alongside this investigations into the different responses of phospho-residues on the same protein both due to stimulation and temporally should be performed. The differential regulation of TAK1 *Thr184* and *Thr187* may be mimicked by other proteins such as SMAD3 that contains several other phospho residues other than those investigated (*Ser423* + *Ser425*). Perhaps phosphorylation of one of these residues is required for the phosphorylation of other molecules such as TAK1, but not in controlling the development of EMT.

Finally, whilst I have described a mechanism that can explain how TNFα accentuates TGF-β1 driven EMT, and highlight key areas where dysregulation may occur, I do not describe how this might come about in a disease state. It is still not known why the normally conflicting functions of TGF-β1 and TNFα are subsumed in this process, and perhaps more importantly still why it is that this occurs only in some people.

7 References

Abbott, D.W., Wilkins, A., Asara, J.M., Cantley, L.C., 2004. Current biology : CB 14, 2217–27.

Abe, R., Donnelly, S.C., Peng, T., Bucala, R., Metz, C.N., 2001. Journal of immunology (Baltimore, Md. : 1950) 166, 7556–62.

Abramoff, M.D., Magelhaes, P., Ram, S.J., 2004. Biophotonics International 11, 36–42.

Adhikari, A., Chen, Z.J., 2009. Developmental cell 16, 485–6.

Aebersold, D.M., Shaul, Y.D., Yung, Y., Yarom, N., Yao, Z., Hanoch, T., Seger, R., 2004. Molecular and cellular biology 24, 10000–15.

Agou, F., Traincard, F., Vinolo, E., Courtois, G., Yamaoka, S., Israël, A., Véron, M., 2004. The Journal of biological chemistry 279, 27861–9.

Akira, S., Takeda, K., 2004. Nature reviews. Immunology 4, 499–511.

Akpinar-Elci, M., Travis, W.D., Lynch, D.A., Kreiss, K., 2004. The European respiratory journal : official journal of the European Society for Clinical Respiratory Physiology 24, 298–302.

Alcorn, J.F., Guala, A.S., Van der Velden, J., McElhinney, B., Irvin, C.G., Davis, R.J., Janssen-Heininger, Y.M.W., 2008. Journal of cell science 121, 1036–45.

Alix-Panabières, C., Vendrell, J.-P., Slijper, M., Pellé, O., Barbotte, E., Mercier, G., Jacot, W., Fabbro, M., Pantel, K., 2009. Breast cancer research 11, R39.

Alkalay, I., 1995. Proceedings of the National Academy of Sciences 92, 10599–10603.

Andersson-Sjöland, A., Erjefält, J.S., Bjermer, L., Eriksson, L., Westergren-Thorsson, G., 2009. Respiratory research 10, 103.

Angel, P., Hattori, K., Smeal, T., Karin, M., 1988. Cell 55, 875–885.

Angel, P., Karin, M., 1991. Biochimica et Biophysica Acta - Reviews on Cancer 1072, 129–157.

Annes, J.P., 2003. Journal of Cell Science 116, 217–224.

Armendariz-Borunda, J., Katayama, K., Seyer, J., 1992. J. Biol. Chem. 267, 14316–14321.

Arsura, M., Panta, G.R., Bilyeu, J.D., Cavin, L.G., Sovak, M.A., Oliver, A.A., Factor, V., Heuchel, R., Mercurio, F., Thorgeirsson, S.S., Sonenshein, G.E., 2003. Oncogene 22, 412–25.

Assoian, R.K., Komoriya, A., Meyers, C.A., Miller, D.M., Sporn, M.B., 1983. The Journal of biological chemistry 258, 7155–60.

ATS, 2000. American journal of respiratory and critical care medicine 161, 646–64.

Avitzour, M., Diskin, R., Raboy, B., Askari, N., Engelberg, D., Livnah, O., 2007. The FEBS journal 274, 963–75.

Barkett, M., Gilmore, T.D., 1999. Oncogene 18, 6910–24.

Bashir, M.M., Sharma, M.R., Werth, V.P., 2009. Archives of dermatological research 301, 87–91.

Baumgartner, K.B., Samet, J.M., Stidley, C.A., Colby, T. V, Waldron, J.A., 1997. American journal of respiratory and critical care medicine 155, 242–8.

Behr, J., Kolb, M., Cox, G., 2009. Respirology (Carlton, Vic.) 14, 1072–1081.

Bellingan, G.J., Caldwell, H., Howie, S.E., Dransfield, I., Haslett, C., 1996. Journal of immunology (Baltimore, Md.: 1950) 157, 2577–85.

Belperio, J.A., DiGiovine, B., Keane, M.P., Burdick, M.D., Ying Xue, Y., Ross, D.J., Lynch, J.P., Kunkel, S.L., Strieter, R.M., 2002. Transplantation 73, 591–9.

Bennett, B.L., Sasaki, D.T., Murray, B.W., O'Leary, E.C., Sakata, S.T., Xu, W., Leisten, J.C., Motiwala, A., Pierce, S., Satoh, Y., Bhagwat, S.S., Manning, A.M., Anderson, D.W., 2001. Proceedings of the National Academy of Sciences of the United States of America 98, 13681–6.

De Bentzmann, S., Roger, P., Dupuit, F., Bajolet-Laudinat, O., Fuchey, C., Plotkowski, M.C., Puchelle, E., 1996. Infection and immunity 64, 1582–8.

Bettermann, K., Vucur, M., Haybaeck, J., Koppe, C., Janssen, J., Heymann, F., Weber, A., Weiskirchen, R., Liedtke, C., Gassler, N., Müller, M., De Vos, R., Wolf, M.J., Boege, Y., Seleznik, G.M., Zeller, N., Erny, D., Fuchs, T., Zoller, S., Cairo, S., Buendia, M.-A., Prinz, M., Akira, S., Tacke, F., Heikenwalder, M., Trautwein, C., Luedde, T., 2010. Cancer cell 17, 481–96.

Black, R.A., Kronheim, S.R., Sleath, P.R., 1989. FEBS letters 247, 386–90.

Borthwick, L.A., Gardner, A., De Soyza, A., Mann, D.A., Fisher, A.J., 2011. Cancer microenvironment: official journal of the International Cancer Microenvironment Society.

Borthwick, L.A., McIlroy, E.I., Gorowiec, M.R., Brodlie, M., Johnson, G.E., Ward, C., Lordan, J.L., Corris, P.A., Kirby, J.A., Fisher, A.J., 2010. American journal of transplantation: official journal of the American Society of Transplantation and the American Society of Transplant Surgeons 10, 498–509.

Borthwick, L.A., Parker, S.M., Brougham, K.A., Johnson, G.E., Gorowiec, M.R., Ward, C., Lordan, J.L., Corris, P.A., Kirby, J.A., Fisher, A.J., 2009. Thorax 64, 770–7.

Boulton, T.G., Nye, S.H., Robbins, D.J., Ip, N.Y., Radziejewska, E., Morgenbesser, S.D., DePinho, R.A., Panayotatos, N., Cobb, M.H., Yancopoulos, G.D., 1991. Cell 65, 663–75.

Boulton, T.G., Yancopoulos, G.D., Gregory, J.S., Slaughter, C., Moomaw, C., Hsu, J., Cobb, M.H., 1990. Science (New York, N.Y.) 249, 64–7.

Brancho, D., Tanaka, N., Jaeschke, A., Ventura, J.-J., Kelkar, N., Tanaka, Y., Kyuuma, M., Takeshita, T., Flavell, R.A., Davis, R.J., 2003. Genes & development 17, 1969–78.

Bucala, R., Spiegel, L.A., Chesney, J., Hogan, M., Cerami, A., 1994. Molecular medicine (Cambridge, Mass.) 1, 71–81.

Burton, C.M., Iversen, M., Carlsen, J., Mortensen, J., Andersen, C.B., Steinbrüchel, D., Scheike, T., 2009. The Journal of heart and lung transplantation: the official publication of the International Society for Heart Transplantation 28, 888–93.

De Caestecker, M.P., Yahata, T., Wang, D., Parks, W.T., Huang, S., Hill, C.S., Shioda, T., Roberts, A.B., Lechleider, R.J., 2000. The Journal of biological chemistry 275, 2115–22.

Cargnello, M., Roux, P.P., 2011. Microbiology and molecular biology reviews: MMBR 75, 50–83.

Carswell, E.A., Old, L.J., Kassel, R.L., Green, S., Fiore, N., Williamson, B., 1975. Proceedings of the National Academy of Sciences of the United States of America 72, 3666–70.

Catalanotti, F., Reyes, G., Jesenberger, V., Galabova-Kovacs, G., De Matos Simoes, R., Carugo, O., Baccarini, M., 2009. Nature structural & molecular biology 16, 294–303.

Chacko, B.M., Qin, B., Correia, J.J., Lam, S.S., De Caestecker, M.P., Lin, K., 2001. Nature structural biology 8, 248–53.

Chai, J.Y., Modak, C., Mouazzen, W., Narvaez, R., Pham, J., 2010. Bioscience trends 4, 130–42.

Chao, Y.L., Shepard, C.R., Wells, A., 2010. Molecular cancer 9, 179.

Charpidou, A., Blatza, D., Anagnostou, V., Anagnostou, E., Syrigos, K.N., 2008. In vivo (Athens, Greece) 22, 529–536.

Chen, R.H., Sarnecki, C., Blenis, J., 1992. Molecular and cellular biology 12, 915–27.

Chen, S.J., Yuan, W., Lo, S., Trojanowska, M., Varga, J., 2000. Journal of cellular physiology 183, 381–92.

Chen, S.J., Yuan, W., Mori, Y., Levenson, A., Trojanowska, M., Varga, J., 1999. The Journal of investigative dermatology 112, 49–57.

Cheung, P.C.F., Campbell, D.G., Nebreda, A.R., Cohen, P., 2003. The EMBO journal 22, 5793–805.

Chow, G., Tauler, J., Mulshine, J.L., 2010. Journal of biomedicine & biotechnology 2010, 485468.

Christie, J.D., Edwards, L.B., Kucheryavaya, A.Y., Aurora, P., Dobbels, F., Kirk, R., Rahmel, A.O., Stehlik, J., Hertz, M.I., 2010. The Journal of heart and lung transplantation : the official publication of the International Society for Heart Transplantation 29, 1104–18.

Chuderland, D., Konson, A., Seger, R., 2008. Molecular cell 31, 850–61.

Cohen, S., Achbert-Weiner, H., Ciechanover, A., 2004. Molecular and cellular biology 24, 475–86.

Connolly, M.K., Bedrosian, A.S., Mallen-St Clair, J., Mitchell, A.P., Ibrahim, J., Stroud, A., Pachter, H.L., Bar-Sagi, D., Frey, A.B., Miller, G., 2009. The Journal of clinical investigation 119, 3213–25.

Cooper, J.D., Billingham, M., Egan, T., Hertz, M.I., Higenbottam, T., Lynch, J., Mauer, J., Paradis, I., Patterson, G.A., Smith, C., 1993. The Journal of heart and lung transplantation : the official publication of the International Society for Heart Transplantation 12, 713–6.

Cuenda, A., Rousseau, S., 2007. Biochimica et biophysica acta 1773, 1358–75.

Câmara, J., Jarai, G., 2010. Fibrogenesis & tissue repair 3, 2.

Dalal, B.I., Keown, P.A., Greenberg, A.H., 1993. The American journal of pathology 143, 381–9.

Davies, S.P., Reddy, H., Caivano, M., Cohen, P., 2000. The Biochemical journal 351, 95–105.

Degryse, A.L., Tanjore, H., Xu, X., Polosukhin, V. V, Jones, B.R., Boomershine, C.S., Ortiz, C., Sherrill, T.P., McMahon, F.B., Gleaves, L.A., Blackwell, T.S., Lawson, W.E., 2011. American journal of physiology. Lung cellular and molecular physiology 300, L887–97.

Delhase, M., Hayakawa, M., Chen, Y., Karin, M., 1999. Science (New York, N.Y.) 284, 309–13.

Dennler, S., Huet, S., Gauthier, J.M., 1999. Oncogene 18, 1643–8.

Dephoure, N., Zhou, C., Villén, J., Beausoleil, S.A., Bakalarski, C.E., Elledge, S.J., Gygi, S.P., 2008. Proceedings of the National Academy of Sciences of the United States of America 105, 10762–7.

Derynck, R., Zhang, Y., 2003. Nature 425, 577–84.

DiDonato, J., Mercurio, F., Rosette, C., Wu-Li, J., Suyang, H., Ghosh, S., Karin, M., 1996. Molecular and cellular biology 16, 1295–304.

Dérijard, B., Raingeaud, J., Barrett, T., Wu, I.H., Han, J., Ulevitch, R.J., Davis, R.J., 1995. Science (New York, N.Y.) 267, 682–5.

Ea, C.-K., Deng, L., Xia, Z.-P., Pineda, G., Chen, Z.J., 2006. Molecular cell 22, 245–57.

Ear, T., Fortin, C.F., Simard, F.A., McDonald, P.P., 2010. Journal of immunology (Baltimore, Md.: 1950) 184, 3897–906.

Ehrlich, H.P., Krummel, T.M., 1996. Wound repair and regeneration: official publication of the Wound Healing Society [and] the European Tissue Repair Society 4, 203–210.

El-Gamel, A., Sim, E., Hasleton, P., Hutchinson, J., Yonan, N., Egan, J., Campbell, C., Rahman, A., Sheldon, S., Deiraniya, A., Hutchinson, I. V, 1999. The Journal of heart and lung transplantation: the official publication of the International Society for Heart Transplantation 18, 828–37.

Elssner, A., Jaumann, F., Dobmann, S., Behr, J., Schwaiblmair, M., Reichenspurner, H., Fürst, H., Briegel, J., Vogelmeier, C., 2000. Transplantation 70, 362–7.

Enslen, H., 1998. Journal of Biological Chemistry 273, 1741–1748.

Eppert, K., Scherer, S.W., Ozcelik, H., Pirone, R., Hoodless, P., Kim, H., Tsui, L.C., Bapat, B., Gallinger, S., Andrulis, I.L., Thomsen, G.H., Wrana, J.L., Attisano, L., 1996. Cell 86, 543–52.

Estenne, M., Maurer, J.R., Boehler, A., Egan, J.J., Frost, A., Hertz, M., Mallory, G.B., Snell, G.I., Yousem, S., 2002. The Journal of heart and lung transplantation: the official publication of the International Society for Heart Transplantation 21, 297–310.

Evans, M.J., Cabral, L.J., Stephens, R.J., Freeman, G., 1973. The American journal of pathology 70, 175–98.

Evans, M.J., Cabral, L.J., Stephens, R.J., Freeman, G., 1975. Experimental and molecular pathology 22, 142–50.

Fan, Y., Yu, Y., Mao, R., Zhang, H., Yang, J., 2010. Cellular signalling.

Fan, Y., Yu, Y., Shi, Y., Sun, W., Xie, M., Ge, N., Mao, R., Chang, A., Xu, G., Schneider, M.D., Zhang, H., Fu, S., Qin, J., Yang, J., 2010. The Journal of biological chemistry 285, 5347–60.

Fanning, A.S., Anderson, J.M., 2009. Annals of the New York Academy of Sciences 1165, 113–20.

Farivar, A.S., Mackinnon-Patterson, B., McCourtie, A.S., Namkung, J., Ward, P.A., Mulligan, M.S., 2005. Experimental and molecular pathology 78, 190–197.

Farooqui, R., Fenteany, G., 2005. Journal of cell science 118, 51–63.

Feng, X.-H., Derynck, R., 2005. Annual review of cell and developmental biology 21, 659–93.

Ferrell Jr., J.E., 1997. Journal of Biological Chemistry 272, 19008–19016.

Forrest, I.A., Murphy, D.M., Ward, C., Jones, D., Johnson, G.E., Archer, L., Gould, F.K., Cawston, T.E., Lordan, J.L., Corris, P.A., 2005. The European respiratory journal: official journal of the European Society for Clinical Respiratory Physiology 26, 1080–5.

Frolik, C.A., Wakefield, L.M., Smith, D.M., Sporn, M.B., 1984. The Journal of biological chemistry 259, 10995–1000.

Fujita, M., Shannon, J.M., Morikawa, O., Gauldie, J., Hara, N., Mason, R.J., 2003. American journal of respiratory cell and molecular biology 29, 669–76.

Fulcher, M.L., Gabriel, S.E., Olsen, J.C., Tatreau, J.R., Gentzsch, M., Livanos, E., Saavedra, M.T., Salmon, P., Randell, S.H., 2009. American journal of physiology. Lung cellular and molecular physiology 296, L82–91.

Funaki, H., Yamamoto, T., Koyama, Y., Kondo, D., Yaoita, E., Kawasaki, K., Kobayashi, H., Sawaguchi, S., Abe, H., Kihara, I., 1998. The American journal of physiology 275, C1151–7.

Furukawa, F., Matsuzaki, K., Mori, S., Tahashi, Y., Yoshida, K., Sugano, Y., Yamagata, H., Matsushita, M., Seki, T., Inagaki, Y., Nishizawa, M., Fujisawa, J., Inoue, K., 2003. Hepatology (Baltimore, Md.) 38, 879–89.

Gardner, A., Borthwick, L.A., Fisher, A.J., 2010. Expert review of respiratory medicine 4, 647–60.

Gauldie, J., Bonniaud, P., Sime, P., Ask, K., Kolb, M., 2007. Biochemical Society transactions 35, 661–4.

Gershengorn, M.C., Hardikar, A.A., Wei, C., Geras-Raaka, E., Marcus-Samuels, B., Raaka, B.M., 2004. Science (New York, N.Y.) 306, 2261–4.

Gery, I., Gershon, R.K., Waksman, B.H., 1972. The Journal of experimental medicine 136, 128–42.

Gharaee-Kermani, M., Hu, B., Thannickal, V.J., Phan, S.H., Gyetko, M.R., 2007. Expert opinion on emerging drugs 12, 627–646.

Ghosh, M., Brechbuhl, H.M., Smith, R.W., Li, B., Hicks, D.A., Titchner, T., Runkle, C.M., Reynolds, S.D., 2011. American journal of respiratory cell and molecular biology 45, 403–10.

Giard, D.J., Aaronson, S.A., Todaro, G.J., Arnstein, P., Kersey, J.H., Dosik, H., Parks, W.P., 1973. Journal of the National Cancer Institute 51, 1417–23.

Gille, H., Kortenjann, M., Thomae, O., Moomaw, C., Slaughter, C., Cobb, M.H., Shaw, P.E., 1995. The EMBO journal 14, 951–62.

Gilles, C., Polette, M., Zahm, J.M., Tournier, J.M., Volders, L., Foidart, J.M., Birembaut, P., 1999. Journal of cell science 112 (Pt 2, 4615–25.

Gorog, D.A., Jabr, R.I., Tanno, M., Sarafraz, N., Clark, J.E., Fisher, S.G., Cao, X. Bin, Bellahcene, M., Dighe, K., Kabir, A.M.N., Quinlan, R.A., Kato, K., Gaestel, M., Marber, M.S., Heads, R.J., 2009. Cell stress & chaperones 14, 477–89.

Grell, M., Douni, E., Wajant, H., Löhden, M., Clauss, M., Maxeiner, B., Georgopoulos, S., Lesslauer, W., Kollias, G., Pfizenmaier, K., Scheurich, P., 1995. Cell 83, 793–802.

Gueders, M.M., Foidart, J.-M., Noel, A., Cataldo, D.D., 2006. European journal of pharmacology 533, 133–144.

Hackett, T.-L., Warner, S.M., Stefanowicz, D., Shaheen, F., Pechkovsky, D. V, Murray, L.A., Argentieri, R., Kicic, A., Stick, S.M., Bai, T.R., Knight, D.A., 2009. American journal of respiratory and critical care medicine 180, 122–33.

Hafkin, J., Blumberg, E., 2009. Current opinion in organ transplantation 14, 483–7.

Hagemann, C., Rapp, U.R., 1999. Experimental cell research 253, 34–46.

Han, J., Jiang, Y., Li, Z., Kravchenko, V. V, Ulevitch, R.J., 1997. Nature 386, 296–9.

Han, J., Lee, J.D., Bibbs, L., Ulevitch, R.J., 1994. Science (New York, N.Y.) 265, 808–11.

Hatano, N., Mori, Y., Oh-hora, M., Kosugi, A., Fujikawa, T., Nakai, N., Niwa, H., Miyazaki, J., Hamaoka, T., Ogata, M., 2003. Genes to cells : devoted to molecular & cellular mechanisms 8, 847–56.

Hawgood, S., Clements, J.A., 1990. The Journal of clinical investigation 86, 1–6.

Hetzel, M., Bachem, M., Anders, D., Trischler, G., Faehling, M., 2005. Lung 183, 225–237.

Heyer, J., Escalante-Alcalde, D., Lia, M., Boettinger, E., Edelmann, W., Stewart, C.L., Kucherlapati, R., 1999. Proceedings of the National Academy of Sciences of the United States of America 96, 12595–600.

Hibi, M., Lin, A., Smeal, T., Minden, A., Karin, M., 1993. Genes & development 7, 2135–48.

Hinz, B., 2007. The Journal of investigative dermatology 127, 526–37.

Hinz, B., Gabbiani, G., 2003. Current Opinion in Biotechnology 14, 538–546.

Hiwatari, N., Shimura, S., Yamauchi, K., Nara, M., Hida, W., Shirato, K., 1997. The Tohoku journal of experimental medicine 181, 285–95.

Hodge, G., Hodge, S., Chambers, D., Reynolds, P.N., Holmes, M., 2009. Transplantation 88, 211–8.

Hoffmann, A., Levchenko, A., Scott, M.L., Baltimore, D., 2002. Science (New York, N.Y.) 298, 1241–5.

Holgate, S.T., Arshad, H.S., Roberts, G.C., Howarth, P.H., Thurner, P., Davies, D.E., 2010. Clinical science (London, England : 1979) 118, 439–50.

Holt, P.G., Oliver, J., Bilyk, N., McMenamin, C., McMenamin, P.G., Kraal, G., Thepen, T., 1993. The Journal of experimental medicine 177, 397–407.

Honorato, B., Alcalde, J., Martinez-Monge, R., Zabalegui, N., Garcia-Foncillas, J., 2008. Gene regulation and systems biology : 2, 63–70.

Hoogewerf, A.J., Kuschert, G.S., Proudfoot, A.E., Borlat, F., Clark-Lewis, I., Power, C.A., Wells, T.N., 1997. Biochemistry 36, 13570–8.

Hou, J.-M., Krebs, M., Ward, T., Sloane, R., Priest, L., Hughes, A., Clack, G., Ranson, M., Blackhall, F., Dive, C., 2011. The American journal of pathology 178, 989–96.

Hu, Y., Baud, V., Delhase, M., Zhang, P., Deerinck, T., Ellisman, M., Johnson, R., Karin, M., 1999. Science (New York, N.Y.) 284, 316–20.

Hudson, A.R., Kilburn, K.H., Halprin, G.M., McKenzie, W.N., 1977. The American review of respiratory disease 115, 89–95.

Humphreys, B.D., Lin, S.-L., Kobayashi, A., Hudson, T.E., Nowlin, B.T., Bonventre, J. V, Valerius, M.T., McMahon, A.P., Duffield, J.S., 2010. The American journal of pathology 176, 85–97.

Huynh, Q.K., Boddupalli, H., Rouw, S.A., Koboldt, C.M., Hall, T., Sommers, C., Hauser, S.D., Pierce, J.L., Combs, R.G., Reitz, B.A., Diaz-Collier, J.A., Weinberg, R.A., Hood, B.L., Kilpatrick, B.F., Tripp, C.S., 2000. The Journal of biological chemistry 275, 25883–91.

Inman, G.J., Hill, C.S., 2002. The Journal of biological chemistry 277, 51008–16.

Iwano, M., Plieth, D., Danoff, T.M., Xue, C., Okada, H., Neilson, E.G., 2002. The Journal of clinical investigation 110, 341–50.

Jacobs, M.D., Harrison, S.C., 1998. Cell 95, 749–58.

Jiang, R., Xia, Y., Li, J., Deng, L., Zhao, L., Shi, J., Wang, X., Sun, B., 2010. International journal of cancer. Journal international du cancer 126, 1263–74.

Jinnin, M., Ihn, H., Tamaki, K., 2006. Molecular pharmacology 69, 597–607.

Kajino, T., Omori, E., Ishii, S., Matsumoto, K., Ninomiya-Tsuji, J., 2007. The Journal of biological chemistry 282, 9475–81.

Kakiashvili, E., Dan, Q., Vandermeer, M., Zhang, Y., Waheed, F., Pham, M., Szászi, K., 2011. The Journal of biological chemistry 286, 9268–79.

Kallunki, T., Su, B., Tsigelny, I., Sluss, H.K., Derijard, B., Moore, G., Davis, R., Karin, M., 1994. Genes & Development 8, 2996–3007.

Karandikar, M., Xu, S., Cobb, M.H., 2000. The Journal of biological chemistry 275, 40120–7.

Kasai, H., Allen, J.T., Mason, R.M., Kamimura, T., Zhang, Z., 2005. Respiratory research 6, 56.

Khokhlatchev, A., Xu, S., English, J., Wu, P., Schaefer, E., Cobb, M.H., 1997. J. Biol. Chem. 272, 11057–11062.

Kim, K.K., Kugler, M.C., Wolters, P.J., Robillard, L., Galvez, M.G., Brumwell, A.N., Sheppard, D., Chapman, H.A., 2006. Proceedings of the National Academy of Sciences of the United States of America 103, 13180–5.

Kim, S.I., Kwak, J.H., Na, H.-J., Kim, J.K., Ding, Y., Choi, M.E., 2009. The Journal of biological chemistry 284, 22285–96.

Kim, Y., Rice, A.E., Denu, J.M., 2003. Biochemistry 42, 15197–207.

Kim, Y.-S., Schwabe, R.F., Qian, T., Lemasters, J.J., Brenner, D.A., 2002. Hepatology (Baltimore, Md.) 36, 1498–508.

Kins, S., Kurosinski, P., Nitsch, R.M., Götz, J., 2003. The American journal of pathology 163, 833–43.

Kis, K., Liu, X., Hagood, J.S., 2011. Expert reviews in molecular medicine 13, e27.

Kishimoto, K., Matsumoto, K., Ninomiya-Tsuji, J., 2000. The Journal of biological chemistry 275, 7359–64.

Kishore, N., Sommers, C., Mathialagan, S., Guzova, J., Yao, M., Hauser, S., Huynh, K., Bonar, S., Mielke, C., Albee, L., Weier, R., Graneto, M., Hanau, C., Perry, T., Tripp, C.S., 2003. The Journal of biological chemistry 278, 32861–71.

Kliment, C.R., Tobolewski, J.M., Manni, M.L., Tan, R.J., Enghild, J., Oury, T.D., 2008. Antioxidants & redox signaling 10, 261–8.

Kojima, H., Sasaki, T., Ishitani, T., Iemura, S., Zhao, H., Kaneko, S., Kunimoto, H., Natsume, T., Matsumoto, K., Nakajima, K., 2005. Proceedings of the National Academy of Sciences of the United States of America 102, 4524–9.

Kolb, M., Margetts, P.J., Anthony, D.C., Pitossi, F., Gauldie, J., 2001. The Journal of clinical investigation 107, 1529–1536.

Kolosova, I., Nethery, D., Kern, J.A., 2010. Journal of cellular physiology 226, 1248–54.

Kondo, M., Osada, H., Uchida, K., Yanagisawa, K., Masuda, A., Takagi, K., Takahashi, T., 1998. International journal of cancer. Journal international du cancer 75, 559–63.

Korthagen, N.M., Van Moorsel, C.H.M., Kazemier, K.M., Ruven, H.J.T., Grutters, J.C., 2012. Immunogenetics 64, 371–7.

Kosters, A., White, D.D., Sun, H., Thevananther, S., Karpen, S.J., 2009. Journal of hepatology 51, 898–908.

Kostura, M.J., Tocci, M.J., Limjuco, G., Chin, J., Cameron, P., Hillman, A.G., Chartrain, N.A., Schmidt, J.A., 1989. Proceedings of the National Academy of Sciences of the United States of America 86, 5227–31.

Koyama, S., Sato, E., Nomura, H., Kubo, K., Miura, M., Yamashita, T., Nagai, S., Izumi, T., 1998. The American journal of pathology 153, 1885–93.

Lacaze-Masmonteil, T., 1995. Journal of Biological Chemistry 270, 12162–12169.

Lange-Sperandio, B., Trautmann, A., Eickelberg, O., Jayachandran, A., Oberle, S., Schmidutz, F., Rodenbeck, B., Homme, M., Horuk, R., Schaefer, F., 2007. American Journal Of Pathology 171, 861–871.

Lapar, D.J., Burdick, M.D., Emaminia, A., Harris, D.A., Strieter, B.A., Liu, L., Robbins, M., Kron, I.L., Strieter, R.M., Lau, C.L., 2011. The Annals of thoracic surgery 92, 470–7.

Lawler, S., Fleming, Y., Goedert, M., Cohen, P., 1998. Current biology : CB 8, 1387–90.

Lee, M.K., Pardoux, C., Hall, M.C., Lee, P.S., Warburton, D., Qing, J., Smith, S.M., Derynck, R., 2007. The EMBO journal 26, 3957–67.

Li, J., Johnson, S.E., 2006. Biochemical and biophysical research communications 345, 1425–33.

Li, Q., Van Antwerp, D., Mercurio, F., Lee, K.F., Verma, I.M., 1999. Science (New York, N.Y.) 284, 321–5.

Lieber, M., Smith, B., Szakal, A., Nelson-Rees, W., Todaro, G., 1976. International journal of cancer. Journal international du cancer 17, 62–70.

Lin, L., DeMartino, G.N., Greene, W.C., 1998. Cell 92, 819–28.

Lin, W.-W., Karin, M., 2007. The Journal of clinical investigation 117, 1175–83.

Lin, X., Duan, X., Liang, Y.-Y., Su, Y., Wrighton, K.H., Long, J., Hu, M., Davis, C.M., Wang, J., Brunicardi, F.C., Shi, Y., Chen, Y.G., Meng, A., Feng, X.-H., 2006. Cell 125, 915–28.

Liu, H., Sidiropoulos, P., Song, G., Pagliari, L.J., Birrer, M.J., Stein, B., Anrather, J., Pope, R.M., 2000. Journal of immunology (Baltimore, Md. : 1950) 164, 4277–85.

Liu, Y., 2010. Journal of the American Society of Nephrology : JASN 21, 212–22.

Locksley, R.M., Killeen, N., Lenardo, M.J., 2001. Cell 104, 487–501.

Lu, G., Kang, Y.J., Han, J., Herschman, H.R., Stefani, E., Wang, Y., 2006. The Journal of biological chemistry 281, 6087–95.

Luzina, I.G., Tsymbalyuk, N., Choi, J., Hasday, J.D., Atamas, S.P., 2006. Journal of cellular physiology 206, 221–8.

Lv, Z.-M., Wang, Q., Wan, Q., Lin, J.-G., Hu, M.-S., Liu, Y.-X., Wang, R., 2011. PloS one 6, e22806.

Löfdahl, J.M., Cederlund, K., Nathell, L., Eklund, A., Sköld, C.M., 2005. The European respiratory journal : official journal of the European Society for Clinical Respiratory Physiology 25, 275–81.

Ma, F.Y., Tesch, G.H., Ozols, E., Xie, M., Schneider, M.D., Nikolic-Paterson, D.J., 2011. American journal of physiology. Renal physiology 300, F1410–21.

Mao, R., Fan, Y., Mou, Y., Zhang, H., Fu, S., Yang, J., 2011. Cellular signalling 23, 222–7.

Maouche, K., Polette, M., Jolly, T., Medjber, K., Cloëz-Tayarani, I., Changeux, J.-P., Burlet, H., Terryn, C., Coraux, C., Zahm, J.M., Birembaut, P., Tournier, J.-M., 2009. The American journal of pathology 175, 1868–82.

March, C.J., Mosley, B., Larsen, A., Cerretti, D.P., Braedt, G., Price, V., Gillis, S., Henney, C.S., Kronheim, S.R., Grabstein, K., 1985. Nature 315, 641–7.

Martin, P., D'Souza, D., Martin, J., Grose, R., Cooper, L., Maki, R., McKercher, S.R., 2003. Current biology : CB 13, 1122–8.

Matsuguchi, T., Masuda, A., Sugimoto, K., Nagai, Y., Yoshikai, Y., 2003. The EMBO journal 22, 4455–64.

Matthews, N., 1978. British journal of cancer 38, 310–5.

May, M.J., D'Acquisto, F., Madge, L.A., Glöckner, J., Pober, J.S., Ghosh, S., 2000. Science (New York, N.Y.) 289, 1550–4.

May, M.J., Marienfeld, R.B., Ghosh, S., 2002. The Journal of biological chemistry 277, 45992–6000.

McDermott, E.P., O'Neill, L.A.J., 2002. The Journal of biological chemistry 277, 7808–15.

Micheau, O., Tschopp, J., 2003. Cell 114, 181–90.

Michel, M., Torok, N., Godbout, M., Lussier, M., Gaudreau, P., Royal, A., Germain, L., 1996. J. Cell Sci. 109, 1017–1028.

Mikuniya, T., Nagai, S., Shimoji, T., Takeuchi, M., Morita, K., Mio, T., Satake, N., Izumi, T., 1997. Sarcoidosis, vasculitis, and diffuse lung diseases : official journal of WASOG / World Association of Sarcoidosis and Other Granulomatous Disorders 14, 39–45.

Miller, B.S., Zandi, E., 2001. The Journal of biological chemistry 276, 36320–6.

Minden, A., Lin, A., Claret, F.-X., Abo, A., Karin, M., 1995. Cell 81, 1147–1157.

Minden, A., Lin, A., Smeal, T., Dérijard, B., Cobb, M., Davis, R., Karin, M., 1994. Molecular and cellular biology 14, 6683–8.

Miyazaki, Y., Araki, K., Vesin, C., Garcia, I., Kapanci, Y., Whitsett, J.A., Piguet, P.F., Vassalli, P., 1995. The Journal of clinical investigation 96, 250–9.

Mizoguchi, E., Mizoguchi, A., Takedatsu, H., Cario, E., De Jong, Y.P., Ooi, C.J., Xavier, R.J., Terhorst, C., Podolsky, D.K., Bhan, A.K., 2002. Gastroenterology 122, 134–44.

Mizuno, R., Oya, M., Shiomi, T., Marumo, K., Okada, Y., Murai, M., 2004. The Journal of urology 172, 723–7.

Moeller, A., Gilpin, S.E., Ask, K., Cox, G., Cook, D., Gauldie, J., Margetts, P.J., Farkas, L., Dobranowski, J., Boylan, C., O'Byrne, P.M., Strieter, R.M., Kolb, M., 2009. American journal of respiratory and critical care medicine 179, 588–594.

Mohit, A.A., Martin, J.H., Miller, C.A., 1995. Neuron 14, 67–78.

Monzen, K., Hiroi, Y., Kudoh, S., Akazawa, H., Oka, T., Takimoto, E., Hayashi, D., Hosoda, T., Kawabata, M., Miyazono, K., Ishii, S., Yazaki, Y., Nagai, R., Komuro, I., 2001. The Journal of cell biology 153, 687–98.

Moran, N., 2011. Nature biotechnology 29, 301.

Morton, R.A., Geras-Raaka, E., Wilson, L.M., Raaka, B.M., Gershengorn, M.C., 2007. Molecular and cellular endocrinology 270, 87–93.

Morton, S., Davis, R.J., McLaren, A., Cohen, P., 2003. The EMBO journal 22, 3876–86.

Murphy, L.O., Smith, S., Chen, R.-H., Fingar, D.C., Blenis, J., 2002. Nature cell biology 4, 556–64.

Nii, A., Sone, S., Orino, E., Ogura, T., 1993. J. Leukoc. Biol. 53, 29–36.

Ninomiya-Tsuji, J., Kajino, T., Ono, K., Ohtomo, T., Matsumoto, M., Shiina, M., Mihara, M., Tsuchiya, M., Matsumoto, K., 2003. The Journal of biological chemistry 278, 18485–90.

Nishimura, M., Shin, M.-S., Singhirunnusorn, P., Suzuki, S., Kawanishi, M., Koizumi, K., Saiki, I., Sakurai, H., 2009. Molecular and cellular biology 29, 5529–39.

Ochs, M., Nyengaard, J.R., Jung, A., Knudsen, L., Voigt, M., Wahlers, T., Richter, J., Gundersen, H.J.G., 2004. American journal of respiratory and critical care medicine 169, 120–4.

Ohkawara, B., Shirakabe, K., Hyodo-Miura, J., Matsuo, R., Ueno, N., Matsumoto, K., Shibuya, H., 2004. Genes & development 18, 381–6.

Ohori, M., Kinoshita, T., Okubo, M., Sato, K., Yamazaki, A., Arakawa, H., Nishimura, S., Inamura, N., Nakajima, H., Neya, M., Miyake, H., Fujii, T., 2005. Biochemical and biophysical research communications 336, 357–63.

Oikonomou, N., Harokopos, V., Zalevsky, J., Valavanis, C., Kotanidou, A., Szymkowski, D.E., Kollias, G., Aidinis, V., 2006. PloS one 1, e108.

Oleinik, N. V, Krupenko, N.I., Krupenko, S.A., 2007. Oncogene 26, 7222–30.

Olson, B.J.S.C., Markwell, J., 2007. Current Protocols in Protein Science Chapter 3, Unit 3.4.

Omenetti, A., Porrello, A., Jung, Y., Yang, L., Popov, Y., Choi, S.S., Witek, R.P., Alpini, G., Venter, J., Vandongen, H.M., Syn, W.-K., Baroni, G.S., Benedetti, A., Schuppan, D., Diehl, A.M., 2008. The Journal of clinical investigation 118, 3331–42.

Omori, E., Matsumoto, K., Zhu, S., Smart, R.C., Ninomiya-Tsuji, J., 2010. Cancer research 70, 8417–25.

Owens, D.M., Keyse, S.M., 2007. Oncogene 26, 3203–13.

Pahl, H.L., 1999. Oncogene 18, 6853–66.

Parish, C.R., 2006. Nature reviews. Immunology 6, 633–43.

Peng, C., Cho, Y.-Y., Zhu, F., Xu, Y.-M., Wen, W., Ma, W.-Y., Bode, A.M., Dong, Z., 2010. The FASEB journal : official publication of the Federation of American Societies for Experimental Biology 24, 3490–9.

Peri, A., Cordella-Miele, E., Miele, L., Mukherjee, A.B., 1993. The Journal of clinical investigation 92, 2099–109.

Perkins, N.D., 2007. Nature reviews. Molecular cell biology 8, 49–62.

Perlson, E., Michaelevski, I., Kowalsman, N., Ben-Yaakov, K., Shaked, M., Seger, R., Eisenstein, M., Fainzilber, M., 2006. Journal of molecular biology 364, 938–44.

Pierreux, C.E., Nicolás, F.J., Hill, C.S., 2000. Molecular and cellular biology 20, 9041–54.

Piguet, P.F., Vesin, C., Grau, G.E., Thompson, R.C., 1993. Cytokine 5, 57–61.

Podolin, P.L., Callahan, J.F., Bolognese, B.J., Li, Y.H., Carlson, K., Davis, T.G., Mellor, G.W., Evans, C., Roshak, A.K., 2005. The Journal of pharmacology and experimental therapeutics 312, 373–81.

Porcheray, F., Viaud, S., Rimaniol, A.-C., Léone, C., Samah, B., Dereuddre-Bosquet, N., Dormont, D., Gras, G., 2005. Clinical and experimental immunology 142, 481–9.

Prajapati, S., Verma, U., Yamamoto, Y., Kwak, Y.T., Gaynor, R.B., 2004. The Journal of biological chemistry 279, 1739–46.

Purkis, P.E., Steel, J.B., Mackenzie, I.C., Nathrath, W.B., Leigh, I.M., Lane, E.B., 1990. Journal of cell science 97 (Pt 1), 39–50.

Quan, T.E., Cowper, S., Wu, S.-P., Bockenstedt, L.K., Bucala, R., 2004. The international journal of biochemistry & cell biology 36, 598–606.

Raingeaud, J., Whitmarsh, A.J., Barrett, T., Dérijard, B., Davis, R.J., 1996. Molecular and cellular biology 16, 1247–55.

Ramirez, A.M., Nunley, D.R., Rojas, M., Roman, J., 2008. Biomarker insights 3, 351–359.

Ramirez, A.M., Shen, Z., Ritzenthaler, J.D., Roman, J., 2006. American journal of transplantation : official journal of the American Society of Transplantation and the American Society of Transplant Surgeons 6, 2080–8.

Ramshaw, J.A., Shah, N.K., Brodsky, B., 1998. Journal of structural biology 122, 86–91.

Reddel, R.R., Ke, Y., Gerwin, B.I., McMenamin, M.G., Lechner, J.F., Su, R.T., Brash, D.E., Park, J.B., Rhim, J.S., Harris, C.C., 1988. Cancer research 48, 1904–9.

Riha, R.L., Yang, I.A., Rabnott, G.C., Tunnicliffe, A.M., Fong, K.M., Zimmerman, P. V, 2004. Internal medicine journal 34, 126–9.

Riise, G.C., Andersson, B.A., Kjellström, C., Martensson, G., Nilsson, F.N., Ryd, W., Scherstén, H., 1999. The European respiratory journal : official journal of the European Society for Clinical Respiratory Physiology 14, 1123–1130.

Rocha, S., Martin, A.M., Meek, D.W., Perkins, N.D., 2003. Molecular and cellular biology 23, 4713–27.

Rock, J.R., Onaitis, M.W., Rawlins, E.L., Lu, Y., Clark, C.P., Xue, Y., Randell, S.H., Hogan, B.L.M., 2009. Proceedings of the National Academy of Sciences of the United States of America 106, 12771–5.

Rogers, A.J., Raby, B.A., Lasky-Su, J.A., Murphy, A., Lazarus, R., Klanderman, B.J., Sylvia, J.S., Ziniti, J.P., Lange, C., Celedón, J.C., Silverman, E.K., Weiss, S.T., 2009. American journal of respiratory and critical care medicine 179, 1084–1090.

Rothe, M., Wong, S.C., Henzel, W.J., Goeddel, D. V, 1994. Cell 78, 681–92.

Van Roy, F., Berx, G., 2008. Cellular and molecular life sciences : CMLS 65, 3756–88.

Royuela, M., Rodríguez-Berriguete, G., Fraile, B., Paniagua, R., 2008. Histology and histopathology 23, 1279–90.

Rubinfeld, H., Seger, R., 2005. Molecular biotechnology 31, 151–74.

Sadir, R., Imberty, A., Baleux, F., Lortat-Jacob, H., 2004. The Journal of biological chemistry 279, 43854–60.

Saklatvala, J., Rawlinson, L., Waller, R.J., Sarsfield, S., Lee, J.C., Morton, L.F., Barnes, M.J., Farndale, R.W., 1996. The Journal of biological chemistry 271, 6586–9.

Sakurai, H., Nishi, A., Sato, N., Mizukami, J., Miyoshi, H., Sugita, T., 2002. Biochemical and biophysical research communications 297, 1277–81.

Sanjabi, S., Zenewicz, L.A., Kamanaka, M., Flavell, R.A., 2009. Current opinion in pharmacology 9, 447–53.

Sano, Y., Harada, J., Tashiro, S., Gotoh-Mandeville, R., Maekawa, T., Ishii, S., 1999. The Journal of biological chemistry 274, 8949–57.

Santos, F.B., Nagato, L.K.S., Boechem, N.M., Negri, E.M., Guimarães, A., Capelozzi, V.L., Faffe, D.S., Zin, W.A., Rocco, P.R.M., 2006. Journal of applied physiology (Bethesda, Md. : 1985) 100, 98–106.

Saunders, R., Siddiqui, S., Kaur, D., Doe, C., Sutcliffe, A., Hollins, F., Bradding, P., Wardlaw, A., Brightling, C.E., 2009. The Journal of allergy and clinical immunology 123, 376–384.

Schildge, J., Nagel, C., Grun, C., 2007. Respiration; international review of thoracic diseases 74, 553–7.

Scholten, D., Osterreicher, C.H., Scholten, A., Iwaisako, K., Gu, G., Brenner, D.A., Kisseleva, T., 2010. Gastroenterology 139, 987–98.

Scholz, R., Sidler, C.L., Thali, R.F., Winssinger, N., Cheung, P.C.F., Neumann, D., 2010. The Journal of biological chemistry 285, 25753–66.

Scott, M.L., Fujita, T., Liou, H.C., Nolan, G.P., Baltimore, D., 1993. Genes & development 7, 1266–76.

Senftleben, U., Cao, Y., Xiao, G., Greten, F.R., Krähn, G., Bonizzi, G., Chen, Y., Hu, Y., Fong, A., Sun, S.C., Karin, M., 2001. Science (New York, N.Y.) 293, 1495–9.

Seternes, O.M., Johansen, B., Hegge, B., Johannessen, M., Keyse, S.M., Moens, U., 2002. Molecular and cellular biology 22, 6931–45.

Sharma, S., Ghosh, B., Sharma, S.K., 2008. Clinical and experimental immunology 151, 251–9.

Shaul, Y.D., Gibor, G., Plotnikov, A., Seger, R., 2009. Genes & development 23, 1779–90.

Shi, M., Zhu, J., Wang, R., Chen, X., Mi, L., Walz, T., Springer, T.A., 2011. Nature 474, 343–9.

Shi, Y., Wang, Y.F., Jayaraman, L., Yang, H., Massagué, J., Pavletich, N.P., 1998. Cell 94, 585–94.

Shim, J.-H., Xiao, C., Paschal, A.E., Bailey, S.T., Rao, P., Hayden, M.S., Lee, K.-Y., Bussey, C., Steckel, M., Tanaka, N., Yamada, G., Akira, S., Matsumoto, K., Ghosh, S., 2005. Genes & development 19, 2668–81.

Shyu, Y.J., Suarez, C.D., Hu, C.-D., 2008. Proceedings of the National Academy of Sciences of the United States of America 105, 151–6.

Siegel, P.M., Shu, W., Cardiff, R.D., Muller, W.J., Massagué, J., 2003. Proceedings of the National Academy of Sciences of the United States of America 100, 8430–5.

Sime, P.J., Marr, R.A., Gauldie, D., Xing, Z., Hewlett, B.R., Graham, F.L., Gauldie, J., 1998. The American journal of pathology 153, 825–32.

Sime, P.J., Xing, Z., Graham, F.L., Csaky, K.G., Gauldie, J., 1997. The Journal of clinical investigation 100, 768–76.

Singhirunnusorn, P., Suzuki, S., Kawasaki, N., Saiki, I., Sakurai, H., 2005. The Journal of biological chemistry 280, 7359–68.

Smith, D.M., Patel, S., Raffoul, F., Haller, E., Mills, G.B., Nanjundan, M., 2010. Cell death and differentiation 17, 1867–1881.

Sorrentino, A., Thakur, N., Grimsby, S., Marcusson, A., Von Bulow, V., Schuster, N., Zhang, S., Heldin, C.-H., Landström, M., 2008. Nature cell biology 10, 1199–207.

Srivastava, A.K., Qin, X., Wedhas, N., Arnush, M., Linkhart, T.A., Chadwick, R.B., Kumar, A., 2007. The Journal of biological chemistry 282, 35113–24.

Stasiak, P.C., Purkis, P.E., Leigh, I.M., Lane, E.B., 1989. Journal of Investigative Dermatology 92, 707–716.

Steinert, P.M., Roop, D.R., 1988. Annual review of biochemistry 57, 593–625.

Strausberg, R.L., Feingold, E.A., Grouse, L.H., Derge, J.G., Klausner, R.D., et al., 2002. Proceedings of the National Academy of Sciences of the United States of America 99, 16899–903.

Stripp, B.R., Reynolds, S.D., 2008. Proceedings of the American Thoracic Society 5, 328–33.

Strippoli, R., Benedicto, I., Foronda, M., Perez-Lozano, M.L., Sánchez-Perales, S., López-Cabrera, M., Del Pozo, M.Á., 2010. Journal of cell science 123, 4321–31.

Strippoli, R., Benedicto, I., Pérez Lozano, M.L., Cerezo, A., López-Cabrera, M., Del Pozo, M.A., 2008. Disease models & mechanisms 1, 264–74.

Su, Y.C., Han, J., Xu, S., Cobb, M., Skolnik, E.Y., 1997. The EMBO journal 16, 1279–90.

Sun, L., Deng, L., Ea, C.-K., Xia, Z.-P., Chen, Z.J., 2004. Molecular cell 14, 289–301.

Szafranska, A.E., Luo, X., Dalby, K.N., 2005. Analytical biochemistry 336, 1–10.

Tanaka, N., Kamanaka, M., Enslen, H., Dong, C., Wysk, M., Davis, R.J., Flavell, R.A., 2002. EMBO reports 3, 785–91.

Tanjore, H., Xu, X.C., Polosukhin, V. V, Degryse, A.L., Li, B., Han, W., Sherrill, T.P., Plieth, D., Neilson, E.G., Blackwell, T.S., Lawson, W.E., 2009. American journal of respiratory and critical care medicine 180, 657–65.

Tanoue, T., Adachi, M., Moriguchi, T., Nishida, E., 2000. Nature cell biology 2, 110–6.

Tanoue, T., Yamamoto, T., Maeda, R., Nishida, E., 2001. The Journal of biological chemistry 276, 26629–39.

Tegethoff, S., Behlke, J., Scheidereit, C., 2003. Molecular and cellular biology 23, 2029–41.

Terada, Y., Nakashima, O., Inoshita, S., Kuwahara, M., Sasaki, S., Marumo, F., 1999. Nephrology, dialysis, transplantation : official publication of the European Dialysis and Transplant Association - European Renal Association 14 Suppl 1, 45–7.

Theiss, A.L., Simmons, J.G., Jobin, C., Lund, P.K., 2005. The Journal of biological chemistry 280, 36099–109.

Therrien, M., Michaud, N.R., Rubin, G.M., Morrison, D.K., 1996. Genes & development 10, 2684–95.

Thornberry, N.A., Bull, H.G., Calaycay, J.R., Chapman, K.T., Howard, A.D., Kostura, M.J., Miller, D.K., Molineaux, S.M., Weidner, J.R., Aunins, J., 1992. Nature 356, 768–74.

Tong, L., Pav, S., White, D.M., Rogers, S., Crane, K.M., Cywin, C.L., Brown, M.L., Pargellis, C.A., 1997. Nature Structural Biology 4, 311–316.

Troyanovsky, S.M., Guelstein, V.I., Tchipysheva, T.A., Krutovskikh, V.A., Bannikov, G.A., 1989. Journal of cell science 93 (Pt 3), 419–26.

Uemura, M., Swenson, E.S., Gaça, M.D.A., Giordano, F.J., Reiss, M., Wells, R.G., 2005. Molecular biology of the cell 16, 4214–24.

Uhlik, M.T., Abell, A.N., Johnson, N.L., Sun, W., Cuevas, B.D., Lobel-Rice, K.E., Horne, E.A., Dell'Acqua, M.L., Johnson, G.L., 2003. Nature cell biology 5, 1104–10.

Upham, J.W., Stick, S.M., 2006. Current drug targets 7, 541–5.

Vaday, G.G., Schor, H., Rahat, M.A., Lahat, N., Lider, O., 2001. Journal of leukocyte biology 69, 613–21.

Valenick, L. V, Hsia, H.C., Schwarzbauer, J.E., 2005. Experimental cell research 309, 48–55.

Vanaudenaerde, B.M., Meyts, I., Vos, R., Geudens, N., De Wever, W., Verbeken, E.K., Van Raemdonck, D.E., Dupont, L.J., Verleden, G.M., 2008. The European respiratory journal : official journal of the European Society for Clinical Respiratory Physiology 32, 832–43.

Vanaudenaerde, B.M., De Vleeschauwer, S.I., Vos, R., Meyts, I., Bullens, D.M., Reynders, V., Wuyts, W.A., Van Raemdonck, D.E., Dupont, L.J., Verleden, G.M., 2008. American journal of transplantation : official journal of the American Society of Transplantation and the American Society of Transplant Surgeons 8, 1911–20.

Varela-Rey, M., Montiel-Duarte, C., Osés-Prieto, J.., López-Zabalza, M.., Jaffrèzou, J.., Rojkind, M., Iraburu, M.., 2002. FEBS Letters 528, 133–138.

Velden, J.L.J. van der, Alcorn, J.F., Guala, A.S., Badura, E.C.H.L., Janssen-Heininger, Y.M.W., 2011. American journal of respiratory cell and molecular biology 44, 571–81.

Verleden, S.E., Vos, R., Mertens, V., Willems-Widyastuti, A., De Vleeschauwer, S.I., Dupont, L.J., Verleden, G.M., Van Raemdonck, D.E., Vanaudenaerde, B.M., 2011. The Journal of heart and lung transplantation : the official publication of the International Society for Heart Transplantation 30, 667–73.

Vermeulen, L., De Wilde, G., Van Damme, P., Vanden Berghe, W., Haegeman, G., 2003. The EMBO journal 22, 1313–24.

Verrecchia, F., Pessah, M., Atfi, A., Mauviel, A., 2000. The Journal of biological chemistry 275, 30226–31.

Verrecchia, F., Vindevoghel, L., Lechleider, R.J., Uitto, J., Roberts, A.B., Mauviel, A., 2001. Oncogene 20, 3332–40.

Verrecchia, F., Wagner, E.F., Mauviel, A., 2002. EMBO reports 3, 1069–74.

Viallet, J., Liu, C., Emond, J., Tsao, M.S., 1994. Experimental cell research 212, 36–41.

Vogelstein, B., Kinzler, K.W., 2004. Nature medicine 10, 789–99.

Voisin, L., Saba-El-Leil, M.K., Julien, C., Frémin, C., Meloche, S., 2010. Molecular and cellular biology 30, 2918–32.

Vos, R., Vanaudenaerde, B.M., Geudens, N., Dupont, L.J., Van Raemdonck, D.E., Verleden, G.M., 2008. The European respiratory journal : official journal of the European Society for Clinical Respiratory Physiology 31, 1037–45.

Vos, R., Vanaudenaerde, B.M., Ottevaere, A., Verleden, S.E., De Vleeschauwer, S.I., Willems-Widyastuti, A., Wauters, S., Van Raemdonck, D.E., Nawrot, T.S., Dupont, L.J., Verleden, G.M., 2010. The Journal of heart and lung transplantation : the official publication of the International Society for Heart Transplantation 29, 1358–68.

Vos, R., Vanaudenaerde, B.M., Verleden, S.E., De Vleeschauwer, S.I., Willems-Widyastuti, A., Van Raemdonck, D.E., Schoonis, A., Nawrot, T.S., Dupont, L.J., Verleden, G.M., 2011. The European respiratory journal : official journal of the European Society for Clinical Respiratory Physiology 37, 164–72.

Walker, S.R., Williams, M.C., Benson, B., 1986. The journal of histochemistry and cytochemistry : official journal of the Histochemistry Society 34, 1137–48.

Wang, C., Deng, L., Hong, M., Akkaraju, G.R., Inoue, J., Chen, Z.J., 2001. Nature 412, 346–51.

Wang, D., Zhang, S., Li, L., Liu, X., Mei, K., Wang, X., 2010. Nature immunology 11, 905–11.

Wang, L., Ma, R., Flavell, R.A., Choi, M.E., 2002. The Journal of biological chemistry 277, 47257–62.

Wang, S., Hubmayr, R.D., 2011. American journal of respiratory cell and molecular biology 44, 692–9.

Wang, X., Sonenshein, G.E., 2005. Journal of virology 79, 95–105.

Ward, C., Forrest, I.A., Murphy, D.M., Johnson, G.E., Robertson, H., Cawston, T.E., Fisher, A.J., Dark, J.H., Lordan, J.L., Kirby, J.A., Corris, P.A., 2005. Thorax 60, 865–71.

Waskiewicz, A.J., Flynn, A., Proud, C.G., Cooper, J.A., 1997. The EMBO journal 16, 1909–20.

Wennerberg, K., Rossman, K.L., Der, C.J., 2005. Journal of cell science 118, 843–6.

Wertz, I.E., O'Rourke, K.M., Zhou, H., Eby, M., Aravind, L., Seshagiri, S., Wu, P., Wiesmann, C., Baker, R., Boone, D.L., Ma, A., Koonin, E. V, Dixit, V.M., 2004. Nature 430, 694–9.

Willis, B.C., Borok, Z., 2007. American journal of physiology. Lung cellular and molecular physiology 293, L525–534.

Willis, B.C., duBois, R.M., Borok, Z., 2006. Proceedings of the American Thoracic Society 3, 377–382.

Wood, C.D., Thornton, T.M., Sabio, G., Davis, R.A., Rincon, M., 2009. International journal of biological sciences 5, 428–37.

Wu, J.W., Hu, M., Chai, J., Seoane, J., Huse, M., Li, C., Rigotti, D.J., Kyin, S., Muir, T.W., Fairman, R., Massagué, J., Shi, Y., 2001. Molecular cell 8, 1277–89.

Wu, Z.-H., Shi, Y., Tibbetts, R.S., Miyamoto, S., 2006. Science (New York, N.Y.) 311, 1141–6.

Wysk, M., 1999. Proceedings of the National Academy of Sciences 96, 3763–3768.

Xia, Y., 2000. Proceedings of the National Academy of Sciences 97, 5243–5248.

Xia, Z.-P., Sun, L., Chen, X., Pineda, G., Jiang, X., Adhikari, A., Zeng, W., Chen, Z.J., 2009. Nature 461, 114–9.

Xu, L., Chen, Y.G., Massagué, J., 2000. Nature cell biology 2, 559–62.

Xu, L., Kang, Y., Cöl, S., Massagué, J., 2002. Molecular cell 10, 271–82.

Xu, Y.D., Hua, J., Mui, A., O'Connor, R., Grotendorst, G., Khalil, N., 2003. American journal of physiology. Lung cellular and molecular physiology 285, 527–539.

Yamaguchi, K., Shirakabe, K., Shibuya, H., Irie, K., Oishi, I., Ueno, N., Taniguchi, T., Nishida, E., Matsumoto, K., 1995. Science (New York, N.Y.) 270, 2008–11.

Yamaoka, S., Courtois, G., Bessia, C., Whiteside, S.T., Weil, R., Agou, F., Kirk, H.E., Kay, R.J., Israël, A., 1998. Cell 93, 1231–40.

Yamashita, M., Fatyol, K., Jin, C., Wang, X., Liu, Z., Zhang, Y., 2008. Molecular cell 31, 918–24.

Yamauchi, Y., Kohyama, T., Takizawa, H., Kamitani, S., Desaki, M., Takami, K., Kawasaki, S., Kato, J., Nagase, T., 2010. Experimental lung research 36, 12–24.

Yang, Y., Xia, F., Hermance, N., Mabb, A., Simonson, S., Morrissey, S., Gandhi, P., Munson, M., Miyamoto, S., Kelliher, M.A., 2011. Molecular and cellular biology.

Yang, Y.-C., Piek, E., Zavadil, J., Liang, D., Xie, D., Heyer, J., Pavlidis, P., Kucherlapati, R., Roberts, A.B., Böttinger, E.P., 2003. Proceedings of the National Academy of Sciences of the United States of America 100, 10269–74.

Yu, F., Chou, C.-W., Chen, C.-C., 2009. Cellular signalling 21, 867–72.

Yu, Y., Ge, N., Xie, M., Sun, W., Burlingame, S., Pass, A.K., Nuchtern, J.G., Zhang, D., Fu, S., Schneider, M.D., Fan, J., Yang, J., 2008. The Journal of biological chemistry 283, 24497–505.

Yujiri, T., 1998. Science 282, 1911–1914.

Zeisberg, M., Yang, C., Martino, M., Duncan, M.B., Rieder, F., Tanjore, H., Kalluri, R., 2007. The Journal of biological chemistry 282, 23337–47.

Zhang, K., Flanders, K.C., Phan, S.H., 1995. The American journal of pathology 147, 352–61.

Zhang, Y., Feng, X., We, R., Derynck, R., 1996. Nature 383, 168–72.

Zhang, Y.-Y., Mei, Z.-Q., Wu, J.-W., Wang, Z.-X., 2008. The Journal of biological chemistry 283, 26591–601.

Zhu, Y., Richardson, J.A., Parada, L.F., Graff, J.M., 1998. Cell 94, 703–14.

8 Appendixes

8.1 Patient Details

BAL Cytokine Assay Non-BOS Patient Details				
Tx #	Sex	Age at Tx	Reason for TX	Sample #
1206	F	21	CF	3
1231	M	57	FA	3
1237	M	45	PF	3
1243	M	54	α1 AD	4
1244	F	49	COPD	3
1254	F	20	CF	3
1263	M	26	CF	5
1268	M	64	Asbestosis	5
1272	M	42	CF	3
1275	M	62	PF	6
1300	M	54	IPF	3
1312	M	29	CF	4
1317	M	45	α1 AD	5
1327	M	52	PH	4
1330	M	27	CF	3
1333	M	57	Emphysema	3
1323	M	46	FLD	5
1348	M	25	CF	3
1374	F	19	CF	3
1378	M	63	PF	3
1379	M	26	CF	5
1459	M	60	Bronchiectasis	3
1460	F	29	CF	3
1498	M	46	FLD	4
1519	M	24	CF	3
1546	M	28	CF	5

Appendix Figure 1 – BAL Cytokine Assay Non-BOS Patient Details

26 patients (5 female, 21 male) with a mean age of 41.2 years and median age of 45 years (19 - 64). All patients gave distinct samples.

CF = Cystic Fibrosis, FA = Fibrosing Alveolitis, PF = Pulmonary Fibrosis, α1 AD = α1 Antitrypsin Deficiency, COPD = Chronic Obstructive Piulmonary Disorder, IPF = Idiopathic Pulmonary Fibrosis and FLD = Fibrotic Lung Disease.

BAL Cytokine Assay BOS Patient Details					
Tx #	Sex	Age at Tx	Reason For Tx	BOS Diagnosis Months post Tx	Sample #
1203	M	39	CF	3	3
1241	M	34	CF	15	4
1259	F	23	CF	12	4
1273	M	25	CF	15	4
1283	M	63	FA	9	6
1284	M	50	Emphysema	24	7
1298	F	63	Emphysema	10	4
1301	M	58	Emphysema	20	5
1304	M	26	CF	19	9
1325	F	63	FLD	12	3
1334	F	33	Emphysema	12	5
1335	M	54	α1 AD	9	6
1352	F	54	Emphysema	10	3
1372	M	43	FLD	13	6
1383	F	28	CF	12	5
1384	M	36	Silicosis	26	5
1399	F	46	COPD	12	8
1403	M	46	Hystiocytosis X	15	6
1424	F	30	CF	12	4
1450	M	40	α1 AD	22	6
1453	M	47	COPD	3	3
1475	M	61	FLD	21	3
1488	M	52	Bronchiectasis	18	3
1501	M	48	Asthma	18	5
1510	M	48	COPD	11	5

Appendix Figure 2 - BAL Cytokine Assay BOS Patient Details

25 patients (8 female, 17 male) with a mean age of 44.4 years and median age of 46 years (23 - 63), mean diagnosis of BOS was 14.1 months (3 – 26). All patients gave distinct samples.

CF = Cystic Fibrosis, FA = Fibrosing Alveolitis, FLD = Fibrotic Lung Disease, α1 AD = α1 Antitrypsin Deficiency, COPD = Chronic Obstructive Piulmonary Disorder.

Cultured Primary Cell Patient Details			
TW #	Age at Tx	Sex	Years Post Transplant
1057	51	F	4
1065	63	F	4
1072	64	F	4
1073	50	M	4
1078	55	M	4
1079	51	M	4
1080	51	F	4
1081	34	F	4
1088	33	F	4
1095	54	M	4
1099	47	M	4
1112	63	M	9
1113	65	M	3
1121	61	M	3
1122	54	F	3
1125	53	M	7
1130	61	M	4
1132	60	M	3
1134	24	F	4
1135	47	F	3
1140	56	M	3
1145	63	M	3
1150	26	M	3
1151	27	M	3
1153	53	F	11
1158	65	F	3
1159	24	M	3
1168	36	F	3
1172	52	F	3
1174	44	F	3
1178	29	F	4
1184	27	M	3
1186	27	M	3
1208	54	F	6
1213	54	M	3
1215	30	F	2
1221	35	F	2
1222	33	M	3
1225	44	F	4
1226	48	F	2
1232	56	M	2
1238	50	F	6
1239	56	F	2
1243	24	M	3
1245	51	F	2
1246	35	F	2
1247	58	M	2

1248	48	F	2
1256	38	M	2
1259	62	M	6
1261	55	M	2
1273	26	F	2
1274	53	M	2
1276	64	F	2
1278	57	F	2
1279	51	F	5
1280	38	M	2
1282	30	M	2
1285	55	M	2
1300	28	M	1

Appendix Figure 3 – Cultured Primary Cell Patient Details

60 patients (29 female, 31 male) with a mean age of 46.2 years and median age of 51 years (24 – 65). Of the 60 patients 21 underwent surgery for Chronic obstructive piulmonary disorder, 19 for cystic fibrosis, 11 for idiopathic pulmonary fibrosis, 3 for bronchiectasis, 3 for lymphangioleiomyomatosis, 2 for sarcoid and 1 for langerhans cell histiocytosis.

8.2 BAL Significance Data

Green shading indicates significance of $p<0.05$, red shading indicates significance of $p>0.05$, tested by two-tailed Mann-Whitney U Test.

TNFα				
Group	Mean (pg/mL)	S.E.M.	Sig. To Non OB	Sig to Non OB C.
OB + 6 C.	129.22	67.56	n/a	0.1639
OB + 6	20.66	9.71	0.7014	n/a
OB + 3 C.	171.60	101.46	n/a	0.1944
OB + 3	26.25	14.64	0.7030	n/a
OB 0 C.	267.46	108.80	n/a	0.0001
OB 0	61.77	33.62	0.0005	n/a
OB - 3 C.	701.12	374.74	n/a	0.0014
OB - 3	105.17	51.37	0.0007	n/a
OB - 6 C.	271.18	139.09	n/a	0.0169
OB - 6	43.86	22.27	0.0343	n/a
OB C.	108.77	46.49	n/a	0.0104
OB	16.86	5.41	0.0407	n/a
Non OB C.	77.95	29.06		
Non OB	24.79	11.75		

Appendix Figure 4 - TNFα statistical significance

IL-1β				
Group	Mean (pg/mL)	S.E.M.	Sig. To Non OB	Sig to Non OB C.
OB + 6 C.	658.26	312.88	n/a	0.0074
OB + 6	105.71	46.01	0.0575	n/a
OB + 3 C.	837.98	463.87	n/a	0.0065
OB + 3	126.23	67.84	0.0503	n/a
OB 0 C.	1831.87	1008.89	n/a	0.0003
OB 0	368.73	208.94	0.0012	n/a
OB - 3 C.	4941.33	3118.07	n/a	0.0025
OB - 3	729.77	459.15	0.0019	n/a
OB - 6 C.	1853.76	1294.58	n/a	0.0316
OB - 6	294.52	212.07	0.0326	n/a
OB C.	483.85	177.14	n/a	0.0004
OB	84.04	23.60	0.0012	n/a
Non OB C.	63.36	14.66		
Non OB	14.95	2.87		

Appendix Figure 5 - IL-1β statistical significance

8.3 Antibody Specificity

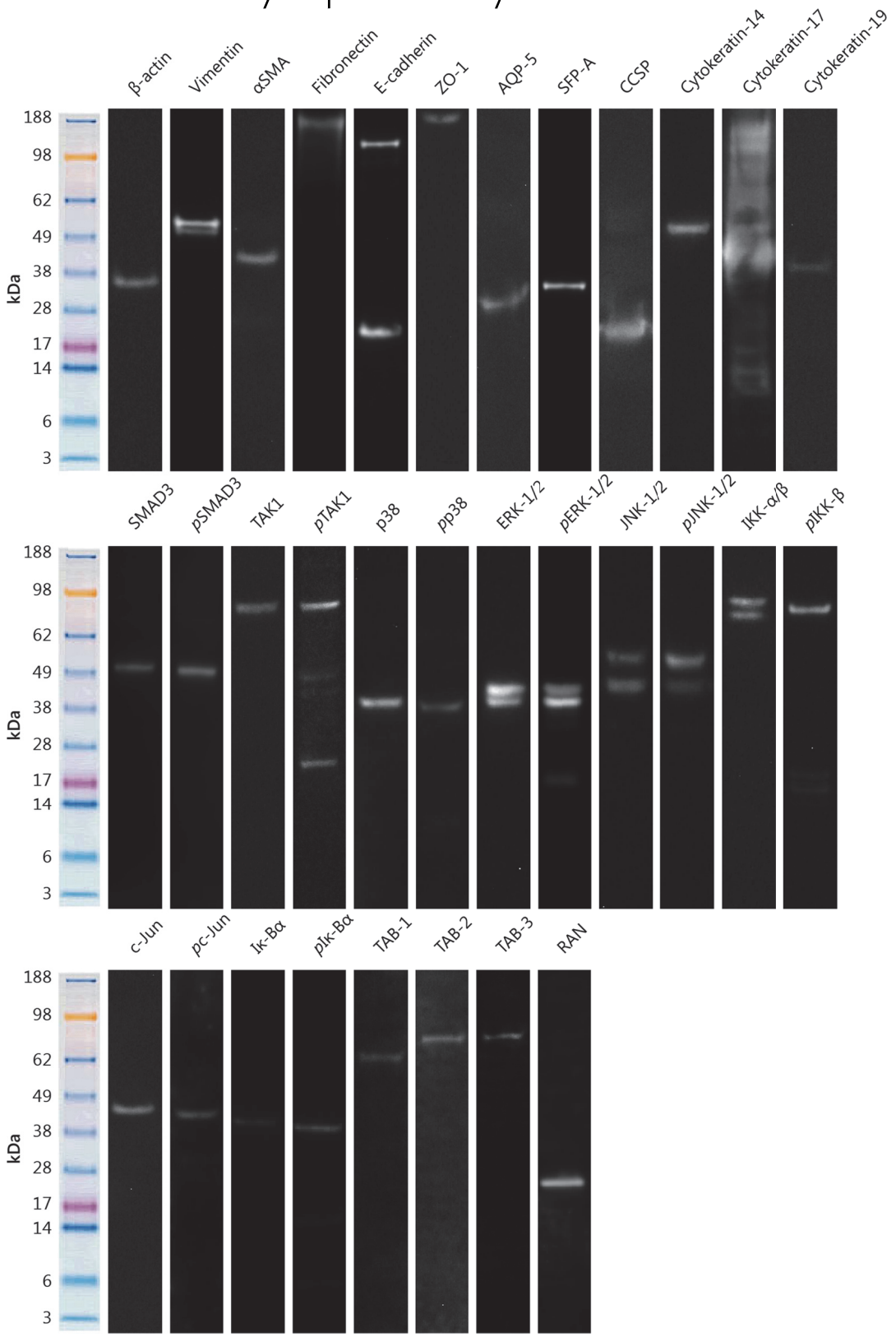

Appendix Figure 6 - Full length PVDF membranes

Between 10µg and 40µgs of PBEC lysate were separated by SDS-PAGE, with the full length of the gel transferred onto PVDF membranes. Each membrane strip was incubated with primary antibodies at concentrations outlined in **2.1.4** with appropriate HRP secondary antibodies used at a 1:2000 concentration.

8.4 Grouped Stimulation Response

Throughout this study, consistent stimulations of 10ng/mL TGF-β1 and 20ng/mL TNFα for 30 minutes and 72 hours have been used to investigate signalling protein phosphorylation and EMT protein expression respectively. Each experiment utilised individual patient samples and contained untreated controls, as such it is possible to group these samples and perform large scale band-densitometry analysis.

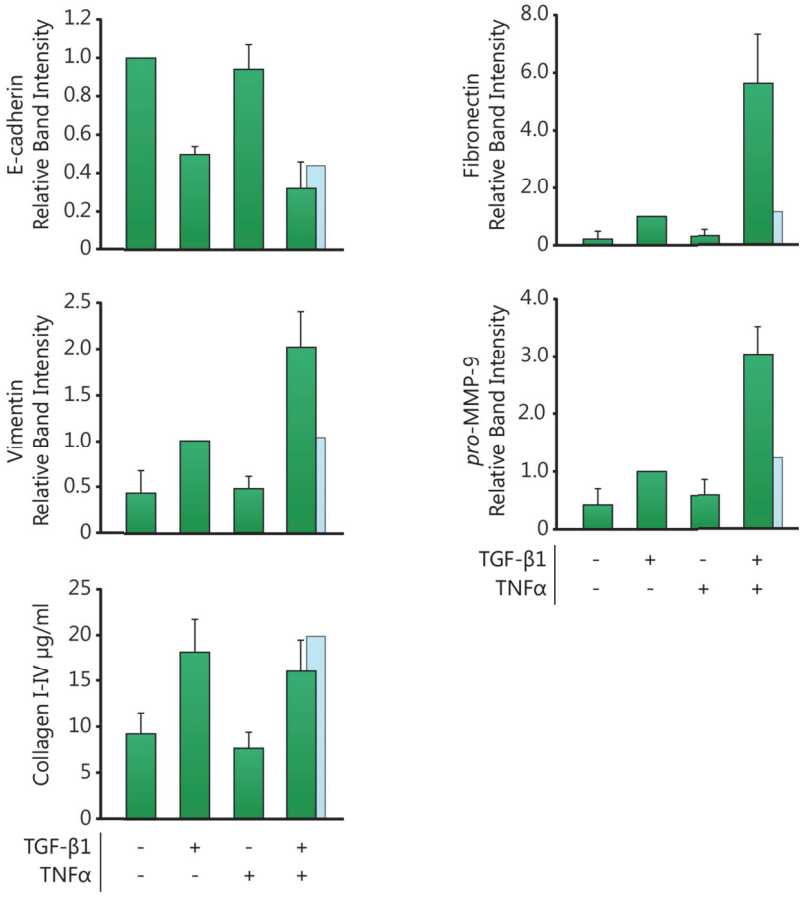

Appendix Figure 7 – Quantified EMT marker protein expression

Stimulation of PBECs (*n*=51 E-cadherin and fibronectin, *n*=40 vimentin, *pro*-MMP-9 and Collagens I-IV) with TGF-β1 (10ng/mL) for 72 hours down-regulated E-cadherin expression, increased fibronectin and vimentin expression and increased *pro*-MMP-9 secretion. This change in EMT marker expression was accentuated by co-stimulation with TNFα (20ng/mL). Collagen I-IV secretion was up-regulated by stimulation with TGF-β1 however no accentuation was observed upon co-stimulation with TNFα. Pale blue bars show additive effect of TGF-β1 and TNFα alone treatments, which, with the exception of Collagens I-IV secretion was lower than the observed result upon co-stimulation.

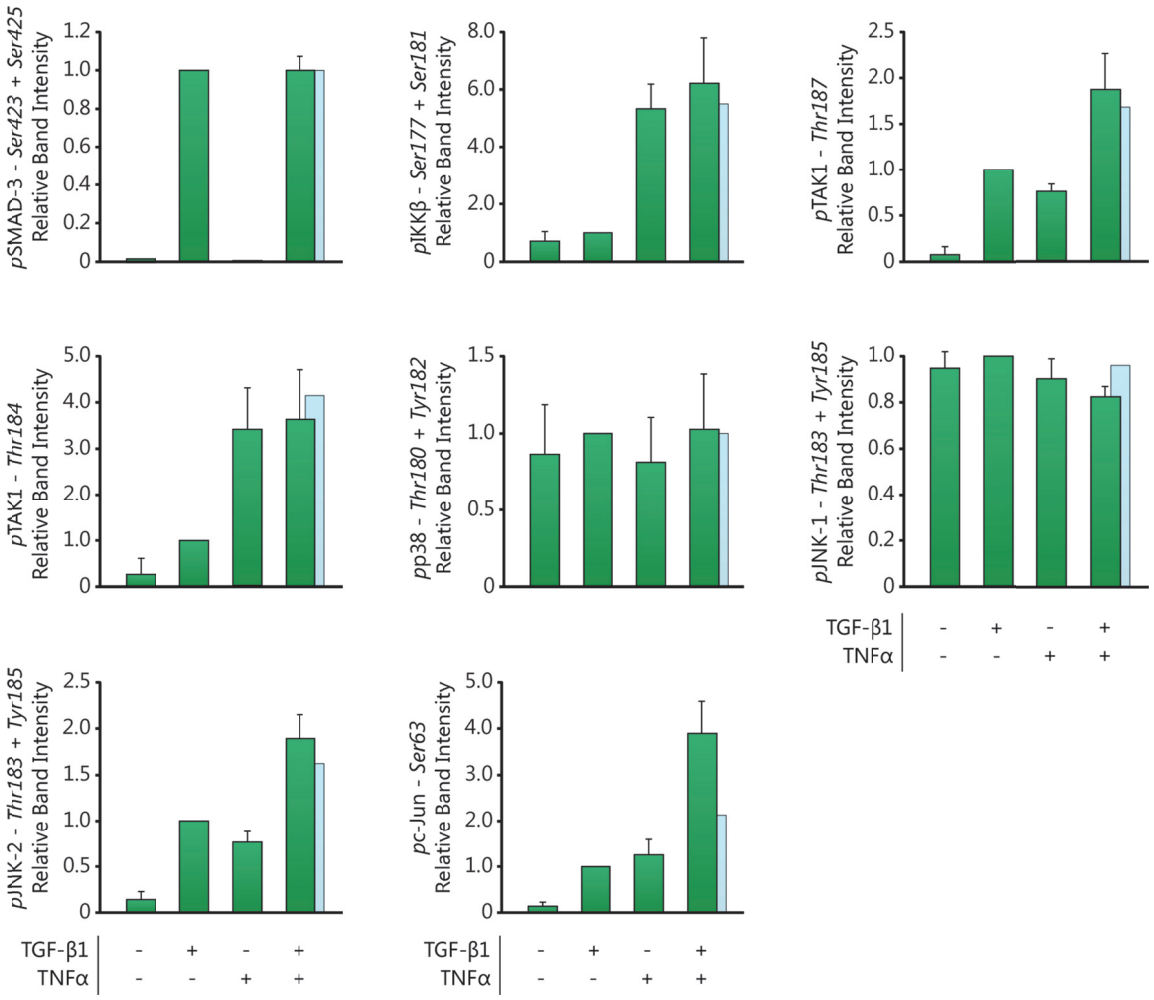

Appendix Figure 8 – Quantified signalling protein phosphorylation

PBECs were stimulated with TGF-β1 (10ng/mL) or TNFα (20ng/mL) for 30 minutes. SMAD-3 (*n*=21) was phosphorylated strongly in response to TGF-β1 but not TNFα with no accentuation observed upon co-stimulation. Conversely, IKKβ (*n*=20) was phosphorylated in response to TNFα but not TGF-β1 with no accentuation observed upon co-stimulation. TAK1 *Thr187* (*n*=22) was strongly phosphorylated in response to both TGF-β1 and TNFα with a slight accentuation observed upon co-stimulation. However, TAK1 *Thr184* (*n*=3) was weakly phosphorylated by TGF-β1 with a strong phosphorylation in response to TNFα stimulation, no accentuation was observed upon co-stimulation. p38 (*n*=18) and JNK-1 (*n*=19) were not phosphorylated above baseline levels by either TGF-β1 or TNFα stimulation. JNK-2 (*n*=19) and c-Jun (*n*=3) were phosphorylated in response to TGF-β1 or TNFα and both displayed an accentuated phosphorylation upon co-stimulation which was especially strong in c-Jun.

8.5 siRNA Phosphorylation Impact

Below are shown the available signalling protein blots post treatment with siRNA, complete sets were not acquired due to the smaller cell number, and the desire to guarantee data on knockdown efficiency.

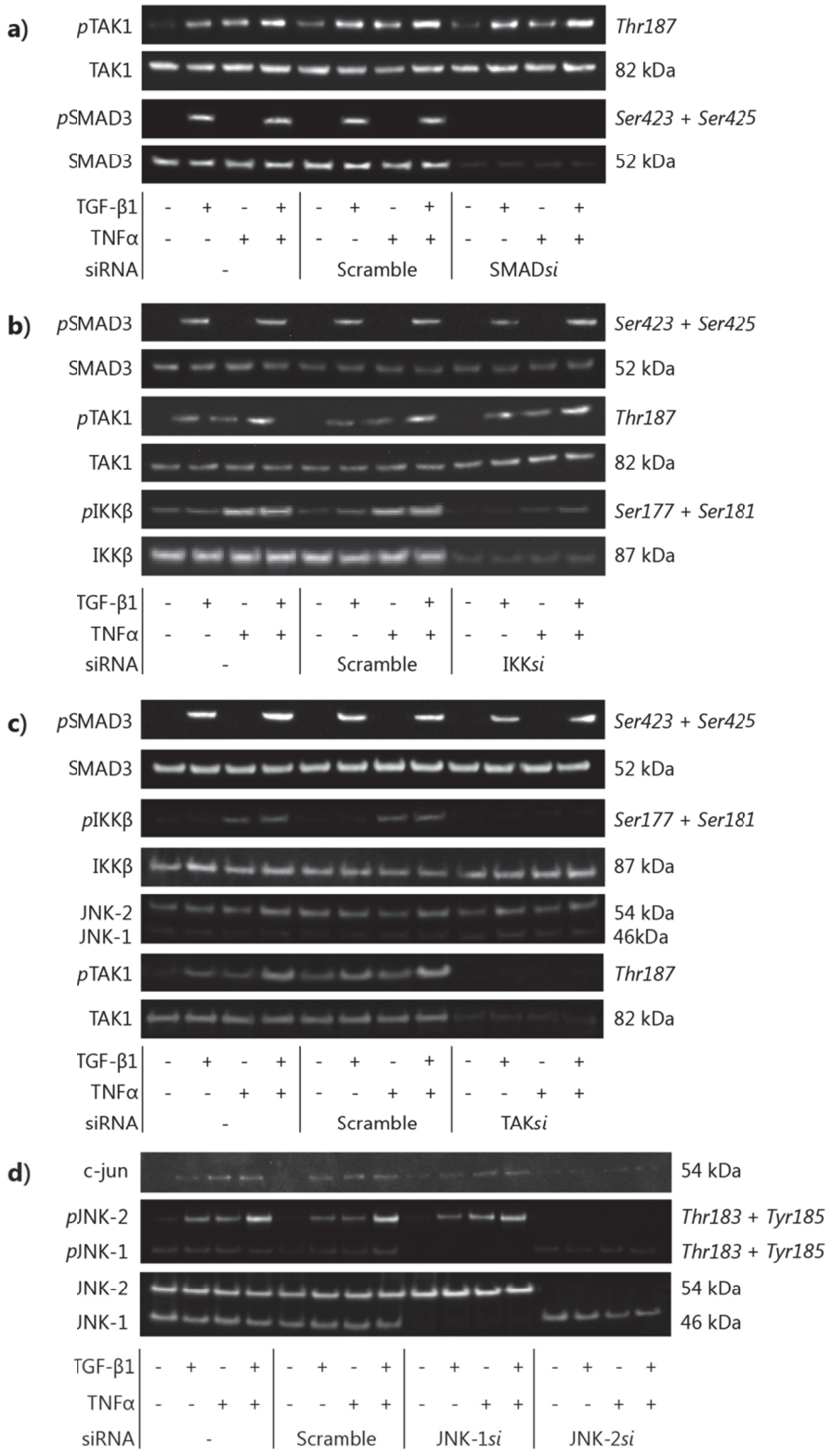

Appendix Figure 9 - siRNA knockdown, effect on phosphorylation

a) PBECs were pre-treated with 5nM SMAD1*si* 24 hours before stimulation with TGF-β1 (10ng/mL) or TNFα (20ng/mL) for 30 minutes. Approximately 90% knockdown of SMAD3 was achieved by SMAD3 targeting siRNA. Neither a sequence scramble control nor the lipid vector had any effect on SMAD3 knockdown, cell viability or morphology. This reduction in total SMAD3 also led to a complete loss of detected phospho-SMAD3 with no effect on SMAD3 phosphorylation seen with either the lipid vector or sequence scramble control. Total TAK1 or phospho-TAK1 were not affected by SMAD*si*.

b) PBECs were pre-treated with 0.1nM IKK*si* 24 hours before stimulation with TGF-β1 or TNFα for 30 minutes. Approximately 90% knockdown of IKKβ was achieved by IKKβ targeting siRNA. Neither a sequence scramble control nor the lipid vector had any effect on IKKβ knockdown, cell viability or morphology. This reduction in total IKKβ also led to a strong reduction in detected phospho-IKKβ with no effect on IKKβ phosphorylation seen with either the lipid vector or sequence scramble control. Total TAK1 and SMAD3 or phospho-TAK1 and SMAD3 were not affected by IKK*si*.

c) PBECs were pre-treated with 3nM TAK*si* 24 hours before stimulation with TGF-β1 or TNFα for 30 minutes. Approximately 80% knockdown of TAK1 was achieved by TAK1 targeting siRNA. Neither a sequence scramble control nor the lipid vector had any effect on TAK1 knockdown, cell viability or morphology. This reduction in total TAK1 also led to a reduction in the detected levels of phospho-TAK1 with no effect on TAK1 phosphorylation seen with either the lipid vector or sequence scramble control. Total SMAD3, JNK-1/2 and IKKβ and phospho-SMAD3 were not affected by TAK*si*. The phosphorylation of IKKβ was inhibited by knockdown of TAK1.

d) PBECs were pre-treated with 5nM JNK1*si* or 10nM JNK2*si* 24 hours before stimulation with TGF-β1 or TNFα for 30 minutes. Approximately 100% knockdown of JNK-1 was achieved by JNK-1 targeting siRNA, with JNK-2 targeting siRNA (10nM) mediating a similar knockdown of JNK-2, neither siRNA demonstrated non-specific knockdown. Neither a sequence scramble control nor the lipid vector had any effect on JNK-1/2 knockdown, cell viability or morphology. This reduction in total JNK-1 or JNK-2 also led to a reduction in the respective levels of phospho-JNK-1/2 with no effect on JNK-1/2 phosphorylation seen with either the lipid vector or sequence scramble control. JNK2*si* but not JNK1*si* reduced the detected amount of c-Jun for all stimulations.

*p*SMAD3 (20μg), *p*IKKβ and *p*p38 (40μg), *p*TAK1, *p*JNK-1/2 and JNK-1/2 (50μg).

Interestingly production of c-Jun was only inhibited by JNK2*si* and not JNK1*si* suggesting that as with the induction of EMT JNK-2 is more important in this system.

8.6 IKKβ Localization

Neither the total or phospho IKKβ antibody worked in ICC experiments, suggesting that the epitope was masked by protein folding or associations, additionally on western blotting no nuclear localization was observed.

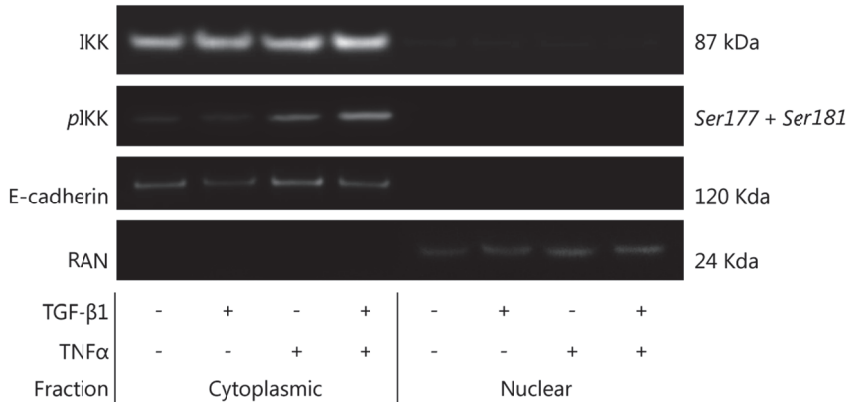

Appendix Figure 10 - Localization of IKKβ and pIKKβ

Total PBEC lysates (*n=3*, representative blots from single patient) treated as above were separated into nuclear and non-nuclear fractions, 35µg of non-nuclear lysate and 10µg of nuclear lysate was then separated by SDS-PAGE and probed for IKKβ and phospho-IKKβ along with E-cadherin and RAN as fractionation controls. Neither total or phospho-IKKβ were detected in the nuclear fraction, although both were detected in the cytoplasm.

8.7 TNF Receptor Work

As described in 1.3.2 TNFα signals through two distinct trans-membrane receptors, TNFR1 and TNFR2 (Locksley et al., 2001). TNFR1 is ubiquitously expressed and can respond to both membrane-bound and soluble forms of TNFα whereas TNFR2 is highly regulated in its expression, mainly on immune cells and responds, efficiently, only to membrane bound TNFα (Grell et al., 1995). Whilst the receptors do provide some form of redundancy they are capable of playing independent roles in cell signalling (16, 26).

It has also been demonstrated that TNFR2 expression over TNFR1 may mediate collagen deposition in response to TNFα (Theiss et al., 2005) and its expression is up-regulated on colonic epithelial cells of patients with Crohn's disease and ulcerative colitis (Mizoguchi et al., 2002). We therefore hypothesized that PBECs from OB patients may express elevated levels of TNFR2 which may mediate the accentuation of TGF-β1 by TNFα by the usage of alternative signalling mechanisms. The below work was carried out in conjunction with Dr Lee Borthwick who contributed the data and analysis to the first figure shown below.

n=6 PBEC cultures from distinct patients were stimulated with TGF-β1 or with soluble TNFα (TNF_{sol}), membrane bound TNFα (TNF_{cys}), TNFR1 specific mutant (Cys-TNF32W/86T) membrane bound TNF ($TNF_{cys}R1$) or TNFR2 specific mutant (Cys-TNF143N/145R) membrane bound TNF ($TNF_{cys}R2$) for 72 hours. Cell lysate and culture media was retained and EMT was assessed using a variety of markers.

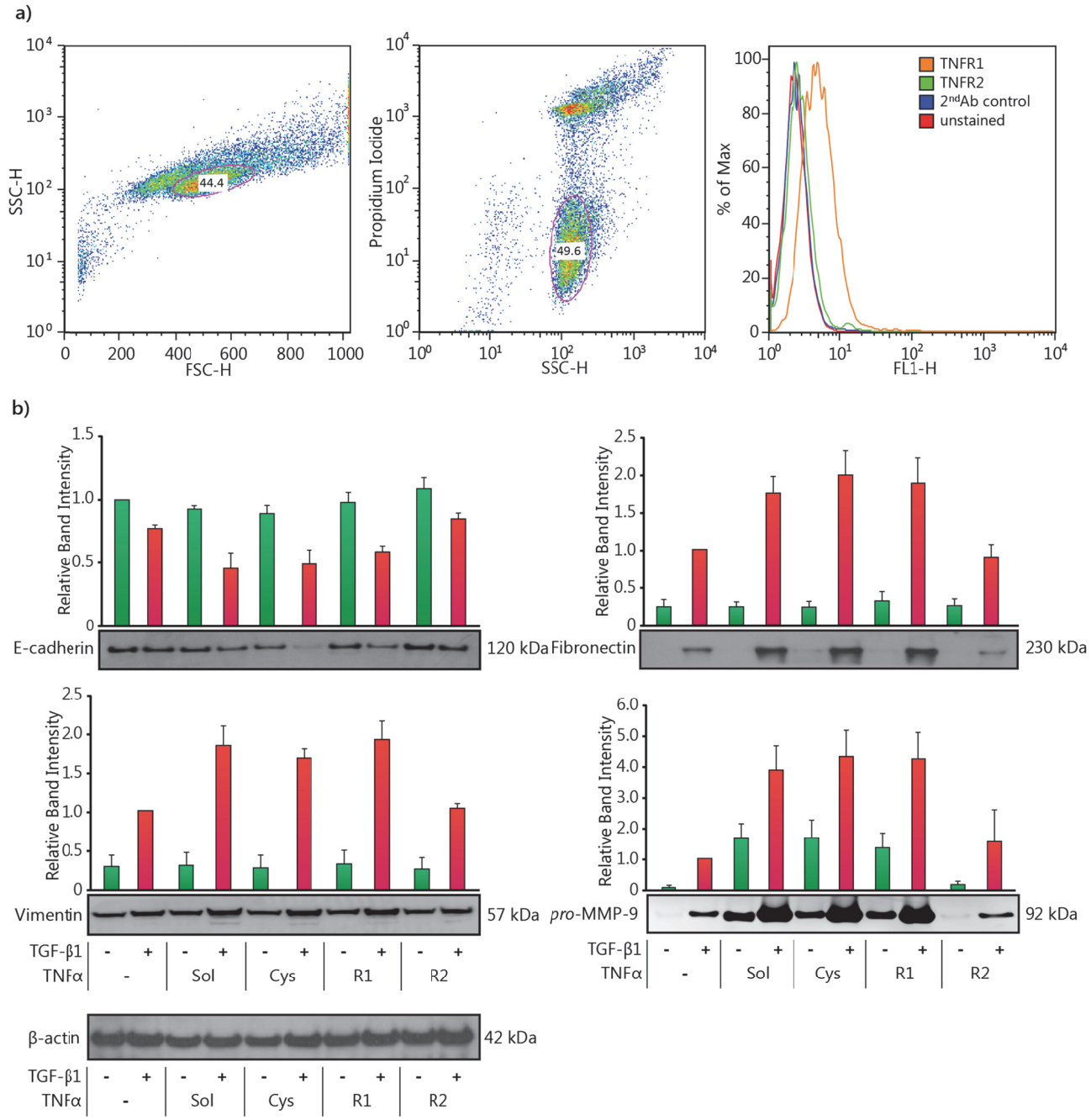

Appendix Figure 11 - TNFR expression, and response to receptor specific expression in PBECs

a) FACS analysis demonstrated that PBECs express TNFR1 on their cell surface but express little to no TNFR2.

b) Stimulation of PBECs (*n=6*) with soluble TNFα (TNF_{sol}), membrane bound TNFα (TNF_{cys}), TNFR1 specific mutant (Cys-TNF32W/86T) membrane bound TNF ($TNF_{cys}R1$) or TNFR2 specific mutant (Cys-TNF143N/145R) membrane bound TNF ($TNF_{cys}R2$) alone has no effect on the expression of E-cadherin, vimentin or fibronectin. However, stimulation with TNF_{sol}, TNF_{cys} or $TNF_{cys}R1$, but not $TNF_{cys}R2$, increased *pro*-MMP-9 secretion. TGF-β1 down-regulated the expression of E-cadherin, increased the expression of vimentin and fibronectin and increased the secretion of *pro*-MMP-9. Co-stimulation of the cells with TGF-β1 and TNF_{sol}, TNF_{cys} or $TNF_{cys}R1$, but not $TNF_{cys}R2$, accentuated the changes in EMT marker expression compared to TGF-β1 alone.

This work was performed by Dr Lee Borthwick and is reproduced here with his consent

Alongside the above investigation I used $TNF_{cys}R1$ and $TNF_{cys}R2$ after pre-treatment with TAK*i*, to investigate if the TNFα mediated accentuation of EMT was associated more strongly with either TNFR1 or TNFR2. *n=4* PBEC cultures from distinct patients were stimulated with TGF-β1 or with $TNF_{cys}R1$ or$TNF_{cys}R2$ for 72 hours. Cell lysate and culture media was retained and EMT was assessed using a variety of markers.

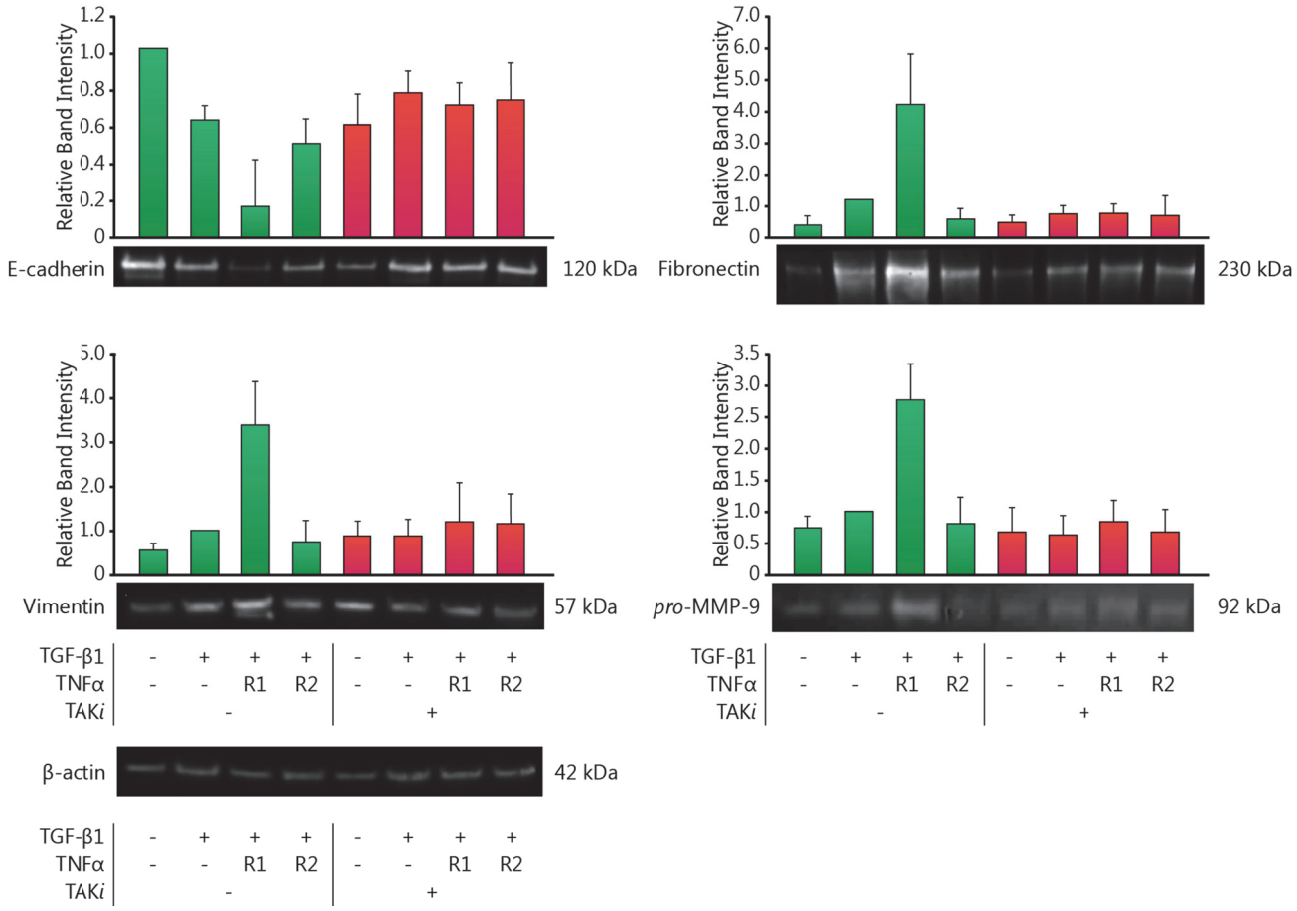

Appendix Figure 12 - Effect of TAKi on EMT induced by TNFR specific isoforms of TNFα

Stimulation of PBECs (*n=4*) with TGF-β1 (10ng/ml) down-regulates E-cadherin expression, increases fibronectin and vimentin expression and increases *pro*-MMP-9 secretion. Co-stimulation with $TNF_{cys}R1$, but not $TNF_{cys}R2$, accentuates the change in EMT marker expression compared to TGF-β1 alone. Pre-treatment with TAKi inhibited EMT driven by both TGF-β1 alone and TGF-β1 and $TNF_{cys}R1$, returning levels of E-cadherin, vimentin, fibronectin expression and *pro*-MMP-9 secretion to baseline.

The above results demonstrated that isolated PBECs expressed TNFR1 with a very low level of TNFR2 detected. Correspondingly, TGF-β1 driven EMT was induced only by TNF isoforms capable of binding to TNFR1, and which TAK*i* was capable of inhibiting. Interestingly unlike in **4.3.2.1** TAK*i* did not induce elevated levels of *pro*-MMP-9 when in the presence of either TNFα isoform. E-cadherin and fibronectin (5µg), vimentin (20µg) and *pro*-MMP-9 (30µL).

8.8 Personal Development

8.8.1 Presentations

- November 2009 - Oral Presentation – North East Post-Graduate Research Conference, Newcastle University, Newcastle-Upon-Tyne, United Kingdom. "*Inflammatory Accentuation of EMT in Fibrotic Lung Epithelium via IKK-NF-κB*"

- June 2010 - Poster Presentation - Institute of Cellular Medicine Research Day, Newcastle University, Newcastle-Upon-Tyne, United Kingdom. "*Inflammatory Accentuation of EMT in Fibrotic Lung Epithelium*"

- March 2010 - Poster Presentation – European Respiratory Society Lung Science Conference, Estoril, Portugal. "*TNFα accentuates TGF-β1 driven epithelial to mesenchymal transition (EMT) in lung epithelium via TNFαReceptor1/TAK-1 dependent signalling*"
  * Awarded European Respiratory Society Lung Science Conference Bursary. €550 travel grant.

- December 2010 - Oral Presentation – British Thoracic Society Winter Meeting, London, United Kingdom. "*The role of Transforming Growth Factor Associated Beta Kinase 1 (TAK1) in the development of airway fibrosis*"

- January 2011 - Poster Presentation – Keystone Symposia on Epithelial Plasticity and Epithelial to Mesenchymal Transition, Vancouver, Canada. "*TNFα accentuates TGF-β1 driven Epithelial to Mesenchymal Transition in lung epithelium via TGF-β activated kinase-1 (TAK1) dependent signalling*"
  * Awarded Newcastle University, Graduate Student Travel Award. £600 travel grant.

- March 2011 - Poster Presentation - European Respiratory Society Lung Science Conference, Estoril, Portugal. "*TNFα accentuates TGF-β1 driven Epithelial to Mesenchymal Transition (EMT) in lung epithelium via TAK1 dependent signalling*"

- June 2011 - Oral Presentation – Institute of Cellular Medicine Research Day, Newcastle University, Newcastle-Upon-Tyne, United Kingdom. "*TNFα accentuates TGF-β1 driven Epithelial to Mesenchymal Transition (EMT) in lung epithelium via TAK1, JNK-1/2 dependent signalling"*

- July 2011 – Oral Presentation, Young Investigator Session - British Association of Lung Research Summer Meeting, Newcastle-Upon-Tyne, United Kingdom. "*TNFα accentuates TGF-β1 driven Epithelial to Mesenchymal Transition in lung epithelium via Transforming growth factor β–activated kinase-1 (TAK1) dependent signalling"*
  * Awarded British Association of Lung Research, Best Oral Presentation by a Young Investigator 2011. £750 travel grant.

- November 2011 – Oral Presentation - Newcastle, Edinburgh, Cambridge & Sheffield Lung Research Meeting, Cambridge, United Kingdom. "*Transforming Growth Factor Beta Activated Kinase 1 (TAK1) as a mediator of the fibrogenic synergy between Transforming Growth Factor Beta 1 (TGF-β1) and Tumour Necrosis Factor Alpha (TNFα)*"

8.8.2 Publications

- Gardner, A., Fisher, A. J., Richer, C., Johnson G. E., Moisey, E. J., Brodlie, M., Ward, C., Krippner-Heidenreich, A., Mann, D. A., and Borthwick, L. A. (2012). **The Critical Role of TAK1 in Accentuated Epithelial to Mesenchymal Transition in Obliterative Bronchiolitis after Lung Transplantation.** The American Journal of Pathology *180 (6),* 2293-2308.

- Borthwick, L. A., Gardner, A., De Soyza, A., Mann, D. A., and Fisher, A. J. (2012). **Transforming Growth Factor-β1 (TGF-β1) Driven Epithelial to Mesenchymal Transition (EMT) is Accentuated by Tumour Necrosis Factor α (TNFα) via Crosstalk Between the SMAD and NF-κB Pathways**. Cancer Microenvironment *5 (1),* 45-57.

- Borthwick, L. A., Botha, P., Verdon, B., Brodlie, M. J., Gardner, A., Bourn, D., Johnson, G. E., Gray, M. A., and Fisher, A. J. (2011). **Is CFTR-delF508 Really Absent from the Apical Membrane of the Airway Epithelium?** PLoS ONE *6*, e23226.

- Gardner, A., Borthwick, L. A., and Fisher, A. J. (2010). **Lung epithelial wound healing in health and disease**. Expert Review of Respiratory Medicine *4*, 647-660.

8.8.3 Memberships

- Student member of the British Thoracic Society, 2010 -

- Silver member of the European Respiratory Society, 2011 -

- Student member of the British Association of Lung Research, 2011 -
  * Also acted as webmaster for the BALR Summer Meeting 2011 that was held in Newcastle-upon-Tyne.

- Member of the North East Post-graduate Research Conference 2010 organising committee, responsible for website design and maintenance, abstract submission and marking as well as design and production of advertising material and abstract booklet.